Evaluating the potential of mechanically ventilated double-skin façades to enhance energy efficiency and thermal comfort of office buildings in different climate zones of India through numerical modelling

Varun Sonpar Kale

TU Delft

“Evaluating the potential of mechanically ventilated double-skin façades to enhance energy efficiency and thermal comfort of office buildings in different climate zones of India through numerical modelling.”

By

Varun Sonpar Kale

Student No.: 4713079

In partial fulfilment of the requirements for the degree of

Master of Science in Civil Engineering

Track: Building Engineering

Specialization: Building Physics and Technology

At Delft University of Technology

July 2019

TU Delft Delft University of Technology

THESIS COMMITTEE

Dr. L.C.M. Itard (Chair)
Delft University of Technology
Faculty of Architecture and the Built Environment
Section of Management in the Built Environment

Dr.ir. W.H. van der Spoel (Supervisor)
Delft University of Technology
Faculty of Architecture and the Built Environment
Section of Architecture Engineering + Technology

Dr.ir. H.R. Schipper (Graduation Co-ordinator)
Delft University of Technology
Faculty of Civil Engineering and Geosciences
Section of Structural Design/Building Engineering

STUDENT

Varun Sonpar Kale
Student No.: 4713079
Faculty of Civil Engineering and Geosciences
Building Engineering *(Building Physics and Technology Specialization)*

ABSTRACT

The air-conditioning of commercial buildings accounts for approximately 50% of the total energy consumed in India's commercial sector. Reducing this load is a key step towards minimizing India's greenhouse gas emissions. One culprit is the routine use of fully glazed façades which are chosen for aesthetics but are neither energy efficient nor effective at providing adequate thermal comfort. A double skin façade (DSF) can help reduce the heat gain of a building by exhaustion heat through cavity ventilation, while still providing the aesthetics of a fully glazed façade. The higher thermal resistance can also help provide better indoor thermal comfort to occupants. However, due to the high cost of DSFs, their complex thermal behaviour and overheating risk in the cavity an assessment of the effectiveness of the system in warmer climates of India is needed.

This study evaluates the energy saving potential and thermal comfort enhancements with mechanically ventilated DSFs in different climate zones of the Indian subcontinent. A numerical model created in the MATLAB/Simulink platform, employing the zonal approach and verified against Design Builder was used for simulating the thermal behaviour. Optimization of the façade design was based on three parameters: 1) cavity width, 2) cavity ventilation rate and 3) glazing systems. The sensitivity of these design parameters to the performance of the DSF was analysed before proposing optimized configurations for different sites based on their local climate. These optimized configurations are then evaluated against a single skin fully glazed façade. The parameters used for evaluating the energy saving potential are annual heat gain and annual heat loss. For thermal comfort and overheating risk, the temperature distributions were analysed.

In comparison with a single skin façade, it is found that the façade orientations with the highest incident solar radiation, usually the South, East and West facing façades, provide the most improvement, up to 50% reduction in heat gain annually. Heat loss was reduced by 25-35% at each site, however, this proves to be irrelevant for sites with mild winters. This corresponded to the arid, semi-arid, humid subtropical and montane climate zones found in India. Thermal comfort was maintained by the DSF for both warm and cool walls. This was also found to be the case for the single skin façade, hence, no additional improvement to thermal comfort was achieved with respect to radiant asymmetries. Overheating in the cavity was mitigated through the application of tinted glazing in the external envelope, ventilation rates of up to 80AC/hr and larger cavity widths. Optical properties of the external envelope have the largest impact on the reduction in heat gain regardless of the façade's spatial orientation and façades with low direct solar radiation were found to be insensitive to changes in cavity width and ventilation rate.

The findings of the study suggest that DSFs have an important energy saving potential in warm climates and the design recommendation can be utilized to mitigate overheating and excess heat gain which is seen as an issue even in cooler climate zones.

TABLE OF CONTENTS

LIST OF FIGURES

LIST OF TABLES

ACKNOWLEDGEMENTS

This thesis was made possible by the insights and feedback of my thesis committee, under whom I have had this wonderful opportunity to progress and learn.

I would like to thank Willem van der Spoel for his insights into numerical modelling and the complexities associated with them. He always made himself available when I needed clarity and his help with setting up and debugging the numerical model is immensely appreciated.

I would like to thank Laure Itard for her constant encouragement throughout the process. Her insights and detail feedback at each of the meetings has helped ensure that the work I did catered to the highest level of quality.

I would like to thank Roel Schipper for the practicality of his feedback. This is greatly appreciated considering the more theoretical nature of the work, helping to ingrain a sense of practical competence and real-world applicability of the proposal.

Lastly, I would like to thank my parents, Sunil Kale and Shobna Sonpar, for their continuous support and unwavering confidence in my abilities.

Figure 1.1: Signature Tower, Gurugram, Delhi NCR (top-left), ICICI Bank Headquarters, Mumbai (top-right), Horizon Centre, Gurugram, Delhi NCR

1. INTRODUCTION

This chapter first presents the current context of the commercial building sector in India and relates the poor design strategies employed to the subpar energy performance of these buildings. This is done by looking at the current trends in façade design of commercial buildings and a brief analysis of the climate zones found in India. Following this, the possible application of double skin façades (DSFs) as a solution to reduce the cooling loads is presented and based of off this, the research focus, it's scope and objectives are presented.

1.1 Background

India is the seventh largest country in the world with a land area of almost 3.7 million km^2. Further, being one of the fastest growing economies there is immense pressure on the construction of commercial and office spaces, especially in major metropolitan cities. These are constantly in need of new office spaces. A large portion of this is designed based on the image of the more "modern" western countries. This has led to an architectural trend in the design of buildings, which makes use of the fully glazed facades. This is unfortunately done without considerations to local climate and context of the users. As a result, the

Figure 1.2: DLF Centre, New Delhi

Figure 1.3: Gateway Tower, Gurugram, Delhi NCR

energy efficiency of the buildings suffers a major setback when it comes to indoor climate control. Fifty percent of the energy demand from the commercial sector is a result of cooling demand which is primarily met through large air-conditioning without the integration of passive design strategies. The large amount of electricity needed for the cooling systems has a significant carbon footprint given that the majority of the electricity is generated from burning fossil fuels. At the other end of the spectrum, there are very few heating costs as most buildings do not have any form of heating systems employed. This comes as a trade-off for the thermal comfort of the occupants. It is not uncommon to be wearing heavy clothing while indoors for maintaining an adequate level of thermal comfort. However, in recent times the use of smaller heating devices such as electric radiators have further increased the energy consumption in buildings. Hence, a façade which can reduce both the cooling and heating needs of the building simultaneously would be beneficial and given the implications of global warming and climate change is the need of the hour.

Creating a façade with the required malleable thermal behaviour while keeping within the architectural demands in the commercial sector which prioritizes fully glazed façades enforces restrictions on the available solutions that can be applied fruitfully. Fully glazed façades offer advantages such as a lighter structure, more daylight availability to the interiors and for many, give a sophisticated appearance to

the buildings. For such reasons, new and upcoming commercial buildings in India are inclined towards fully glazed facades *(Fig. 1.1, 1.2, 1.3)*. Given the high summer temperatures and large solar radiation received on building façades this choice is sub-optimal for promoting energy efficiency and thermal comfort. Nevertheless, the trend exists and a façade system capable of reducing internal heat gains while accommodating this aesthetic demand is needed.

DSFs are gaining recognition as a technology that, while giving a modern transparent appearance to buildings, has the capability to moderate the indoor thermal conditions and the potential to reduce energy demands (Barbosa, 2015). It is a hybrid system made of an external glazed skin and the actual building façade, which constitutes the inner skin. The two layers are separated by an air cavity which has fixed or controllable inlets and outlets and may or may not incorporate fixed or controllable shading devices (Pomponi, et al., 2016). The ability of a DSF to behave differently based on the airflow scheme in the cavity *(Fig. 1.4)* offers a possible solution to enhanced thermal comfort and energy savings at sites with large climatic variations. In summer times the façade could make use of the chimney effect and help create ventilation in the buildings, thereby decreasing the load on the HVAC system. This coupled with the insulating behaviour of the cavity and the added shading device can help mitigate the extreme heat during summers. It also allows a convenient solution to integrate night-time ventilation because the second skin reduces the ingress of precipitation and particulate matter while allowing ample ventilation. The research of Barbosa (2015) on the application of naturally ventilated DSFs in the hot and humid climate of Brazil (Barbosa, 2015) and that of Yellamraju (2014) in the hot climate of India (Yellamraju, 2014) show a promising future for the use of this system in hot climates. Given the well-established research as well as the application of DSFs in cooler climates there are possible advantages in energy saving and thermal comfort to be gained both in summer as well as winter for the seasonal variations seen in the different climate zones in India.

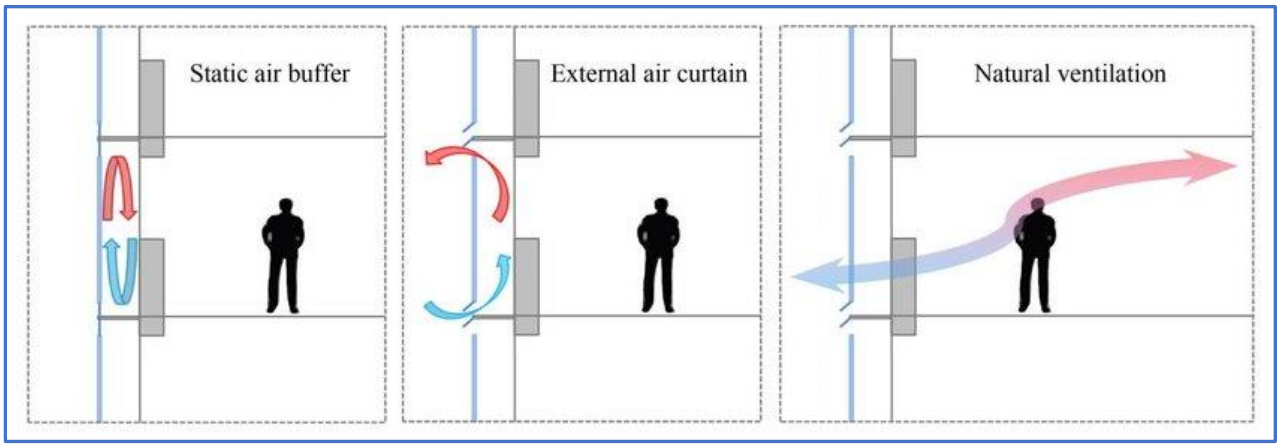

Figure 1.4: Seasonal airflow operating method of a DSF: (a) Static air buffer as winter airflow operating method; (b) External air curtain as summer airflow operating method; (c) Natural ventilation as summer airflow operating method.
SOURCE: *Assessment of Seasonal Energy Efficiency Strategies of a Double Skin Façade in a Monsoon Climate Region - Scientific Figure on ResearchGate. Available from: https://www.researchgate.net/figure/Seasonal-airflow-operating-method-of-a-DSF-a-Static-air-buffer-as-winter-airflow_fig3_276035983 [accessed 14 Dec 2018]*

India's large land area coupled with a variety of geographical features such as the Himalayan Mountains to the North and East, the Thar Desert to the West and a peninsula to the South have resulted in a multitude of climate zones *(Fig. 1.5)*. The following is a brief description of the same:

I. **Alpine/Tundra:** This climate type is only found in a small portion of the Himalayan Mountains within India. The temperature in these areas rarely exceeds 10°C.
II. **Humid Sub-tropical**: This climate features mean temperatures in the coldest month between 0 °C or −3 °C and 18 °C and mean temperatures in the warmest month, 22 °C or higher. Rainfall often shows a summer peak, especially in India where monsoon seasons are well developed.
III. **Tropical Wet and Dry:** These regions have monthly mean temperatures above 18 °C in every month of the year and typically a pronounced dry season, with the driest month having less than 60 mm of precipitation and less than 100 [total annual precipitation {mm}/25] of precipitation.
IV. **Tropical Wet:** The temperature variation in this clime is usually between 20°C and 34°C with an average of 27°C throughout the year. But this coupled with high humidity often leads to much higher perceived temperatures. Additionally, there is regular rainfall throughout the year with roughly 250cm of annual rainfall.
V. **Semi-arid:** These climates tend to have hot, sometimes extremely hot, summers and warm to cool winters, with some to minimal precipitation. In India, due to the seasonal effects of monsoons, a short well-defined wet season is also experienced but it is not sufficiently wet overall to qualify as a tropical wet and dry climate. The winter temperature may be as low as 0 °C with summer temperatures exceeding 30 °C.
VI. **Arid:** In these locations, hot desert climates as seen in India are generally hot, sunny and dry year-round. Hot-month average temperatures are normally between 29 and 35 °C and midday readings of 43–46 °C are common. During colder periods of the year, night-time temperatures can drop to freezing or below due to the large radiation loss under the clear skies. However, very rarely do temperatures drop far below freezing.

1.2 Research Focus

A DSF system is one of the few solutions available to improve the performance of fully glazed façades beyond that which is achieved from using different glazing types. External shading is one of the most effective strategies to reduce heat gains within buildings but prevents the façade from achieving a flush, fully glazed exterior. Hence, due to architectural and aesthetical reasons these are not always employed. A DSF system gives the opportunity to employ shading devices within the cavity, thereby maintaining the aesthetical appeal from the exterior while still having a similar effect as external shading with respect to the internal envelope of the building. When it comes to the heating season, i.e. winter, the cavity acts as an extra buffer space, improving the thermal insulation of the façade. Adding to this, the greenhouse effect within the cavity can take advantage of the solar radiation and daylight hours

even during winter months to capture and store heat. Given that the occupants in office buildings of India are accustomed to wearing heavier clothing indoors, one could argue that the thermal comfort of the occupants can be greatly enhanced without the need for heating devices, based solely on the combination of the already heavier clothing and higher insulation provided by the DSF.

Research into the thermal behaviour of DSFs along with their energy saving and thermal comfort enhancing ability has caught pace over the past decade. The need for more energy efficient buildings as well as higher occupant demand for indoor comfort have fuelled this trend. The current state of research is however largely dominated by the application of such systems in cooler climates, with few in

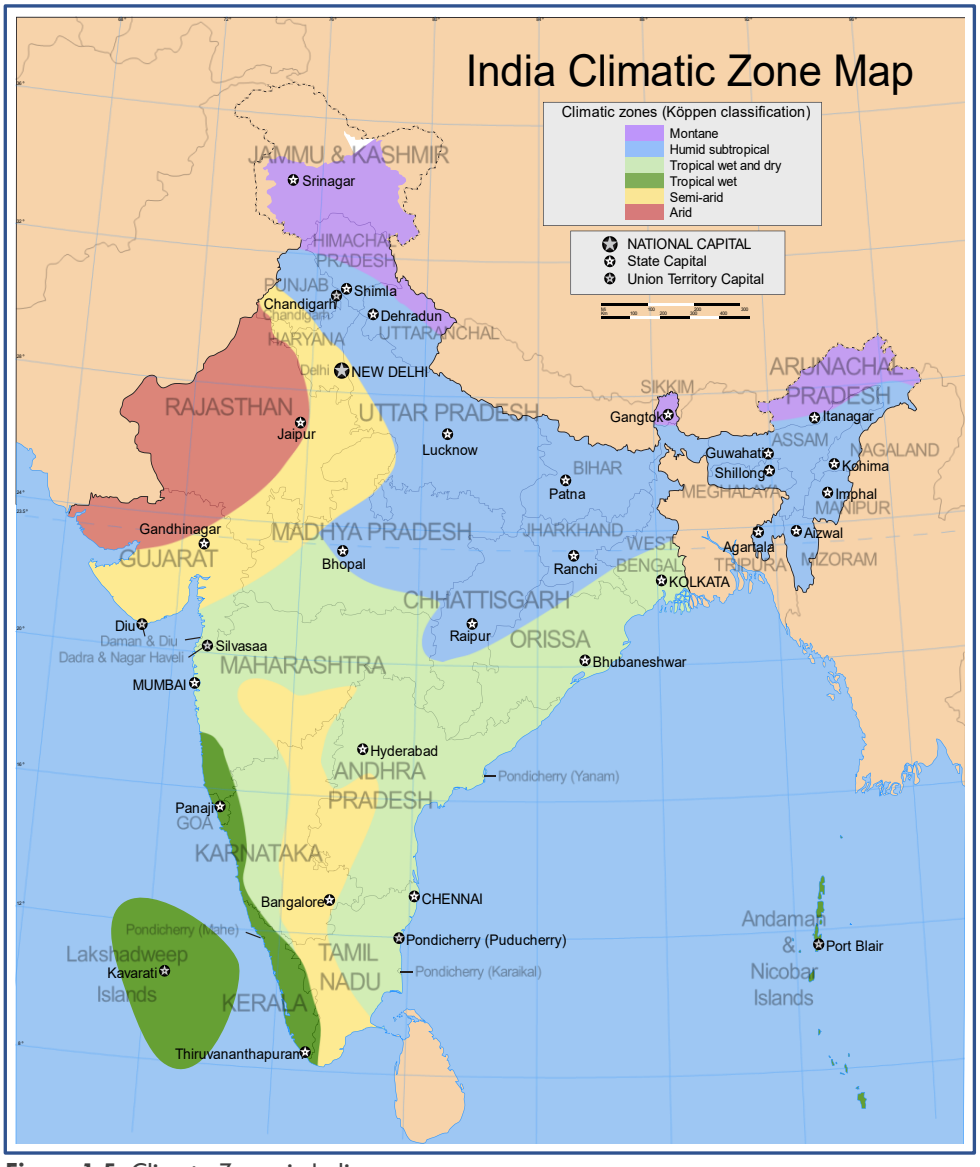

Figure 1.5: Climate Zones in India

SOURCE: *By Saravask, based on work by Planemad and Nichalp - Own workInternational Borders: University of Texas map library - India Political map 2001Disputed Borders: University of Texas map library - China-India Borders - Eastern Sector 1988 & Western Sector 1988 - Kashmir Region 2004 - Kashmir Maps.State and District boundaries: Census of India - 2001 Census State Maps - Survey of India Maps.Other sources: US Army Map Service, Survey of India Map Explorer, Columbia UniversityMap specific sources: india_climate_map.jpg., CC BY-SA 3.0, https://commons.wikimedia.org/w/index.php?curid=1810580*

cooling demand dominant regions such as India. Further, only a handful of articles delve into the behaviour of the DSF in climates with high temperature and humidity variation, with only a few studies in China analysing the behaviour in such climates. However, looking at a combination of the studies for the applicability of DSFs in different climate zones, one can see how the façade can be employed in climates with a high annual variation.

The malleability of the thermal behaviour of a DSF based on the air flow in the cavity as explained in the previous section offers a promising technique to employ the façade in regions with high temperature variance. This allows the designer to prioritize different aspects of the façade to cater to better energy efficiency and optimum thermal comfort. The added insulation for winter conditions and a reduction in the temperature of the interior envelope in summers can benefit the occupant's thermal comfort. By applying night-time ventilation, shading within the cavity, a suitable ventilation strategy in the cavity and appropriate inner and exterior glazing types a reduction in heat gain to the building can be achieved when compared to the traditionally used fully glazed systems in India.

The high cost of DSFs presents the need for an accurate energy simulation model to judge its performance in each context and region. Numerical models such as zone models are one such method and can be employed for the purpose of analysing heat flow and thermal comfort predictions. The process of creating and applying such models is however complicated by a large number of variables involved such as heat transfer coefficients, material properties, etc. in which small changes may have a large impact on the assessment criteria. Many of the variables are determined empirically to save time lest complex computational fluid mechanics (CFD) calculations are involved which are time-consuming and require far too much detailed input which is unavailable in the early stages of the design process.

Using a numerical model to evaluate the behaviour of a DSF in the various climate zones of India and respective contexts offers a perspective into the application of the façade system. Further, it sheds light on the different properties of the façade that have a profound effect on performance or those that are more or less redundant when it comes to the thermal and energy saving capacity of the DSF with respect to its design and operation in hot climates.

1.3 Aim

This study aims to develop a zonal model of a DSF to assess its performance in different climate zones of India. Data pertaining to important design parameters and operation related mechanisms of a DSF will be evaluated as per their impact on decreasing cooling and/or heating energy and the level of thermal comfort achieved.

1.4 Research Questions

The main research objective: **To model and evaluate the thermal performance of different double-skin façade configurations for office buildings in different climate zones and the context of India.**

Research questions to achieve the main objective can be classified into those pertaining to the contextual evaluation, modelling approach and interpretation and analysis of the data. These are presented below.

1.4.1 Contextual Evaluation

a) What are the unique characteristics of the climatic regions in India?
b) How can one apply an appropriate adaptive thermal comfort model to Indian office buildings?

1.4.2 Modelling and Simulation

a) Which boundary conditions and assumptions can be applied for an accurate simulation of the thermal behaviour of a DSF?
b) Which design parameters have the most significant effect on the thermal performance of a DSF?
c) How can overheating in the cavity be minimized?

1.4.3 Performance Evaluation and Analysis

a) What enhancements in thermal comfort in office spaces are achieved using the DSF as compared to a single skin system?
b) What enhancements in energy savings for office spaces are achieved using the DSF as compared to a single skin system?
c) What are the most effective design configurations of the DSF for reducing the energy consumption of the HVAC system at different sites?
d) What is the minimum required rate of ventilation to prevent overheating for a given DSF configuration and climate zone?
e) How can one justify additional energy used for mechanical ventilation in the façade?

Figure 2.1: One Angel Square, Manchester, England. Detail of the double skin façade (during construction) that increases natural ventilation. There is a walkway between the inner and exterior façade panels for maintenance and solar shading.

2. Literature Review

Buildings in the commercial sector of India account for the largest proportion of energy consumption within the country. There is a trend of rising popularity for fully glazed facades in urban areas resulting in large energy consumption during summers for cooling. Double skin façades provide an attractive mitigating strategy to decrease the cooling loads by extracting the excess heat energy through ample ventilation within the façade cavity (Rajesh & Purohit, 2014). This chapter, first, analyses the available literature on the application of DSFs in hot climates. Second, discusses the different numerical modelling methodologies available, weighing their pros and cons. And lastly, presents the effectiveness of different design parameters such as cavity width, ventilation rate, etc. on heat gain and temperature distribution within the façade.

2.1 Overview of Double Skin Facades

Multiple studies show that DSFs help save energy even in warmer climates when compared to the traditional single or double glazing that is employed in such regions. In the research of Muliyadi (2012) which is based on analysing a DSF in Indonesia, he has shown that the DSF minimizes heat gain when compared to single-skin and pair glass window systems (Mulyadi, 2012). While other studies have shown that a mixed approach to DSFs, in which an opaque and transparent façade cladding are used together can be much more fruitfully applied (Yellamraju, 2014). Further yet, a study in the hot arid region of Brazil on a naturally ventilated DSF found that the thermal acceptance rate was less than 20% for the DSF, hence concluding that despite benefits of natural ventilation the less expensive single skin façade seems to perform better with respect to thermal comfort. In the same study, an acceptance rate of 60-80% was found for the DSF in the coastal regions of Brazil (Barbosa, 2015). This study however only compared naturally ventilated DSF and not those that are mechanically ventilated which have better performance and lower energy consumption (Su, et al., 2017).

DSFs have proven their energy saving capacity in many low energy buildings in Europe by using features such as low U-value glazings and heat recovery. However, even in these cases, there are examples of buildings in which the cooling load during summer has increased due to the insulating effect of the double skin. This is primarily due to the high heat retention in façade cavity (Barbosa, 2015). Another study conducted for the cooling and heating seasons in China found that the heat loss during the heating season for an opaque façade was 89% more than that of a double skin while heat gain in the cooling season was 30% less for the opaque façade as compared to the double skin. Despite this, the overall energy saving of a double skin was still better as compared to the opaque façade (Xue & Li, 2015). These studies show the complex nature of a DSF and how perhaps the current designs are much more suited to the heating seasons (winter conditions) as opposed to the cooling seasons (summer conditions).

The main strategy employed to address this issue, especially in countries with more severe summer conditions, is to provide ample ventilation in the cavity. With respect to night-time ventilation, the façade has shown a positive effect on decreasing cooling loads during summers. This is a key aspect as without night-time ventilation the insulating behaviour of the façade will decrease the heat loss of the building at night (Hashemi, et al., 2010). Night-time cooling and ventilation rate in the cavity play a significant part in the performance of the DSF in the cooling season. In the hot arid climate of Iran, it was found that the cavity of a DSF with poor ventilation was 2-10°C higher than the external air temperature while in a section of the same façade which was ventilated adequately, it was only 2-4°C higher than the external air temperature. Further, a combination of the naturally ventilated DSF which is integrated with the HVAC system of a building was found to increase the coefficient of performance of the cooling system, hence providing further benefit in terms of decreasing the energy needs (Mulyadi, 2012).

Lateral ventilation, air movement in the horizontal direction can also be used as a ventilation strategy to cool the cavity air, however this method is based on wind speed as opposed to the buoyancy forces and

therefore depends largely on external climatic conditions, façade orientation as well as the relative positions of the surrounding buildings (Larsen, et al., 2015).

Changes in the façade configuration can also have a profound effect on the thermal behaviour. Simulations of a DSF in Hong Kong have shown that a configuration which uses double reflective glazing as the external skin and single glazing on the internal skin can reduce cooling loads by 26%. However, the large payback period which was estimated at 81 years resulted in the design being economically unfeasible for the Hong Kong climate conditions (Chan, et al., 2009).

Photo-voltaic (PV) integrated DSF also offer a possible solution to decrease not only the cooling load but overall energy consumption of an office building. The shading effect of opaque PV panels reduces the overheating issue observed in the cavity during summers. Further, by using translucent PV panels a balance can be achieved between daylight entry, shading and heat gain. A right combination of these factors could play a vital role in achieving zero energy buildings as well. In particular, the use of semi-transparent PVs (transmittance 70%), allows reaching the nearly zero energy goal for an indoor space area up to 27 m2 (Ioannidis, et al., 2017). The ventilation in the façade cavity can help cool the PV panels which may increase their efficiency (Peng, et al., 2016). However, the effect of temperature on the efficiency of the PV panels is negligible. The combination is still effective to produce energy as well as decrease cooling demand in subtropical climates (Han, et al., 2013).

The complex behaviour of the DSF due to different configurations, design strategies, ventilation schemes, etc, coupled with the high investment cost dictate the need for a simulation platform which can be used to predict the possible energy saving and indoor thermal comfort levels when a DSF is employed at a particular site. And even if these initial assessments show positive results, there are still multiple issues pertaining to acoustic behaviour, moisture condensation and fire safety to be considered (Ghaffarianhoseini, et al., 2016). From an economic standpoint, unless designed and operated correctly, the DSF can result in a very high payback period which could turn investors away.

2.2 Modelling and Simulation

Many different modelling techniques have been developed to simulate the thermal behaviour of a DSF. A brief overview of a few are presented as follows:

2.2.1 Analytical or Lumped Models

This modelling approach is one of the simplest approaches. Each component of the façade, external glazing, cavity and inner envelope is represented as a single node accounting for all the properties of the component (Zhou & Chen, 2010). Such a model can provide specific information at the design stage as well as facilitate the development of the optimal control strategy. Due to the simplified approach of such models, many hypotheses must be assumed (Gracia, et al., 2013). These models cannot be used to estimate natural ventilation within the cavity due to a lack of discretization.

2.2.2 CFD Models

CFD or Computational Fluid Dynamic Models are among the most accurate simulation methods available. The entire façade is divided and subdivided into many discretised units. These are used to create a very detailed nodal mesh of the entire system. The system can be solved for the conservation of mass, energy and momentum between the nodes to obtain a very detailed distribution of temperature, velocity and pressure as well as convective heat transfer coefficients (Zhou & Chen, 2010). Further, the extremely detail capabilities of this method allows the simulation of complex geometries such as those of the venetian blinds present in the cavity (Gracia, et al., 2013). However, due to the very detailed analysis and the large number of equations and relations to be solved, this method is very time consuming and requires large computing power. The high level of detail also makes the models extremely dependant on the assumption and the accuracy of the input data. Such accurate input data may not be available at the early design stages of a project and hence this method often cannot be used in such situations to assess the design (Zanghirella, et al., 2011) (Elarga, et al., 2015).

2.2.3 Zone Approach

The zone approach can be described as an intermediate between lumped and CFD models. The discretised units in this method are much larger than those used in CFD models. Each unit or volume is represented by a node to which all the properties of the volume are attributed (Zanghirella, et al., 2011). A two- or one-dimension network of these nodes is solved using energy and mass conservation equations. For simplicity, this method often makes use of empirical methods to estimate convective heat transfer coefficients (Zhou & Chen, 2010). Due to fewer and less complex equations to be solved this method is much faster to use than the CFD approach and at the same time is much more accurate in its results of air flow and temperature distribution as compared with the lumped model approach (Gracia, et al., 2013). Often studies have found deviation in this model from the more accurate CFD models (Elarga, et al., 2015) and site measurements (Wang, et al., 2016). These deviations usually occur at high solar loads and are attributed to either the thermal storage in the system or the simplified convective and radiative heat transfer coefficients.

2.3 Design Parameters

This section presents the available literature on the different design parameters of a DSF and how these influence the thermal behaviour. This sheds light on which parameter can be considered in more detail for achieving the desired thermal performance as well as reducing the overheating in the cavity.

2.3.1 Ventilation Scheme

Existing studies have shown that a static air buffer is optimal in winter because it acts as a thermal buffer whereas in summer it is recommended to utilize an external air curtain configuration to remove the heat generated in the cavity due to high solar loads. However, in evenings if the external temperature drops

below the required indoor temperature natural ventilation can be employed to cool the building (Hong, et al., 2013). The research of Yellamraju reiterates the point of a static buffer during winters while an externally ventilated cavity in summers for hot climates (Yellamraju, 2014).

The importance of nighttime ventilation has been highlighted in multiple studies to decrease the cooling loads during summers (Hong, et al., 2013) (Hashemi, et al., 2010). It is important to note however that natural ventilation and/or night-time ventilation may not be suitable in all summer scenarios, especially if it allows hotter external air into the interiors (Yellamraju, 2014).

2.3.2 Orientation and Window to Wall Ratio (WWR)

The WWR needs to be optimized based on orientation (Peng, et al., 2016). This can be attributed to the importance of wind and solar radiation because these are the two main determinants as a natural stimulus of thermal and airflow behaviour (Stec & Paassen, 2005). The solar heat gain coefficients are significantly more in East and West facing facades as compared to North or South facing facades. A Significant decrease in WWR up to 0.3 shows an appreciable decrease in solar heat gains, with a WWR of 0.9 having a diminished potential to decrease solar heat gains (Chou, et al., 2009).

2.3.3 Glazing Properties

Glazing properties have an appreciable effect on the thermal loads, with an appropriate selection of glazing types possibly reducing the thermal loads by almost an order of magnitude (Perez-Grande, et al., 2005). A larger temperature difference between the interior and exterior leads to a higher benefit from the insulating properties of the façade (Mingotti, et al., 2013).

For Double skin facades with single glazing on the exterior envelope and double glazing on the interior envelope, it was found that the largest impact on energy consumption with respect to the glazing properties was for variations in the external glazing light of the inner envelope. While the inner glazing light of the internal envelope had the least impact (Joe, et al., 2014).

2.3.4 Cavity Dimensions and Opening Size

Most studies that have considered a variety of cavity depths have determined that it has a negligible effect on the thermal performance of a DSF (Pappas & Zhai, 2008). There is however some evidence to suggest that a cavity, if too narrow, may perform poorly due to restricted airflow (Rajesh & D.G.M.Purohit, 2014). Cavity height affects the performance due to the generated stack effect and buoyancy-driven forces which are more profound at greater heights. Taller cavities produce stronger buoyancy forces, resulting in greater airflow (Pappas & Zhai, 2008). Further, it has been seen that a multi-story DSF could save 5% more energy than a corridor type DSF in the Mediterranean climate (Torres, et al., 2007).

Opening size has a predominant effect on decreasing cooling loads (Torres, et al., 2007). CFD simulations of DSF for climate of Shanghai in China have found that with an increase in opening width there is a

significant decrease in the heat gain of the cavity, this effect has been attributed to the natural ventilation in the cavity which is enhanced by increasing the opening width up to 0.1m, after which there is no significant benefit (Su, et al., 2017). It is important to note that the design of the cavity width, height and opening size are all interdependent and must be optimized based on the climate for the region. For instance, a large multi-story DSF would need large openings but could benefit from a narrower cavity to reduce the overall volumetric flow rate of air required for adequate ventilation for cooling. Alternatively, a smaller opening would benefit a DSF in decreasing heating loads as it will increase the thermal air buffer (Torres, et al., 2007).

2.3.5 Thermal mass & Shading device

Shading device is an important aspect of the DSF for controlling solar gains. The shading absorbs and re-radiates short wave radiation which does not pass through the inner glazing, thus reducing the solar gains of the room. Further, a combination of opaque materials and glazing is recommended for hot climates to control solar loads (Yellamraju, 2014). Nonetheless, the shading device can reach significantly high temperatures which can not only result in higher cavity air temperatures but also higher temperature on the inner envelope (Stec & Paassen, 2005), thus affecting the thermal comfort of occupants.

Thermal mass can help reduce the cavity temperature by absorbing solar heat and releasing it slowly with time. By doing so, it reduces the amount of heat that needs to be exhausted at peak solar load durations in the cavity. Integration of thermal mass into a DSF has shown a saving of 21-26% in summers and 41-59% in winters (Fallahi, et al., 2010).

2.4 Summary

Double skin façades are a proven design for lowering overall energy demand in heating and cooling, but this is often attributed to energy reductions in heating only while cooling loads increase due to the thermally insulating behaviour of the façade. This can be prevented firstly, by providing adequate ventilation in the cavity for the extraction of heat through the façade. Secondly, the cooling effect can be enhanced using nighttime ventilation. And lastly, integration of the DSF with the HVAC system of a building can increase the operating efficiency of the HVAC system, thus reducing energy consumption for indoor climate control.

The high cost of DSFs is a deterring factor for investors, therefore there is a need for an accurate method to predict the behaviour and performance of a DSF. The zonal approach offers one such method. It is relatively faster than a detailed CFD analysis but can still provide accurate data for energy use and allows for the simulation of air flow which is key to predicting the combined effect of the DSF and HVAC system along with the effects of nighttime cooling/ventilation.

There is a lack of information regarding the use of DSFs in warmer climate zones, as is the case in many of the climate zones in India. Most studies present are usually carried out in regions with milder

temperature and humidity variations. However, studies show that a DSF can perform better than traditional single or double glazing in warmer climates as well, but issues of overheating and internal condensation need to be evaluated for the same. A proper design considering the local climatic conditions in relation to the design parameters such as ventilation in the cavity, opening sizes, cavity dimensions, shading, glazing selection and possibly applying thermal mass can yield a DSF with a significant potential for reducing cooling loads in summer conditions.

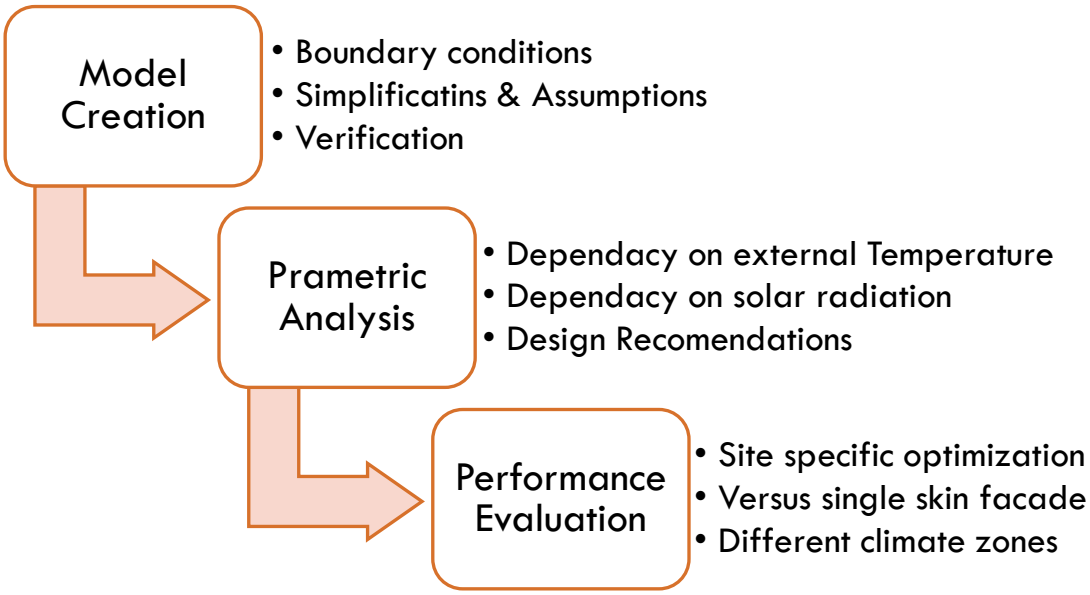

Figure 3.1: Flow chart of progression from model creation to evaluation and applicability of the DSF

3. Methodology

The main objective of this research revolves around simulating the thermal behaviour of a DSF. This is done via the MATLAB/Simulink platform because of its versatility in solving dynamic environments. Before being applied, the model must be verified to check the validity of the working principles and underlying assumptions. For this purpose, the MATLAB/Simulink model is verified against a model with similar working boundaries in Design Builder *(Ch. 4)*. Once verified, an in-depth thermal behavioural analysis for the influence of different design parameters on heat flows and temperature distributions within the DSF is done *(Ch. 5)*. The findings from the behavioural analysis are subsequently used to present optimized configurations of the DSF at different sites. These optimized configurations are weighed against a single skin fully glazed façade based on various performance markers such as annual heat gain to assess the advantages of implementing a DSF when compared to the conventional single skin. And finally, an intercomparison of the effectiveness of the DSF at different sites is made to better present the dependency of the DSF on site climatic conditions and spatial orientation *(Ch. 6)*.

3.1 Introduction to the Numerical Model

For the purpose of modelling the façade, the zonal approach is used. This entails discretization of the system into multiple "zones" each represented by a node containing all the properties and associated mass and volume of the designated zone. Using the heat balance equations for all the nodes, a system of differential equations is obtained which is solved in Simulink to generate the temperatures of all the nodes. The simulations are run using hourly weather data and hence the temperature of each node can be obtained for every hour in the year.

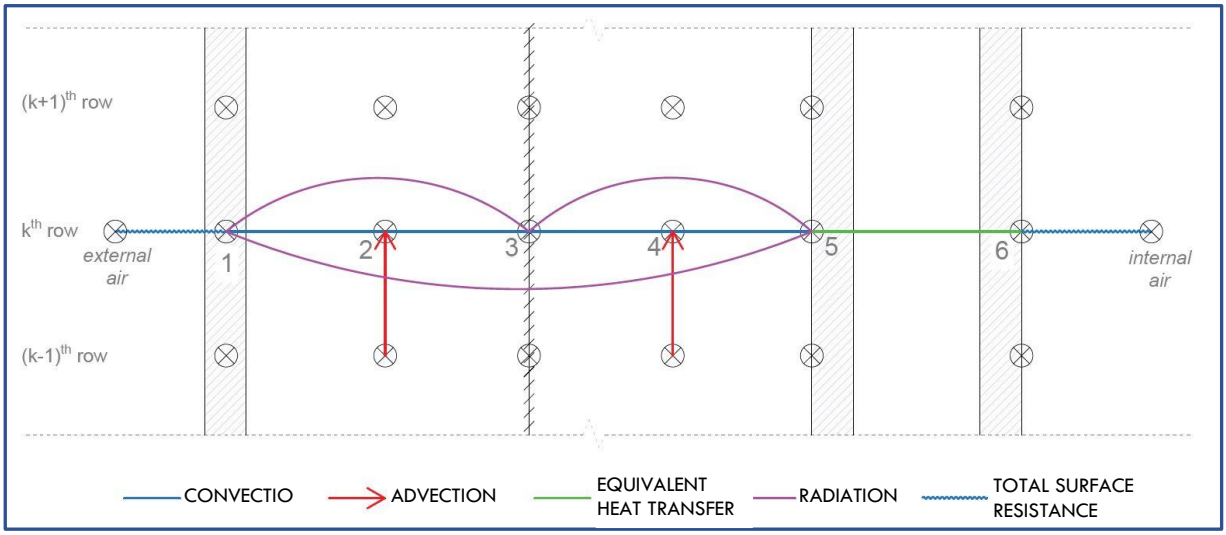

Figure 3.2: Nodal Diagram showing all the heat transfer mechanisms present between the different nodes. ***NOTE 1:*** *The solar radiation components are not shown in this diagram.* ***NOTE 2:*** *The bottom most row, i.e. row number 1 will have advective components linked to external air.*

The system of equations used can be represented as follows in matrix format (van der Spoel, 2017):

$$[M]_{K,K} * [T']_{K,1} + [S]_{K,K} * [T]_{K,1} = [Q]_{K,1}$$

Where *M* represents the mass matrix containing the thermal mass of each node, *T'* represents the rate of temperature change with respect to time, i.e., the first derivative of temperature with respect to time. *S* is the stiffness matrix which consists of all the thermal coupling coefficients among the nodes, *T* is the temperature at each node and Q is the heat gain within a node. *K* is the total number of nodes in the system including nodes with known temperatures such as the node representing the external air. In the given system, the i^{th} row represents the equation pertaining to node number "i" as portrayed in Appendix A. The mass matrix is a diagonal matrix with the thermal mass along the diagonal while the stiffness matrix is configured to contain the coupling coeffects from the heat balance equation at node "i" to node "j" in element (i,j).

$$\begin{bmatrix} M_1 & & 0 \\ & M_2 & \\ 0 & & M_K \end{bmatrix} \begin{bmatrix} T'_1 \\ T'_2 \\ \vdots \\ T'_{K-1} \\ T'_K \end{bmatrix} + \begin{bmatrix} S_{1,1} & S_{1,2} & \cdots & \\ S_{1,1} & S_{2,2} & & \\ \vdots & & \ddots & S_{K-1,K} \\ & & S_{K,K-1} & S_{K,K} \end{bmatrix} \begin{bmatrix} T_1 \\ T_2 \\ \vdots \\ T_{K-1} \\ T_K \end{bmatrix} = \begin{bmatrix} Q_1 \\ Q_2 \\ \vdots \\ Q_{K-1} \\ Q_K \end{bmatrix}$$

Given that some of the nodes have known temperatures, such as the node representing external air, all the rows representing these nodal equations may be eliminated. Further, the coupling coefficients from the *S* matrix pertaining to the connections to the known temperature nodes, i.e. columns containing coupling coefficients to the known nodes, can be moved to the right-hand side of the equation. This results in:

$$[M]_{K',K'} * [T']_{K',1} + [S]_{K',K'} * [T]_{K',1} = [Q]_{K',1} - [Sb]_{K',K'} * [Tb]_{K',1}$$

Where *Sb* and *Tb* represent the coupling coefficients and temperatures respectively of the known (or bound) nodes and *K'* is the number of nodes with unknown temperatures.

In Simulink, the above differential equation can be solved for *T'* given the initially assumed temperature of all nodes at time t=0 as follows.

$$[T']_{K',1} = [M]_{K',K'}{}^{-1} * \int \{[Q]_{K',1} - [Sb]_{K',K'} * [Tb]_{K',1} - [S]_{K',K'} * [T]_{K',1}\}$$

The discretization of the system has been programmed such that the number of rows into which the system is discretised may be varied as this can affect the accuracy of the temperatures calculated and the time taken by the solver.

The nodes have been set in each row as follows:

Table 3.1: Node Descriptions, *refer Fig. 3.2*

Node No.	Description
1	The single glazing of the outer envelope, located at the centre of the glazing
2	The air cavity between the external envelope and the blind system, located at the centre of the cavity
3	The blind system, located at the centre of the blind
4	The air cavity between the internal envelope and the blind system, located at the centre of the cavity
5	The outer glazing light of the double glazing of the internal envelope, located at the surface towards the cavity
6	The inner glazing light of the double glazing of the internal envelope, located at the surface towards the interior room

It is important to note that the overall node number of a node with respect to the entire system i.e. the node number "i" as used in the numerical modelling set up in MATLAB/Simulink is from bottom to top, left to right *(ref. Appendix A)*.

For simplification of the thermal system the following assumptions have been made:

1. Heat transfer within the DSF is only in the horizontal direction, except for the advective flow within the cavity.
2. Conduction within the glazings and the blind is neglected.

3. The convective heat transfer coefficient is assumed as constant for interfaces, i.e. does not vary with time, temperature or air velocity of the concerned nodes.
4. Radiation view factors are calculated using the factitious cavity method as done in previous research work (Jiru & Haghighat, 2008) (Park, 2003).
5. Emissivities of all surfaces are close to one, therefore reflections in longwave radiation are neglected
6. Internal room temperatures are assumed to be constant throughout the day. Only monthly changes are used based on the Indian Model for Adaptive (Thermal) Comfort (IMAC) (Manu, et al., 2014). The IMAC prescribes indoor temperature ranges for adequate thermal comfort in various Cities located throughout India.

3.2 Heat Transfer Mechanisms

Multiple forms of heat transfer have been integrated into the model design to best predict the behaviour of the DSF. These can be classified as follows.

3.2.1 Convection

Heat transfer involving motion in a fluid and its interaction with a surface, in this case, air and the various DSF components, falls under this category. When the motion of the fluid is instigated due to a difference in densities and the action of gravity, it is referred to as natural or free convection. On the other hand, when the motion of the fluid is driven due to external actions such as mechanical ventilation it is referred to as forced convection. Heat transfer coefficients associated with gases for natural convection are generally much lower than those for forced convection, and it is therefore important not to ignore radiation in calculating the total heat loss or gain when natural convection is present (ASHRAE, 2013).

In building modelling, external and internal exposures are often differentiated. In the former case, convection is usually wind induced and considered as forced whereas, with internal surfaces, natural and/or forced air movement can occur depending on the location of mechanical equipment and the flow field to result (Clarke, 2001).

For forced or natural convections many modelling attempts have previously used empirical formulae involving dimensionless numbers such as Reynold's number *(Re)*, Prandtl number *(Pr)*, Rayleigh's number *(Ra)*, Grashof number *(Gr)*, and the Nusselt number *(Nu)*. The Nusselt number is finally used to evaluate the convective heat transfer coefficient using the following formula.

$$h_{conv} = \frac{Nu * k_a}{l_{ch}}$$

Where h_{conv} is the convective heat transfer coefficient, k_a is the thermal conductivity of the fluid and l_{ch} is the characteristic length (Elarga, et al., 2015) (Zanghirella, et al., 2011) (Jiru & Haghighat, 2008). The relations used were derived from those for the fluid properties in ducts, flat plates and narrow cavities.

It is also possible to calculate the total heat transfer within a cavity by assuming an equivalent conductivity based on the radiation and convective heat transfer (ISO-15099, 2003). This method also involved the use of empirical formulae and dimensionless numbers.

A distinction can be made between the natural, forced or mixed convection, applying different formulae based on the conditions that prevail, such as the McAdam's formula for forced convection as provided in the ASHRAE handbook. Further distinctions can be made based on the behaviour of the blinds which are, in terms of airflow, more complex than the boundaries of the glazing lights of the DSF. The convective heat transfer coefficient for the blinds can be estimated as a function of the temperature of the blinds and the cavity air (Wang, et al., 2016) or by analysing the mixed convection that takes place along its boundaries, which gives a heat transfer coefficient approximately twice as large as that for the glazing surfaces (Jiru & Haghighat, 2008).

Looking at the values for the convective heat transfer coefficient taken in different models and the recommendations provided in international standards it was chosen to use 2.2 W/m^2K for the glazing surfaces within the cavity and 4 W/m^2K for the venetian blind. Similar values have been previously used in zonal models with a value of 2.2 W/m^2K, 1.5 W/m^2K and 4.4 W/m^2K being employed for the convective heat transfer coefficient for the external envelope, internal envelope and venetian blind within the DSF cavity respectively (Jiru & Haghighat, 2008).

For the outer- and innermost surfaces of the façade, i.e. with the external air and inside the room, 17.7 W/m^2K and 1.7 W/m^2K were chosen respectively. In previous cases for external convection due to wind, the McAdams formula has been used (Ong, 2003) which is based on the wind speed. The internal convection coefficient for the room can be calculated using the Grashof and Prandtl numbers for the natural convection along a flat surface *(ref. Appendix B)*.

All the coefficients are treated as constants. However, it is important to note that the coefficients will change with time, based on temperature and air velocities in a real scenario. Hence, a sensitivity analysis shall be used to assess the magnitude of change associated with the value of the convective heat transfer coefficients at various surfaces.

Knowing the convective heat transfer coefficient, the heat flux between two nodes can be calculated as:

$$Q_{conv} = h_{conv} * Ar * \Delta T$$

Where Q_{conv} is the total convective heat flux to or from a node, *Ar* is the designated area for the node and ΔT is the temperature difference between the two respective nodes (van Paassen, 2004).

3.2.2 Radiation

Radiation heat transfer occurs due to the energy transported in the form of electromagnetic waves with a wavelength between 0.1 mm and 1000 mm. This includes the short wave (solar radiation), which has a wavelength between 0.3 mm and 2.5 mm; and the long wave (emitted by surfaces at terrestrial temperatures) which have wavelengths between 5 mm and 50 mm (Jiru & Haghighat, 2008).

Long Wave Radiation:

Inter-surface longwave radiation is a function of the prevailing surface temperatures, the surface emissivities, the extent to which the surfaces are in visual contact, referred to as the view factor, and the nature of the surface reflection (diffuse, specular or mixed) (Clarke, 2001). Two objects or surfaces at different temperatures will both emit, absorb and reflect heat radiation to and from one another. On balance, heat will flow from the entity at a higher temperature to the one at a lower temperature (Linden, et al., 2013). The rate and characteristic of radiation emitted from a surface depend only on the material characteristics and absolute temperature of the surface. It is independent of the properties and orientation of the surrounding surfaces. However, the amount of radiation incident on a surface depends on the temperature of the surrounding surfaces as well as their spatial orientations (ASHRAE, 2013). In case reflectance is accounted for, which in the case of this study is neglected, the radiation emitted from a surface can also contribute to the incident radiation on the same surface.

The total radiative heat flux from the i^{th} to the j^{th} surface (or node) can be calculated as follows.

$$Q_{rad} = Ar * \alpha_r * F_{ij} * (T_i - T_j)$$

Where Q_{rad} is the total heat flux due to longwave radiation, Ar is the designated area for the nodes, α_r is the radiation heat transfer coefficient, T_i and T_j are the respective temperatures and F_{ij} is the view factor from the i^{th} to the j^{th} surface (van Paassen, 2004). As reflections are neglected in this case, emissivities of the materials are assumed close to one. This assumption is valid for most non-metallic materials such as the glass in the glazing units and painted or coated metallic surfaces such as the venetian blind system.

In normal building practice, the value of α_r is often between 4.7 and 5.2 W/m^2K (Linden, et al., 2013). This approximation may be wrong in principle and hence the value taken will be further used for a sensitivity analysis to judge the magnitude of change induced due to changes in the radiation coefficient. Ideally speaking, the radiation heat transfer coefficient for two surfaces depends on the temperatures (T_1 and T_2) and emissivity (ε_1 and ε_2) as given in the following equation (Ong, 2003)

$$\alpha_r = \sigma * \frac{({T_1}^2 + {T_2}^2) * (T_1 + T_2)}{(1/\varepsilon_1) + (1/\varepsilon_2) - 1}$$

Where σ is the Stephan-Boltzmann constant. Substituting room temperature (≈22°C) and emissivities close to 1 (≈0.95) we arrive at a heat transfer coefficient of roughly 5 W/m^2K which has been used in the numerical model *(ref. Appendix B)*.

The view factors from the i^{th} to the j^{th} node *(ref. Fig. 3.2)*, F_{ij} were calculated based on the fictitious cavity method *(ref. Appendix C)* using the following formulae as has been done in previous modelling attempts (Jiru & Haghighat, 2008).

$$F_{13} = 2 - \sin\left(\frac{90 - \phi}{2}\right) - \sin\left(\frac{90 + \phi}{2}\right)$$

$$F_{35} = F_{13}$$

$$F_{15} = \sqrt{2} * \cos\left(\frac{\phi}{2}\right) - 1$$

Where ϕ is the horizontal angle of the slats in the venetian blinds. This angle was set to 0° for the blinds in the off condition and 45° for when the blinds are active.

Solar Radiation:

In the case of completely transparent structures, the shortwave energy impinging on the outermost surface is partially reflected and partially transmitted. Within the glazing layers and substrates of the system, many further reflections take place and some portion of the energy is absorbed within the material to raise its temperature. This temperature rise will augment the normal transient conduction process and, thereby, help to establish inner side and outer side surface temperatures which, in turn, will drive the surface convection and longwave radiation flow paths. Thus, in effect, absorbed shortwave radiation penetrates the building via convection and longwave radiation (Clarke, 2001).

For solar radiation incident on a glazing surface, the transmittance (τ), reflectance (ρ) and absorptance (α) of the glazing layer contain the effects of multiple reflections between the two interfaces of the layer as well as the effect of the absorption during the passage of the radiation through the layer. The said properties of τ, ρ and α of a layer are formally defined as the fractions of the incident solar radiation that are transmitted, reflected and absorbed by the layer respectively. The sum of these quantities being unity, i.e.,

$$\tau + \rho + \alpha = 1$$

The variation in these properties is small for an angle of incidence less than 40° but becomes significant for larger angles (ASHRAE, 2013).

The solar radiation has often been divided among three components, direct, diffuse and once reflected (from the base of the façade). The latter refers to the component of radiation falling on the floor of the DSF which is reflected upwards to the respective components such as the shading device and the inner envelope. Normally, the top and bottom surfaces of the DSF cavity are not made of reflective materials, hence 90% of the solar energy is absorbed after being reflected twice or more by the ceiling or base of the cavity, making the intensity an order of magnitude less than the incident radiation and thus, can be ignored. The diffuse radiation is received by the whole glazing or shading component equally while the direct and once reflected components depend on the solar altitude and the shading effect of the DSF configurations (Xue & Li, 2015).

The required dimensions as shown in *Fig. 3.3* can be calculated for the shading system and inner glazings based on the effective depth, *D* and the solar altitude, *A'* as follows,

$$H_{dir} = \begin{cases} H - D * tanA' & ; \quad D * tanA' < H \\ 0 & ; \quad D * tanA' \geq H \end{cases}$$

$$H_{re} = \begin{cases} D * tanA' & ; \quad D * tanA' < H \\ 2 * H - D * tanA' & ; \quad H \leq D * tanA' < 2 * H \\ 0 & ; \quad D * tanA' \geq 2 * H \end{cases}$$

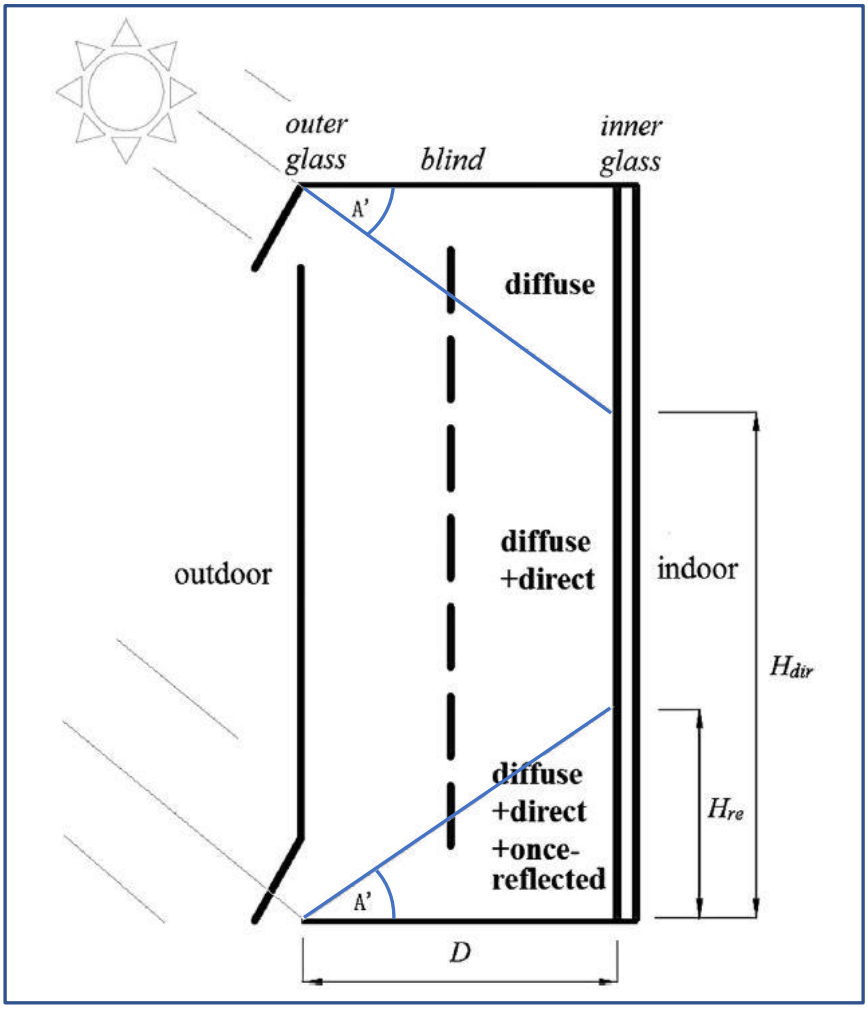

Figure 3.3: Short wave radiation received by inner glazing unit. Sections of the façade components that receive diffuse, direct + diffuse and direct + diffuse + once reflected components of the solar radiation.
***ADAPTED*:** (Xue & Li, 2015)

Where *H* is the total height of the cavity (Xue & Li, 2015). These formulae can be used in the same manner for all components by adjusting the effective depth as shown in *Appendix A*.

A similar method has also been employed in previous research (Su, et al., 2017) (Xue & Li, 2015), however, the absorptance of the glazing surfaces was treated as constant due to angle of incidences less than 60° (Jiru & Haghighat, 2008). This assumption cannot be made for the sun altitudes found in India where it can be almost perpendicular to the horizontal. Hence, the optical properties of the glazings are evaluated based on the sun altitudes at each time step.

The incident radiation intensities of the three sections in the facade mentioned above can be calculated by solar diffuse radiation, solar direct radiation, solar altitude and the optical properties of each surface. The shading coefficient of the blind can be treated as a constant value based on the respective case of

the blinds being active or inactive. The respective values of the transmittance and absorptance of the glazings are evaluated at each time step based on the glazing properties and the solar altitude.

$$Q_{diff,i} = Q_{diff} * (\tau_{i-1} * \tau_{i-2} * \dots) = Q_{diff} * RF_{diff,i}$$

$$Q_{dir,i} = Q_{dir} * (\tau_{i-1} * \tau_{i-2} * \dots) = Q_{dir} * RF_{dir,i}$$

$$Q_{re,i} = Q_{dir} * \rho_s * (\tau_{i-1} * \tau_{i-2} * \dots) = Q_{dir} * RF_{dir,i} * \rho_s$$

Where $Q_{diff,i}$, $Q_{dir,i}$ *and* $Q_{re,i}$ are the diffuse, direct and once reflected components of radiation on the i^{th} node. Q_{diff} and Q_{dir} are the intensities of radiation on the outer glazing and τ_i is the transmittance for all the i^{th} glazing layers or shading coefficient for the blind system. Lastly, ρ_s is the average reflectivity of the façade base. The reduction factor, RF_i, is the fraction of incident radiation on the external envelope that is incident on an inner i^{th} component *(ref. Appendix D & Fig. 3.4)*.

To evaluate the transmittance (τ) and absorptance (α) of the glazing layers the WINDOW *7.7* application by Berkeley Labs was used. The values for the τ and α for direct incident radiation were calculated for angle of incidences at 10◦ intervals between 0◦ and 90◦. Further, linear interpolation was used to arrive at the required value of the property for the actual solar altitude at each time step in the Simulink model. The same properties were also evaluated for diffuse solar radiation, which is independent of the angle of incidence as presented in the WINDOW *7.7* application, hence a single constant value could be used for every time step *(ref. Appendix E)*.

Lastly, the shading coefficient and the absorptance of the shading device were calculated, this too was done using the WINDOW *7.7* application for both cases of the blinds on as well as off. This was accomplished by simulating the behaviour of a venetian blind at 0◦ and *45*◦ slat angles. The respective properties of the blinds were treated as constant, independent of the angle of incidence and hence do not vary with time.

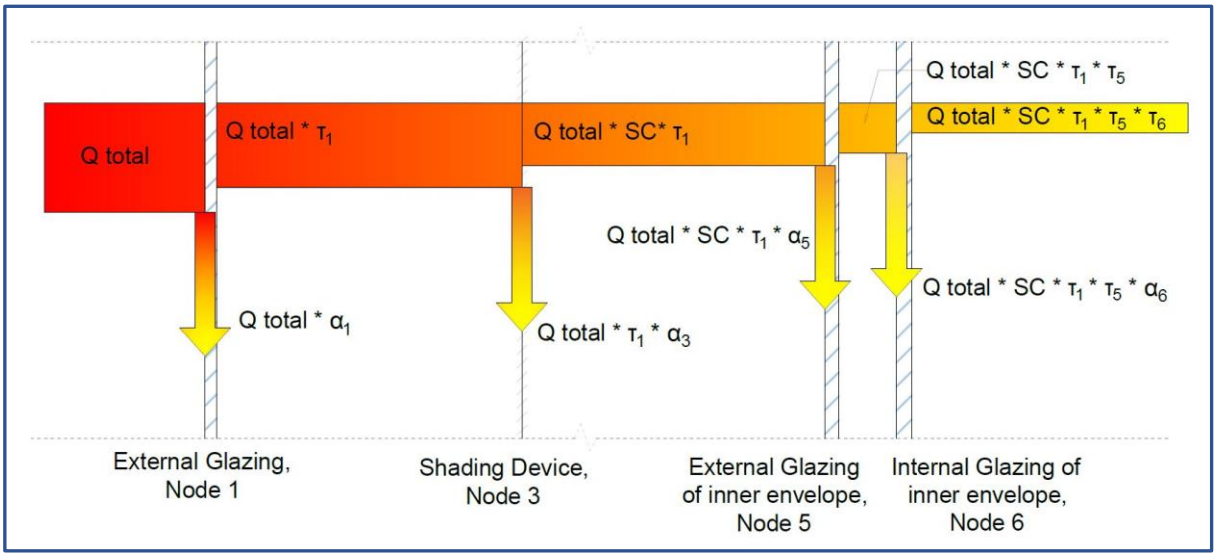

Figure 3.4: Solar load absorptance and transmittance at different components in the DSF

Knowing the required optical properties of the glazing units and shading device, the following equations were used to calculate the total solar heat gain, Qze for the i^{th} node.

$$Qze = \begin{cases} Ar * SC_i * \left(Q_{diff} * RF_{diff,i} * \alpha_{diff,i}\right) & ; CASE\ 1 \\ Ar * SC_i * \left(Q_{diff} * RF_{diff,i} * \alpha_{diff,i} + Q_{dir} * RF_{dir,i} * \alpha_{dir,i}\right) & ; CASE\ 2 \\ Ar * SC_i * \left(Q_{diff} * RF_{diff,i} * \alpha_{diff,i} + Q_{dir} * RF_{dir,i} * \alpha_{dir,i} * (1 - \rho_s)\right) & ; CASE\ 3 \end{cases}$$

CASE 1,2 and 3 respectively refer to the *diffused only*, *diffused + direct* and *diffuse + direct + once reflected* modes of incident solar radiations. The application of these cases is based on the height of the node in the façade system as has been explained previously (*ref. Fig. 3.3*).

SC_i is the applicable shading coefficient (=1 for external glazing and shading device, variable based on shading configuration for inner envelope components), $\alpha_{diff,i}$ and $\alpha_{dir,i}$ are the absorptance of the i^{th} layer for diffuse and direct radiation respectively, RF_i is the reduction factor for the incident direct or diffused radiation and ρ_s is the base reflection. The base reflection has been set for the reflectivity of common terracotta floor tiles i.e. 0.28.

3.2.3 Equivalent Resistances

Equivalent resistances have been used to simplify the behaviour of the façade. These have been made for the total surface resistance and the thermal transmittance (U-value) of the double-glazing unit.

Surface Resistance:

The total surface resistance can be calculated as a function of the convective and radiative heat transfer coefficients from a surface. The convective coefficient depends on the wind/air speed while the radiative coefficient depends on material properties and surface temperature as explained in the previous sections. The total resistance has been calculated as follows.

$$r = \frac{1}{\alpha_{conv} + \alpha_{rad}}$$

Where r is the total surface resistance, α_{conv} is the convective coefficient and α_{rad} is the radiation coefficient. In keeping with respective values for the heat transfer coefficients from the previous sections, the total surface resistance for the internal (towards the room) and external (towards outside air) surfaces of the façade were calculated.

U-value of Double-Glazing Unit:

The U-value of the double-glazing unit was calculated using the WINDOW 7.7 application. The software contains a large database of glazing options which one can use to create custom glazing units and calculate the respective properties which have been implemented in the modelling process. The calculated U-value from WINDOW 7.7 was then adjusted to compensate for the surface resistances that are included as separate components.

$$U_{adj} = \frac{1}{\frac{1}{U_{glz}} - r_{cavity} - r_{room}}$$

Where U_{adj} is the adjusted resistance between the two surfaces of the double glazing, U_{glz} is the actual U-value of the glazing unit which already includes the surface resistance, r_{cavity} is the surface resistance towards the cavity air while r_{room} is the surface resistance towards the air in the room.

3.2.4 Advection

The advective heat transfer component accounts for the heat transferred within the air cavity due to the movement of air. This component may be equal to zero if no ventilation is present and can otherwise be calculated as a function of the mass flow rate (χ), the thermal heat capacity of air (C_p) and temperature difference. This component of heat transfer is applied in the vertical direction at nodes 2 and 4, which represent the air within the cavity *(ref. Fig. 3.2)*. Hence, it is applied between the respective air nodes of the k^{th} row with those at the $(k-1)^{th}$ row in the discretization.

It is assumed that air movement is only in the upward direction while the mechanical ventilation is on. If no mechanical ventilation is applied, the cavity openings are sealed and hence there is no significant air movement, making this component of heat transfer negligible, or zero.

The heat flux, Q_{adv}, through advection can be calculated as follows.

$$Q_{adv} = vf * \rho_{air} * C_{p,air} * \Delta T$$

Where vf is the volumetric flow rate, ρ_{air} is the density of air and $C_{p,air}$ is the specific heat of air (van Paassen, 2004). The mass flow rate, χ, can be computed based on the volumetric flow rate as follows,

$$\chi = vf * \rho_{air}$$

Which gives,

$$Q_{adv} = \chi * C_{p,air} * \Delta T$$

3.3 Nodal Heat Balance

Given the above assumptions, nodal connections and heat transfer coefficients, the following nodal equations are derived based on the nodal diagram *(ref. Fig. 3.2)*:

Node 1:

$$Ar * \left(\frac{1}{r_{ext}}\right) * (T_1 - T_{ext}) + Ar * \alpha_{c,IC} * (T_1 - T_2) + Ar * \alpha_r * F_{13} * (T_1 - T_3) + Ar * \alpha_r * F_{15} * (T_1 - T_5) = Q_1$$

Node 2:

$$Ar * \alpha_{c,IC} * (T_2 - T_1) + Ar * \alpha_{c,BL} * (T_2 - T_3) + c_{air} * \chi * (T_{2,k} - T_{2,k-1}) = 0$$

Node 3:

$$Ar * \alpha_{c,BL} * (T_3 - T_2) + Ar * \alpha_{c,BL} * (T_3 - T_4) + Ar * \alpha_r * F_{31} * (T_3 - T_1) + Ar * \alpha_r * F_{35} * (T_3 - T_5) = Q_3$$

Node 4:

$$Ar * \alpha_{c,IC} * (T_4 - T_5) + Ar * \alpha_{c,BL} * (T_4 - T_3) + c_{air} * \chi * (T_{4,k} - T_{4,k-1}) = 0$$

Node 5:

$$Ar * \alpha_{c,IC} * (T_5 - T_4) + Ar * \alpha_r * F_{53} * (T_5 - T_3) + Ar * \alpha_r * F_{51} * (T_5 - T_1) + Ar * U_{adj} * (T_5 - T_6) = Q_5$$

Node 6:

$$Ar * \left(\frac{1}{r_{int}}\right) * (T_6 - T_{int}) + Ar * U_{adj} * (T_6 - T_5) = Q_6$$

Note: The view factors indicated here for radiative interactions between Node 1, 3 and 5 will change based on the slat angle of the venetian blind *(ref. Sec. 3.1.2, Longwave Radiation)*.

Nomenclature:

Ar	*designated horizontal area per node, function of "K"*
$\alpha_{(c,IC)}$	*convective coefficient for glazing surfaces and air*
$\alpha_{(c,BL)}$	*convective coefficient for venetian blind and air*
α_r	*radiative transfer coefficient*
F_{ij}	*view factor from node i to j*
r_{ext}	*total surface resistance to external environment*
r_{int}	*total surface resistance to internal environment*
c_{air}	*specific heat capacity of air*
χ	*mass flow rate of air within the cavity*
U_{adj}	*Adjusted U-value of the inner double-glazed envelope*
T_i	*temperature of i^{th} node*
$T_{i,k}$	*temperature of the i^{th} node in the k^{th} row*
Q_i	*total solar heat gain on the i^{th} node*

3.4 Control Scheme

The thermal behaviour of the DSF can be primarily altered through two mechanisms, the blind control and the ventilation control. The control systems make use of set points to change from one state to another.

3.4.1 Shading Control

The model simulates a venetian blind system in which the blinds are off at slat angle of 0° and on at 45°. The slat angle is set to the required angle based on the total incident solar radiation on the outer glazing unit. This condition is implemented in Simulink through an *if block*. Two separate stiffness (S) and internal heat gain (Q) matrices are created for the different slat angles. The respective view factors are applied in the two different *S* matrices while the respective shading coefficients are applied in the two different Q matrices. If the solar load is greater than equal to 250W/m^2 the blinds on condition is used. Otherwise, the condition of blinds off is used.

3.4.2 Ventilation Control

The control for the ventilation affects the advective component of heat transfer. Only mechanical ventilation is applied within the cavity, i.e. natural ventilation is not applicable. If the outside temperature is lower than a set point (default of 15°C), and the shading device is enabled (solar radiation greater than 250 W/m^{2}K by default) the ventilation in the cavity is switched on.

This condition is applied in Simulink through an if block. By default, the ventilation is on, but if it must be off the if block subtracts the required advective component from the original stiffness matrix for both the bound (Sb) and free (S) nodes, hence simulating the case of no ventilation. This is further elaborated in section 3.4.3.

3.5 MATLAB/Simulink Programming

This section provides an insight into the programming done in MATLAB and Simulink.

3.5.1 Matlab Initialization Function

A section wise explanation is provided as follows. More details can be found in *Appendix F* which contains the full code with descriptive comments.

I. **WEATHER DATA INPUT:** This section is used to load the hourly temperature and solar radiation data into the respective matrices which are used in Simulink. The hourly temperature data was taken from the EPW file of the respective site and an excel sheet was used to convert global direct and diffuse solar radiation (also found in EPW file) to the required intensities on vertical faces at various orientations taking into account ground reflected radiation for a reflectivity of 0.3. The same excel sheet also contained the hourly angle of incidence.

II. **LOAD MATERIAL DATA FOR GLAZING OPTICAL PROPERTIES:** A table containing the angular properties of all the glazing panes is first loaded and then converted to an array for ease of access. The table contains optical properties for different angles of incidence, thicknesses of the glass panes as well as the U-value for the inner envelope with double glazing. All these values were calculated using the WINDOWS 7.7 programme from Berkeley Lab (ref. Appendix E).

III. **THERMAL COMFORT DATA TO SET INTERNAL TEMPERATURE:** Here, the internal temperature for every hour is set. The temperatures required were found using the IMAC tool (an excel worksheet) which gives the temperatures on a monthly basis. These temperatures are then assigned to an hourly basis to facilitate the use in Simulink.

IV. **PHYSICAL INPUT:** All the physical properties of the façade and its respective components are declared. The structured array variable "layer(i)" contains the respective properties of the façade components. "i" here denotes the node equivalent as in table 3.1. Also, the shading depth for each component is calculated which is used to set the "Q" matrix in Simulink

V. **SIMULATION SPECIFIC INPUT FOR SIMULINK:** Basic inputs pertaining to the execution of the solver in Simulink are specified.

VI. **DISCRETISATION INPUT:** Declaration of the number of nodes in each component in the vertical direction "K" followed by setting the node number of known nodes, etc. Further, the area assigned to each node is calculated based on "K".

VII. **HEAT TRANSFER AND AIR FLOW PARAMETERS:** All the respective heat transfer parameters are declared in this section along with flow rates of the ventilation and the required effective U-value of the inner envelope is calculated.

VIII. **VIEW FACTORS:** Based on the fictitious cavity method, all the view factors are calculated here. F_ij indicates view factor from i^{th} node to j^{th} node where i and j are node numbers as per fig 3.1 in each k^{th} layer.

IX. **CREATING "S" MATRIX, STIFFNESS MATRIX WITHOUT BLINDS:** All coupling coefficients for the "S" matrix as described at the beginning of this chapter are made. "(i,j)" refers to the nodal equation of node "i" and the coupling coefficient with node "j". The bottom air nodes are set separately since their advective component is connected to the outside air which is a bound node.

X. **CREATING "S_blind" MATRIX, STIFFNESS MATRIX WITH BLINDS:** The stiffness matrix for the "blinds on" case is created by altering the S matrix. Essentially only the radiation view factors change and the same is applied in this section.

XI. **CREATING "Sb" MATRIX, KNOWN TEMPERATURE COUPLINGS:** The stiffness matrix for all bound nodes is created, i.e. containing the coupling coefficients between the external or internal air with the respective DSF component.

XII. **SETTING PARTIAL STIFFNESS MATRIX FOR ADVECTION ADJUSTMENT:** First, the set point for controlling when the ventilation can be switched on is declared (control also depends on solar radiation which is accommodated in Simulink). This is followed by creating an adjustment stiffness matrix that when subtracted from the main stiffness matrix cancels the advective components, hence creating the ventilation off scenario.

XIII. **CREATING "M" MATRIX, MASS MATRIX:** The mass matrix containing all the thermal masses assigned to each node is created.

XIV. **CREATING "Q" MATRIX, SOLAR/INTERNAL HEAT LOADS:** Partial Q matrix is created here. 2 versions are created, one with details of blinds "on" while the other for blinds "off". Only the shading coefficient of the blind and area of the respective nodes are included here. All other

assignments such as optical properties and incident radiation are added within Simulink in a separate MATLAB block.

3.5.2 Matlab Function in Simulink for Calculating Solar Loads and Solar Heat Gain

This function takes various inputs from Simulink at each time step and calculates the "Q" matrix as described in ch3.1.2 and the total solar heat gain into the room for each time step. A section wise explanation is provided as follows. More details can be found in *Appendix G* which contains the full code with descriptive comments.

I. **SETTING CONDITION FOR BLIND ON OR OFF:** In this section, the appropriate partial Q matrix is assigned based on blind control, i.e., blind on if direct and diffuse radiation is greater than the setpoint (250 W/m^2), otherwise the blinds are off. The matrix value is saved in two variables, "x" and "a". "x" is used to calculate the respective solar load at each component in the DSF (the Q matrix) while "a" is used in the calculation of the total solar gain into the room.

II. **SETTING SHADING LENGTH:** The shading length from the self-shading effect of the façade ceiling is calculated using the tangent of the angle of incidence and the respective depths of the components.

III. **SETTING HT OF ONCE REFLECTED FROM BASE:** The "hre" height *(ref. Appendix: A)* for once reflected radiation from the base of the façade is calculated for the respective components.

IV. **SETTING INCIDENT ANGLE FOR INTERPOLATION:** The angle of incidence based on the solar radiation is calculated from the tangent of the angle which was used as input.

V. **SELECTING PROPERTIES BASED ON SOLAR ANGLE:** Knowing the angle of incidence the respective absorptance and transmittance for diffuse and direct radiation are calculated for each component. Matrix "T" contains the glazing details as described in the MATLAB initialization function. Linear interpolation is used to calculate the exact optical properties for the angle of incidence using a linear interpolation function ("intpol"). This is followed by setting the reduction factors for each component.

VI. **SETTING "x" AS Q:** The variable "x" is modified by multiplying/adding the required reduction factor and solar load to form the full Q matrix (containing heat load vectors) to be used in the solution generation of each time step.

VII. **INTERNAL SOLAR GAIN INTO THE ROOM:** The internal solar gain is calculated using the "a" matrix which contains the nodal areas and shading coefficient and applying the respective reduction factors and transmission for the inner-most glazing.

VIII. **LW SKY RADIATION:** This section was **unused.** It was intended to add ground and sky radiation exchange to the external glazing as part of the heat load vector. **NOTE:** In case this is to be used, the nodal connection in the main initiation function for the external envelope with outside air must be modified to remove the radiative heat transfer coefficient.

3.5.3 Simulink Model

The Simulink model consists of five main blocks (fig. 3.4). Following is a description of the tasks performed in each of the blocks. Full detail of the setup is shown in *Appendix G*.

I. ***Solar loads and Q matrix*** *(indicated in red in fig 3.4)*: This block only contains the MATLAB function described in section 3.4.2 with its respective inputs. The outputs from this block are, the total solar heat gain into the room, the "Q" matrix for solution generation and the total incident solar radiation (direct and diffuse) on the external skin.

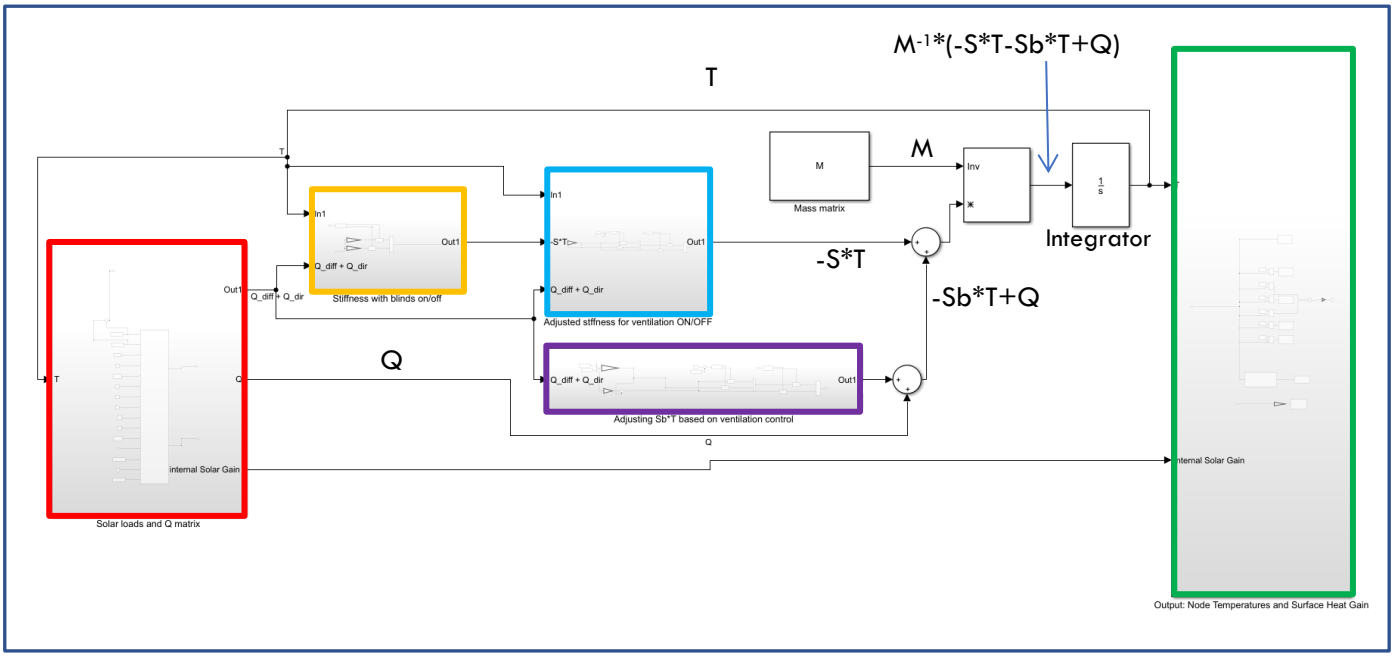

Figure 3.5: Screen shot of full Simulink Model with the various blocks colour coded.

II. ***Output*** *(indicated in green in fig 3.4)*: This block primarily contains scope blocks to store the temperatures, surface heat gain and solar heat gain for each time step. A Matlab function is created to calculate the surface heat gain based on the nodal temperatures of the inner-most glazing surface at each time step. The inputs for this block are the temperature signal ("T" matrix) and solar heat gain.

III. ***Stiffness Matrix Adjustment for Blinds*** *(indicated in orange in fig 3.4)*: This block contains an if statement which selects the appropriate stiffness matrix ("S" or "S_blind") to be used based on the intensity of incident solar radiation. The setpoint can be adjusted in the if statement block, set to 250W/m^2 by default. The inputs of this block are the solar load for checking the if statement and the temperature signal "T". The output of this block consists of the temperature signal multiplied by the appropriate stiffness matrix "T*S".

IV. ***Stiffness Matrix Adjustment for Ventilation*** *(indicated in blue in fig 3.4)*: Here the stiffness matrix is adjusted based on the ventilation control. Two if statement blocks are employed, one to check the incident solar radiation and the other to check the external air temperature. "S_adjust", the partial stiffness matrix is subtracted from the signal in case ventilation is meant to be switched

off. The inputs of this block are the product of the temperature and appropriate stiffness matrix "T*S", the temperature signal "T" and solar radiation. The latter is used in one of the if statements. Depending on the adjustment needed the output signal may be "T*S" if ventilation is supposed to be on, otherwise, it is "T*S-T*S_adjust" for removing the advective component, hence ventilation is off.

V. ***Bound Stiffness Matrix Adjustment for Ventilation*** *(indicated in purple in fig 3.4)*: In this block, the bound stiffness matrix (*Sb*) is first multiplied by the known temperatures (*Tb*) and is subsequently adjusted for the ventilation control. The input to this block is only the solar radiation, used in the if statements for ventilation control. The output of this block is the product of the bound stiffness matrix and bound nodal temperatures, i.e., "Sb*Tb" with the appropriate ventilation setting.

NOTE: Additional components are included within each block to provide the required inputs which are declared within the initiation function. This includes among other constants, the outside temperature, room temperature, direct and diffuse solar radiation etc.

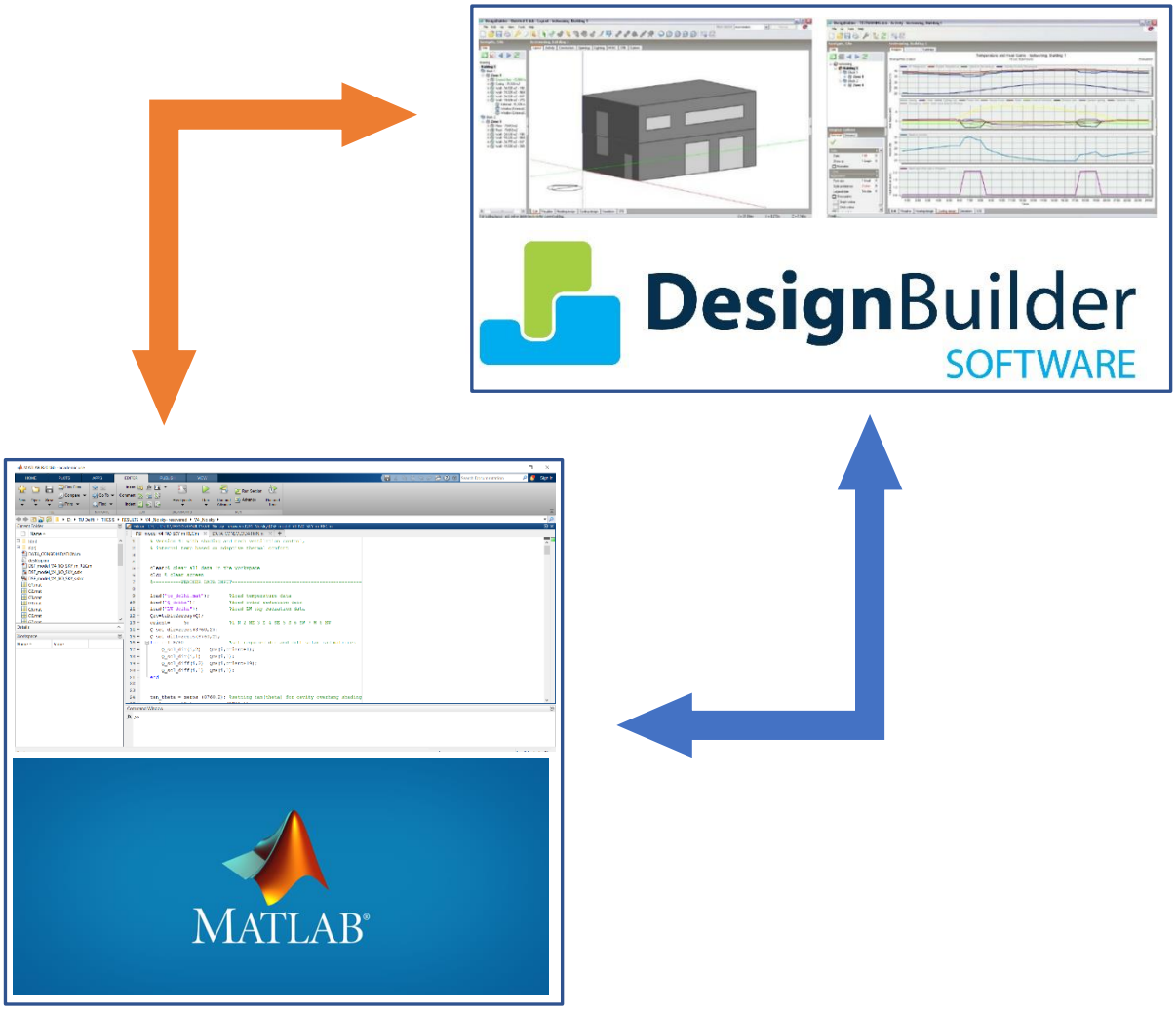

Figure 4.1: The two software packages with their respective interface used for the intercomparison and verification

4. Model Verification

The numerical model created with the Matlab/SIMULINK (M/S) platform was compared with a DSF model created in Design Builder (DB). A DSF is a complex system and hence, many simplifications and alterations had to be made to both models to obtain comparable thermal environments considering their boundary conditions, external influences and working assumptions. This chapter explains the calibration of the two models to obtain comparable boundary conditions. This is followed by the results in terms of heat flows through the façade which are used to verify the M/S model. The reasons for not using DB itself for the purpose of this study are addressed in Ch. 7.

DB simulates the behaviour of an entire building and not just a façade. Hence, many settings in DB had to be changed, to ensure that the temperature distribution and heat flows were under the same criteria as intended within M/S. Further, due to lack of certain controls in DB, the M/S model was altered to adequately match the behaviours. These alterations and adjustments are elaborated in sections 4.1 and 4.2.

The simulations used for the validation purpose were carried out for the site location of New Delhi with a DSF of 0.5 m width facing North or South and a ventilation rate of 100 m^3/hr in the cavity. An additional comparison is made in the South facing façade for ventilation rate of 600 m^3/hr as this rate better represents the requirements for decreased risk of overheating from a practical perspective.

A look into the temperature distribution of the components and net heat flow to the room were used to assess the accuracy and possible reasons for discrepancies between the two platforms.

4.1 Overview of the Design Builder Model

4.1.1 Building Setup

The DB model consists of a building with a floor plan of 10x10m and a height of 3m. The DSF is on one of the four exterior walls. DB does not provide the option of mechanically ventilating the cavity with

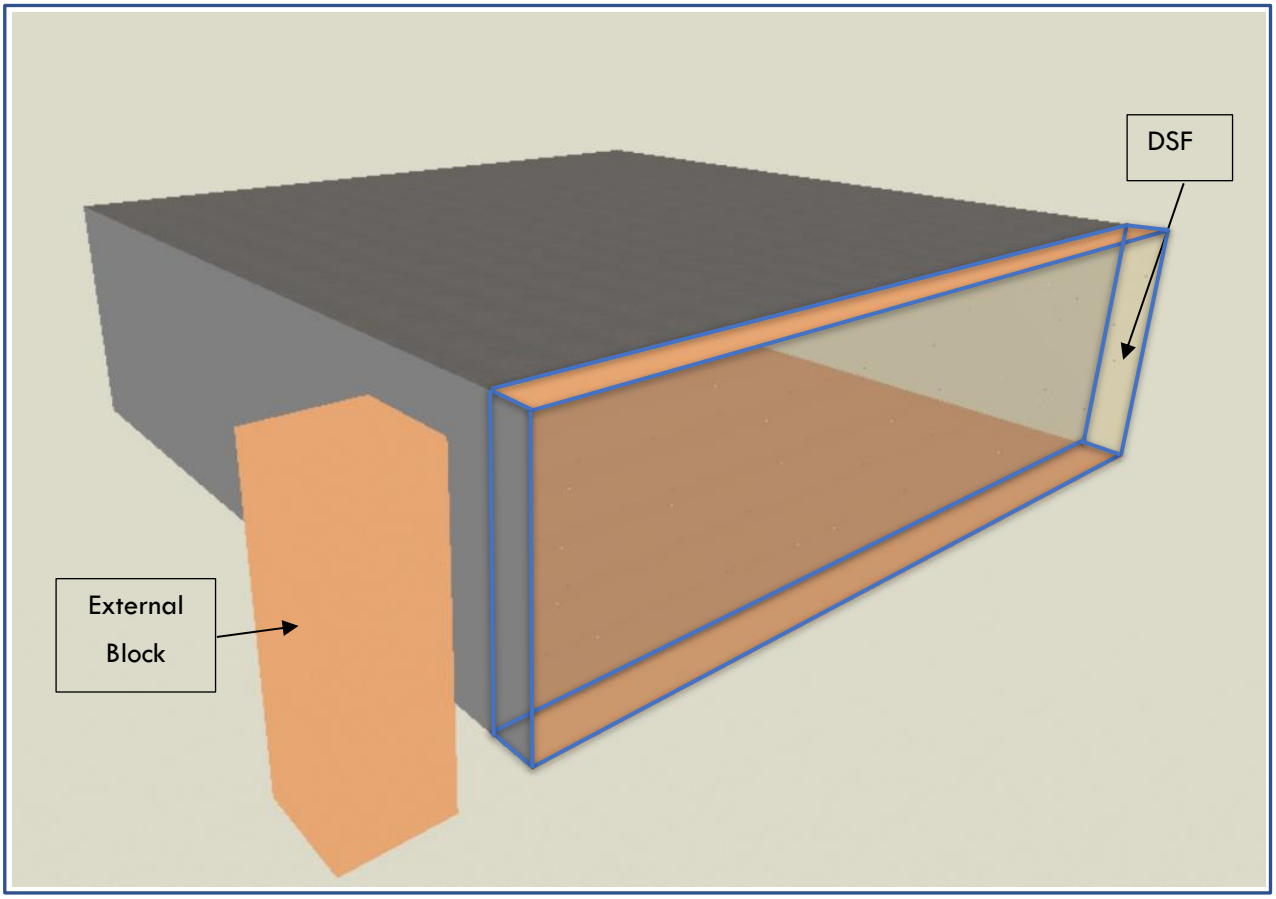

Figure 4.2: Design Builder Model Visualization

outside air. Hence, the building was created by six floor levels (zones) of 0.5 m height each. After doing so, the floors were removed from each zone to obtain an empty cavity from the ground level to the ceiling. This enabled one to set the movement and rate of air from each zone to the zone above, hence simulating bottom up mechanical ventilation. Further, the ventilation in the cavity is defined to and from an external block *(ref. Fig. 4.2)* which is ventilated heavily with outside air. Thus, this external block essentially contains outside air which is circulated to the cavity at the required ventilation rate.

4.1.2 HVAC Settings

The HVAC system for the interior of the building was calibrated to ensure that the inside air temperature remains constant at 23°C. In order to achieve this despite the changing external climatic conditions, the heating and cooling capacities were set to an extremely high value at each zone level *(ref Fig 4.3)*. This enables the internal temperature to remain constant since ample capacity is provided within the HVAC system. Thus, the internal boundary condition was matched with that of the M/S model, i.e., a constant temperature.

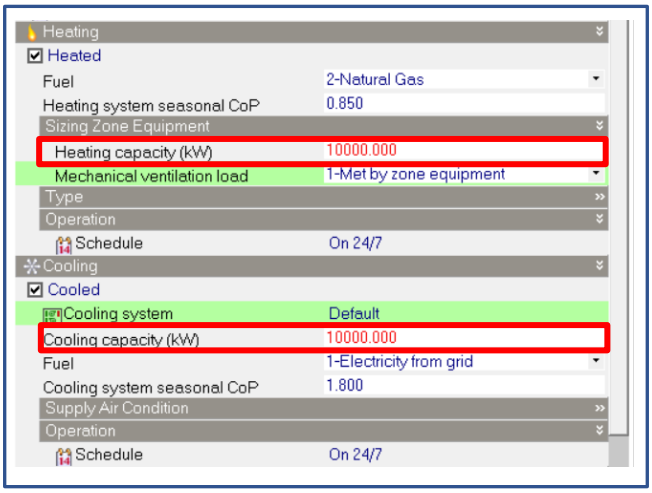

Figure 4.3: HVAC system set-up at zone level in Design Builder

4.1.3 Material Selection

The material selection for the verification was kept simple. The external envelope was fully glazed with 6mm clear glass while the internal envelope was 4/16/4 double glazed clear glass with argon gas.

The shading system comprised of the "Venetian Blind – medium (modelled as diffusing)" which was then altered to match the specifications in the M/S model *(ref. Fig. 4.4)*. The altered properties were as follows:

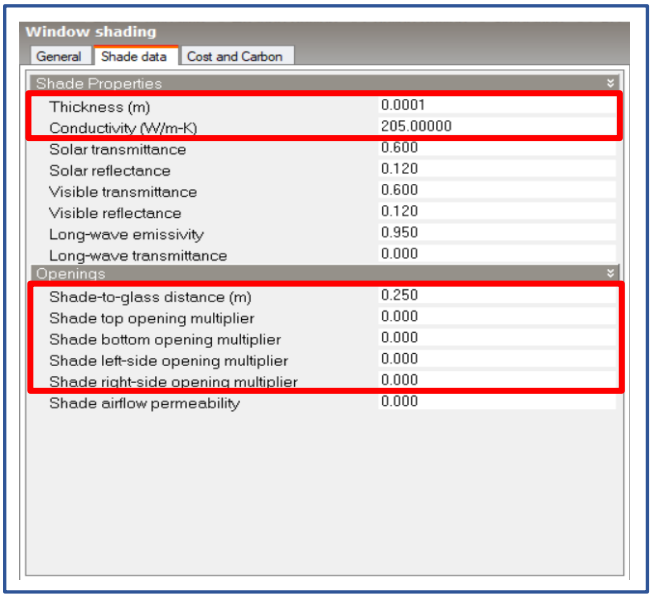

Figure 4.4: Shading Properties in Design Builder

1. Conductivity, set to that of Aluminium
2. Thickness of 0.1mm (slat thickness)
3. Shade-to-glass distance of 0.25m (centre of the cavity)

4. All opening multipliers around the edges were set to zero to eliminate solar radiation passing through the edges of the blind system.

Lastly, the building's construction was set to lightweight super insulated, once again to ensure that the internal room temperature always remains at 23°C.

4.1.4 Control Schemes

Due to the already complex setup required to simulate the mechanical ventilation in the DSF, it was chosen not to integrate any ventilation control in the DB model. Hence, the ventilation in the cavity was set to a constant value (100 or 600 m^3/hr) throughout the duration of the simulation.

The shading control was set to the same settings as in the M/S model, i.e., the blinds are switched on only if the solar load on the external glazing exceeds 250 W/m^2.

4.1.5 Calculation Algorithms

It was initially found that the external convective coefficient and thereby the external surface resistance was far lower than the expected values based on the empirical formulae. The convective coefficient estimated by DB's default algorithm DOE-2 gave values close to 6.0 W/m^2K, far below the expected 17.7 W/m^2K based on the wind speed and empirical formulae *(ref. Appendix B)*. Hence it was chosen to use the "Simple Combined" algorithm for calculating the external convective coefficient which along with giving more realistic coefficients also eliminated complexities due to sky radiation on the external glazing. This moreover reduced the number of uncertain parameters and made it easier to track the causes of discrepancies.

The internal convective coefficient algorithm was set to "CIBSE" method as this gives roughly a constant value of 3.1 W/m^2K. This value was incorporated into the M/S model for the validation purpose only as it is relatively high for internal convection coefficients which as per the empirical formula available are often less than 2 W/m^2K in building applications.

4.1.6 Summary

By adjusting the HVAC system and external wall construction it was possible to obtain a constant internal temperature as is the case in the M/S model. The alterations to the shading device properties and employed ventilation with the external block can be said to fairly replicate the mechanical ventilation and venetian blinds in the M/S model as well. Lastly, a suitable selection of convection algorithms allowed for surface resistances which could be implemented within the M/S model for its validation.

However, due to lack of possible controls in the ventilation scheme and large variance in the external convective coefficients, alterations had to be made to the M/S model in order to calibrate it with respect to the simulations carried forth in DB. This aided in reducing the number of unaccounted variables and thus, assisted in identifying the possible causes in discrepancies.

4.2 Matlab/SIMULINK Model Calibration

Some parameters of the M/S model could not be incorporated adequately in DB, thus, changes were made to the M/S to replicate the boundary conditions and behaviour of the DB model instead.

Firstly, the internal room temperature was set to a constant 23°C rather with the monthly variations as per the IMAC.

Secondly, the longwave radiation exchange between the external glazings with the external environment and sky was removed. This was done as a first iteration to decrease the number of variables influencing the model. As a second iteration, a model with the external radiation components was made as these influences cannot be neglected for real-world scenarios.

Third, due to the large hourly variation in the external convective coefficient (ranging from 8.2 to 23.6 W/m^2K), despite the "Simple Combined" algorithm in DB, it was decided to extract the hourly external convective coefficient values from DB and use the same in the M/S model. Hence, the external surface resistance was evaluated for each hour based on the extracted convective coefficient as opposed to the constant value originally intended.

Lastly, the internal convective coefficient was changed to 3.1 W/m^2K in accordance with the values calculated via the "CIBSE" algorithm in DB as opposed to the original values of 1.7 W/m^2K.

4.3 Observations

Graphical plots of the outputs can be found in *Appendix H* which have been used for the purpose of verifying the M/S model against DB. *Table 4.1* gives the percentage difference in heat gains among the two models for various simulations. The difference in total heat gain is minor although the difference in surface and solar heat gain is more pronounced.

Firstly, comparisons between the temperature of the outer glazing surface, cavity air and inner surface of the inner envelope showed that the temperature discrepancies between the M/S and DB models vary primarily with an increase in the incident direct solar radiation. This idea is supported firstly by a better correlation in the temperature distribution of the North facing façade rather than the South façade which receives much more solar radiation throughout the year. Secondly, in the South facing façade, the temperature distribution is better correlated in the month of June when the direct solar load on the façade is lower owing to high sun altitudes while the correlation is poorer in March and December when direct solar loads are more severe due to lower sun altitudes.

Secondly, increasing the ventilation rate within the cavity improves the correlation between the temperature distribution of the two models. The simulations with 600 m^3/hr ventilation rate coincide better with each other as compared to the comparisons between the models at 100 m^3/hr ventilation rate. However, the surface heat gain deviates significantly, up to 23% with an increase in ventilation

rate. The overall effect of this deviation is minor since surface heat gain forms a smaller fraction of the total heat gain, around one-third, while the rest is contributed to by the solar heat gain.

Table 4.1: Comparison of annual heat gain components in M/S and DB for different orientations and ventilation rates at New Delhi.

Orientation	Ventilation Rate	Platform	Total Heat Gain (kWh)	Surface Heat Gain (kWh)	Solar Heat Gain (kWh)
South	100m^3/hr	M/S	11575.6	4209.6	7366
		DB	11265.3	4671.2	6594.1
		% Change	-2.7	9.9	-11.7
South	600m^3/hr	M/s	10818.5	3452.4	7366.1
		DB	11068.3	4474.2	6594.1
		% Change	2.3	22.8	-11.7
North	100m^3/hr	M/s	7001	2297.7	4703.3
		DB	7413.2	1736.2	5677
		% Change	5.6	-32.3	17.4

Third, looking at the heat gain into the room it is apparent that the trend is very similar to that seen in the temperature distribution, i.e., the discrepancies in the two models are higher during higher solar loads. Moreover, it is observed that the differences in surface heat gain and solar heat gain often compensate for each other resulting in a total heat gain that is similar in both models. This indicates a difference in the optical properties of the glazings and blind system. For instance, a higher absorptance of glazing in the models will increase heat transfer due to surface convection while decreasing heat transfer by solar radiation, hence balancing the net heat transfer to a large extent. However, this compensation is not present when there are no solar loads and leads to a discrepancy primarily due to the difference in surface resistance at night.

Lastly, the M/S model with the sky and ground radiation components included correlates more poorly with the DB model for low ventilation rates as well as low solar loads as opposed to the M/S model which neglects these radiation components. There is an unexpected behaviour in the M/S model with 100 m^3/hr ventilation rate at low solar loads (in June) where the inner envelope temperature is affected more severely than the external envelope, this is rather absurd given that the radiation exchange added only affects the external envelope. Coupled with the insulating nature of the cavity between the envelopes, one can see how this change in behaviour is an absurd result. Further, the total heat gain into the room is also largely increased, at points almost by 50% more than that observed in DB.

4.4 Conclusion

Looking at the temperature distributions and heat flows in the two simulations *(ref. Appendix H)* it can be said in some confidence that the Matlab/SIMULINK model which neglects sky and ground radiation provides a good degree of accuracy when compared with the output from Design Builder, especially at ventilation rates of 600 m^3/hr.

The M/S model which incorporates sky and ground reflected radiation is disregarded due to the unexpected nature of the output under certain boundary cases as mentioned in the previous section. Further, the heat gain and internal glazing temperature are the primary parameters intended to be used in this study for the evaluation of the DSF, as these parameters do not correlate well with those seen in DB this particular model configuration cannot be said to aptly represent the intended behaviour of the system. Therefore, it was chosen to use the model neglecting sky and ground radiation components for the purpose of this study. Relying only on the surface equivalent resistance which includes a radiative loss of 5 W/m^2K.

The overall working methodology of the Matlab/SIMULINK model employed has been verified as a large portion of the discrepancies observed in the comparisons can be attributed to the physical inputs of the model such as material properties and heat transfer coefficients.

The possible causes for discrepancies, in varying degrees, have been listed below:

1. Differences in the optical properties of the glazings.
2. Difference in the optical and thermal properties of the venetian blind as well as air flow through the blinds which is not taken into consideration in M/S.
3. Radiative heat exchange of the inner glazing surface with walls, ceiling and floor of the room. This is accounted for in Design Builder but not considered in detail in Matlab/Simulink which uses only an internal surface resistance equivalent.
4. The temperature of the cavity floor, this is neglected in Matlab/Simulink, however, this is not the case in Design Builder and could influence the system in terms of absorption of heat as well as radiative exchange with other components.

Given that the application of the Matlab/SIMULINK model is for a relative comparison of design parameters and configurations. It can be stated that any discrepancies with the Design Builder model will be apparent in all model configurations and thus, as a relative measure of performance can be neglected under the given boundary conditions. The heat flows through the façade are correlated well for the two models. However, due to different physical properties, the mechanism through which the heat transfer takes place, solar heat gain or surface heat transfer vary. The similar trends in temperature change with time for the sample weeks indicate good working principles in the M/S model.

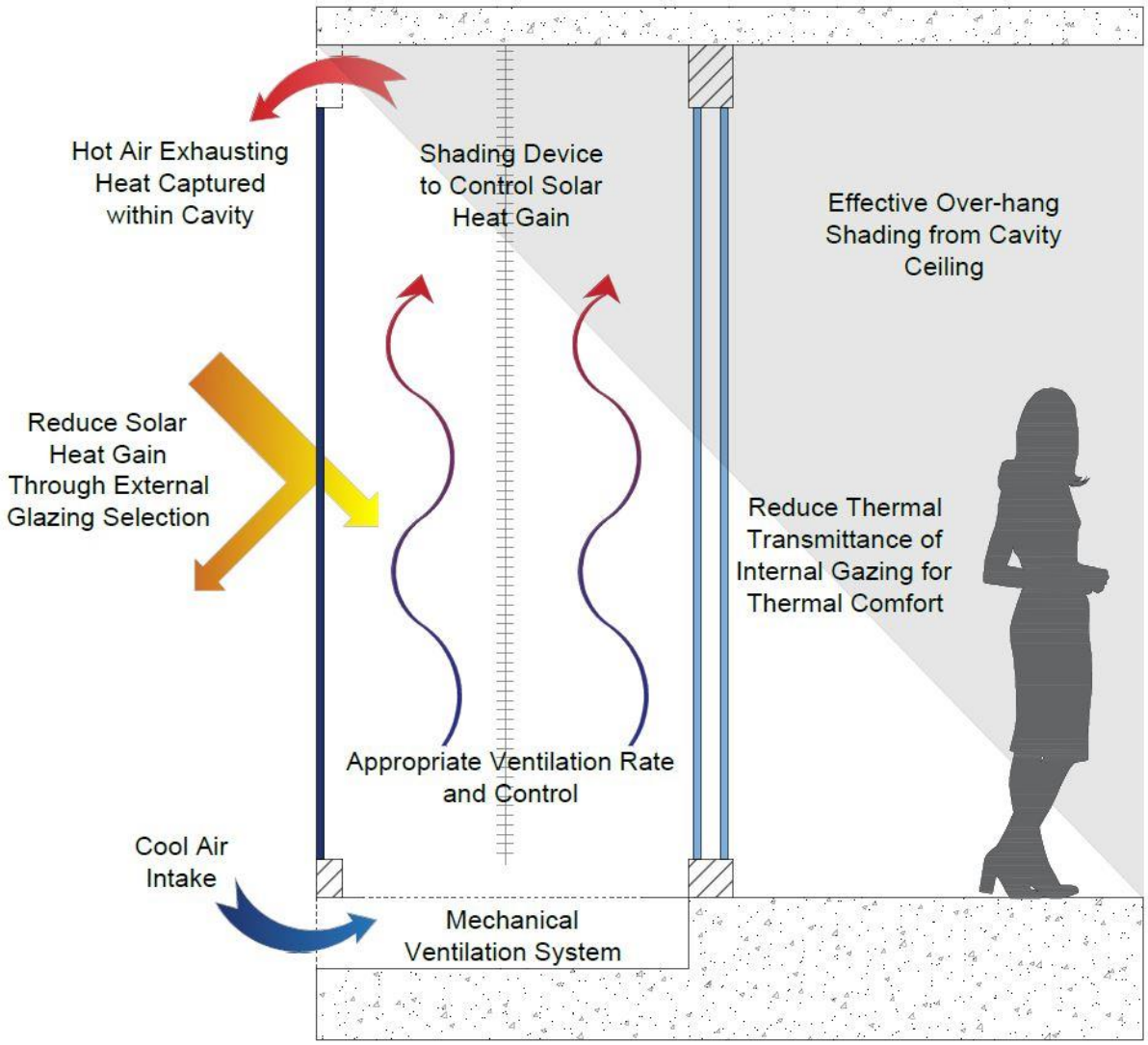

Figure 5.1: Sectional view of a ventilated DSF showing the effect of various components on mitigating heat gain/loss

5. Behavioural Analysis of DSF

This chapter describes the analysis of the changes in the performance parameters, such as heat gain and thermal comfort, with respect to the DSF configuration, particularly ventilation rate, cavity width and glazing properties. New Delhi has been chosen as the location for this detailed analysis as it offers a wide range of seasonal variations within a year. A brief description of the climatic conditions of New Delhi is provided followed by the respective analysis. In addition, an inter-comparison for all sites is briefly presented to add perspective to the effectiveness of using different design strategies. The inferences drawn from the observed behaviour of the DSF with respect to changes in design configuration are utilized in the subsequent chapter to derive the optimized configurations for specific site locations catering to their temperature variations and solar loads.

The simulations were conducted for different orientations, namely, North, South and East. For each orientation, different façade parameters were changed. Detailed results of the simulations can be found in *Appendix I* for all sites, although this chapter only discusses the results for New Delhi in detail. The parameters analysed were as follows:

1. **Cavity Depth:** 0.2m, 0.5m, 0.8m, 1.0m, 1.2m and 1.5m deep cavities were used. The variations in the depth were simulated for two ventilation schemes, a constant rate of air changes (80 AC/hr) and a constant volumetric flow rate (120m^3/hr per meter length of façade).
2. **Ventilation Rate in the Cavity:** The ventilation (mechanical) rate was varied from 0 AC/hr, no ventilation (sealed cavity), to 400 AC/hr.
3. **Glazing Properties:** The external and internal envelope glazing systems were varied in different combinations. A wide selection of optical properties for both envelopes was used. The external envelope was single-glazing, which was either clear, tinted or reflective. The inner envelope was a double-glazed unit in which the external light was varied in terms of its optical properties while the inner light was restricted to 3 or 4 mm clear glazing. The restriction on the inner glazing was made due to its relative ineffectiveness as has been discussed in the literature review. Further, the inner envelope was evaluated for special features such as glazings with low-E coatings and high-performance double-glazing units.

The base configuration for the DSF is presented below *(ref. Table 5.1)*. **Only one design parameter** at a time was changed from this base configuration for each simulation.

Table 5.1: Base configuration of DSF

PROPERTY	VALUE
Cavity Depth	0.5m
Façade height (held constant)	3.0m
Façade length (held constant)	10.0m
Ventilation Rate	1200m^3/hr (80 AC/hr)
External Envelope	Single-glazing, 6mm, clear
Internal Envelope	Double-glazing, 4/16/4, clear, Argon gas

5.1 Parameters Used for Analysis

5.1.1 Annual Solar Heat Gain to the Room

This accounts for the total heat entering the room due to the solar radiation. The solar gain at each time step is calculated by applying the suitable reduction factor and glazing transmission coefficient to the incident radiation for the inner-most glazing unit. The solar radiation transmitted at each node of the inner-most glazing is then summed to obtain the total solar load transmitted through the façade at the respective time step as explained in *section 3.4.2*. The solar gain is consequently summed for each time step to obtain the annual solar heat gain.

$$Q_{Sol} = Ar * \sum_{i=5*k+1}^{6*k} Q_{ze} * SC * \tau_1 * \tau_5 * \tau_6$$

Where Q_{sol} is the total diffuse/direct solar gain in one time step and *Ar* is the area represented by each node. The terms within the summation denote the intensity of solar radiation entering the room. This is evaluated based on the incident direct/diffuse radiation (Q_{ze}), shading coefficient (SC) and transmission (τ) for direct/diffuse radiation incident on the respective nodes based on their height *(ref. Fig. 3.3)*. *k* denotes the total number of nodes in the vertical direction, i.e., the number of discretized layers over the height of the façade. The above formula is implemented separately to calculate the diffuse and direct components of radiation entering the room and the sum of these gives the total solar gain.

5.1.2 Annual Heat Gain to The Room

The annual heat gain represents the total net heat flow into the room. It is calculated as a sum of the solar and surface heat gain for all hours when there is net heat flow into the room.

$$Q_{HG} = Q_{Sol} + Ar * \sum_{i=5*k+1}^{6*k} \frac{\Delta T_i}{r}$$

Q_{HG} is the total heat gain at each time step. The summation of Q_{HG} for all hours for which it is greater than zero gives the annual heat gain. The second term on the right-hand side of the equation represents the surface heat flow where *Ar* is the area represented by each node, i is the node number, *k* is the discretization in the vertical direction, ΔT_i is the temperature difference between the i^{th} node and the room temperature and r is the equivalent surface resistance as calculated in *section 3.1.3*.

5.1.3 Annual Surface Heat Gain to the Room

This is used to evaluate the component of heat gain to the room due to the convective and radiative exchange from the inner-most surface of the façade. It is calculated as the difference between the annual heat gain and annual solar heat gain. It is important to note that the surface gain can be negative despite net heat gain owing to a situation of high solar radiation but low external air temperatures.

$$Q_{Surf,a} = Q_{HG,a} - Q_{Sol,a}$$

Where, $Q_{Surf,a}$ is the annual surface heat gain, $Q_{HG,a}$ and $Q_{Sol,a}$ are the annual total heat gain and solar gain respectively.

5.1.4 Annual Heat Loss from The Room

This component represents the total heat flowing out of the room. It is calculated as the same for the total heat gain at each hour, but it is summed for all time steps during which the total heat gain is negative, indicating net heat flow out of the room.

5.1.5 Thermal Comfort Indicator

The temperature of the inner-most glazing surface is compared to a maximum limit for thermal comfort. The temperature of the node at mid-height of the glazing was chosen for this purpose and the number of hours during which the temperature exceeds 45°C is used as an indicator for adequate thermal comfort throughout the year. Temperature asymmetries for a warm wall are recommended to be kept below 23°C, i.e., the difference between the room dry bulb temperature and temperature of the wall surface should not exceed this value (ASHRAE, 2004). Given the room air temperature varies between 23°C and 27°C annually for all sites considered in this study, the 45°C mark was chosen as an appropriate value to judge the adequacy of thermal comfort. However, this is a rather high temperature and therefore in addition to it, the number of hours with glazing surface temperature above 28°C is also noted as a comparative performance measurement for temperature distribution in the façade.

A minimum mark of 16°C is kept for winter thermal comfort. The radiant temperature asymmetry, in this case, should be limited to 10°C (ASHRAE, 2004).

5.1.6 Overheating Risk in The Cavity

The overheating risk of the cavity is assessed as the number of hours during the year in which the cavity air temperature exceeds 40°C. This temperature was chosen as it reflects a fair degree of heat accumulation in the cavity. The average temperature of the air nodes at mid-height of the façade, either side of the venetian blind were used for this purpose.

5.2 Climatic Analysis – New Delhi

The climate of New Delhi is an overlap between monsoon-influenced humid subtropical (Köppen climate classification Cwa) and semi-arid (Köppen climate classification BSh). This overlap of climate types can be attributed to New Delhi's proximity to the Himalayan Mountain Ranges to the North and the Thar Desert to the West. This has resulted in a humid subtropical climate very different from what is classically expected due to frequent dust storms and haze which are more prominent in arid climate zones. *Fig. 5.2* gives a brief look into the hourly temperature distribution over the year. It is important to point out that due to periods of high humidity the perceived temperature during the months of June, July and August are significantly higher and thermal comfort is diminished below what one would expect based on temperature conditions. The dotted lines in *Fig. 5.4* are a clear indicator of this phenomenon which coincides with the higher humidity levels as displayed in *Fig. 5.5*.

Located at 28.6° N and 77.2° E *(ref. Fig. 5.3)* the daylight hours vary approximately between a minimum of 10.5 hours at the lowest in December to a maximum of 14 hours in July. However, when considering solar radiation incident on vertical faces, such as those of buildings, one must keep in mind that due to the closer proximity to the equator the angle of incidence is significantly larger in summers as compared to winters. This results in higher intensities of solar radiation on South facing façades during winters rather than in summer. The latitude is above 23.5° N (Tropic of Cancer), hence there is never a period during

which the North facing façades receive significant direct solar radiation. The East and West oriented façades receive almost the same amount of direct radiation with only the time of day, before or after noon, changing.

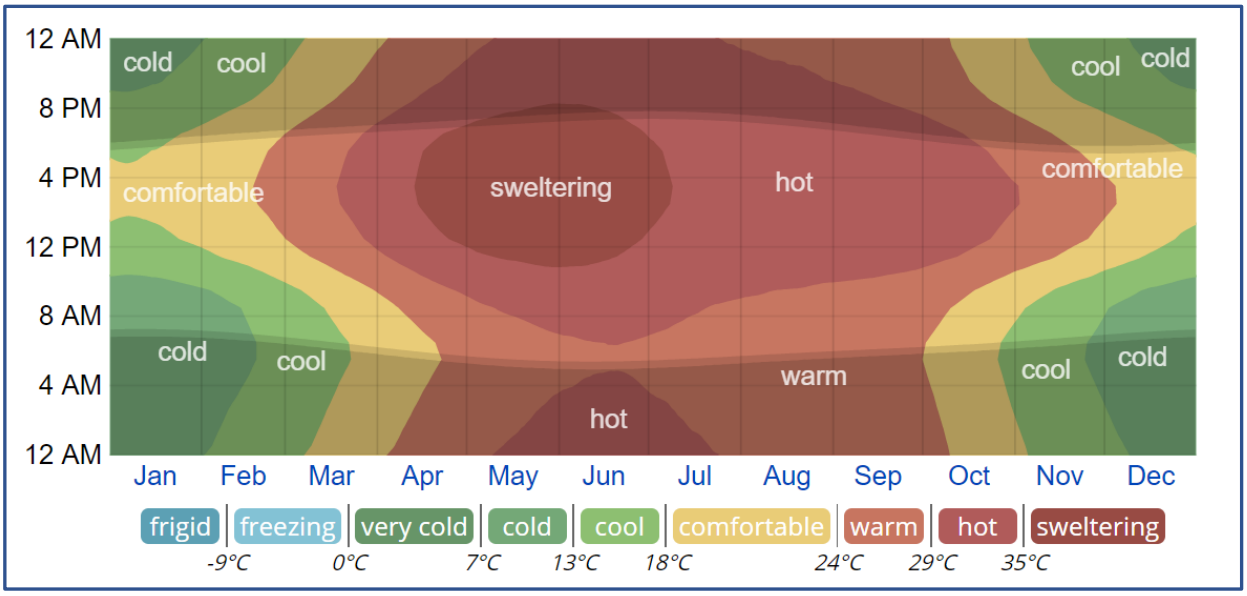

Figure 5.2: New Delhi:The average hourly temperature, colour coded into bands. The shaded overlays indicate night and civil twilight. The horizontal axis is the day of the year, the vertical axis is the hour of the day, and the colour is the average temperature range for that hour and day.
Source: **https://weatherspark.com/y/109174/Average-Weather-in-New-Delhi-India-Year-Round#Sections-Temperature**

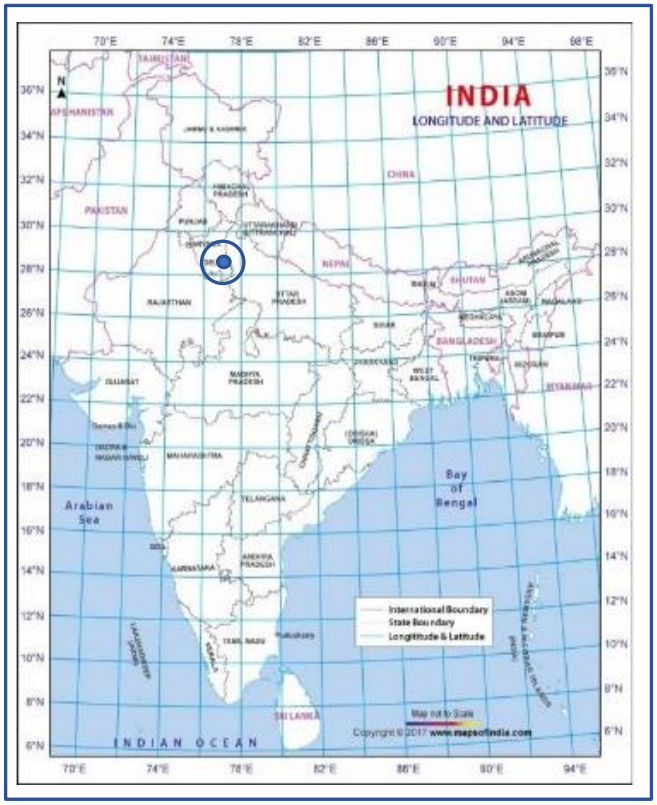

Figure 5.3: Location of New Delhi on political map of India with longitudes and latitudes. Indicated at centre of target

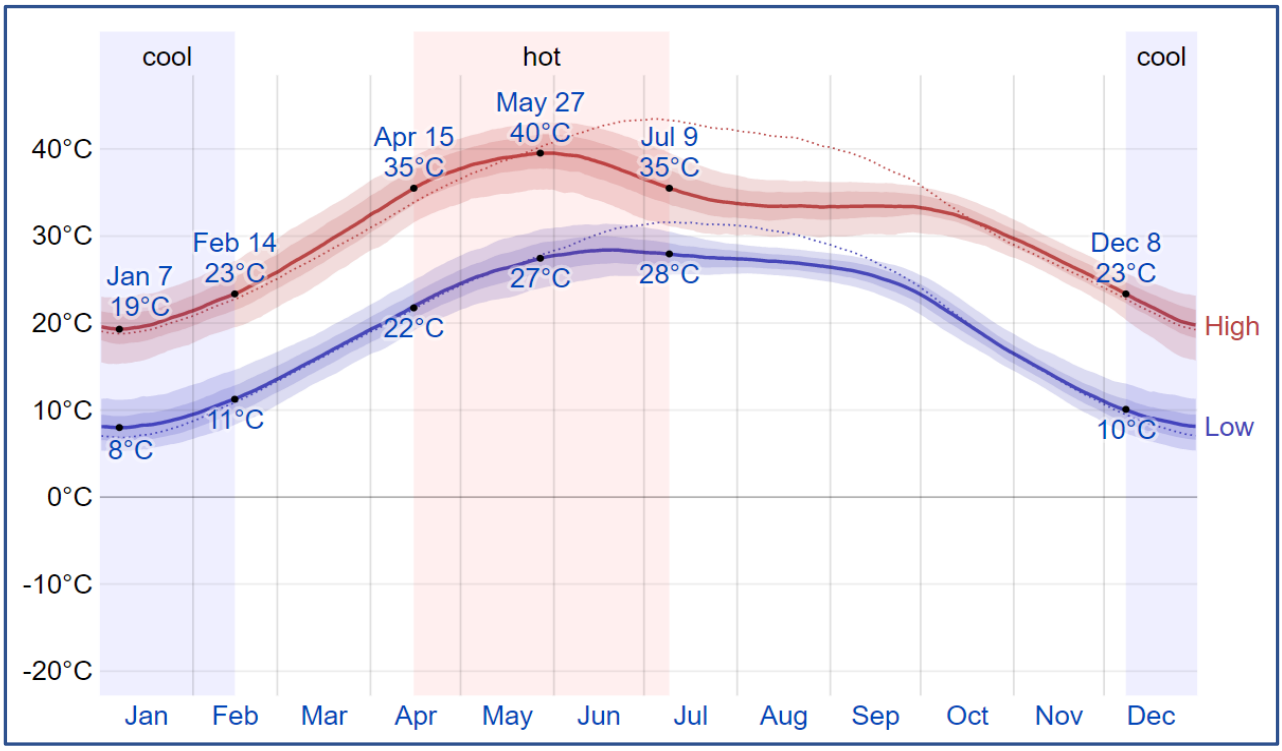

Figure 5.4: New Delhi: The daily average high (red line) and low (blue line) temperature, with 25th to 75th and 10th to 90th percentile bands. The thin dotted lines are the corresponding average perceived temperatures.
***Source*:** **https://weatherspark.com/y/109174/Average-Weather-in-New-Delhi-India-Year-Round#Sections-Temperature**

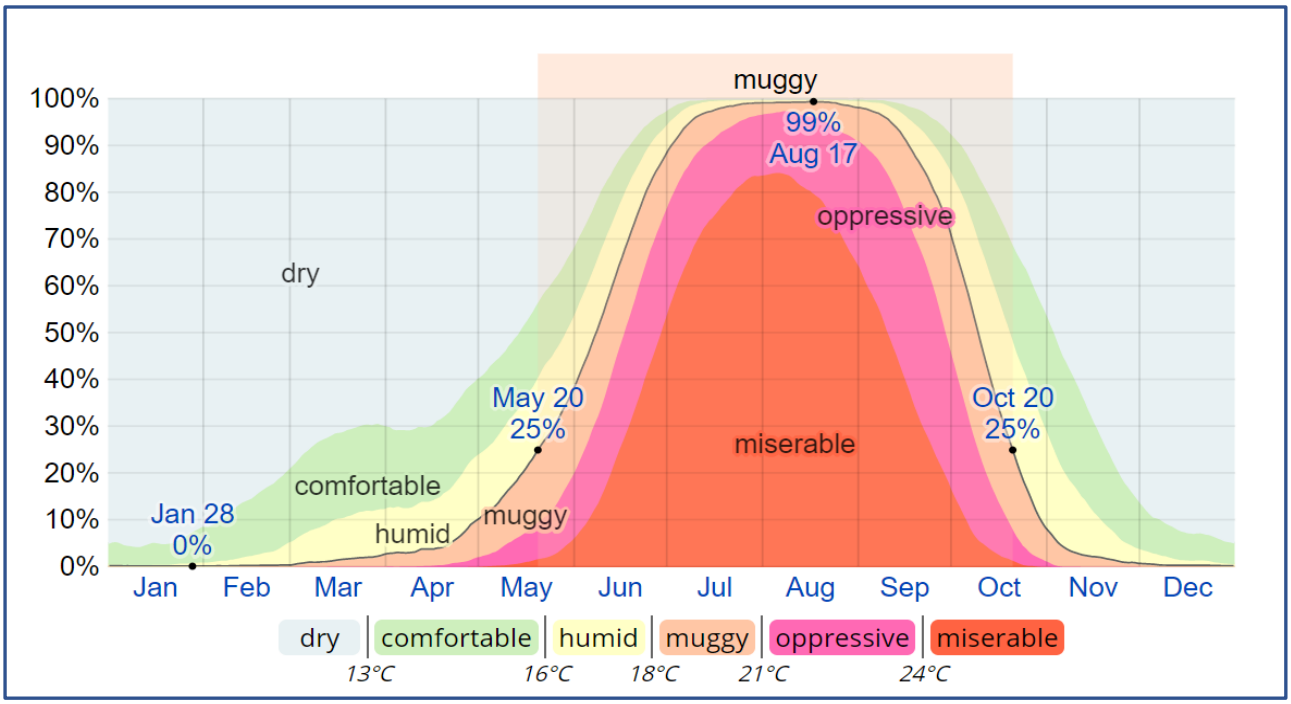

Figure 5.5: New Delhi: The daily percentage of time spent at various humidity comfort levels, colour coded and categorized by dew point.
***Source*:** **https://weatherspark.com/y/109174/Average-Weather-in-New-Delhi-India-Year-Round#Sections-Temperature**

5.3 Simulation Results

5.3.1 Ventilation Rate:

Increasing the ventilation rate in the cavity reduced the annual heat gain into the room for the South and East oriented façades. This can be attributed to a reduced surface heat gain as some of the heat "deposited" into the cavity due to solar loads is exhausted via the mechanical ventilation rather than being absorbed and transmitted through the inner envelope. It is apparent from *Fig. 5.8* and *Fig. 5.9* that periods of higher solar radiation (in December) show a much greater effect from ventilation rate as compared to lower solar radiation (in June). In June, all ventilation rates yield the same result as seen by the overlapping lines. This

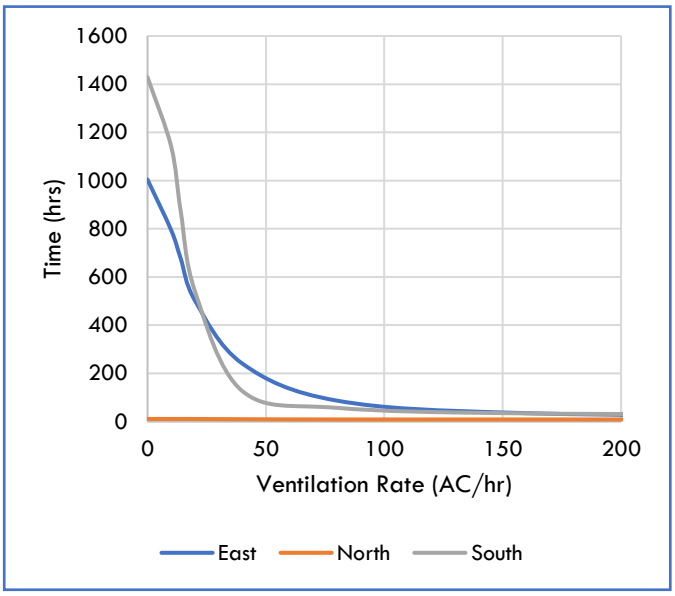

Figure 5.6: Number of hours with cavity air temperature above 40°C for different ventilation rates along three façade orientations (colour coded)

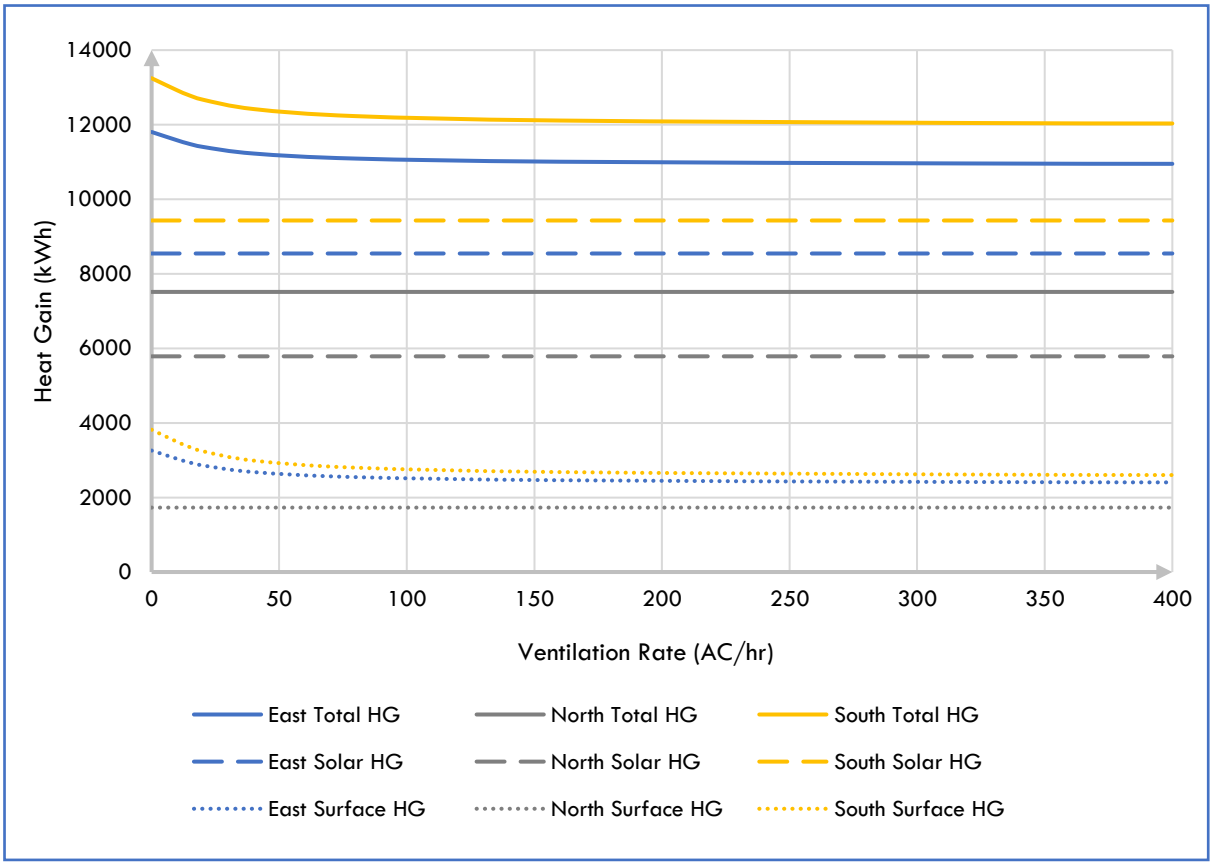

Figure 5.7: Change in annual heat gain with increase in ventilation rate at different orientations (colour coded). The heat gain is displayed as total heat gain and its two components, i.e., solar and surface heat gain (different line styles)

indicates that the control for the ventilation was never activated owing to low solar radiation. The lower cavity temperatures as compared to the external air in June indicate that the selected control strategy is effective *(ref. Sec. 3.3.2)*.

The decrease in heat gain was marginal for ventilation rates above 80AC/hr. From zero to 80AC/hr there was a reduction of 7.68% in total heat gain for the South oriented façade and roughly 6% for the East oriented façade. Increasing the ventilation beyond 80AC/hr to 400AC/hr only provided a benefit of 1.6% and 1% respectively for the South and East façades. The North façade was unaffected

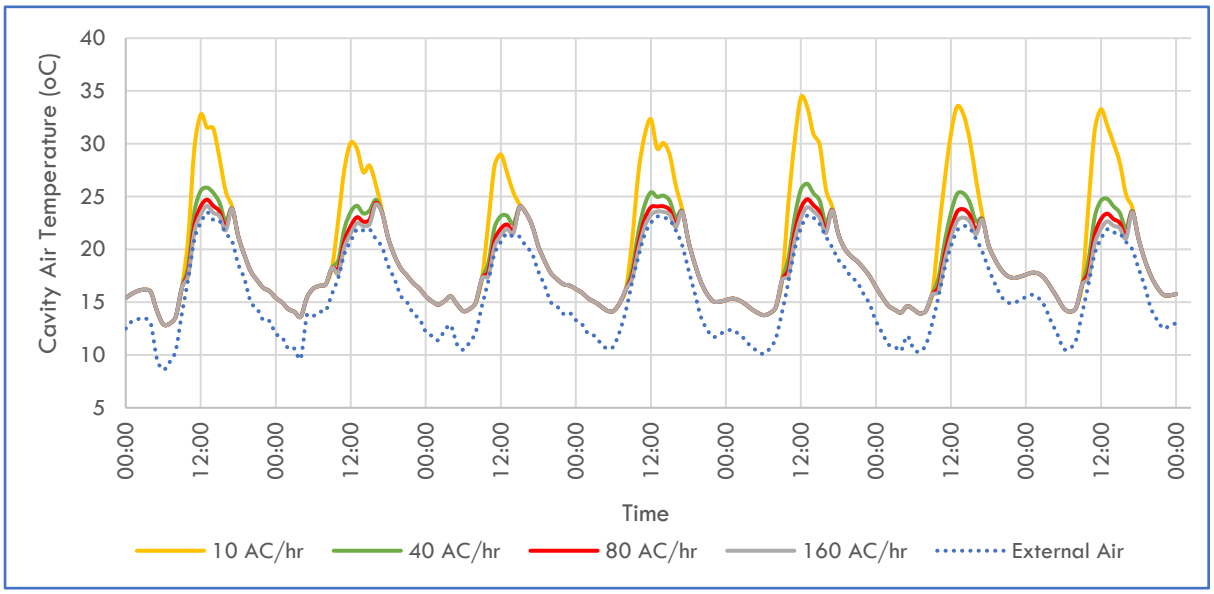

Figure 5.8: Hourly cavity air temperture for different ventilation rates (colour coded) for a sample week in December on a South facing DSF

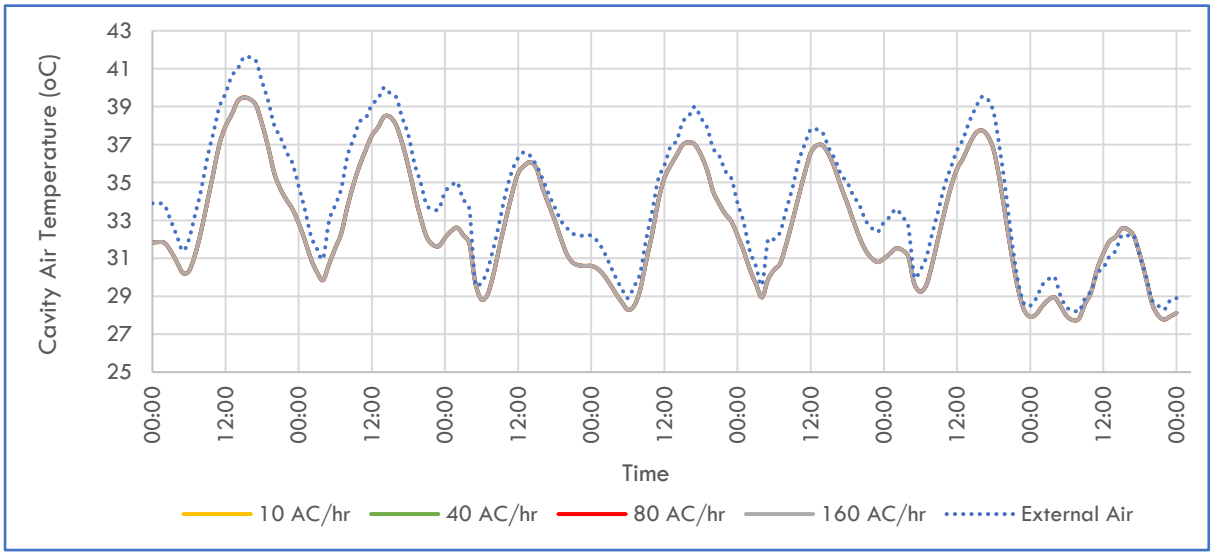

Figure 5.9: Hourly cavity air temperature for different ventilation rates (colour coded) for a sample week in June on a South facing DSF

NOTE: *Ventilation control is in "off" state hence ventilation rate is irrelevant (all lines overlap), cavity air temperature is equivalent of a sealed cavity (no air exchange with external elements)*

by changes in the ventilation rate with a reduction of only 0.4kWh of yearly total heat gain (less than 0.1%) when ventilation rate was varied from zero to 400AC/hr.

Heat loss from the room was not affected by any significant margin (less than 0.1% change from no ventilation to 400 AC/hr). This is to be expected since the default control settings in the simulations would dictate ventilation off condition for cooler external air temperatures (less than 15°C) and lower solar radiation.

Fig. 5.7 clearly indicates the redundancy of ventilation rates above 80AC/hr for the South and East oriented façades as well as the North oriented façade's relatively unchanged thermal behaviour with an increase in ventilation rates.

The ventilation rate plays a key role however in reducing the cavity air temperature and thereby reducing the risk of overheating. This can be especially seen in the South and East façades where increasing the ventilation rate from zero to 80AC/hr decreased the number of hours with cavity air above 40°C significantly. In the South façade, the reduction was from 1429 to 57 hours. Just as in the case of heat gain this reduction diminishes in magnitude for ventilation rates above 80AC/hr and is negligible for the North façade which has almost no overheating risk, to begin with *(ref. Fig. 5.6)*.

5.3.2 Cavity Width:

As in the case of ventilation rate, cavity width had a significant impact on the South and East façades but produced only marginal improvements for the North façade *(Fig. 5.10)*. Increase in cavity depth from 0.2 to 1.5 m in the South façade decreased the total yearly heat gain by more than 150kWh per meter length of façade. The surface heat gain was reduced by 19% and 6% for ventilation rates of 80AC/hr and 1200m^3/hr respectively when cavity width increased from 0.2 to 1.5 m in the East façade. This difference can be attributed to the poor performance of the 0.2 m wide cavity at 80AC/hr which showed a significantly higher risk of overheating in the South and East façades when compared with all other configurations *(ref Appendix I, tables on cavity width)*. On the other hand, larger cavity widths were more resilient to overheating at lower ventilation rates. On the South façade, at 1.5 m, the risk of overheating at 80AC/hr and 1200m^3/hr (26.7AC/hr) were equally low with 24 and 36 hours of cavity air temperature above 40°C respectively.

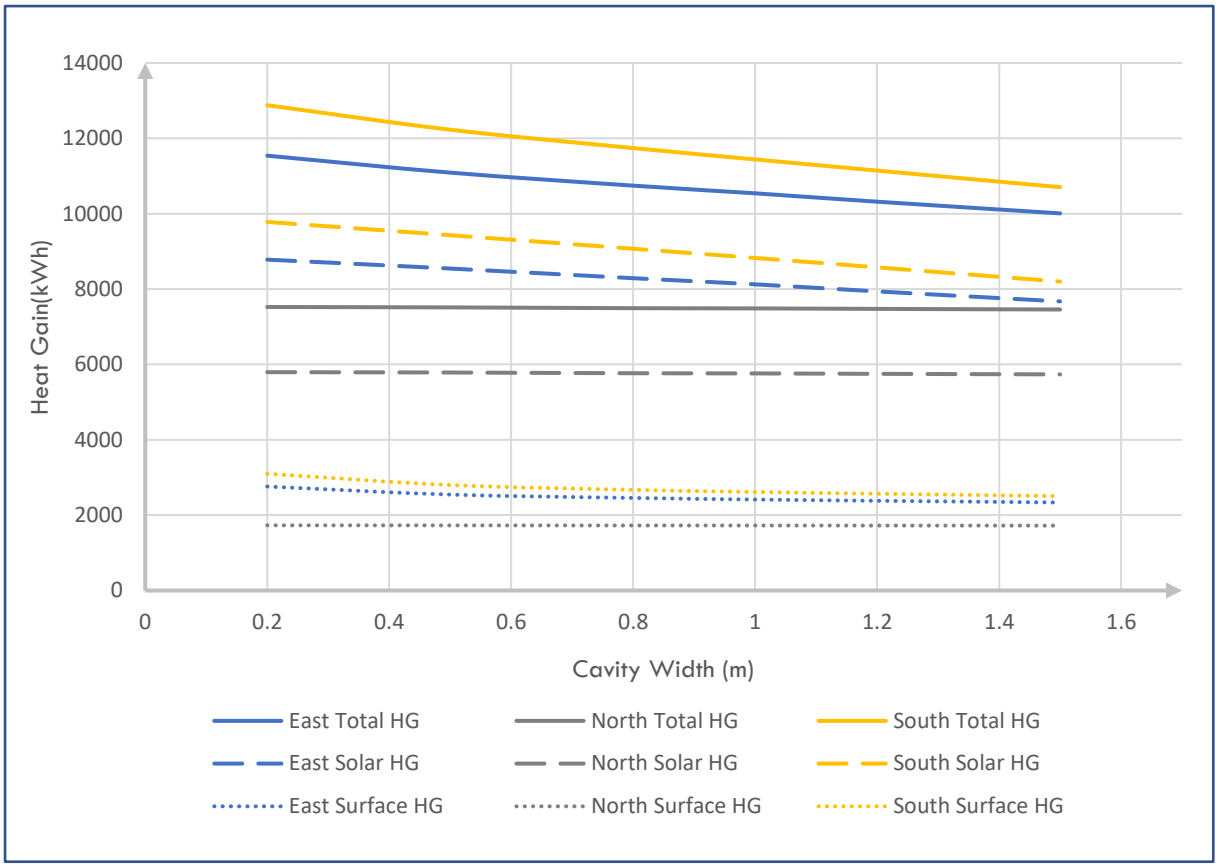

Figure 5.10: Change in annual heat gain with increase in cavity width at different orientations (colour coded). The heat gain is displayed as total heat gain and its two components, i.e., solar and surface heat gain (different line styles)

5.3.3 Glazing Units:

The key phenomena observed was an increase in the risk of overheating in the cavity when glazing units with better thermal performance were applied on the inner envelope. The highest risk of overheating accompanies the configurations which used high-performance glazings on the inner envelope. For the South façade, using tinted glazing on the external envelope reduced the total heat gain by almost half when compared to the base configuration with clear glazing. Further, it reduced solar heat gain by 60%. Reflective glazing on the external envelope proved most effective in reducing the risk of overheating in the cavity while tinted glazings increased the risk when applied to either of the envelopes. This can be due to the high absorptance in tinted glazings, hence they may be effective at decreasing solar heat gains but significantly increase surface heat gains to the room if applied on the inner envelope. However, thermal comfort was not compromised at any point in any of the orientations with the inner-most glazing surface temperature always within the set limits.

The total heat loss over the year was primarily influenced by the U-value of the internal envelope, with changes in the external envelope showing insignificant variation. A low-E coated inner envelope decreased the heat loss by roughly 32% while the high-performance vacuum glazing reduced it by over 60%. Similar trends are seen in all façade orientations for the heat loss.

5.3.4 Summary:

Ventilation rate is important for preventing overheating. However, ventilation rates beyond 80AC/hr provide minor benefits with further increase. The positive effects of ventilating the cavity can only be seen at high solar loads where the ventilation helps to cool the cavity air and façade components.

Wider cavities are more resilient to overheating while narrow cavities are more susceptible. Façades with low direct solar radiation, such as North oriented (in the case of New Delhi) have only marginal benefits from changes in cavity width.

Using well-insulated glazings on the inner envelope increases the risk of overheating, on the other hand, reflective glazings, when applied to the external envelope, can significantly reduce the risk of overheating.

Increasing ventilation and cavity width have a negligible impact on decreasing heat loss from the room. The primary influencer for decreasing heat loss is the U-value of the inner envelope.

Thermal comfort was never compromised in any of the tested configurations at the site. The inner-most glazing temperature remained within the range, never going below 16°C and never exceeding 45°C. However, there is significant variation in the hours for which the glazing temperature exceeds 28°C and this is primarily dependant on the degree of overheating in the cavity.

The control strategy employed has shown the desired effect. Excess heat, when deposited in the cavity due to high solar loads on the façade, is mitigated suitably. However, the setpoint temperature may be reduced at colder climates to ensure that the ventilation is activated appropriately.

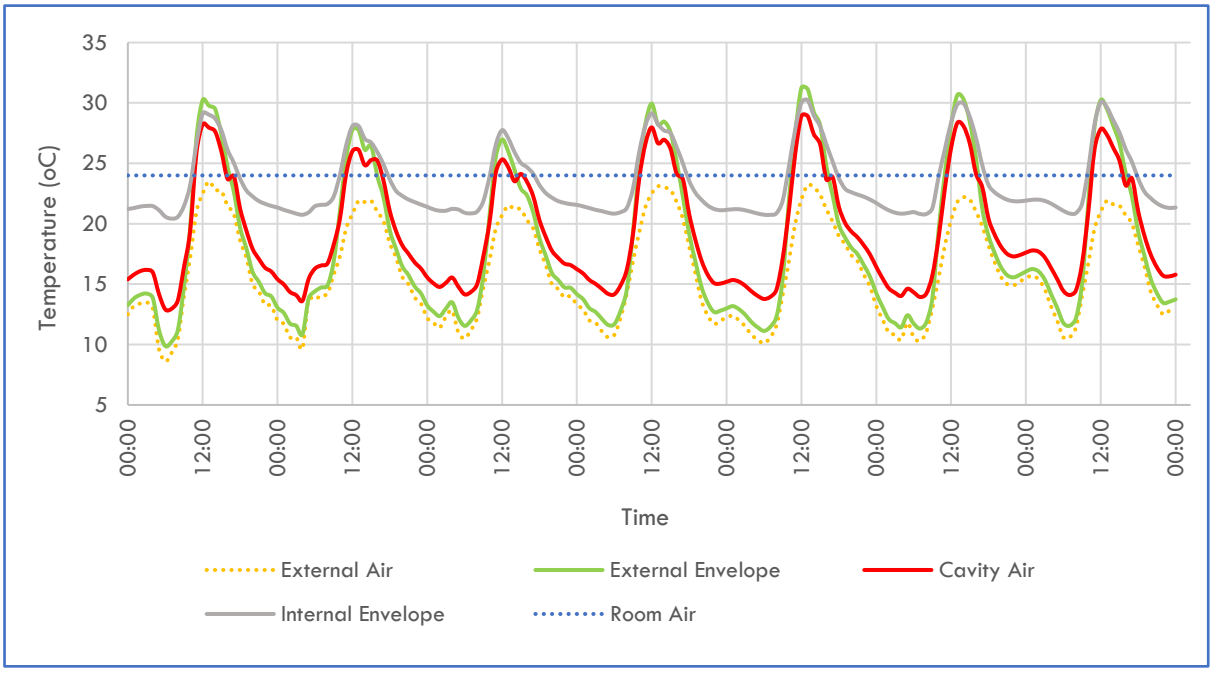

Figure 5.11: Hourly temperature distribution of different components (colour coded) for a sample week in December

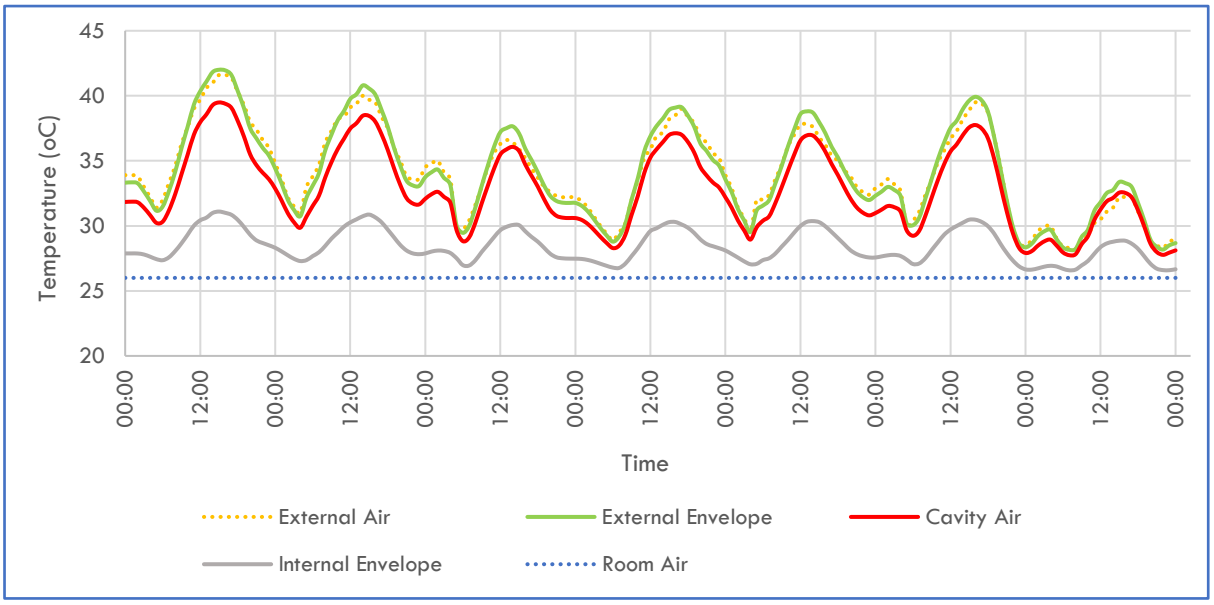

Figure 5.12: Hourly temperature distribution of different components (colour coded) for a sample week in June

It is clear from the temperature distribution *(ref. Fig. 5.11 & Fig. 5.12)* that the excess heat deposition in the façade is much higher in winters (December) than in summers (June). Peak temperatures in the façade exceed the external air temperature in winters while those in summer are primarily between the internal and external air temperature.

5.4 Inter-site Comparison

This section presents the changes in the performance parameters at the different sites to add perspective to the possible application of different strategies based on each site. The explanations presented here are only with respect to the façade's behaviour and not interpreted as per the climatic context which is done in detail in the following chapter *(Ch. 6)*.

Fig. 5.13 indicates the different heat transfer mechanisms (surface transfer and solar radiation) that contribute to the net annual heat gain when using the base configuration of the DSF at the different sites considered for this study. It is apparent that solar heat gain forms a much higher proportion of the total heat gain than the component through surface convection and radiation. The South façade is most susceptible to heat gain at all sites other than Chennai, further, as site locations move South, towards the equator, the heat gain at the East façade becomes more prominent.

For the South orientation, it is apparent that all sites benefit with an increase in cavity width and ventilation rate. However, the magnitude of the decrease in annual heat gain varies from site to site *(ref Fig. 5.14 & Fig. 5.16)*. Chennai shows the least sensitivity while Kathmandu, Jaisalmer, New Delhi and Bhopal show similarly decreasing trends. It can be further observed that ventilation rates beyond 80 AC/hr at all sites yield a minor decrease in heat gain while an increase in cavity width indicates almost a linear trend.

For the North façade, the sensitivity to cavity width and ventilation rate are negligible at all sites. Chennai showing only minor benefits with an increase in ventilation rate and cavity width while other sites display almost no reduction in heat gain with an increase in these parameters *(ref. Fig. 5.15 & Fig.5.17)*.

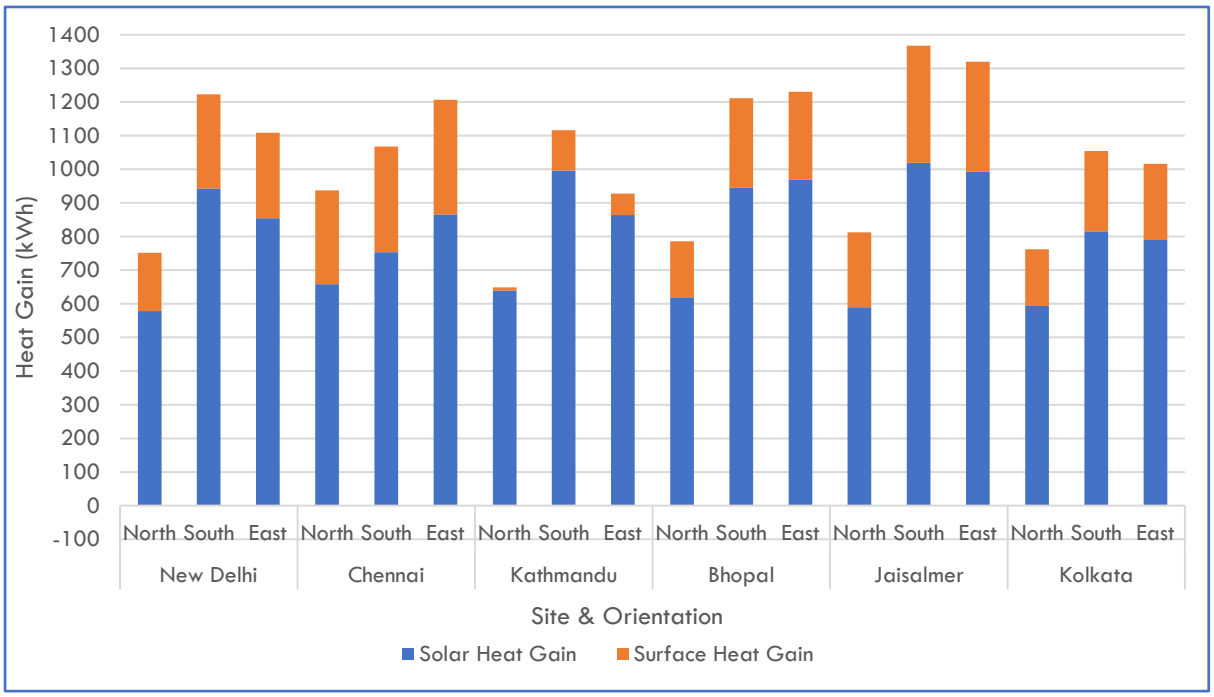

Figure 5.13: Stacked bar graphs representing the annual net surface and solar heat gains (colour coded) per meter length of façade at the respective sites and orientations for the base configuration of the DSF.

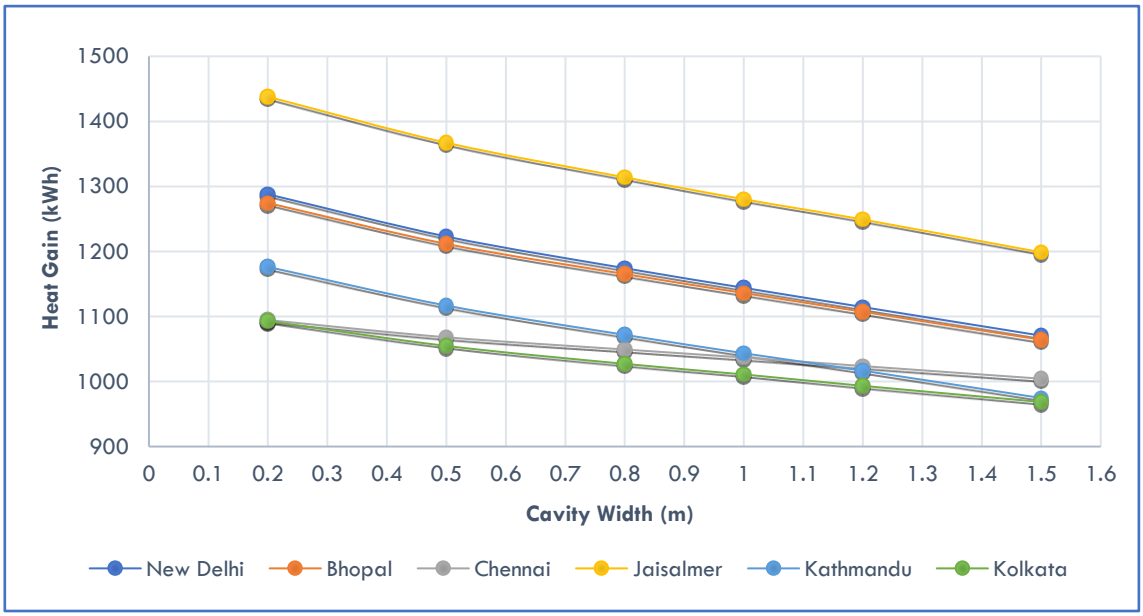

Figure 5.14: Annual heat gain per meter length of facade verses increase in cavity width for the base configuration at various sites in a South oriented DSF

A common denominator among all the observed behaviour at the sites is a sensitivity proportional to incident solar radiations. Hence, DSFs facing North show much less benefit from greater cavity widths and ventilation rates as opposed to those facing South.

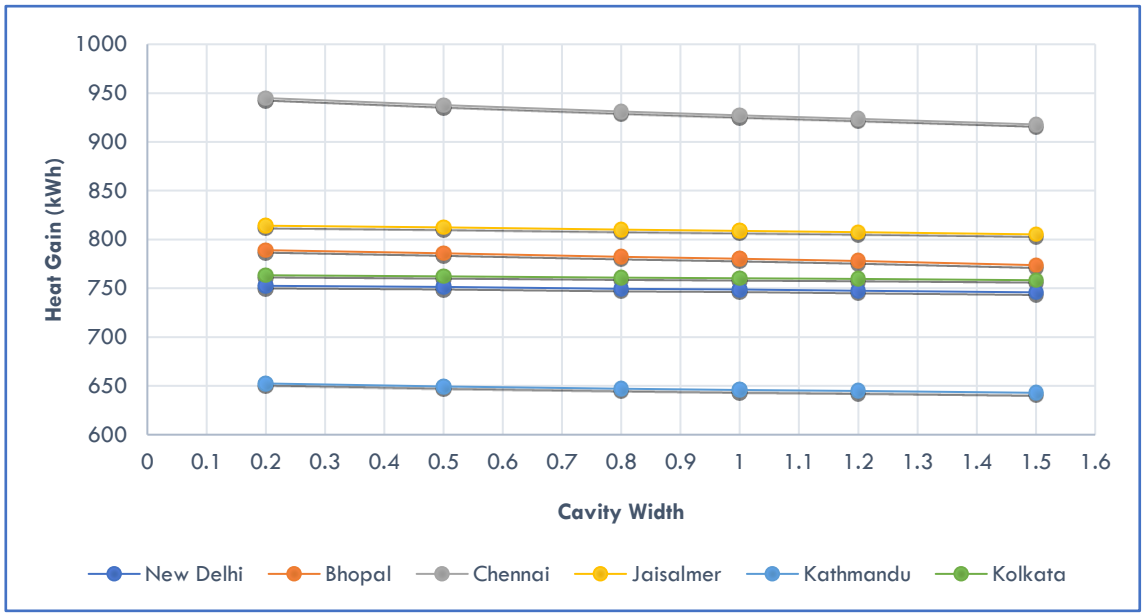

Figure 5.15: Annual heat gain per meter length of facade verses increase in cavity width for the base configuration at various sites in a North oriented DSF

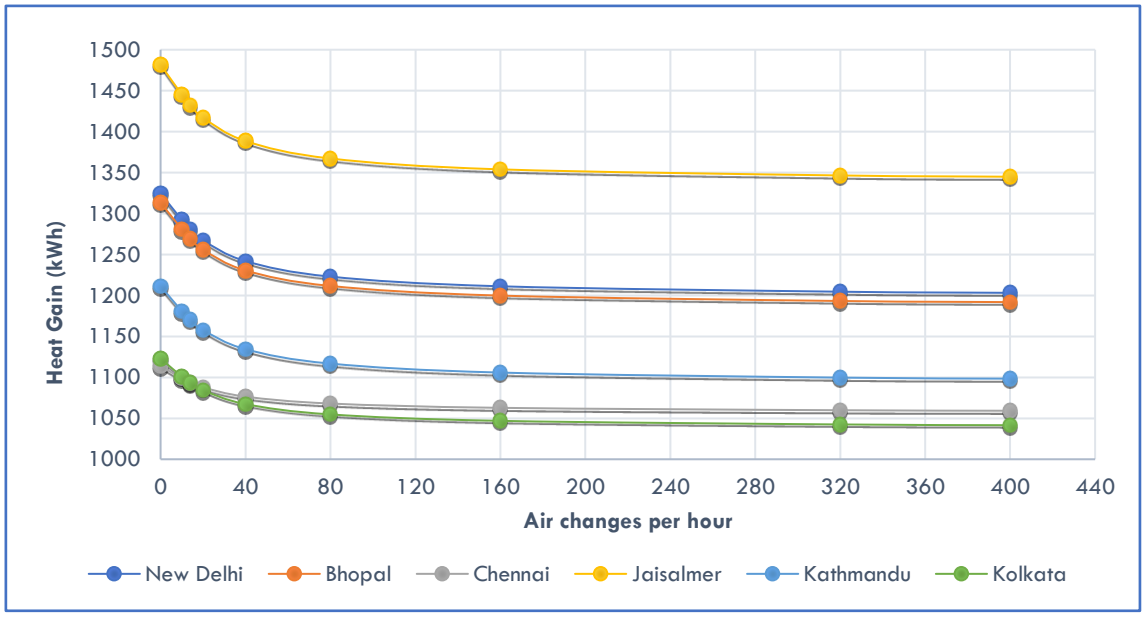

Figure 5.16: Annual heat gain per meter length of facade verses increase in ventilation rate for the base configuration at various sites in a South oriented DSF

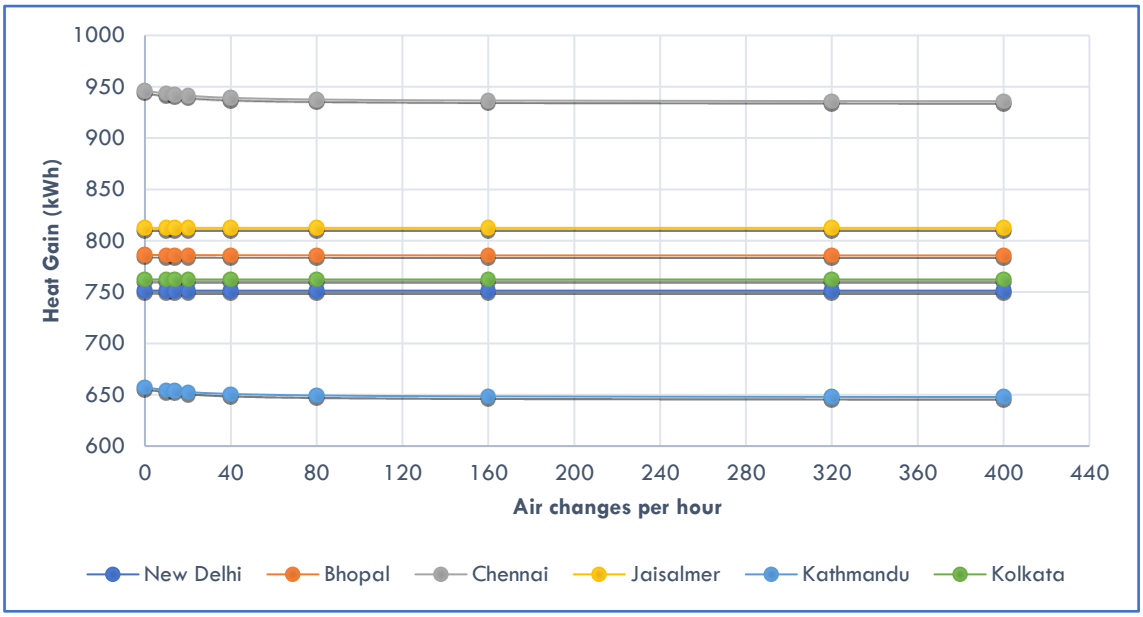

Figure 5.17: Annual heat gain per meter length of facade verses increase ventilation rate for the base configuration at various sites in a North oriented DSF

5.5 Inferences

Each of the parameters varied, namely, cavity width, ventilation rate and glazing system have important ramifications for the effective use of each other.

Although ventilation rates above 80 AC/hr seem to produce insignificant improvements, when combined which better insulating glazings on the inner envelope it may not only make a higher ventilation rate beneficial but possibly even necessary for a suitable reduction in the risk of overheating.

Sites with higher sun altitudes could potentially be equally successful with narrower cavity widths, less than 0.5 m, as the self-shading effect from the cavity width becomes more pronounced. This, however, must be balanced with an adequate ventilation rate since the risk of overheating is higher at lower cavity widths.

Overheating in the South and East façade is much more severe as compared to the North façade. This can be attributed to the direct solar radiation. Further, variation in the sun altitude throughout the year is a critical factor for assessing the risk of overheating within the cavity. This is clearly indicated by the higher risk in winters (lower sun altitudes) than in summers (almost perpendicular sun altitudes). The overheating risk has a fair degree of dependence on the direct solar radiation incident on the façade, hence for sites at lower latitudes, the risk of overheating may be greater in the North façade during summers as the sun path shifts to the North of the site.

Heat loss is affected significantly only by the U-value of the inner envelope, in colder climates, a better insulating glazing system on the inner envelope would be more beneficial as compared to climates where external temperatures do not significantly drop below the required indoor temperature.

DSFs facing North are nominally affected by changes in cavity depth and ventilation rate, the maximum sensitivity to the mentioned parameters for the overall behaviour is seen in the South oriented DSF. This can be attributed to the DSFs ability to decrease solar heat gains, hence façades with higher exposure to solar radiation are likely to benefit more from a DSF. Glazing selection has the largest impact on the thermal performance of the façade in all orientations. Properties of the external glazing are a crucial consideration for mitigating overheating in the cavity.

Thermal comfort is not compromised in any of the configurations despite the increased risk of overheating. Although an increase in the temperature of the inner-most glazing is observed in some situations, it is never high enough to cause a significant reduction in thermal comfort.

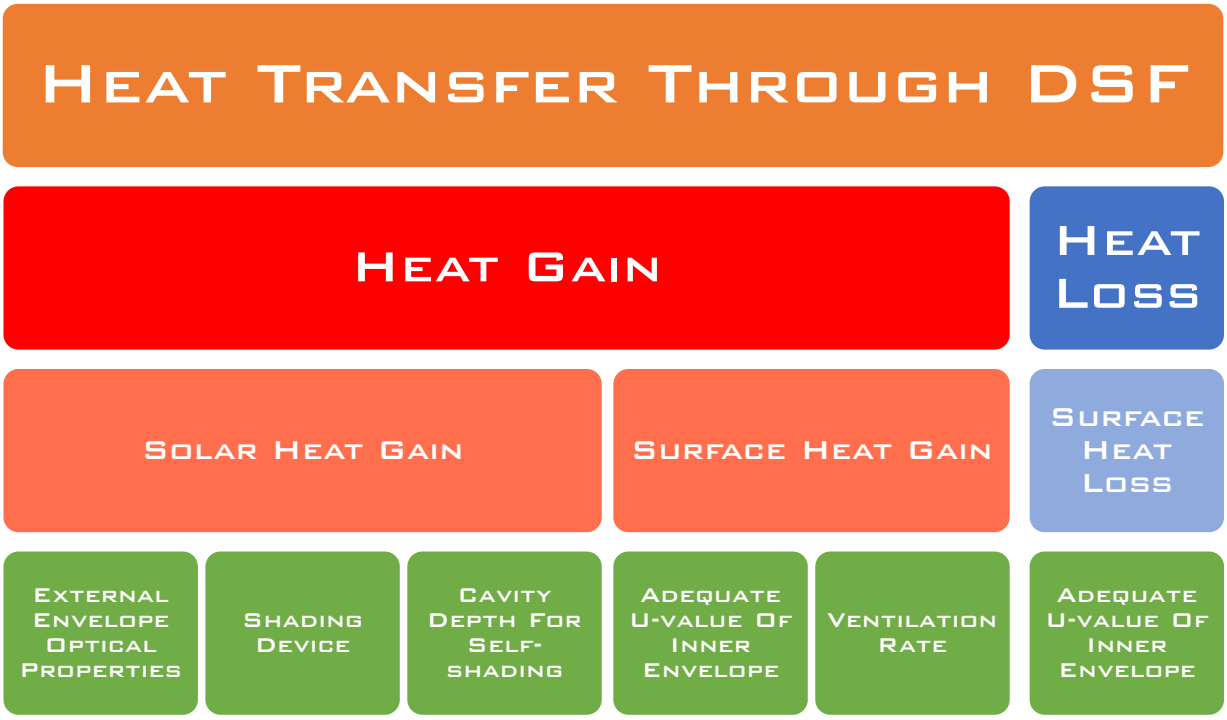

Figure 6.1: Design considerations for limiting different heat transfer mechanisms

6. Site Specific Optimization and Performance Evaluation

This chapter presents the site-specific recommendations based on local climate followed by a performance evaluation of an optimized configuration of the DSF as compared with a single skin façade. There are countless possibilities and combination of paraments which can yield similarly beneficial designs owing to their interdependencies as explained in the previous chapter. Here, only one or two such possible designs are presented and evaluated. The evaluation is based on the same markers as used in the previous chapter for the behavioural analysis. The details of the glazing system used in the single skin façade can be found in *Appendix E*. Each façade is assumed to be 3 m in height and the simulations were made for a façade length of 10 m. A brief description of the climate and topology of each site is given prior to the recommendations and optimized design to provide the climatic context.

In order to facilitate a more practical design approach to the DSF the following restrictions are imposed on the façade configurations for the purpose of this study:

I. Maximum cavity width of 1.3 m and a minimum of 0.3 m.
II. The external envelope must have a glazing thickness of at least 6mm for structural safety.
III. The total visible light transmission for the DSF system must be at least 0.5. This is to ensure adequate daylight is available for the occupants.

6.1 New Delhi

6.1.1 Climatic Overview

The climate of New Delhi has already been extensively discussed in the previous chapter *(ref. Sec. 5.1)*. The key features for design consideration are the higher latitude, above 23.5^0 N, which dictates that there will be negligible direct solar radiation on the North façade. Further, the maximum solar radiation incident on the South façade is during winters, which can potentially lead to overheating issues despite the relatively lower air temperatures.

6.1.2 Recommendations

New Delhi's climate has cold winters and very hot summers, hence there is a high potential to take advantage of the malleable thermal behaviour of the DSF.

For a South, East or West facing façade, a larger cavity width would be more beneficial as compared to a narrower cavity since the additional width further increases the shading effect of the ceiling. Moreover, it will also decrease the risk of potential overheating in winters.

The ventilation rate can be lowered (less than 40 AC/hr) owing to the larger cavity width. Of course, if the cavity width is made smaller a higher ventilation rate would be needed. A maximum of 80 AC/hr is the highest recommended ventilation rate, beyond which additional benefits will be insignificant.

Glazing selection must be made to reduce solar heat gains at the external envelope in order to mitigate overheating while the inner envelope must possess an adequate U-value to reduce heat loss during winters. Further, a lower U-value will also combat the thermal discomfort that may accompany periods where overheating in the cavity is unavoidable.

For a North oriented façade, the DSF does not seem to provide any significant advantageous behaviour with the primary influencer being the glazing selection which can potentially be adapted to a suitable glazing selection in a single skin façade as well. Hence, a North oriented DSF cannot be recommended in New Delhi. If indeed a DSF is desired regardless, a clear external envelope to maximize daylight entry, which may be limited due to lack of direct solar radiation, can be employed. Cavity width selection can be done as per ease of construction and maintenance as it has minimal effect on performance. The ventilation rate can be kept low due to its lack of influence on the thermal behaviour in this orientation

as well as due to low overheating risk. The inner glazing, as in the other orientations can be selected to increase thermal performance during winters, hence a lower U-value would be beneficial.

6.1.3 Design Optimization

One possible optimized configuration of the DSF is presented below in *Table 6.1*.

Table 6.1: Optimized facade properties for New Delhi

PROPERTY	VALUE
Façade depth	1.3m
Ventilation rate	1200m³/hr (30.5 AC/hr)
External Envelope	Single glazing, 6mm, tinted
Internal Envelope	Double-glazing, 9/12/3, low-E, Argon gas

In addition to the above-mentioned properties, the set point for activating the mechanical ventilation was decreased from 15◦C to 10◦C owing to the higher risk of overheating in winters due to more direct solar radiation on the façade.

For the South façade, this configuration results in roughly a 66% reduction in heat gain as compared to the base configuration while heat loss was reduced by 38%. The risk of overheating in the cavity was increased as compared to the base configuration with 318 hrs of cavity air temperature above 40◦C as compared to 57 hours. However, the hours with innermost glazing surface temperature above 28 ◦C was reduced by roughly half to 1020 hrs. Thermal comfort was however never compromised with glazing temperatures never exceeding 45◦C in either of the configurations.

To compensate for the higher cavity air temperatures a higher ventilation rate was implemented but its effects were found to be minimal. A better solution may be to have reflective glazing, but this would be a trade-off against daylight quality.

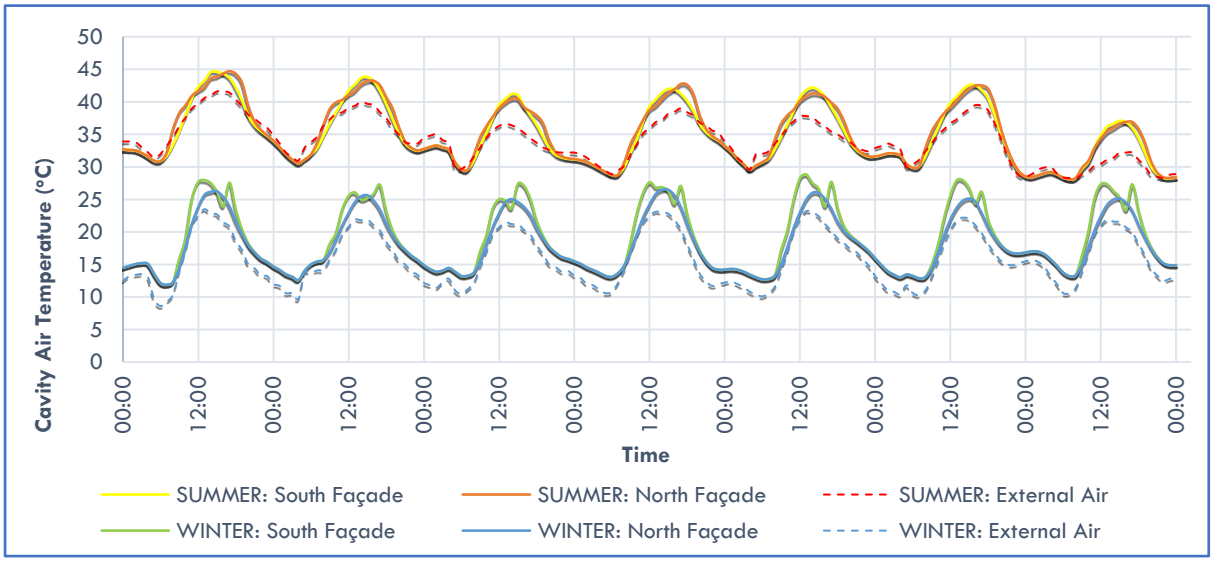

Figure 6.2: Cavity air temperature for the optimized DSF in the north and south orientations (colour coded) for New Delhi

6.1.4 Performance Evaluation

Table 6.2 compares the various performance parameters for the proposed optimized DSF configuration with those of the single skin façade for three different orientations, namely North, South and East. The total heat gain at each orientation is reduced for the DSF primarily due to a decrease in the solar heat gain. This can be credited to the added shading from the cavity depth and venetian blind system present within the cavity. It is interesting to note that the DSF increases the surface heat gain when compared with a single skin albeit, the total heat gain is still less. Hence, one can infer that the DSF can aid in reducing yearly cooling loads when compared to a single skin façade but that comes at the cost of a minor reduction in the level of thermal comfort due to the overheating effect in the cavity and higher surface temperatures.

The maximum benefit for reducing cooling loads is observed in the South oriented façade with a reduction of 46% in the total heat gain annually. The East oriented façade also showed a significant decrease in total heat gain at 41% while the North oriented façade showed the least benefit, at only a 16% reduction. All orientations resulted in an almost equal performance in winter conditions, with a roughly 25% reduction in heat loss annually.

Table 6.2: Comparing the proposed optimized DSF with a single skin facade for different orientations in New Delhi. **NOTE:** *Façade of 10m length and 3m in height is taken.*

Details		Total Heat Gain (kWh)	Total Heat Loss (kWh)	Solar Heat Gain (kWh)	Surface Heat Gain (kWh)	Hours with glazing surf above 45 °C	Hours with glazing surf above 28 °C
South	Double Skin	4115	619	2264	1852	0	1020
	Single Skin	7632	843	6007	1625	0	768
	% Reduction	46.1	26.6	62.3	-13.9	0	-32.8
North	Double Skin	2927	664	1520	1407	0	850
	Single Skin	3499	868	2310	1189	0	593
	% Reduction	16.3	23.5	34.2	-18.3	0	-43.3
East	Double Skin	3877	629	2105	1777	0	1121
	Single Skin	6591	844	5085	1506	0	883
	% Reduction	41.2	25.5	58.6	-17.7	0	-26.9

The temperatures of the innermost glazing surface paints a poorer picture for performance evaluation. In all orientations, there is a significant increase in the number of hours with glazing temperature above 28°C. The North façade, suffering the most with an increase of 43%. This coupled with its less impressive reduction in heat gain reinforces the recommendation of avoiding the use of North facing DSF systems in New Delhi. This increase in glazing temperature is however not high enough to negatively impact thermal comfort. No additional benefit can be drawn in this respect as the single skin façade and DSF, both never have inner surface temperatures above 45°C. In neither of the cases, the DSF or single skin was the innermost glazing surface temperature ever below 16°C either. Hence thermal comfort during winter was not of paramount consequence.

6.1.5 Summary

The advantages of the proposed DSF configuration for a reduction in cooling and heating energy demand has been well established for the South and East facing façades. Given the similarity in external conditions for the East and West oriented façade, it can be well argued that the DSF system will be equally beneficial in a West facing façade as well. In the North, it gives the least additional benefit although it would still perform better than a single skin for a reduction in energy consumption for cooling and heating.

No advantage to thermal comfort can be derived from the DSF as the single skin façade itself provides adequate levels of thermal comfort which are matched equally well by the DSF. However, the DSF does show relatively higher temperatures of the inner-most glazing surface as compared with the single skin albeit, never at risk of deteriorating thermal comfort.

Further optimization of the design with reflective glazing on the external envelope or drastically higher ventilation rates within the cavity may provide mitigative strategies for cavity overheating. The former being of consequence to daylight quality indoors and the latter expected to have only minor benefits.

6.2 Chennai

6.2.1 Climate Overview

Chennai's climate is tropical wet and dry (Köppen climate classification Aw). Being located on the coast as well as the thermal equator (defined by the set of locations having the highest mean annual temperature at each longitude around the globe), provides it with a climate that lacks variation

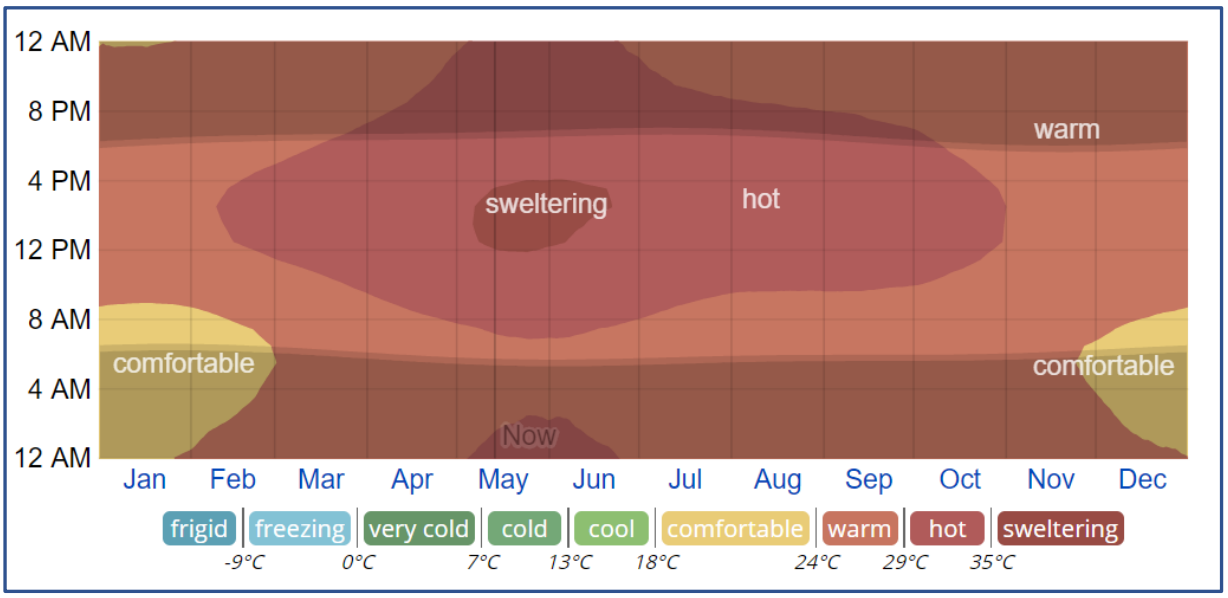

Figure 6.3: Chennai: The average hourly temperature in Chennai, colour coded into bands. The shaded overlays indicate night and civil twilight. The horizontal axis is the day of the year, the vertical axis is the hour of the day, and the colour is the average temperature range for that hour and day.
Source: **https://weatherspark.com/y/110123/Average-Weather-in-Chennai-India-Year-Round**

throughout the year although the average temperatures are consistently hot. Summer temperatures vary between 35°C to 40°C while winter temperatures are between 20°C to 25°C. *Fig. 6.3* gives an insight into the hourly variations in temperatures throughout the year.

The maximum daylight hours in June is roughly 13 hours whereas the minimum in December is approximately 11 hours and 30 minutes. Chennai's location at 13.1°N, 80.3°E *(ref. Fig. 6.4)*, which lies between the Tropic of Cancer and the Equator, results in a situation where during peak summers the sun path shifts from South to North of Chennai. Hence, when it comes to building façades, it is the North façade which receives higher direct solar radiation as opposed to the South façade.

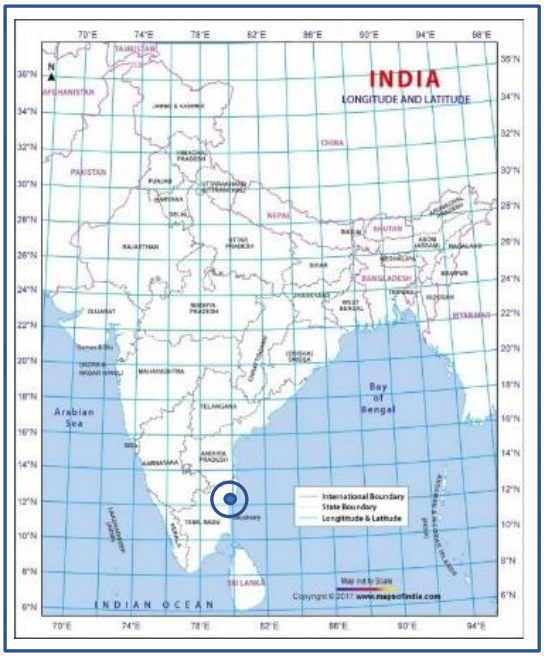

Figure 6.4: Location of Chennai on political map of India with longitudes and latitudes. Indicated at centre of target

However, due to high sun altitudes, the angle of incident on the North and South façade is relatively large, resulting in a lower intensity of incident radiation.

6.2.2 Recommendation

With respect to thermal and energy needs for buildings, Chennai's climate results in cooling needs mostly, with very little to none for heating.

It is reasonable to assume that any heating needs can be neglected as these will primarily be at night when offices are unoccupied. Further, free cooling may be beneficial at night to help reduce cooling loads during the day. Hence the façade design should be primarily geared to reduce heat gain. This would imply that the U-value of the inner envelope may be of less importance as compared with locations with more severe winters.

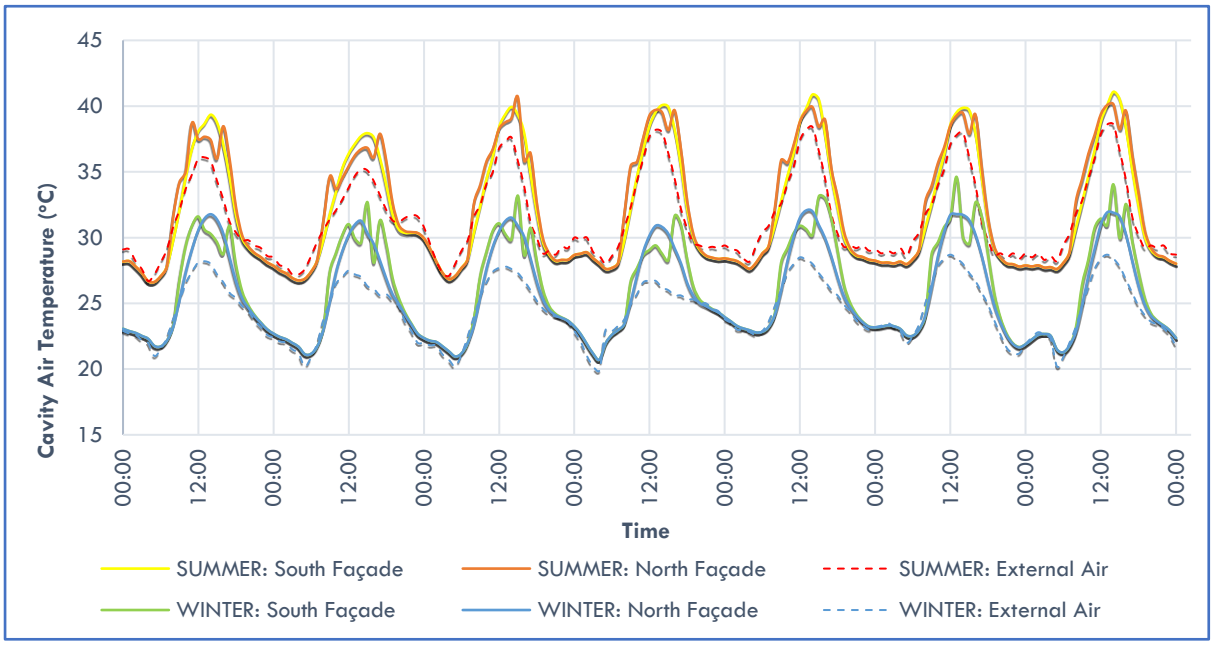

Figure 6.5: Cavity air temperature for the optimized DSF in the north and south orientations (colour coded) for Chennai

Due to higher sun altitudes throughout the year, it would be possible to opt for lower cavity widths with adequate ventilation as the self-shading effect of the cavity is amplified. However, given the somewhat linear relationship between decreasing heat gain and cavity width, a larger cavity width may also be justified.

The glazing selection for the external skin should be, as in the case of New Delhi, geared to reducing heat gain. Hence, a reflective or tinted external envelope should be selected. The inner double-glazing selection could be kept relatively simple. However, given the tendency for the cavity to overheat and thereby affect thermal comfort, a low-E coated external glazing light for the internal skin can be justified. This, however, will depend on the effectiveness of the ventilation rate on mitigating the excess heat deposited within the cavity and the temperature distribution on the inner envelope with respect to thermal comfort standards.

Unlike in New Delhi, the benefits of a DSF could be applied to any façade orientation in Chennai owing to the relative shifting of the sun path to the North and South throughout the year.

6.2.3 Design Optimization

Two potentially optimized configurations have been presented below *(table 6.3)*. Configuration A focusses on favouring a slightly wider cavity with a clear inner envelope glazing while configuration B uses a narrower cavity width but with a low-E coated inner envelope.

Table 6.3: Optimized facade properties for Chennai

PROPERTY	CONFIGURATION A	CONFIGURATION B
Façade width	0.5m	0.3m
Ventilation rate	1200m^3/hr (80 AC/hr)	1200m^3/hr (123 AC/hr)
External Envelope	Single glazing, 6mm, tinted	Single glazing, 6mm, tinted
Internal Envelope	Double-glazing, 4/16/4, clear, Argon gas	Double-glazing, 9/12/3, low-e, Argon gas
Visible Light Transmission	0.537	0.517

The setpoint for activation of the mechanical ventilation was kept at 15°C, this is of little consequence as temperatures rarely fall below 20°C. Hence, just as the control for the venetian blinds, the mechanical ventilation will be only depending on the solar load setpoint (250W/m^2 by default).

Both DSF configurations showed relatively minor changes in performances with respect to orientation. Reduction in total heat gain as compared with the base configuration was roughly 43% and 60% for configuration A and B respectively in all orientations, North, South and East.

In the North orientation, Configuration A performed poorer with respect to the temperature distribution in the inner envelope. The hours with the inner-most glazing temperature above 28°C was increased when compared with the base case and in the East and South orientation was only slightly better. Configuration B however, showed a significant decrease in this parameter but at the cost of an increased risk of overheating within the cavity.

Thermal comfort was however unaffected in all cases with the inner-most glazing temperature never dropping below 16°C nor exceeding 45°C in any of the orientations with either of the DSF configurations.

6.2.4 Performance Evaluation

Both configurations, A and B have been compared to the single skin façade via the various measurement parameters, the details of which are presented in *Table 6.4*.

Table 6.4: Comparing the proposed optimized DSFs with a single skin facade for different orientations in Chennai.
NOTE: *Façade of 10m length and 3m in height is taken.*

Details		Total Heat Gain (kWh)	Total Heat Loss (kWh)	Solar Heat Gain (kWh)	Surface Heat Gain (kWh)	Hours with glazing surf above 45 °C	Hours with glazing surf above 28 °C
South	Single Skin	6141	51	4076	2065	0	0
	Config A	6148	61	2973	3174	0	815
	% Reduction	-0.1	-18.5	27.1	-53.7	0	-INF
	Config B	4300	36	2022	2278	0	0
	% Reduction	30	29.9	50.4	-10.3	0	-INF
East	Single Skin	7136	51	4976	2160	0	45
	Config A	6833	61	3449.5	3383	0	1274
	% Reduction	4.3	-18.5	30.7	-56.6	0	-2731.1
	Config B	4797	36	2356	2441	0	114
	% Reduction	32.8	29.7	52.7	-13	0	-153.3
North	Single Skin	4817	51	2898	1919	0	0
	Config A	5547	61	2598	2950	0	719
	% Reduction	-15.2	-19.2	10.4	-53.7	0	-INF
	Config B	3879	37	1751	2128	0	4
	% Reduction	19.5	28.9	39.6	-10.9	0	-INF

Configuration A leads to minor advantages in terms of heat gain in the East orientation and performs poorer than the single skin façade in the North and South orientations. On the other hand, Configuration B shows reasonable benefit to reducing heat gain in all orientations, with similar reduction of 30% and 32% in the South and East orientations respectively while the reduction in the North façade is 20%. It is important to note however that in both cases the reduction in total heat gain is primarily due to a reduction in solar gains while surface gains are actually increased.

Thermal comfort as in the case of New Delhi is never compromised with the inner-most glazing temperature always remaining within the required range. The temperature distribution of the inner envelope, however, is poorer in both the DSF configurations with Configuration A drastically increasing the number of hours with inner-most glazing surface temperature above 28°C. Configuration B is relatively much better, however still poorer than the single skin façade. A wider cavity width of 1.2m was also simulated with Configuration A, however, it had a negligible effect on reducing the overheating risk.

6.2.5 Summary

The advantageous use of a DSF to reduce heat gain in Chennai has been verified. This, however, was only a viable case for configuration B and not configuration A when compared to the single skin façade. Hence the importance of a low-E coated inner glazing cannot be undermined. Chennai's location allows for the use of a suitably designed DSF in all orientations as a reasonable reduction in heat gain is seen

regardless of orientation in configuration B, albeit the results in the South and East facades are more impressive than in the North.

Thermal comfort is never compromised. However, the inner-most glazing temperatures are higher for the DSF as compared with the single skin.

There appear to be very limited options in order to reduce the overheating risk in Chennai with wider cavity widths and increased ventilation rate having minimal effects. Glazing properties seem to be the main influencer for the viability of a DSF.

6.3 Kathmandu (Nepal)

Kathmandu has been chosen as one of the sites for this study despite its location outside India, in Nepal, because the required weather data for Indian cities located at higher altitudes in the Himalayan Ranges in the North of India were not available. Kathmandu's climate represents that of many colder towns and cities located at high altitudes in North India. This provides an opportunity to compare the DSFs advantages in warmer climates to those observed in relatively cooler climates subject to similar solar radiation.

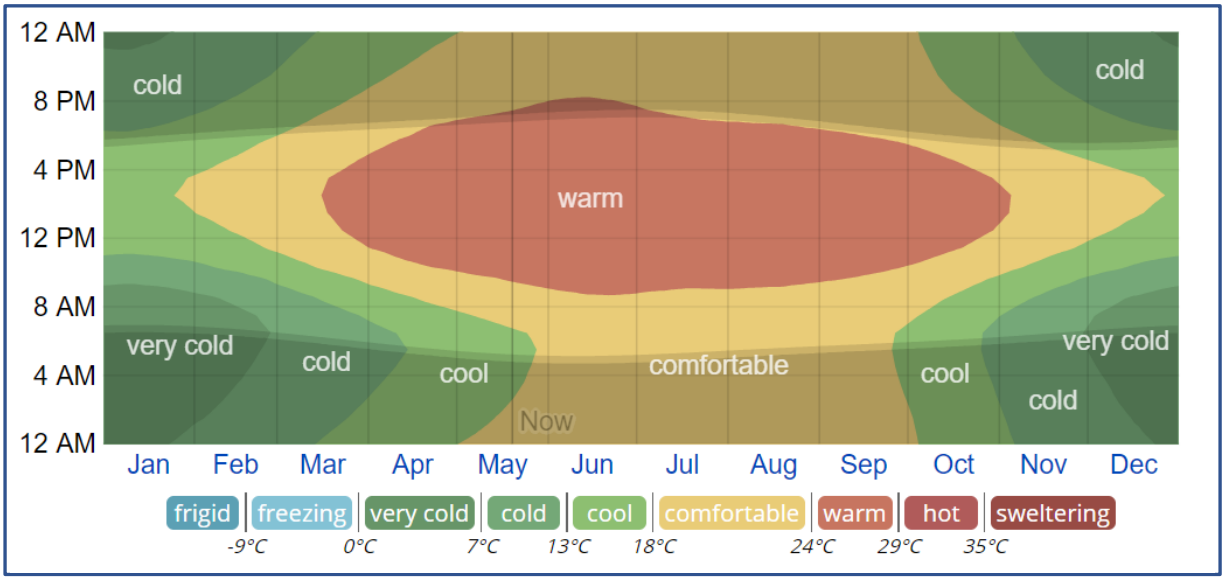

Figure 6.6: Kathmandu: The average hourly temperature in Kathmandu, colour coded into bands. The shaded overlays indicate night and civil twilight. The horizontal axis is the day of the year, the vertical axis is the hour of the day, and the colour is the average temperature range for that hour and day.
***Source*:** **https://weatherspark.com/y/111107/Average-Weather-in-Kathmandu-Nepal-Year-Round**

6.3.1 Climate Overview

Kathmandu is located in the Kathmandu Valley and has an average elevation of 1400m above sea level. Under Köppen's climate classification, portions of the city with lower elevations have a humid subtropical climate (Cwa), while portions of the city with higher elevations generally have a subtropical highland climate (Cwb). Winter temperatures can drop quite low to below zero degrees occasionally while summer temperatures vary between 25°C to 28°C *(ref. Fig. 6.6)*.

Daylight varies with a maximum of almost 14 hours during June and a minimum of 10 hours and 30 minutes in December. Located above the topic of Cancer, at 27.7°N, 85.3°E *(ref. Fig. 6.7)*, the solar radiation is primarily on the South facing façade while the North façade receives no direct solar radiation, even during peak summers. The high altitude leads to a situation where air temperature may be cool despite very high solar radiation intensities.

6.3.2 Recommendations

Kathmandu's climatic variation is like that of New Delhi, however with relatively cooler summer temperatures and slightly more severe winters. The daylight and solar radiation patterns are almost identical. Hence, a similar design strategy can be employed since both cooling and heating needs are present.

Cavity width is kept large to reduce the risk of overheating at periods of high solar radiation. A low-E coated glazing system for the inner envelope should be employed for decreasing heat loss. The external envelope must be made tinted or reflective, although a case could be made for clear glazing as a trade-off between the heating and cooling needs. However, the decrease in cooling needs from tinted glazing far exceeds the decrease in heating needs of using clear glazing instead. Therefore, it would be more appropriate to use a tinted or reflective external skin to reduce the overall energy consumption *(ref. Appendix I)*.

Table 6.5: Optimized DSF configuration for Kathmandu

PROPERTY	VALUE
Façade width	1.3m
Ventilation rate	1200m^3/hr (30.5 AC/hr)
External Envelope	Single glazing, 6mm, tinted
Internal Envelope	Double-glazing, 9/12/3, low-e, Argon gas

The ventilation rates beyond 80AC/hr yields insignificant improvements. A lower ventilation rate may also be successful due to the cooler external air temperatures. However, owing to the lower temperatures in winters the ventilation set point should be reduced to below 15°C to ensure activation of the mechanical ventilation.

6.3.3 Design Optimization

One possible optimized configuration is presented in *Table 6.5*. In addition, the ventilation setpoint is reduced to 10°C. The presented configuration yields a significant improvement in all orientations for a reduction in heat gain with roughly 60% in the South, East and North façades when compared with the base configuration. The heat loss is also equally decreased in all orientations at roughly 35% each.

As expected, the cavity overheating risk is increased, however, the thermal comfort is never compromised in either the base or optimized configuration. Further, the temperature

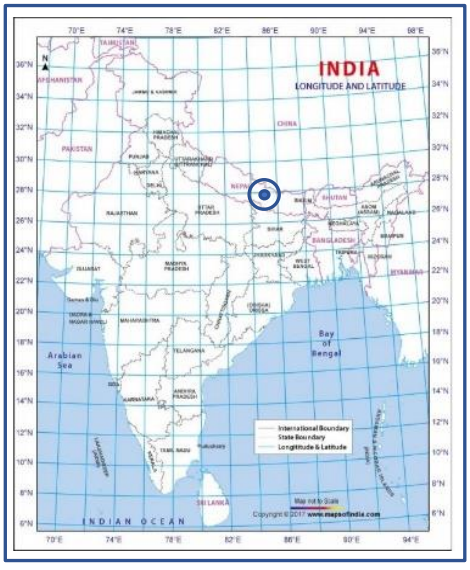

Figure 6.7: Location of Kathmandu on political map of India with longitudes and latitudes. Indicated at centre of target

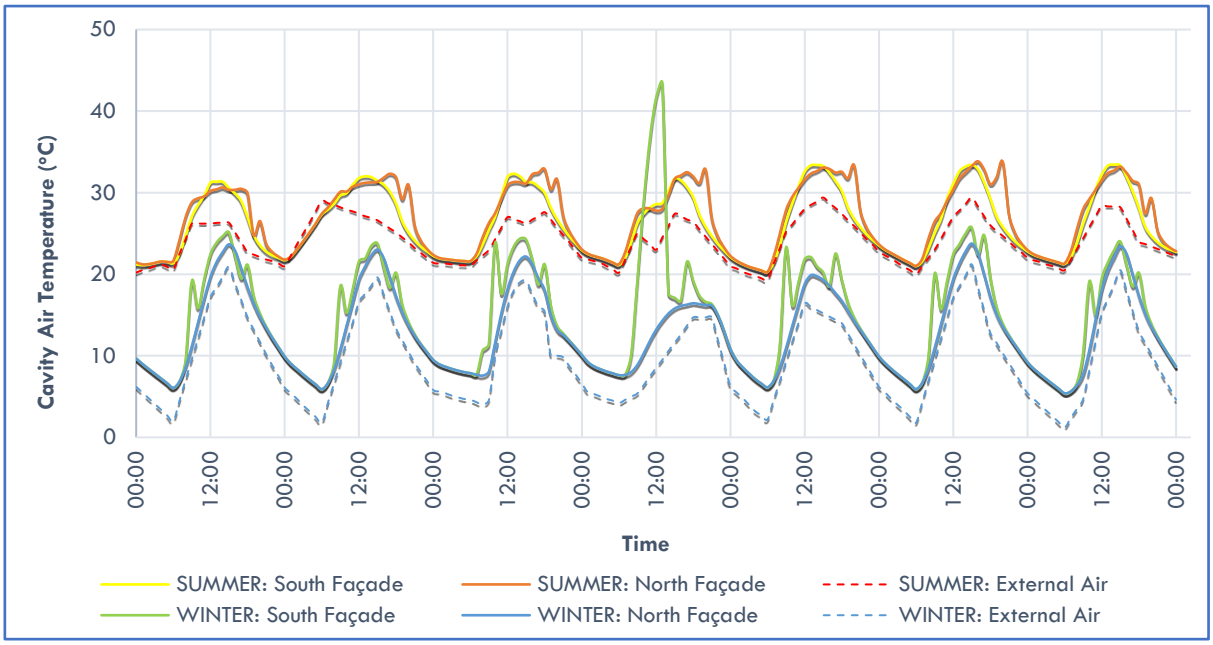

Figure 6.8: Cavity air temperature for the optimized DSF in the north and south orientations (colour coded) for Kathmandu

distribution of the inner envelope is made more favourable with a fewer number of hours during which the inner-most glazing is above 28°C.

The temperature spikes seen in the cavity air during winter *(ref. Fig. 6.8)* can be attributed to poor performance of the ventilation control. The lower air temperature (below 10°C) results in the ventilation of the cavity being switched off. This, coupled with the high solar loads in winter leads to high temperatures in the cavity.

6.3.4 Performance Evaluation

The above-presented configuration has been compared to the single skin façade via the various measurement parameters and the details are presented in *Table 6.6*. The effectiveness of the DSF for reducing heat gain is apparent in the South and East orientations while that of the North is less impressive. Although total heat gain is reduced by as much as 50%, the surface heat gain is increased by a significant amount, especially in the East façade. For both the North and East SS façade it is observed that the surface component of heat gain is negative, i.e., despite net heat gain to the room the surface component is a heat loss with heat gain primarily being attributed by the solar radiation.

Heat loss is reduced by 25% at all orientations.

Thermal comfort is never compromised in either the single or DSF with inner-most glazing surface temperatures always above 16°C and below 45°C. Unlike in the previous sites analysed, a higher temperature distribution on the inner-most glazing surface is not observed to a significant effect. Almost no hours during which the inner-most glazing surface is above 28°C are found. Both the SS and DSF perform adequately in terms of thermal comfort and maintain lower glazing temperatures as compared with other sites throughout the year.

Table 6.6: Comparing the proposed optimized DSF with a single skin facade for different orientations in Kathmandu. ***NOTE*:** *Façade of 10m length and 3m in height is taken.*

Details		Total Heat Gain (kWh)	Total Heat Loss (kWh)	Solar Heat Gain (kWh)	Surface Heat Gain (kWh)	Hours with glazing surf above 45 °C	Hours with glazing surf above 28 °C
South	Double Skin	3095	1103	2440	654	0	0
	Single Skin	6568.3	1507	6330	237	0	0
	% Reduction	52.9	26.8	61.5	-175.5	0	0
East	Double Skin	2730	1088	2246	483	0	0
	Single Skin	4674	1478	4682	-8	0	0
	% Reduction	41.6	26.4	52	-6007	0	0
North	Double Skin	2027	1239	1681	346	0	5
	Single Skin	2627	1632	2710	-83	0	0
	% Reduction	22.8	24	38	-516.8	0	-INF

6.3.5 Summary

The DSF shows significant benefit to in the South and East façade in reducing both heat gain and heat loss. For the North façade, the decrease in heat gain is almost half as compared to the other orientations. However, the decrease in heat loss is equally at par with the improvements in the other orientations.

Thermal comfort is of little consequence as both the single skin as well as DSF perform adequately well with respect to the recommended temperature distribution of the inner-most glazing surface.

Despite the lower external air temperatures, ventilation rate is still only effective till a limit of 80AC/hr for the presented cavity width *(ref. Appendix I)*. Further improvements to reduce heat gain and cavity overheating risk can only be influenced by suitable glazing selection.

The temperature setpoint for the ventilation was seen to be too high. A lower value, below 10°C, should be employed to ensure proper activation of ventilation in peak winter conditions. It may also be important in this respect that the temperature set is varied perhaps monthly to accommodate the changes in temperature and intensity of incident solar radiation.

6.4 Jaisalmer

6.4.1 Climate Overview

Jaisalmer is located in West India well within the Thar Desert *(ref. Fig. 6.10)* as a result of which the climate is typical of a hot desert (Köppen climate classification BWh). There is a large variation in daily temperatures, almost 20°C. In summer, daytime temperatures can reach as high as 50°C while the night time temperatures are around 25°C. During winters, the temperatures ranges between 23°C in the day and 5°C at night. *Fig. 6.9* provides a brief overview of the daily temperature variations throughout the year.

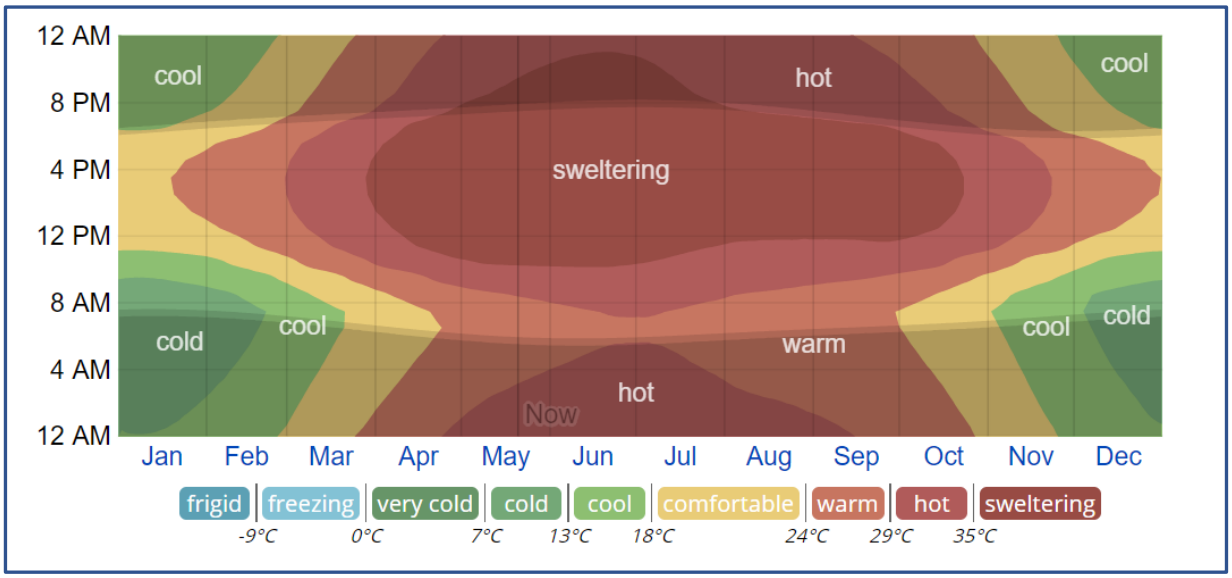

Figure 6.9: Jaisalmer: The average hourly temperature in Kathmandu, colour coded into bands. The shaded overlays indicate night and civil twilight. The horizontal axis is the day of the year, the vertical axis is the hour of the day, and the colour is the average temperature range for that hour and day.
***Source*: https://weatherspark.com/y/106969/Average-Weather-in-Jaisalmer-India-Year-Round**

Daylight hours vary from a maximum of 14 to a minimum of 10 hours and 30 minutes. Located just above the Tropic of Cancer, the direct solar radiation is incident on the South façade for the majority of the year. During peak summers, the high solar altitudes will result in lower incident solar radiations on the South façade.

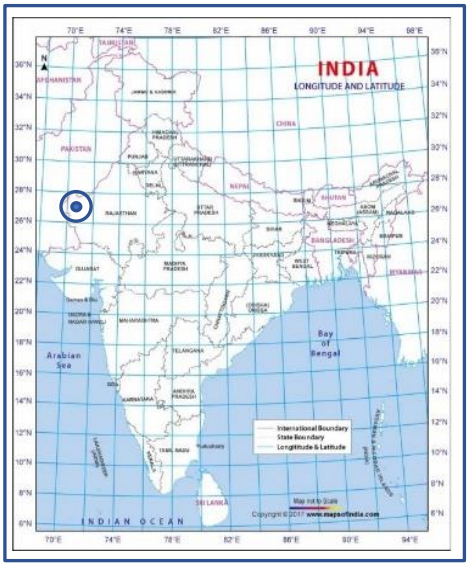

Figure 6.10: Location of Jaisalmer on political map of India with longitudes and latitudes. Indicated at centre of target.

6.4.2 Recommendations

Jaisalmer presents itself as an ideal location for a DSF owing not only to its high seasonal variation but also daily variation in temperatures.

A tinted or reflective external envelope is almost certainly needed. The combination of high solar loads and hot external air temperatures during peak summer require a focussed

approach to reduction in heat gain. A wider cavity will facilitate this by increasing the self-shading effect along with increased robustness against the overheating risk. On the other hand, the inner envelope must possess a suitably low U-value for adequate performance during winter conditions.

The North façade, as in the case of New Delhi, may not benefit significantly due to the absence of significant direct solar radiation owing to the city's location.

Lastly, ventilation rates must be selected taking into consideration the cavity width, 80AC/hr would be suitable for most cavities as there is little benefit to higher rates of ventilation, however with a wider cavity, it may be decreased *(ref. Appendix I)*.

6.4.3 Design Optimization

One possible optimized configuration of the DSF is presented in *Table 6.7*.

Table 6.7: Optimized DSF configuration for Jaisalmer

PROPERTY	VALUE
Façade width	1.3m
Ventilation rate	1200m³/hr (30.8 AC/hr)
External Envelope	Single glazing, 6mm, tinted
Internal Envelope	Double-glazing, 9/12/3, low-e, Argon gas

The configuration is the same as that for New Delhi, however, due to the higher daily variation in temperatures the ventilation set point was kept at 15°C as opposed to 10°C in the case of New Delhi. The temperature setpoint is seen to work adequately as no unusually high temperatures in the cavity are seen *(ref. fig. 6.11)*.

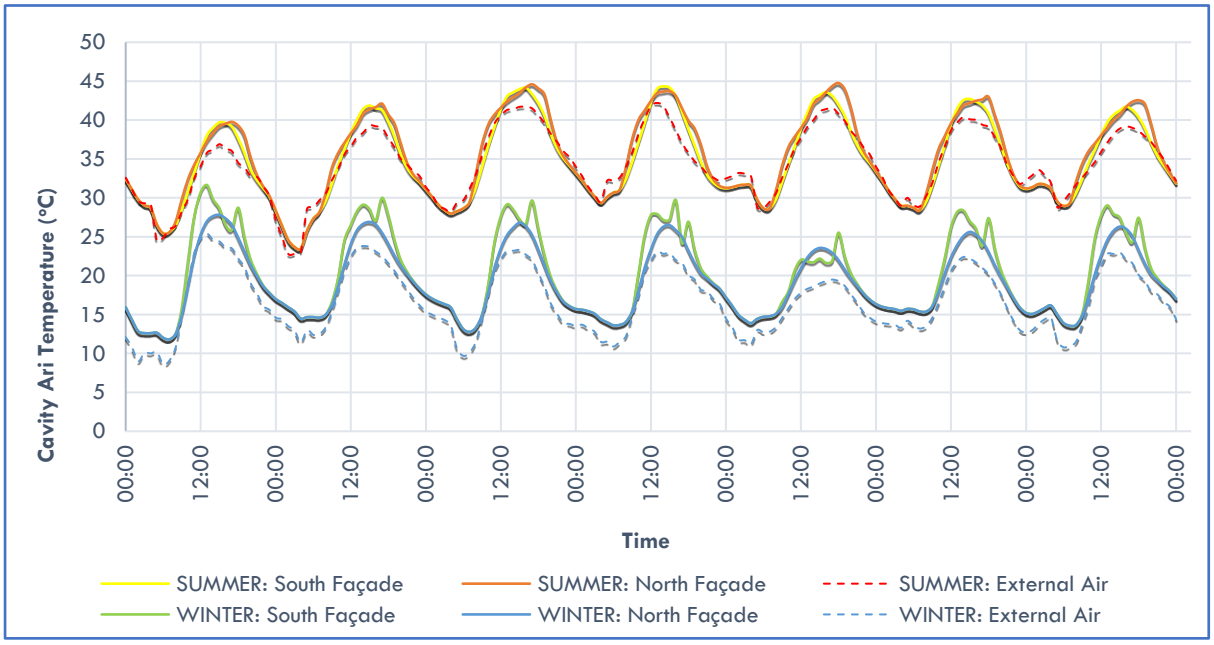

Figure 6.11: Cavity air temperature for the optimized DSF in the north and south orientations (colour coded) for Jaisalmer

The presented configuration yields a significant improvement in all orientations when compared to the base configuration. Reduction in heat gain is roughly 60% in the South, East and North façades. The reduction in heat loss is also similar at each orientation at roughly 37%.

As expected, the cavity overheating risk is increased, especially in the North façade. However, the thermal comfort is never compromised in either the base or optimized configuration. Further, the temperature distribution of the inner envelope is made more favourable with a fewer number of hours during which the inner-most glazing is above 28°C.

6.4.4 Performance Evaluation

Significant reduction in heat gain can be observed in the South and East façades when comparing the DSF to the single skin with a decrease of 45% and 40% in the South and East orientations respectively. The benefit to the North façade is relatively much less at 16% reduction in heat gain. The reduction in heat loss is the same for all orientations at roughly 25% *(ref. Table 6.8)*.

As in the previous sites, a relative increase in the temperature of the inner-most glazing surface is observed with a greater number of hours with glazing surface temperature above 28°C. However, this increase is never significant enough to compromise thermal comfort for warm walls. For winter conditions, the glazing surface temperature never drops below 16°C in either of the façade systems. Hence, thermal comfort is maintained for both the façade systems in all orientations.

Table 6.8: Comparing the proposed optimized DSF with a single skin facade for different orientations in Jaisalmer. ***NOTE:*** *Façade of 10m length and 3m in height is taken.*

Details		Total Heat Gain (kWh)	Total Heat Loss (kWh)	Solar Heat Gain (kWh)	Surface Heat Gain (kWh)	Hours with glazing surf above 45 °C	Hours with glazing surf above 28 °C
South	Double Skin	4749	-518	2462	2286	0	1318
	Single Skin	8729	-716	6636	2093	0	983
	% Reduction	45.6	27.7	62.9	-9.3	0	-34.1
East	Double Skin	4792	-525	2540	2251	0	1328
	Single Skin	7944	-716	5957	1987	0	945
	% Reduction	39.7	26.6	57.3	-13.3	0	-40.5
North	Double Skin	3294	-561	1547	1747	0	614
	Single Skin	3942	-739	2353	1588	0	452
	% Reduction	16.4	24.1	34.3	-10	0	-35.8

6.4.5 Summary

The DSF shows a significant benefit for the South and East orientations, specifically for decreasing heat gain when compared to the single skin envelope. Benefits to the reduction in heat loss are consistent in all orientations, however less impressive than the advantages seen in the reduction for heat gain.

Thermal comfort is not compromised for either warm or cool walls in either the single or double skin façade.

6.5 Bhopal

6.5.1 Climate Overview

Bhopal, located in central India, has a humid subtropical climate (Köppen climate classification Cwa). Peak temperatures can rise to above 40°C in May and winter temperatures can drop close to 0°C in the month of January. The monsoon season plays a crucial role in lowering the temperatures during the months of July and August after which there is again an increase in temperatures till October until winter begins. *Fig. 6.12* provides a brief overview of the daily temperature variations throughout the year.

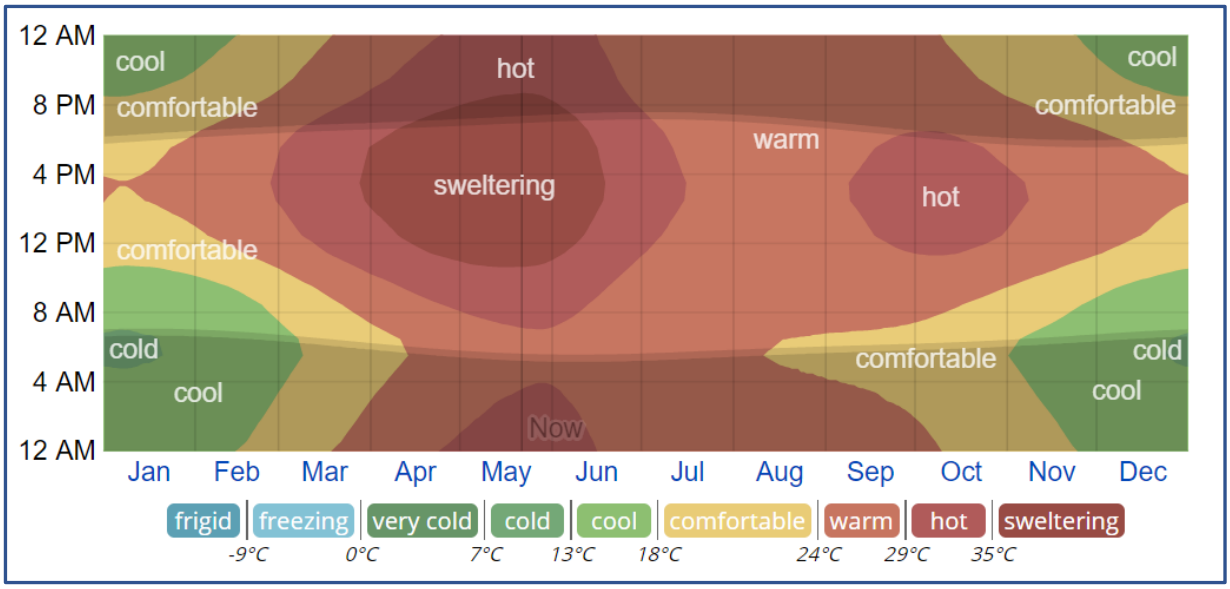

Figure 6.12: Bhopal: The average hourly temperature in Kathmandu, colour coded into bands. The shaded overlays indicate night and civil twilight. The horizontal axis is the day of the year, the vertical axis is the hour of the day, and the colour is the average temperature range for that hour and day.
***Source*:** https://weatherspark.com/y/109103/Average-Weather-in-Bhopal-India-Year-Round

Daylight varies between a maximum of 13 hours and 30 minutes in June and a minimum of roughly 10 hours and 30 minutes in December.

The tropic of Cancer is located just above Bhopal which lies at 23.26°N *(ref. Fig. 6.13)*. This would imply a low level of direct solar radiation on the North and South façade during peak summer due to the high solar altitudes. The maximum solar radiation would be in the winter time, on the South façade.

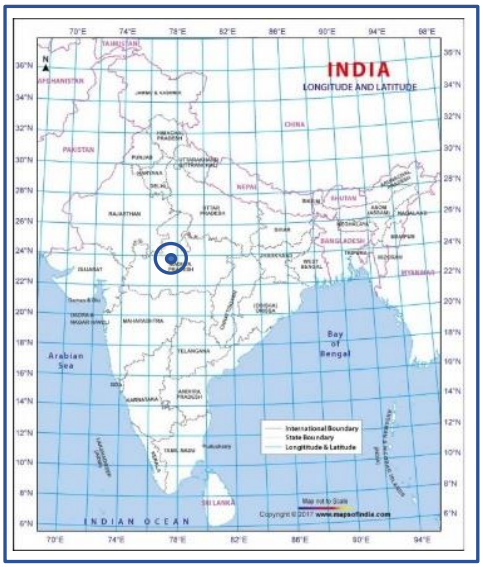

Figure 6.13: Location of Bhopal on political map of India with longitudes and latitudes. Indicated at centre of target

6.5.2 Recommendations

Bhopal's climate is like that of New Delhi in many ways. The main difference being a milder summer due to the monsoons

and the higher solar altitudes during summertime owing to the lower latitude.

Looking at the temperature range which varies from cold in winters to hot in summers the glazing selection for the external envelope should be geared to reducing heat gain while the inner envelope should provide an adequate U-value for winter conditions. A tinted or reflective external glazing would benefit the most for reducing heat gain and controlling the risk of cavity overheating. While a low-E coated double glazing on the inner envelope will help to control heat loss as well as nullify any detrimental effects from the overheating in the cavity.

Cavity width can be kept moderate, the higher solar altitudes in summer would enhance the self-shading effect of the cavity. Larger cavity widths offer little advantage in improved performance while smaller cavity width may be much more prone to overheating in winters (ref appendix I).

Increase in ventilation rate above 80AC/hr would provide little benefit in reducing heat gain, the only benefit usually observed is a reduction in the temperature of the inner-most glazing surface but as the temperature never exceeds the limit to maintain thermal comfort it would not be of any particular benefit to the user. Hence, a ventilation rate of 80AC/hr or lower should suffice based on the cavity width.

6.5.3 Design Optimization

Table 6.9 provides the details of a proposed optimized design. This configuration yields a significant improvement when compared to the base configuration in the reduction of heat gain at almost 60% in all orientations while the heat loss is reduced by roughly 35% in all orientations. A large portion of the improvement in reducing total heat gain can be attributed to the reduction of solar heat gain which was reduced by almost 75% in each orientation.

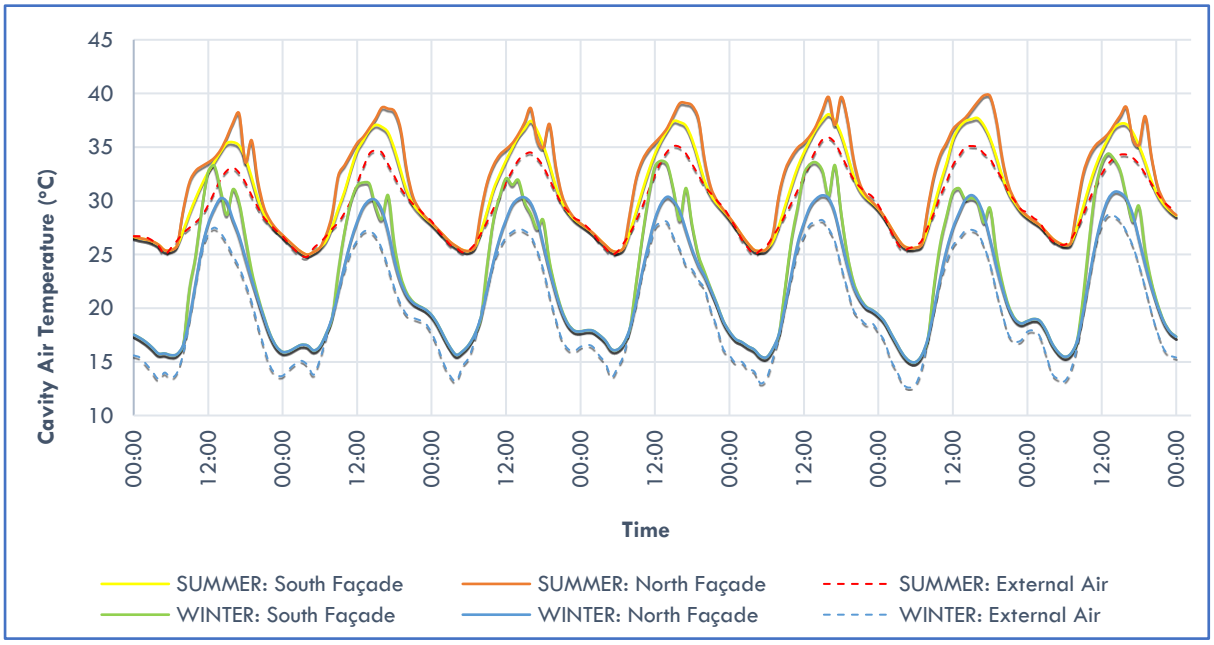

Figure 6.14: Cavity air temperature for the optimized DSF in the north and south orientations (colour coded) for Bhopal

The cavity overheating risk, as in all other sites, was increased. This increase was most pronounced in the North façade owing to very low risk in the base case which drastically increases in the presented optimized configuration. However, the thermal comfort of occupants is never affected since the temperature of the inner-most glazing surface is always within the set limits for warm and cool walls.

Table 6.9: Optimized DSF configuration for Bhopal

PROPERTY	VALUE
Façade width	0.8m
Ventilation rate	1200m^3/hr (50 AC/hr)
External Envelope	Single glazing, 6mm, tinted
Internal Envelope	Double-glazing, 9/12/3, low-E, Argon gas

6.5.4 Performance Evaluation

The optimized DSF yields the most improvement when compared to the single skin façade in the South and East façades. A reduction in total heat gain of roughly 40% is observed in each case. For the North façade, this effect is less pronounced at only 16%. On the other hand, the heat loss is reduced by roughly 25% at each orientation *(ref. Table 6.10)*.

Although the time during which the inner-most glazing surface is above 28°C is increased for the DSF in relation to the single skin this increase in the temperatures is never high enough to compromised thermal comfort. In both the single skin and DSF, thermal comfort is always maintained for cool and warm walls.

Table 6.10: Comparing the proposed optimized DSF with a single skin facade for different orientations in Bhopal

Details		Total Heat Gain (kWh)	Total Heat Loss (kWh)	Solar Heat Gain (kWh)	Surface Heat Gain (kWh)	Hours with glazing surf above 45 °C	Hours with glazing surf above 28 °C
South	Double Skin	4255	468	2442	1812	0	728
	Single Skin	7518	650	5990	1528	0	411
	% Reduction	43.4	27.9	59.2	-18.6	0	-77.1
East	Double Skin	4427	476	2591	1836	0	745
	Single Skin	7348	652	5858	1489	0	547
	% Reduction	39.7	26.9	55.8	-23.3	0	-36.2
North	Double Skin	3005	492	1634	1371	0	372
	Single Skin	3604	661	2497	1106	0	263
	% Reduction	16.6	25.4	34.6	-23.9	0	-41.4

6.5.5 Summary

The DSF has the potential for significant improvement when applied to the South and East façade of a building in Bhopal. The benefits to the North façade are less impressive and may not justify the use of such a complex façade system. Despite the overheating risk, the thermal comfort is not compromised at any time for warm walls. This however is not an additional advantage as the same is also accomplished by the single skin façade.

6.6 Kolkata

6.6.1 Climate Overview

Kolkata, being located on the coast towards the Bay of Bengal has a climate with moderate to warm temperatures throughout the year. The climate is typical of a tropical wet-and-dry (Köppen climate classification Aw). Peak summer temperatures, usually around May can go as high as 35°C while the minimum in winters is just below 15°C. As in the case of Bhopal, there is a slight drop in temperatures after May due to the Monsoon season and the temperature variation remains roughly the same till winter

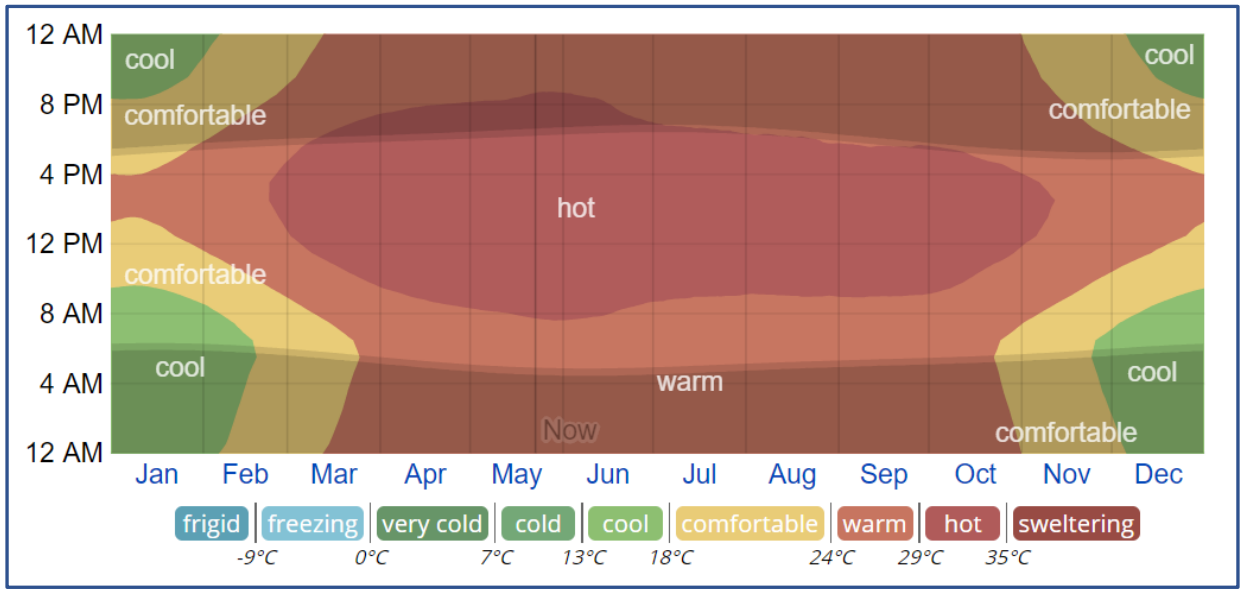

Figure 6.15: Kolkata: The average hourly temperature in Kolkata, colour coded into bands. The shaded overlays indicate night and civil twilight. The horizontal axis is the day of the year, the vertical axis is the hour of the day, and the colour is the average temperature range for that hour and day.
***Source*:** https://weatherspark.com/y/111532/Average-Weather-in-Kolkata-India-Year-Round

begins. *Fig. 6.15* gives a brief overview of the hourly temperature variations throughout the year.

Located just below the tropic of cancer *(ref. Fig. 6.16)*, the incident solar radiation on building façades facing both North and South would be considerably low during peak summers due to the high solar altitudes. Daylight variation is between 13 hours and 30 minutes in June to 10 hours and 45 minutes in December.

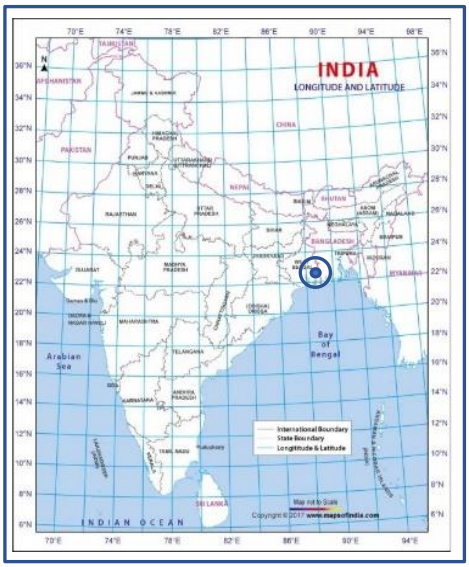

Figure 6.16: Location of Kolkata on political map of India with longitudes and latitudes. Indicated at centre of target

6.6.2 Recommendations

Due to the relatively milder climate throughout the year as opposed to the other sites considered in this study the

advantages derived from a DSF over a single skin may be limited.

The benefits of a DSF on the North façade will be less since there is lower incident solar radiation.

As the temperatures during winter are not particularly low it may suffice to proceed with clear inner glazing without a low-E coating, however, this may be inadequate in preventing the overheating of the cavity from affecting the heat gain into the room and the thermal comfort of the occupants.

A narrow to moderate cavity width can be suitable as solar altitudes are relatively high during summertime.

Ventilation rate can once again be set to roughly 80AC/hr as the added benefit for higher rates is minor. However, this may be reduced for wider cavities due to their increased robustness against overheating and potentially decrease air temperatures due to the self-shading.

6.6.3 Design Optimization

Two configurations were tested for this site. As in the case of Chennai, since there is no real need for heating design of the building a DSF with an inner envelope of clear double glazing and wider cavity width (configuration A) is compared with one with a low-E coated inner envelope and narrower cavity width (configuration B). Both configurations consist of a tinted external envelope *(ref. Table 6.11)*.

Table 6.11: Optimized facade properties for Kolkata

PROPERTY	CONFIGURATION A	CONFIGURATION B
Façade width	0.8m	0.3m
Ventilation rate	1200m^3/hr (50 AC/hr)	1200m^3/hr (123 AC/hr)
External Envelope	Single glazing, 6mm, tinted	Single glazing, 6mm, tinted
Internal Envelope	Double-glazing, 4/16/4, clear, Argon gas	Double-glazing, 9/12/3, low-E, Argon gas
Visible Light Transmission	0.537	0.517

Configurations A and B produce roughly, in all orientations, a 45% and 60% reduction in total annual heat gain when compared with the base configuration. The change in heat loss in negligible for configuration A, this can be attributed to the same inner envelope glazing system as in the base configuration. This reinforces the dependency of the reduction in heat loss on the U-value of the inner envelope. Configuration B reduces heat loss by roughly 36% in all orientations. However, given the site's climatic conditions the advantages from the reduction may be neglected from a practical perspective.

As expected, the cavity overheating risk is most for Configuration B and even in configuration A the risk is increased as compared with the base case, this may be attributed to the high absorptance of the tinted glazing.

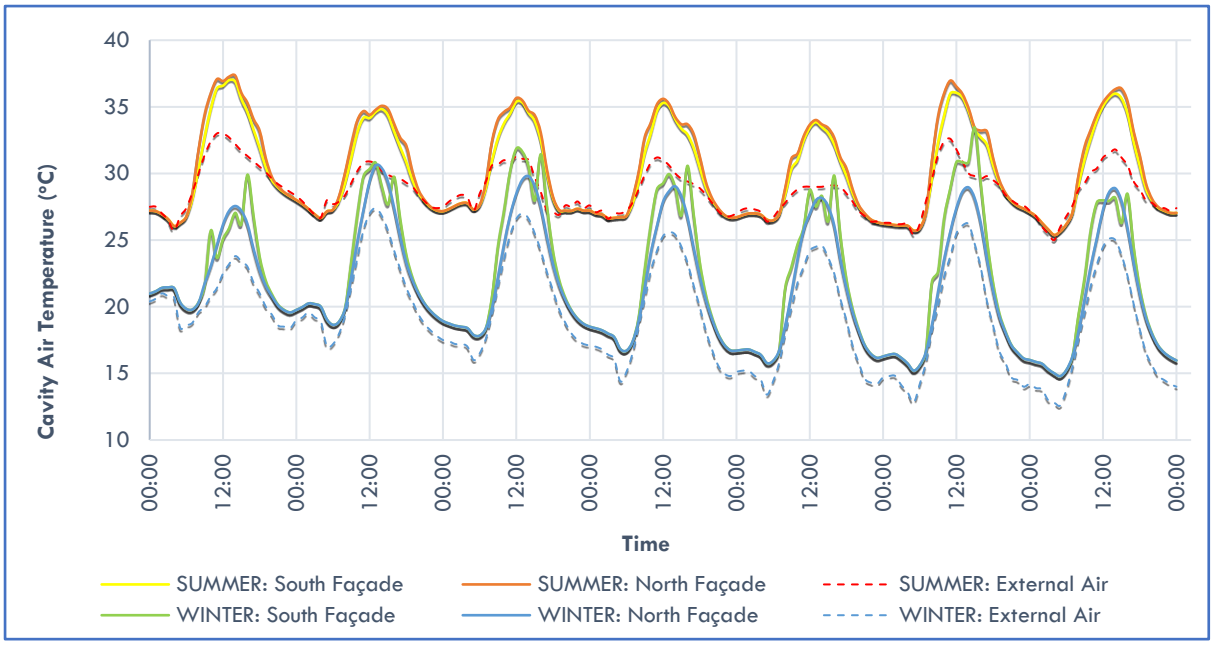

Figure 6.17: Cavity air temperature for the optimized DSF (configuration B) in the north and south orientations (colour coded) for Kolkata

Looking at *Fig. 6.17* it is apparent that the overheating in the cavity is present to a significant degree even in summer conditions despite the lower incident solar radiations, unlike for all other sites considered in the study. This can perhaps be attributed to the lower cavity depth in configuration B and therefore can justify a higher ventilation rate.

6.6.4 Performance Evaluation

Table 6.12 provides a comparison between the two optimized configurations of the DSF for Kolkata with the single skin façade.

Configuration A provides very little benefit when compared with the single skin façade, only a marginal decrease in heat gains along the South and East façade and an increase in heat gain on the North façade. Further, the heat loss, albeit unimportant for this site, is higher for configuration A when compared with the single skin. For these reasons, it can be said that configuration A is undesirable for this site, it can even be described as a poorer façade than the single skin system for the prevalent climatic conditions.

Configurations B provides a reasonable reduction in heat gain for the South and East orientations at 36% and 32% respectively. The reduction in heat gain for the North façade is much less at 16%. Heat loss, on the other hand, is reduced by roughly 26% at each orientation.

Thermal comfort is never compromised in either of the DSFs nor the single skin system. There is however, just as in all other sites analysed, an increase in the temperature of the inner-most glazing surface for the DSF systems.

Table 6.12: Comparing the proposed optimized DSFs with a single skin facade for different orientations in Kolkata
NOTE: *Façade of 10m length and 3m in height is taken.*

Details		Total Heat Gain (kWh)	Total Heat Loss (kWh)	Solar Heat Gain (kWh)	Surface Heat Gain (kWh)	Hours with glazing surf above 45 °C	Hours with glazing surf above 28 °C
South	Single Skin	6158	417	4749	1409	0	180
	Config A	5490	496	3152	2337	0	1807
	% Reduction	10.9	-18.9	33.6	-65.8	0	-903.9
	Config B	3919	304	2204	1714	0	613
	% Reduction	36.4	27.1	53.6	-21.6	0	-240.6
East	Single Skin	5671	417	4322	1348	0	325
	Config A	5378	498	3106	2272	0	1630
	% Reduction	5.2	-19.3	28.1	-68.5	0	-401.5
	Config B	3824	308	2144	1680	0	774
	% Reduction	32.6	26.2	50.4	-24.6	0	-138.2
North	Single Skin	3499	423	2375	1124	0	101
	Config A	4213	508	2333	1879	0	1176
	% Reduction	-20.4	-20.2	1.8	-67.2	0	-1064.4
	Config B	2961	317	1569	1391	0	421
	% Reduction	15.4	25.1	33.9	-23.8	0	-316.8

6.6.5 Summary

The DSF with a simple clear double glazing on the inner envelope as in the case of configuration A performs poorer than the single skin system for the given site conditions. The benefits seen from a better inner glazing system, as in configuration B is primarily for the South and East façades where heat gain and heat loss are reduced significantly.

The smaller cavity depth in configuration B has resulted in increased cavity air temperature even when incident solar radiation is minimal. This further highlights the caution to be used when employing DSFs with low cavity depths.

6.7 Inter-site Comparison

Comparing the thermal behaviour of the DSF and the energy saving potential for the different sites included in this study will further aid in understanding the applicability of the DSF to different climates. *Fig. 6.18* gives a brief overview of the annual temperature variations for the six cities considered in the study.

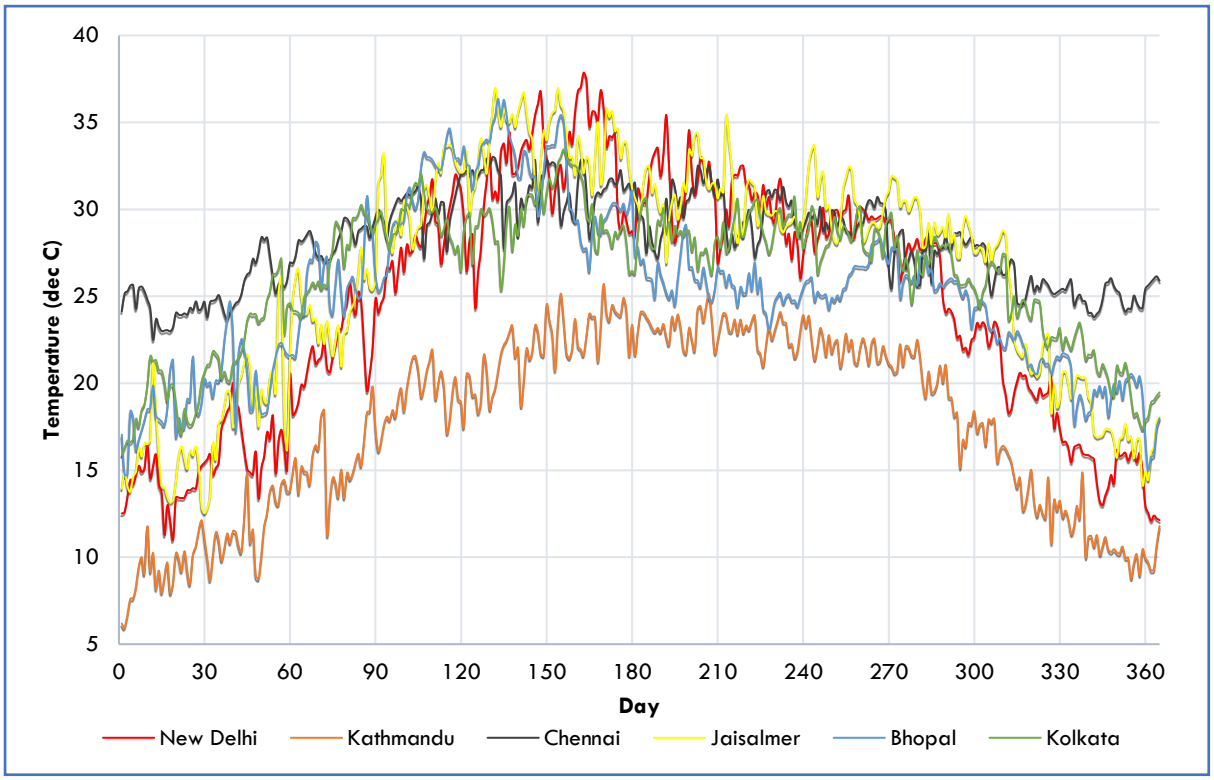

Figure 6.18: Graphical representation of daily average temperatures throughout the year for the respective sites (colour coded) included in this study.

It is clear that New Delhi has the highest variation in temperatures while Chennai has the least. Kathmandu is by far the site with the lowest average temperatures throughout the year. Kolkata and Chennai both have milder climatic variations throughout the year with respect to all other sites selected in the study.

However, temperature alone does not adequately represent the climatic conditions in order to evaluate the performance of a façade. Solar heat gains forms a large portion of the total heat gain through the façade and hence the solar radiation incident on the façade plays a vital role. The latitude of the location of a site gives vital insight into this. Sites above or close to the Tropic of Cancer (23.5° N) have very low incident radiation on the South and North façades when temperatures are at their highest in summers (May to July) while the incident radiation for the South façade is maximum in winter time (Nov to Feb). *Fig. 6.19* represents the solar and surface heat gains in the optimized configuration of the DSF for North, South and East orientations at each site.

The North oriented façade has the least heat gain in all cities. Chennai, being the closest to the equator has the highest heat gain through the North façade in relation to other sites due to the relative shifting of the sun path.

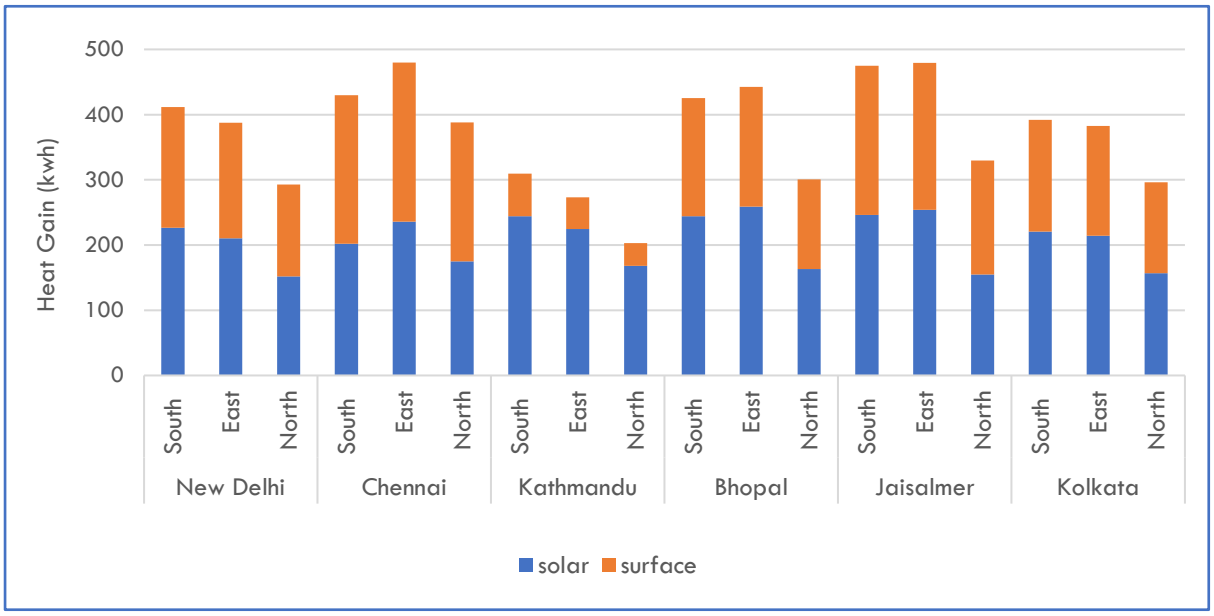

Figure 6.19: Annual heat gain per meter length of the optimized DSF for various sites and orientation. The heat gain is presented in its components of solar and surface heat gain (colour coded)

Further, it is observed that on moving closer to the equator, the heat gain on the East façade increases in relation to the South and North façades at each site.

The advantage of the DSF is clearly seen in cities with higher climatic variation, Bhopal, New Delhi, Kathmandu and Jaisalmer show the maximum reduction in total heat gain for the optimized DSF when compared to the base configuration *(Ref Fig. 6.19 & Fig. 5.13)*. The effectiveness of the optimized DSF in reducing solar heat gain is clearly shown. Hence, a much larger proportion of the total heat gain is taken up by the surface transfer mechanisms as opposed to the distribution seen in the base configuration.

The heat gain in the base configuration of New Delhi and Jaisalmer on the South and East façades were higher than those of Chennai, but by employing the optimized configuration the heat gain is reduced to values comparable or below those of Chennai.

6.7.1 Advantage of a DSF Over the Single Skin Façade

Although the optimized designs presented in the previous sections for each site may provide relative benefits of similar magnitudes when compared to the single skin façade, it is important to consider the benefits in absolute terms as well.

Fig. 6.20 shows the total heat gain for the optimized DSF presented in the previous sections versus that for the single skin façade in different orientations at each of the sites analysed in the study. The advantages of using a DSF versus a single skin in the North facing façades is significantly less compared to the South and East facing façades. Further, cities with higher temperature variations throughout the

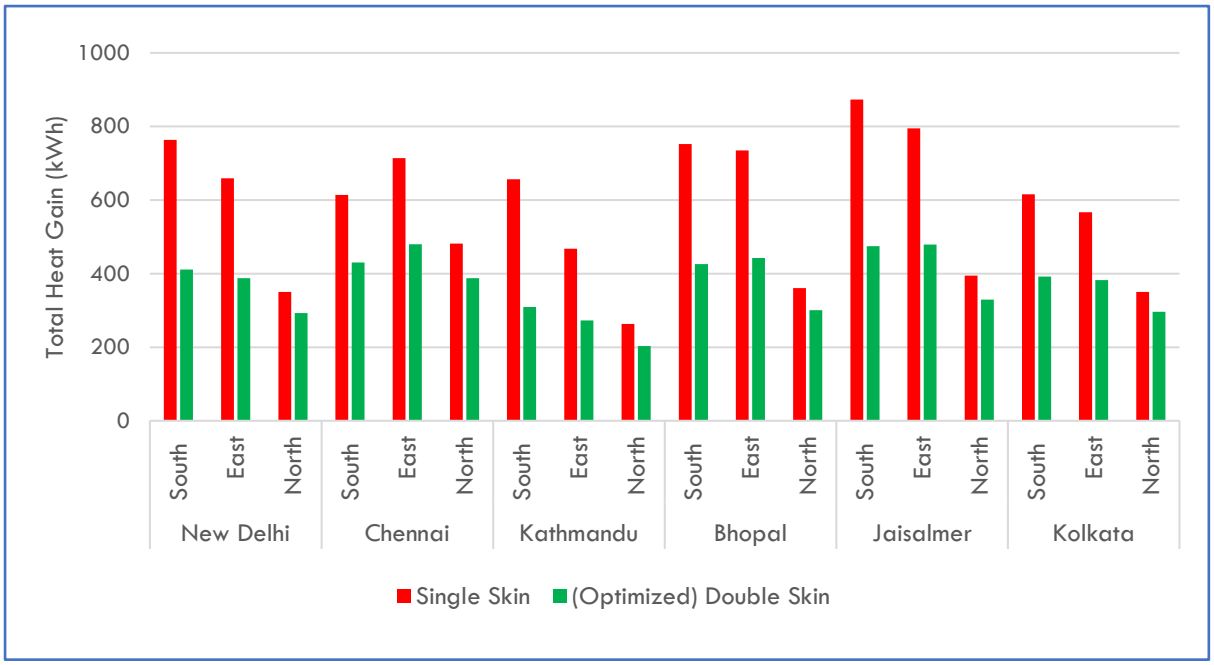

Figure 6.20: Comparison of annual heat gain for the optimized DSF and the single skin facade at various sites and orientations

year such as New Delhi, Kathmandu, Bhopal and Jaisalmer benefit the most when it comes to reduction in heat gain. Kolkata which has a milder climate and Chennai which has relatively the same albeit, warmer temperatures throughout the year have less impressive reductions in heat gain. The sites and orientations with the highest solar radiation incident on the façade seem to benefit the most.

The advantage seen in the DSF versus the single skin for a reduction in heat loss is similar in terms of percentages for all sites. However, due to the large difference in magnitude of overall heat loss the effective advantage in much higher in cities with colder climates such as Kathmandu and New Delhi *(ref.*

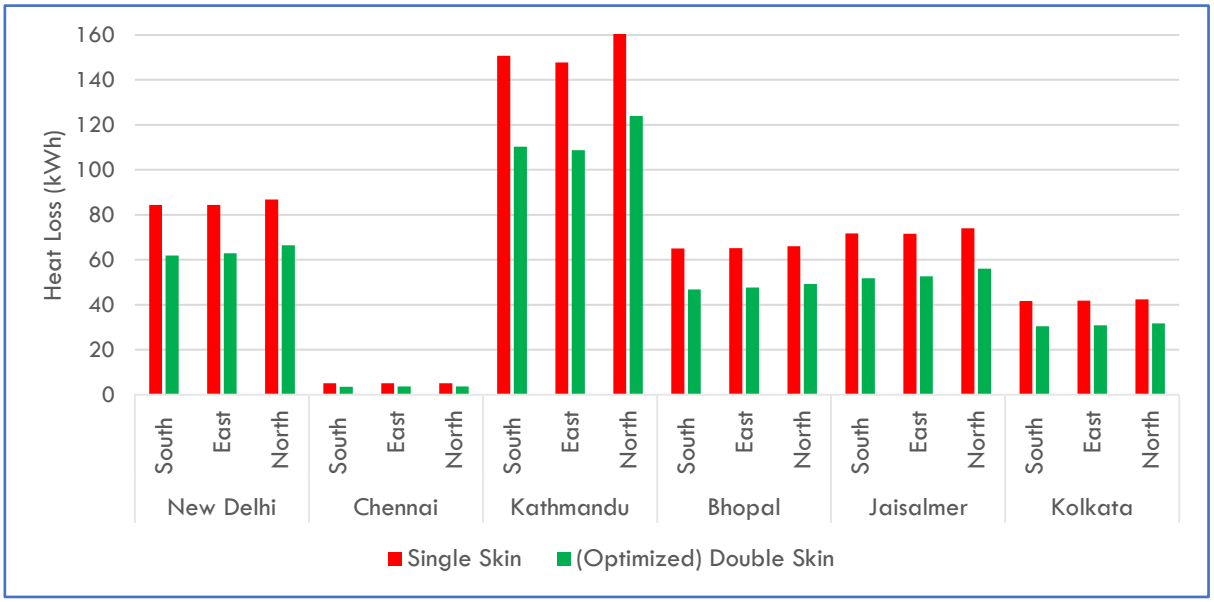

Figure 6.21: Comparison of annual heat loss for the optimized DSF and the single skin facade at various sites and orientations

Fig. 6.21). A trend of a slight increase in heat loss for the North façade at each site as compared to other orientations can be observed and is attributed to the difference in incident solar loads on the façade.

6.7.2 Evaluating Electrical Energy Consumption

The yearly electricity consumption to compensate for the heat flows through the façade are presented in this section. The electrical energy needed is calculated assuming all the heat gain through the façade needs to be compensated by cooling. This assumption is simplifying the rather complex systems used for cooling as well as its dependencies on the occupants of the office space. The results presented here do not account for working hours or additional internal heat generation, it only presents the electricity that would be consumed to compensate for the heat gain through the façade. Additionally, the energy used for the mechanical ventilation of the cavity is accounted for and added to the total energy consumption of the DSF.

In order to estimate the electricity consumption for cooling, a cooling efficiency (coefficient of performance, COP) of 3 is taken for the air conditioning (AC) unit. This will, of course, depend on many factors including, but not limited to, outside air temperature, relative humidity, the design of the air conditioning unit itself as well as the setpoint temperatures for controlling the AC. Due to the high temperature and humidity, the COP of AC units can be as low as 2. For mechanical ventilation, a fan of efficiency 0.8 is assumed. The results are presented in T*able 6.13*.

For the air conditioning,

$$Electrical\ energy\ needed\ = \frac{Heat\ gain}{COP\ of\ AC\ unit}$$

For mechanical ventilation,

$$Electrical\ energy\ needed\ = \frac{Q\ *\ \Delta P}{Efficiency\ of\ Fan}$$

Where Q refers to the volumetric flow rate of air in m^3/s and ΔP is the pressure difference, calculated as,

$$\Delta P = \rho * g * \Delta h$$

Where ρ is the density of air, taken as $1.2kg/m^3$, g is the acceleration due to gravity, taken as $9.81m/s^2$ and Δh refers to the height different between the inlet and outlet, which for the DSF is the height of the façade, i.e., 3m. The inlet, outlet and other losses for the flow of air are neglected in this calculation.

Table 6.13: Annual electrical power consumed for compensating total heat gain in the single skin (SS) and optimized DSF for the respective orientations at each site sites per meter of façade width.
***NOTE*:** Power consumption for cooling is based on total heat gain and does not account for working hours or days of the office building.

City	Orientation	Annual Electrical Energy per meter length of façade (kWh)					% Reduction in cooling energy
		Cooling in SS	Cooling in DSF	Ventilation in DSF	Total in DSF	Energy saved	
New Delhi	South	254	137	3	140	117	46
	East	220	129	2	131	91	41
	North	117	98	0	98	19	16
Chennai	South	205	143	2	145	62	30
	East	238	160	2	162	78	33
	North	161	129	1	130	32	20
Kathmandu	South	219	103	3	106	116	53
	East	156	91	2	93	65	42
	North	88	68	0	68	20	23
Bhopal	South	251	142	3	145	109	43
	East	245	148	2	150	97	40
	North	120	100	0	100	20	17
Jaisalmer	South	291	158	3	161	133	46
	East	265	160	2	162	105	40
	North	131	110	0	110	21	16
Kolkata	South	205	131	2	133	74	36
	East	189	127	2	129	62	33
	North	117	99	0	99	18	15

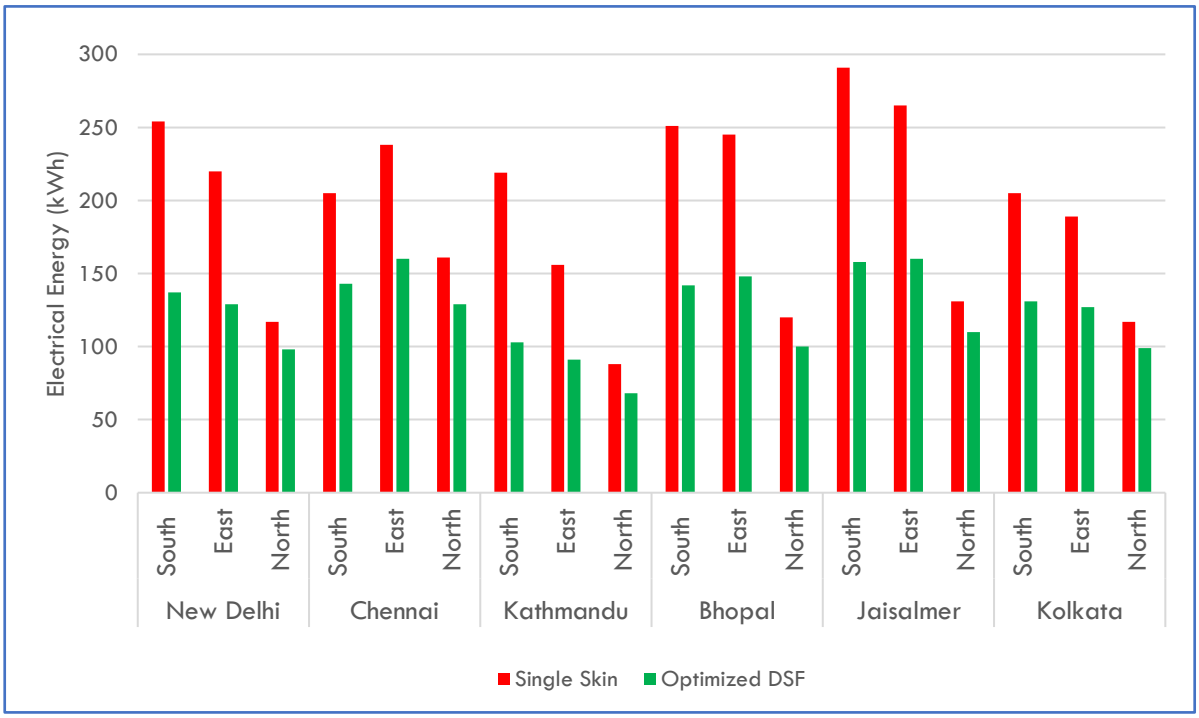

Figure 6.22: Comparison of annual energy consumption to compensate for the excess heat gain through the optimized DSF (excluding energy for ventilation) and the single skin facade at various sites and orientations

Table 6.13 presents the annual electricity consumption for compensating the heat gain through the façade from the external environment per meter length of the façade. This is assuming a façade height of 3 m. It is quite apparent that the power needed for ventilating the cavity is insignificant with respect to the power needed to compensate for the heat gain through the façade. As the power consumption is directly proportional to the heat gain (neglecting the energy needed for mechanical ventilation) the trends observed for the electrical energy used are very similar to those for the heat gains, as can be seen in *Fig. 6.22*.

For electricity needed for heating, most electric radiators use a COP of nearly 1. Hence, the energy saved is the same as the decrease in heat loss. But once again, given the different climate zones in India, this will be far more beneficial to areas with more severe winters such as New Delhi, Jaisalmer, Kathmandu and Bhopal.

6.7.3 Summary

The solar radiation incident on the façade is the primary source of heat gain which can be mitigated significantly by the DSF. Thus, the solar altitudes and seasonal changes in the sun path must be analysed to achieve a better understanding and estimation of the energy saving potential of the DSF. The advantages of the DSF are extenuated in sites and orientations with higher incident solar radiations and larger seasonal variations in temperature. Lower sun altitudes throughout the year correspond to higher solar gains and thus make the DSF more suitable, such as in the case of New Delhi, as opposed to in locations where sun altitudes are relatively high throughout the year such as Chennai. However, improvements using the DSF are seen in all sites analysed for each of the orientations albeit in varying magnitudes. Given the high cost of the DSF as opposed to a conventional single skin façade, the application may be restricted to those sites and orientations where significant improvements are expected such as the South and East façades of New Delhi, Kathmandu, Bhopal and Jaisalmer.

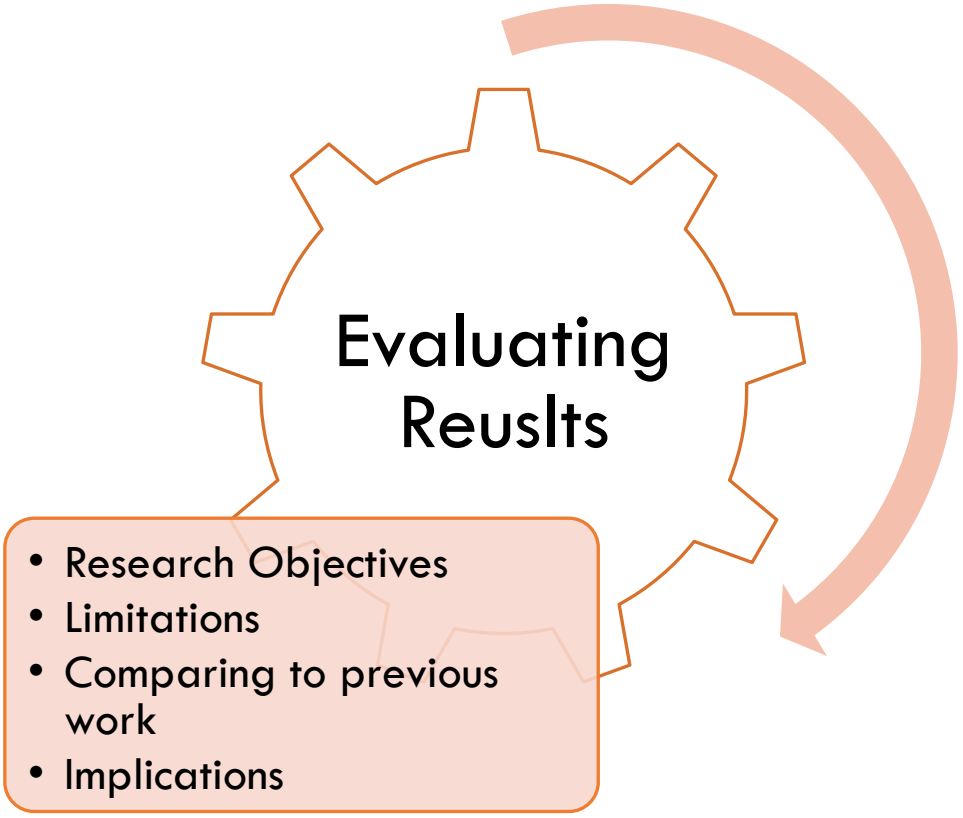

Figure 7.1: Discussion themes

7. Discussions

This chapter, firstly, presents the views and interpretations of the results and contextualizes them with respect to the aim and objectives of the research. Second, a critical assessment and pitfalls of the simulation technique employed are discussed. And last, a comparative assessment of the results with respect to previous work done in this field of study are presented.

7.1 Reviewing the Research Questions

The research questions were divided into three categories, namely, a) Contextual Evaluation, b) Modelling and Simulation and c) Evaluation and Analysis. The interpretations of the results with respect to these research questions can be described as a) Site Analysis, b) Modelling and Parametric Analysis and c) Performance Assessment respectively. The results are discussed under these themes as follows.

7.1.1 Site Analysis

Analysis of the climatic conditions at each site is imperative to design the DSF for maximum benefit, the primary influencer for heat gain being the incident solar radiation which can be mitigated by significant margins (up to 70%). Hence, the latitude of a location and changes in the sun path are vital site-specific parameters that must be addressed.

The solar heat gain far outweighs the surface heat gain *(ref. fig. 6.19)*. External air temperatures have a much lower impact on heat gain when compared to the solar radiation, especially for South, East and West facing façades.

The internal room temperatures were set according to the Indian Model of Adaptive (Thermal) Comfort (IMAC) for each site (Manu, et al., 2014). This allowed the simulations to better represent the heat flows through the DSF with seasonal changes and to a minor extent account for changes in occupancy behaviour with respect to external temperatures. It must be noted that in the case of Kathmandu the IMAC results for the city of Dehradun in India were chosen. Dehradun, despite being in the Himalayan Mountain Ranges, is at a lower altitude than Kathmandu and has slightly higher temperatures. However, the expected difference in the room temperatures as per the IMAC is minor and was hence ignored.

7.1.2 Modelling and Parametric Analysis

The model discretization *(ref. Appendix A)* has proven to be accurate in representing the thermal behaviour of the DSF. This is seen by the verification and comparison made with an equivalent façade system in Design Builder. Design Builder itself was not chosen for the analysis due to the following reasons.

1. Longer processing time for each simulation (up to 30 mins versus at most 2 mins in Matlab/SIMULINK).
2. Lack of implementable control scheme for mechanical ventilation within the cavity.
3. Highly complex simulation technique and output data making it extremely difficult to pinpoint the cause and effect of design parameters.

The assumptions regarding the behaviour of the different components of the façade with respect to heat transfer coefficients have been proven to replicate the behaviour of a DSF to a good level of accuracy. It can be said that the impact of these simplifications on heat gain is small. However, the sensitivity of the temperature distribution to changes in the heat transfer coefficients is much higher than that for heat gain *(ref. appendix J)*. The comparative nature of the study makes any skewing of the results less significant as the impact would be equally present in all the simulations. This makes any relative changes in

behaviour primarily attributed to the façade configuration and external site conditions as opposed to the assumed boundary conditions and heat transfer mechanisms.

The properties of the glazing units were found to be most conducive to changes in thermal behaviour. Cavity width has a lower impact on the decrease of heat gain when compared to glazing properties and has almost no impact on decreasing heat loss *(ref. Appendix I)*. The decrease in heat gain was almost linear in nature with an increase in the cavity width *(ref. fig. 5.10, 5.14, 5.15)*. The ventilation rate as expected only showed significant advantage up to a particular rate after which only marginal benefits could be derived *(ref. fig. 5.7, 5.16, 5.17)*. It is important not to forget that the effectiveness of a parameter is influenced to a large extent by the solar radiation intensities as explained in the previous section as well as the overall configuration of the façade components. Further, the set points for activation of the blinds and ventilation system should be considered based on seasonal variation of temperature and solar radiation. As seen in the case of Kathmandu, low temperatures with high solar loads during winter can result in improper activation of the ventilation system. Thus, leading to overheating and high fluctuations in the cavity air temperature.

The primary concern with the DSF was that of overheating as pointed out in the literature review. The phenomenon of overheating in the cavity is very real and its dependence on the insulating properties of the inner glazing *(ref. Ch. 5.3.3)* present mixed and opposed concerns. The risk of overheating as described in this study, when the air temperature in the cavity is above 40◦C, is profoundly increased with a decrease in the U-value of the inner glazing. Given the concept of exhausting air and hence heat through the cavity as one of the main driving forces for decreasing heat gain, one can argue that an increase in the overheating risk could actually be a positive marker for performance in the sense that more heat is deposited in the cavity and less passes through to the interior. Adding to the this, the high tolerance to warm walls for thermal comfort (up to 23◦C of radiation asymmetry as per ASHRAE guidelines) and inherently lower inner surface temperatures of the better insulating double-glazing units makes the negative effects of overheating more acceptable. Especially when weighed against the energy saving potential of a DSF.

Regardless, the overheating risk can be mitigated to a large extent using a suitable external glazing selection, by increasing the cavity width or increase in ventilation rate coupled with an appropriate control scheme as explained in chapter 5. Once again, it is important to reiterate the interdependencies of these design parameters. For example, a wider cavity width has a lower risk of overheating and therefore can be used in conjunction with a lower ventilation rate, while the opposite may be true for narrow cavity widths.

The energy used for ventilation proves to be negligible compared to that needed for compensation of the heat gain as cooling energy. The decrease in cooling energy for the optimized DSF configurations when compared with a single skin façade ranged anywhere from 15% to 50% depending on the site and orientation of the DSF. The energy needed for ventilation constituted less than 1% of the energy

needed for compensating the heat gain, hence the additional power needed to mechanically ventilate the cavity is justified *(ref. Ch. 6.7.2 & table 6.13)*.

7.1.3 Performance Assessment

The optimized configurations of the DSF yield no additional benefits to thermal comfort as compared to the single skin system as demonstrated in chapter 6. If anything, the thermal comfort may be slightly reduced due to higher glazing temperatures, however, this is insignificant owing to the high tolerance for radiation asymmetries in warm walls.

For all the sites analysed, the glazing systems employed had the largest impact. Particularly with a combination of a tinted or reflective external glazing and a low-E coated internal glazing. The reduction in cavity overheating risk and heat gain throughout the year were significant. However, this is subject to the orientation of the façade, with North facing façades, in general, having little benefit from the DSF as compared to the single skin (ref. fig. 6.20). The cavity width showed a decrease in heat loss in a somewhat linear trend, primarily due to a decrease in solar heat gain owing to the shading effect of the cavity ceiling. Hence, smaller cavity widths could be employed in sites closer to the equator where sun altitudes are relatively higher throughout the year. Increasing the ventilation rate decreased heat gain only up till a rate of 80AC/hr (for a façade height of 3m and a 0.5m cavity width the equivalent of 120m^3/hr volumetric flow rate per meter length of the façade). The effects of increased cavity width and ventilation rates were only seen on the South and East facing façades with little to no benefit in the North orientation. Changes in the performance of the DSF in the North orientation when ventilation rate or cavity width are increased are negligible. The only exception to this being Chennai, owing to its lower latitude, where also the changes in the behaviour of the North façade was still limited when compared to other orientations.

All the optimized configurations of the DSF at the respective sites employed tinted external glazing and Low-E coated double glazing on the inner envelope. The cavity depth was suitably reduced at sites closer to the equator and was found to still provide additional benefits as opposed to the single skin façade. Overheating was mitigated and thermal comfort was ensured using a combination of a low-E coated internal envelope and adequate ventilation rate.

Given the overall energy savings provided by the DSF as compared to the single skin, it is easy to justify the cost of mechanical ventilation in the cavity. The energy used for ventilation proves to be negligible compared to that needed for compensation of the heat gain as cooling energy. The decrease in cooling energy for the optimized DSF configurations when compared with a single skin façade ranged anywhere from 15% to 50% depending on the site and orientation of the DSF. The energy needed for ventilation constituted less than 1% of the energy needed for compensating the heat gain, hence the additional power needed to mechanically ventilate the cavity is justified. One could even add that higher ventilation rates despite their minor benefits could be employed as the additional power consumption would remain significantly lower than the energy saved in air conditioning. However, a detailed analysis of the

additional power used in ventilation versus that saved in cooling needs will have to be performed to arrive at any definitive advantageous rates of ventilation.

7.2 Critique of the Simulation Technique

The associated discretization, assumptions and simplifications which govern the setup of the numerical model employed for the purpose of this study can have a profound impact on the output of the simulations. In this section, the various reasonings associated with these assumptions and settings within the MATLAB/Simulink model are discussed. It is important to assess these details as they can be the cause of discrepancies from past studies as well as for studies conducted in the future for this field.

The number of layers for discretization in the vertical direction was kept at 12. This was done to facilitate the comparison with the Design Builder model, which had 6 zones in the vertical direction *(ref. Ch. 4.1.1)*. Once the verification was satisfactory, it was decided to keep the same discretization. A smaller number of layers would have decreased the time taken for the simulations. However, with a smaller number of layers the rounding error while assigning solar loads becomes significant and can give inaccurate results (up to 25% deviation was observed for 6 layers instead of 12 in the base configuration of the DSF). These errors are associated with the different heights of the components which are exposed to *diffuse*, *direct + diffuse* or *direct + diffuse + once reflected* shortwave solar radiation *(ref. Fig. 3.3)*. Only one of these conditions can be imposed on a given node. Hence, nodes which contain the interface of these conditions have an error. Only one condition is chosen to act over the entire area represented by the node despite some of the area being under a different solar load condition. Given the importance of solar loads on the thermal behaviour of the DSF, perhaps an even higher number of layers could have been used. However, for the purpose of this study, the selected number of layers at 12 has proven sufficient as demonstrated in *Table 4.1* and *Appendix H*.

The intensity of diffuse radiation at the shading device (venetian blind) and the inner envelope is treated independently of the self-shading effect due to the cavity ceiling. Shading caused by facade obstructions (such as overhangs and window recesses or in this case the ceiling of the DSF) should also be applied to the diffuse beam since the effective solid angle of the external scene, as subtended at the surface in question, is markedly reduced (Clarke, 2001). The error induced due to the negligence of this effect is unknown. It can be speculated that due to the reduction in the intensity of radiation owing to the external glazing and inherently lower intensity of incident diffuse radiation this error will be negligible. Further, it is an assumption made in many other works pertaining to the modelling of the DSF which have been verified against other simulation platforms and/or mark-ups (Jiru & Haghighat, 2008) (Xue & Li, 2015).

Conduction within the glazing lights has been omitted and given the narrow thickness of the glazings, it is not of much consequence. Nonetheless, it must be acknowledged that the assumption may provide less accuracy for glazings with high absorptance such as tinted glazings. Especially when used in the inner envelope in which the incident solar radiation can vary significantly with height based on the conditions

of *diffuse*, *direct + diffuse* or *direct + diffuse + once reflected radiation*. Due to conduction in the vertical direction, the temperature distribution along the height of the glazing may change.

The convective and radiative heat transfer coefficients have been kept constant in the simulations. These coefficients will realistically vary with time, based on the temperature of the node as well as the velocity of air in the case of convection. The inaccuracies associated with these may be pronounced in the case of high temperature nodes such as with tinted glazings and the metallic venetian blind systems. Further, larger ventilation rates and/or lower cavity width will result in increased air velocity which can have a significant impact on the convective coefficient within the cavity. The selected values of the respective coefficients within the cavity have been satisfactorily verified against the results from Design Builder for higher ventilation rates. Adding to this, the importance of solar heat gain as compared to surface heat gain diminishes the expected error in the total heat gain due to these heat transfer coefficients. The sensitivity of the total heat gain to changes in convective and radiative heat transfer coefficients is rather small, however, the temperature distribution in the components and heat loss can change profoundly when the same quantities are varied *(ref. Appendix J)*. The later can be ignored as the boundary conditions for heat loss would imply the cavity is not ventilated (act as a thermal buffer) and therefore the convection coefficients will not be affected by higher flow rates.

Within the cavity, no mixing of air either side of the venetian blind is accounted for. Given that air movement through the venetian blind is very much possible, especially in the "blind off" state this assumption can raise questions regarding the accuracy of the simulations. However, the Matlab/Simulink model is verified against Design Builder which does account for the air movement through the blind system based on the slat angles. This could be one of the reasons for the difference in results among the two platforms. However, the output from the MATLAB/Simulink simulations gave only minor temperature differences between the air on either side of the blinds, less than 1°C. Lastly, during the "ventilation on state", the fresh air is introduced either side of the blind which would nullify the discrepancy due to possible mixing of the air through the blind.

During the validation process, two phenomena remain unexplained. The first, a better correlation between ventilation rate of 600 m^3/hr versus that at 100 m^3/hr. It is quite apparent that the discrepancies primarily vary due to a difference in dealing with short wave solar radiation between the MATLAB/Simulink and Design Builder platforms. A greater difference in temperature distribution and heat gain occurs during hours with high incident solar radiation. A higher ventilation rate could perhaps be reducing the contribution of solar radiation to the temperature distribution in favour of other heat transfer mechanisms which may lead to a reduction in the discrepancies between the two models. Secondly, the unexplained behaviour of the MATLAB/Simulink model with external long wave sky and ground radiation which had a profound effect on the temperatures of the inner envelope rather than that of the external. This too, like in the previous case decreases with higher ventilation rates and thus, can be attributed to a change in the governing heat transfer mechanism at higher ventilation rates. Considering the large discrepancy observed in the second case *(ref. Appendix H)* it was decided to use

a generic surface resistance which accounts for radiative loss *(ref. ch. 3.2.3)* as opposed to the detailed long-wave radiation exchange with sky and ground.

The single envelope evaluated for comparison with the DSF omits the effect of internal shading devices such as curtains, venetian blinds etc.. Although the internal shading does not actually reduce the heat entering the room it can influence its distribution through absorption and consequently re-radiation and surface convection from the blind surface. The parameters used for the comparison in this study primarily deal with heat gain into the room, hence this omission is of little consequence. It must be said that a small fraction of heat gain could be sent back out of the room due to re-distribution of the heat energy from the shading system when applied to the single skin.

For assessing thermal comfort, the temperature of the glazing at the mid-height of the DSF is taken. Owing to the distribution in solar loads over the height of façade it is likely that the temperature at the bottom-most nodes of the inner envelope is higher than that at the top or middle. However, for a simulation in a South facing DSF (base configuration) in New Delhi, this difference was found to never exceed 1◦C.

The absorption and shading coefficient of the shading device, the venetian blind, is treated is as constant for the given slat angles (0◦ and 45◦). However, just as in the case of the optical properties of the glazing device this may vary based on the relative angle of incidence. A more detailed calculation methodology taking into consideration the solar altitude, slat angle and slat width could perhaps increase the accuracy of the model.

At high solar altitudes, a case of only *diffuse + once reflected* solar load may arise at some of the sections in the blind and internal envelope without any *direct radiation* component. In this case, the once reflected component in neglected owing to the low transmission of the external envelope at large angles of incidence. This coupled with the reduction in the intensity of radiation after being reflected from the base of the façade results in incident radiation less than an order of magnitude when compared to the diffuse radiation. For the base configuration of the DSF at New Delhi facing South the error in this was found to be less than 0.1% but for a larger cavity depth, 1.5m, it increased to 2.5%. However, once the external glazing was changed to a tinted or reflective glazing the error was negligible regardless of cavity width.

7.3 Revisiting the Literature Survey

The work of Barbosa on a naturally ventilated DSFs in the hot and humid climate of Brazil concluded that the thermal acceptance of the DSF was lower than the single skin in arid regions (Barbosa, 2015). The higher temperatures of the inner-most glazing surface in the DSF as compared to the single skin bring forth the possibility of lower thermal acceptance of the DSF, but in this study, the ventilation provided by mechanical means was found to be adequate in mitigating this phenomenon.

A larger temperature difference between the interior and exterior leads to a higher benefit from the insulating properties of the façade (Mingotti, et al., 2013). Looking at the cities where the DSF provided

maximum benefit, i.e., New Delhi, Jaisalmer, Bhopal and Kathmandu it is apparent that the climate zones with more severe winter and/or summer temperatures benefit the most, in accordance with the work of Mingotti et al (2013).

The advantage of mechanically ventilating the DSF is clearly presented in previous research works (Su, et al., 2017). The heat gain into the building was suitably reduced in all cases when the cavity was ventilated as opposed to being closed off (ventilation rate set to zero). However, this does not compare to natural ventilation and no comments can be made with that respect. The above-mentioned study also highlights the high climatic dependency for the optimum use and design of a DSF. Given the different configurations and effectiveness of the DSF at the various sites analysed in India, this point is strongly advocated.

In Korea, it was found that the glazing properties of the outer glazing light in the inner envelope had the highest impact on reducing energy consumption, especially when employing Low-E coatings (Joe, et al., 2014). Although the importance of the low-E coated glazings cannot be undermined in this study, especially owing to an improved U-value, it must be said that the external envelope's optical properties can have a larger impact on energy consumption than the inner envelope *(ref tables on glazing variations in Appendix I)*. This difference in opinion can be explained based on the climatic contexts. Korea has much more severe winters and lower solar radiation intensities than any of the sites included in this study, hence the U-value of the inner envelope takes precedence. It has been found in this study as well that reduction in heating needs is largely affected by the U-value of the inner envelope, in agreement with the work of Joe et al. However, reduction in cooling needs, which form majority of the energy consumption in commercial building in India, is more strongly affected by the external envelope's optical properties and will thereby have a more profound effect on overall energy consumption.

With an increase in cavity width from 0.2 to 0.8 m a reduction of 4.3% was found for heat gain in the city of Shanghai for a naturally ventilated DSF (Su, et al., 2017). New Delhi and Shanghai have similar climatic variations and lie on roughly the same latitude. In this study, a difference of roughly 8% and 6.5% were found in the South and East façade orientations in the base configuration when the cavity width was changed similarly. However, this study does utilize mechanical ventilation which may indicate better performance.

Smaller cavities have a higher risk of overheating due to restricted airflow (Rajesh & Purohit, 2014). The findings here agree with this statement. The overheating risk for a cavity width of 0.2m was far higher than those for wider cavities at constant rates or air change. This issue was however mitigated through a suitable increase in the ventilation rate.

Barbosa et al. (2014) have conducted an extensive review of the effects of various design and spatial parameter on the behaviour of the DSF, especially oriented towards a reduction in heat gain (Barbosa & Ip, 2014). Many of the findings of this study agree with those presented by them. This includes the following:

1. The major influence of the façade orientation on annual cooling load.

2. Better performance in the South facing façade as compare to North in Hong Kong. Although no particular exception was found to this, the performance between the two orientations seems to become similar for site locations closer to the equator and the trend will certainly reverse for cities South of the equator.
3. Increase in cavity width reduces solar heat gain.
4. Solar energy absorbed in the DSF is effectively removed with mechanical ventilation
5. Reduction in the transmissivity of the external glazing can have a significant reduction in solar heat gain.

Additionally, the above-mentioned study also highlighted the possibility of having an external envelope with double-glazing and a single glazed inner envelope. This configuration can also reduce the cooling loads in buildings (Barbosa & Ip, 2014). However, this was not tested in this study and hence cannot be commented on.

7.4 Summary

The results of the research conducted have provided vital insight into the thermal behaviour of the DSF in warmer climates of India. Most importantly, the high dependency of the advantages of a DSF on the incident solar radiation has been brought to light. For this very reason, one must look beyond the generic temperature data of a site and go in depth into the details pertaining to sun angles and façade orientations.

All the research questions have been answered within the scope of this study and by doing so, the objective of the research has been accomplished. The modelling methodology has been verified to an acceptable degree and the same has been utilized in gathering and analysing data for the DSF performance at the six different sites. Further, the intercomparison of the various sites has presented the climatic conditions in which the advantage of the DSF, in absolute terms, is more than that of a single skin. Hence, providing a better understanding of the site details that make a DSF more viable.

It is important to take note of the limited scope of this study. The behaviour and efficiency of the DSF are dependent on multiple design parameters and configurations, many of which have not been considered in the optimization carried out in this study. This includes, but is not restricted to, combining an external double-glazed envelope with a single-glazed inner envelope, cavity height, mixed transparent and opaque inner envelopes (window to wall ratio) as well as set points for the shading and ventilation system. Further, the possibility of ventilating the cavity with inside air-conditioned air or using natural or mixed-mode ventilation were not explored. The former being left out, firstly, as it is expected to increase cooling loads for the air conditioning system due to loss of cool air from the room. And secondly, any increase in thermal comfort would be insignificant owing to the high level of tolerance to radiation asymmetries of warm walls. The latter, natural ventilation, was not explored owing to its lower efficiency and increased risk of overheating when compared to mechanical ventilation as demonstrated in the literature review.

The study challenges the prevailing ideas surrounding DSFs which focus on its application in temperate and cool climates. The results have shown that there is a significant reduction in heat gain through the application of a well-designed DSF. Nonetheless, as discussed above, these reductions are very much dependant on the site-specific climate and spatial details at the site. Many of which agree with the findings of previous research in this area while others present new possibilities for mitigating heat gain and reducing overheating risk in the cavity. The latter being time and again presented as one of the pitfalls of a DSF.

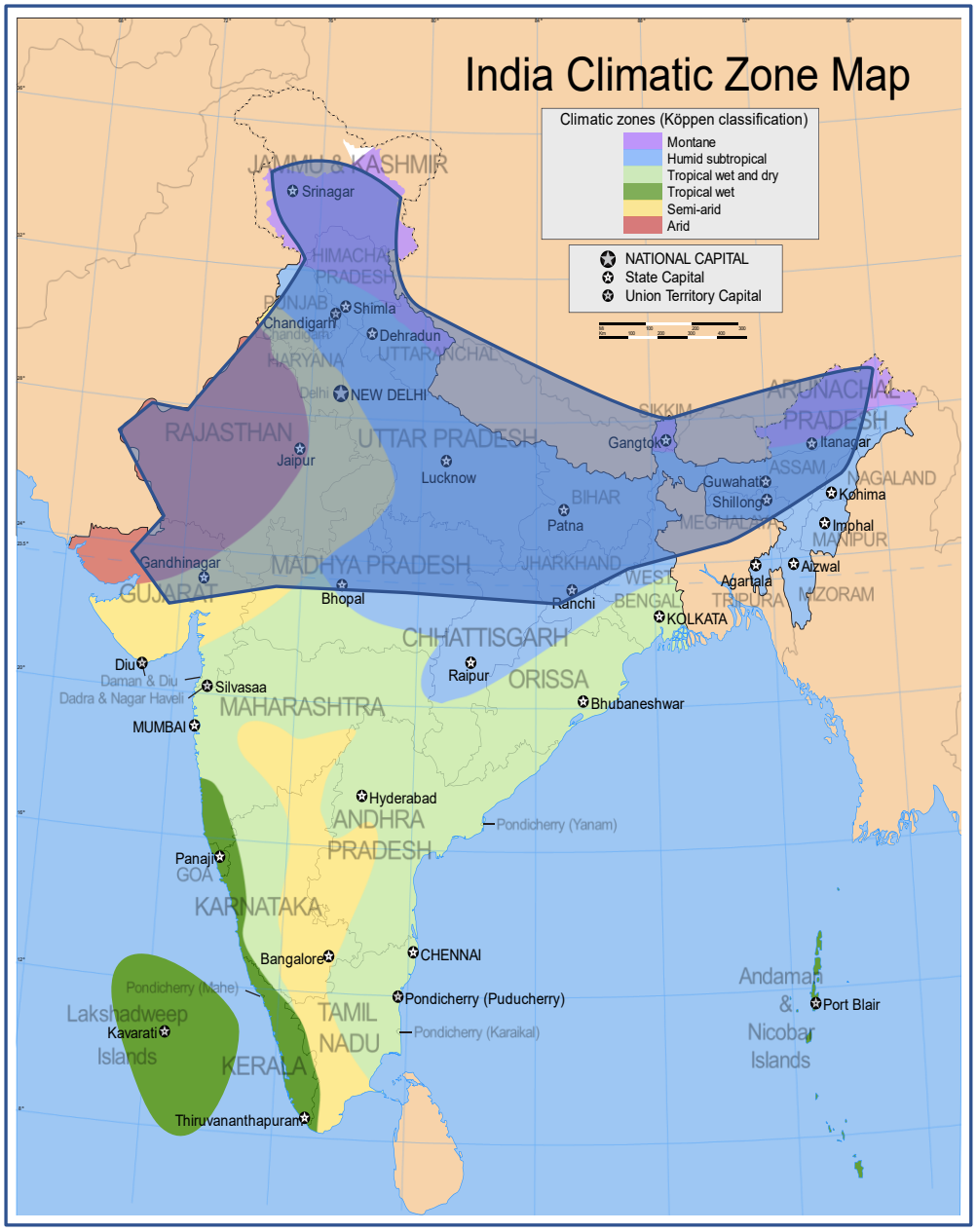

Figure 8.1: Climate Zones in India, Highlighted areas indicate the region where DSF can be used to derive significant reductions in cooling demand.

ADAPTED FROM: *https://commons.wikimedia.org/w/index.php?curid=1810580*

8. Conclusions

This chapter, first, presents the conclusions of the study based on the results and analysis of the simulation outputs and secondly, suggests possible directions for future research in the field. The limitations of the study having already been discussed extensively in Ch. 7 are only presented briefly to provide context to the concluding statements where necessary.

8.1 Introduction

This thesis presents a study on the thermal behaviour of different DSF configurations for various climate zones of India. Unlike the use of DSF in the cooler climate of Europe to increase energy efficiency by decreasing heating demand, the application of DSF in the warmer climate of the Indian subcontinent for a decrease in cooling demand has been analysed. This is driven by popular aesthetic demand for fully glazed facades in commercial and corporate buildings. The DSF offers the external appearance

Figure 8.2: CBI Headquarters in New Delhi. A fully glazed façade using reflective glazing. A building design that has undergone criticism for its poor occupant comfort despite the use of reflective glazings and its high cost.

comparable to that of a fully glazed system but can provide benefits similar to if not better than those achieved by external shading devices. The study does not advocate for the use of fully glazed systems for the given climatic conditions but rather presents the possibility of using a DSF to cater to the aesthetic demand while reducing energy consumption for cooling, which currently accounts for up to 50% of the electricity consumption in the commercial sector, and enhancing thermal comfort in both warm and cool climates owing to its malleable thermal behaviour.

The analysis has been carried out by developing a numerical model based on the zonal approach. Three main parameters for the design of a mechanically ventilated DSF are analysed, namely, ventilation rate, cavity width and glazing units. The behavioural analysis, having been extensively conducted for the site location in New Delhi was extrapolated to the other sites in order to provide recommendations and optimized designs of the DSF. The DSF at each site is compared to a single skin façade to judge the improvement seen in energy saving and thermal comfort. This was accomplished by analysing annual heat gain, annual heat loss and the temperature distribution among the façade components. The cavity air temperature was used to judge the overheating risk while that of the innermost glazing surface was used to assess thermal comfort.

8.2 Key Findings

The reduction in heat gain from the application of a DSF in place of a single skin (SS) envelope is primarily dependent on the solar radiation incident on the façade. Hence, the spatial orientation of the façade and the angle of incidence of solar radiation play a vital role in anticipating the benefits of a DSF. Both these aspects are primarily influenced by the sun path and its seasonal changes in relative

position with respect to a location. The latitude of a site is a good indicator for assessing the above-mentioned parameters for different façade orientations. Latitudes further North of the Tropic of Cancer received much higher solar radiation on the South façade while those closer to the equator received a higher intensity on the East façade.

The decrease in total heat gain, compared to a SS, in the South façade of most sites was between 30% and 50% while that in the North was at most 22%. Site variations in performance also showed that increased seasonal and/or daily temperature variations increase the benefits derived from implementing a DSF.

The DSF provides no added benefit for thermal comfort. The SS itself provided sufficient thermal comfort for both warm and cool walls at all sites. The inner-most glazing surface temperatures are higher for the DSF when compared to the SS. This can be attributed to the greenhouse effect in the cavity which leads to an increase in the cavity air temperature. However, the temperatures of the inner-most glazing surface are never high enough to compromise thermal comfort despite the overheating in the cavity.

Glazing properties of the envelopes have the greatest impact on the performance of the façade. External envelopes composed of tinted or reflective glazing have the largest impact on reducing heat gain and overheating risk. On the other hand, it is the thermal transmittance (U-value) of the inner envelope which is the primary factor to consider for reducing heat loss. By implementing the DSF the heat loss was decreased by roughly 25-35% when compared to a SS regardless of site, orientation or climatic condition. In absolute terms, this proves to be negligible for sites with year-round warm temperatures such as Chennai. However, the effective benefit can be seen in cities with colder winters such as New Delhi, Kathmandu, Bhopal and Jaisalmer *(ref. Fig. 8.1)*. Most buildings, if applicable usually employe electric radiators for heating needs. The efficiency of such devices is close to one, hence a similar decrease in energy consumption of heating can be expected as that for the decrease in heat loss.

Cavity width affects the behaviour in two ways. First, larger cavity widths offer greater self-shading from the cavity ceiling and secondly, they increase the volume of air and thereby reduce the risk of overheating. The advantages of larger cavity widths are also dependent on the incident solar radiation. Reductions in heat gain were insignificant for all site orientations where direct solar radiation was negligible throughout the year such as the North façade for all sites except Chennai.

Mechanical ventilation is important to mitigate cavity overheating. However, ventilation rates above 80 AC/hr provide no further significant reduction in heat gain. The effectiveness of the ventilation rate like that of the cavity width is negligible at orientations with low incident solar radiation. It is important to point out that narrow cavities need higher ventilation rates to mitigate overheating whereas larger cavities can implement lower rates, in terms of air changes per hour (AC/hr). Owing to the solar radiation patterns in India for façades which is higher is winters than summers it was seen that the cavity ventilation control is opposite to that expected, with the cavity acting as a buffer in summers and ventilating in winters when excess heat is accumulated.

Table 8.1: Considerations for different design variables, site selection and spatial orientation on DSFs in hot climates

Design Variable	Considerations
Site Location	Better performance with higher seasonal temperature variations and lower solar altitudes
Orientations	Higher incident solar radiation increases overall efficiency as well as sensitivity to changes in ventilation rate and cavity width
Cavity Width	Greater cavity width: • Decreases overheating risk • Allows effective use of lower ventilation rates • Decreases solar heat gain
Ventilation Rate	Higher ventilation rate: • Provides benefit up to 80AC/hr • Controls overheating in the cavity • Decreases temperature of the inner envelope
External Envelope Glazing (Single Glazing)	Thermal Transmittance (lowering the U-value): • No significant effect Optical properties: • Most effective parameter at reducing heat gain • Reflective glazing yields maximum benefit followed by tinted glazing • Insignificant effect on heat loss
Internal Envelope Glazing (Double Glazing)	Thermal Transmittance (lowering the U-value): • Decreases heat loss • Increases heat captured in the cavity, hence increasing overheating risk but reduces heat gain • Maintains adequate surface temperature for thermal comfort Optical Properties: • Absorptive (tinted) glazings should be avoided

The reduction in cooling load from the application of a DSF can lead to a reduction of up to 0.07 ton per meter length of façade in the carbon footprint when compared to a SS *(ref. appendix K)*. The energy used for mechanical ventilation is far outweighed by that saved in terms of cooling energy. Given the scale and size of building façades and the implications of climate change and global warming, it is a significant reduction that can be achieved by applying an appropriately configured DSF *(ref. table 8.1 and fig. 8.1)*. The successful application of DSFs in the Indian subcontinent can be extrapolated to many

other parts of the globe where cooling demand dominates a building's energy consumption. Further, the recommendation presented here can aid in the design of DSFs in temperate climates which suffer from severe overheating due to high solar radiation, as is the case for many energy efficient buildings in Europe which have utilized DSFs.

8.3 Suggestions for Future Research

Considering the limited scope of the study as presented in Ch. 7.4, further parametric analysis of the DSF is needed in hot climates. Most of the parametric analyses presented in previous work in hot climates are based on naturally ventilated cavities and the same must be evaluated for mechanically ventilated DSFs. This study has limited itself to only three design and operation parameters, cavity width, ventilation and glazing systems. Further, the possibility for utilizing natural ventilation, especially for façades with a continuous cavity along the height (not separated at floor levels) should be analysed. In such a case, the solar heat gain from the external envelope to the cavity must be sufficiently high to induce buoyancy driven forces required for the natural ventilation but at the same time must reduce the heat gain to the inside of the building. The heat captured in the cavity to induce natural ventilation would have to be balanced with that which is let into the building.

The success of mechanically ventilated cavities has been assessed here as well as in previous works. A better optimization based on the control strategies such as the shading and ventilation control is needed, as demonstrated in the case of Kathmandu *(ref. Sec. 6.3)*. Assessing daylight quality while using tinted glazings along with the shading device should be looked into in order to strike a balance between heat gain and natural daylight entry. Further, a mixed mode ventilation system which only uses mechanical ventilation to supplement natural ventilation or uses variable ventilation rates can be explored.

The modelling of DSFs in India, or in general, at locations closer to the equator appears more complex due to the high variation in the glazing optical properties at high solar altitudes. Actual measurements in a mark-up will help provide credibility to the simulation models and techniques. This is especially needed owing to the importance of solar radiation and its ramifications in terms of heat gain.

Owing to the high cost of DSFs a lifetime analysis considering the monetary savings in terms of electricity cost for cooling and/or heating versus the initial cost of investment is needed to offer this façade system as an attractive option to the commercial and corporate building designers.

Lastly, the assessment of thermal comfort in summer conditions based on the intensity of solar radiation entering the room needs to be evaluated. Although it has been found that the temperature of the glazings in both the DSF and SS are within the limits, high solar transmission can lead to discomfort for occupants seated close to the façade if no shading device is present.

8.4 Summary

In sum, the present study indicates that while DSFs did not contribute to higher levels of thermal comfort, it is promising for reducing energy consumption without compromising thermal comfort. Since it was found that sites having high incident solar radiation have a higher reduction, site location is an important variable with sites located at higher latitudes, at or above the Tropic of Cancer, likely to benefit most from DSF usage in the Indian subcontinent.

The South, East and West facing façades are expected to benefit the most by employing a DSF. New Delhi, Jaisalmer, Kathmandu and Bhopal all show promising results for the application of DSF. Kolkata and Chennai on the other hand show less impressive improvements and owing to the high cost of DSF systems, a recommendation to use the same cannot be made without more detailed feasibility analysis. Looking at the sites in which the DSF performed most impressively it can be said that cites in the arid, semi-arid, humid subtropical and montane climate zones of India and other parts of the world can utilize the DSF for a reduction in cooling and/or heating demand.

The strategies employed here to reduce heat gain and overheating in the cavity can also be employed at locations in cooler climates such as in Europe. Many of the current DSFs employed in cooler climates have resulted in an increase in cooling demand despite an overall reduction in energy need due to a lowering of heating demand. The recommendations presented here can help achieve a more balanced design of the DSF in these locations as well.

Glazing selection is the most influential design parameter for reducing heat gain, especially in the external envelope. The overheating effect in the cavity has been shown to not have any detrimental effects on thermal comfort and can be suitably mitigated through mechanical ventilation.

REFERENCES

ASHRAE, 2004. Radiat Temperatrue Asymmetry. In: *ASHRAE STANDARD 55-2004*. Atlanta: American Society of Heating, Refrigerating and Air-Conditioning Engineers, Inc., pp. 7-8.

ASHRAE, 2013. *Handbook - Fundamentals*. SI ed. Atlanta: American Society of Heating, Refrigerating and Air-Conditioning Engineers, Inc..

Barbosa, S. A., 2015. *Thermal performance of naturally ventilated office buildings with double skin façade under Brazilian climate conditions,* Brighton: University of Brighton.

Barbosa, S. & Ip, K., 2014. Perspectives of double skin façades for naturally ventilated buildings: A review. *Renewable and Sustainable Energy Reviews,* Volume 40, pp. 1019-1029.

Chan, A., Chow, T., Fong, K. & Lin, Z., 2009. Investigation on energy performance of double skin facade in Hong Kong. *Energy and Buildings,* Volume 41, pp. 1135-1142.

Chou, S., Chua, K. & Ho, J., 2009. A study on the effects of double skin façades on the energy management in buildings. *Energy Conversion and Management,* Volume 50, pp. 2275-2281.

Clarke, J. A., 2001. *Energy Simulation in Building Design.* 2nd ed. Oxford: Butterworth-Heinemann.

Elarga, H., Carli, M. D. & Zarrella, A., 2015. A simplified mathematical model for transient simulation of thermal performance and energy assessment for active facades. *Energy and Buildings,* Volume 104, pp. 97-107.

Fallahi, A., Haghighat, F. & Elsadi, H., 2010. Energy performance assessment of double-skin facade with thermal mass. *Energy and Buildings,* Volume 42, p. 1499–1509.

Ghaffarianhoseini, A. et al., 2016. Exploring the advantages and challenges of double-skin façades (DSFs). *Renewable and Sustainable Energy Reviews,* Volume 60, pp. 1052-1065.

Gracia, A. D. et al., 2013. Numerical modelling of ventilated facades: A review. *Renewable and Sustainable Energy Reviews,* Volume 22, pp. 539-549.

Han, J., Lu, L., Peng, J. & Yang, H., 2013. Performance of ventilated double-sided PV facade compared with conventional clear glass facade. *Energy and Buildings,* Volume 56, p. 204–209.

Hashemi, N., Fayaz, R. & Sarshar, M., 2010. Thermal behaviour of a ventilated double skin facade in hot arid climate. *Energy and Buildings,* Volume 42, pp. 1823-1832.

Hong, T. et al., 2013. Assessment of Seasonal Energy Efficiency Strategies of a Double Skin Façade in a Monsoon Climate Region. *Energies,* Volume 6, pp. 4352-4376.

Ioannidis, Z., Buonomano, A., Athienitis, A. & Stathopoulos, T., 2017. Modeling of double skin fac¸ ades integrating photovoltaic panels and automated roller shades: Analysis of the thermal and electrical performance. *Energy and Buildings,* Volume 154, pp. 618-632.

ISO-15099, 2003. *Thermal performance of windows, doors and shading devices — Detailed calculations.* 1st ed. Switzerland: International Standards.

Jiru, T. E. & Haghighat, F., 2008. Modeling ventilated double skin facade—A zonal approach. *Energy and Buildings,* Volume 40, p. 1567–1576.

Joe, J., Choi, W., Kwak, Y. & Huh, J.-H., 2014. Optimal design of a multi-story double skin facade. *Energy and Buildings,* Volume 76, p. 143–150.

Larsen, S. F., Rengifo, L. & Filippín, C., 2015. Double skin glazed facades in sunny Mediterranean climates. *Energy and Buildings,* Volume 102, p. 18–31.

Linden, A. C. v. d., Erdtsieck, P., Gaalen, L. K.-v. & Zeegers, A., 2013. *Building Physics.* 1st ed. Amersfoort: Thieme Meulenhoff.

Manu, S. et al., 2014. *An Introduction to the Indian Model for Adaptive (Thermal) Comfort, IMAC,* Ahmedabad: Centre for Advanced Research in Building Science and Energy, CEPT University, India. IMAC TOOL: http://www.carbse.org/wp-content/uploads/2015/08/IMAC_Assistant-V2.xlsx Accessed on 3rd December 2018

Mingotti, N., Chenvidyakarn, T. & Woods, A., 2013. Combined impacts of climate and wall insulation on the energy benefit of an extra layer of glazing in the facade. *Energy and Buildings,* Volume 58, p. 237–249.

Mulyadi, R., 2012. *Study on naturally ventilated dounble-skin facade in hot and humid climate,* Nogaya: Nogaya University.

Pappas, A. & Zhai, Z., 2008. Numerical investigation on thermal performance and correlations of double skin facade with buoyancy-driven airflow. *Energy and Buildings,* Volume 40, p. 466–475.

Park, C. S., 2003. *A Thesis Report: Occupant Responsive Optimal Control of Smart Facade Systems,* Atlanta: Georgia Institute of Technology.

Peng, J. et al., 2016. Numerical investigation of the energy saving potential of a semi-transparent photovoltaic double-skin facade in a cool-summer Mediterranean climate. *Applied Energy,* Volume 165, p. 345–356.

Perez-Grande, I., Meseguer, J. & Alonso, G., 2005. Influence of glass properties on the performance of double-glazed facades. *Applied Thermal Engineering,* Volume 25, p. 3163–3175.

Pomponi, F. et al., 2016. Energy performance of Double-Skin Façades in temperate climates: A systematic review and meta-analysis. *Renewable and Sustainable Energy Reviews ,* Volume 54, pp. 1525-1536.

Rajesh, S. & Purohit, D., 2014. Energy efficient facades for Hot and Dry climate in India. *IJISTE - International Journal of Innovative Science, Engineering & Technology,* 1(6), pp. 536-542.

Stec, W. & Paassen, D. v., 2005. Sensitivity of the double skin facade on the outdoor conditions. *Proceedings: Indoor Air,* pp. 1371-1376.

Su, Z., Li, X. & Xue, F., 2017. Double-skin façade optimization design for different climate zones in China. *Solar Energy,* Volume 155, p. 281–290.

Torres, M. et al., 2007. Double skin facades - Cavity and exterior openings dimensions for saving energy on Mediterranean climate. *Proceedings: Building Simulation,* pp. 198-205.

van der Spoel, W. H., 2017. *Playing with heat balances - An introduction to numerical modelling of heat transfer problems.* Delft: TU Delft, Faculty of Architecture - Building Technology - Building Physics.

van Paassen, . A. H. C., 2004. *Indoor Climate Control Fundamentals (Module - 3): Heating and Cooling Capacities.* Delft: TU Delft Section Energy Technology.

Wang, Y., Chen, Y. & Zhou, J., 2016. Dynamic modeling of the ventilated double skin façade in hot summer and cold winter zone in China. *Building and Environment,* Volume 106, pp. 365-377.

Xue, F. & Li, X., 2015. A fast assessment method for thermal performance of naturally ventilated double-skin facades during cooling season. *Solar Energy,* Volume 114, pp. 303-313.

Yellamraju, V., 2014. *Evaluation and Design of Double-skin Facades for Office Buildings in Hot Climates,* College Station: Texas A&M University.

Zanghirella, F., Perino, M. & Serra, V., 2011. A numerical model to evaluate the thermal behaviour of active transparent facades. *Energy and Buildings ,* Volume 43, pp. 1123-1138.

Zhou, J. & Chen, Y., 2010. A review on applying ventilated double-skin facade to buildings in hot-summer and cold-winter zone in China. *Renewable and Sustainable Energy Reviews ,* Volume 14, pp. 1321-1328.

APPENDICES

Appendix A

Full Discretised Façade Diagram

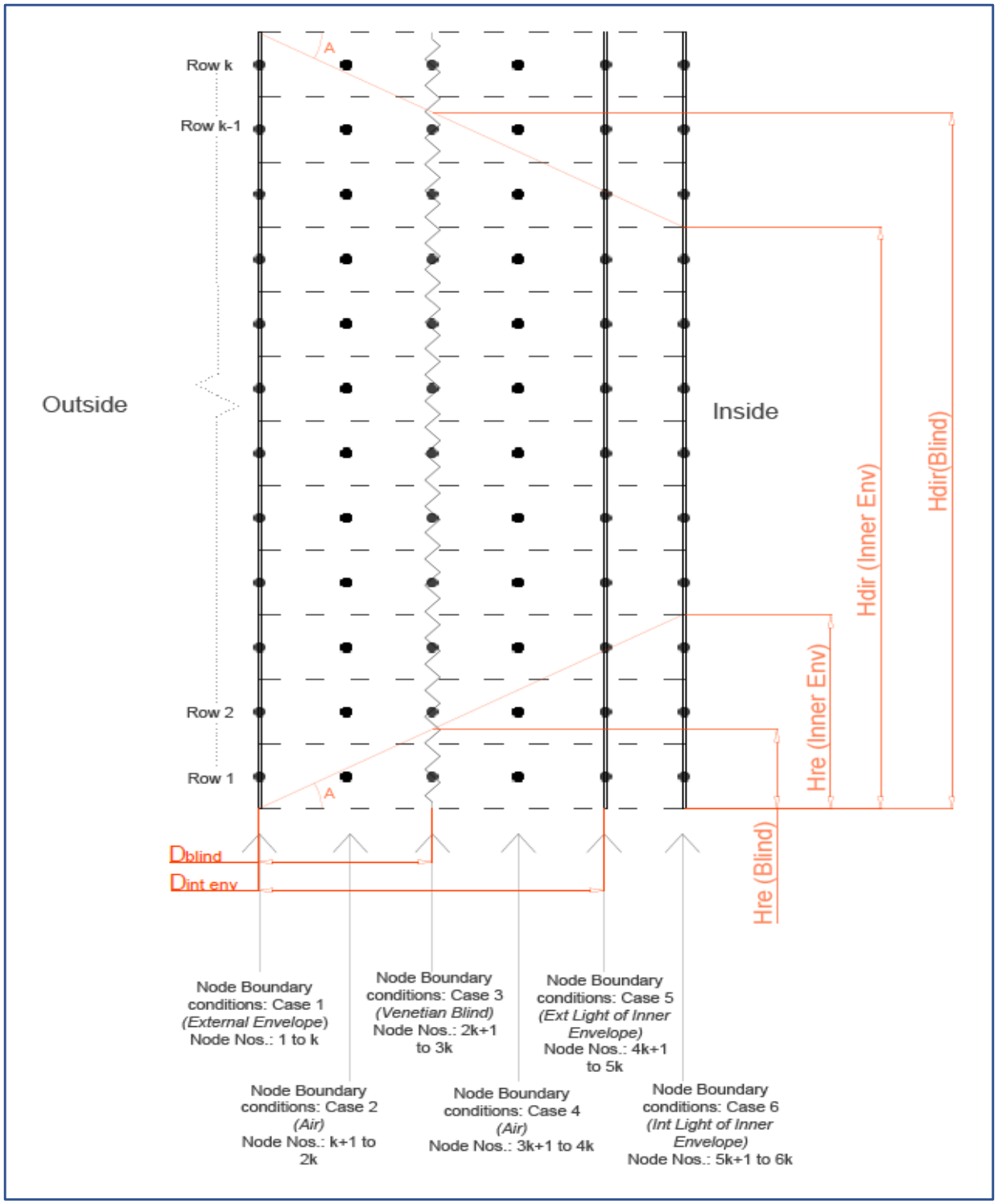

Figure A-1: A full discretized façade for 12 rows (k=12) along the height of the DSF. Each black circle represents a node. In red are indicated the details for the incident solar load, diffuse, diffuse + direct and diffuse + direct + once reflected for angle of incidence "A" on the respective components. To the bottom are described the component details with the boundary condition case (ref. fig. 3.1) followed by the node number (bottom to top) as referred to in the MATLAB/Simulink model.

Appendix B

Convective and Radiative Heat Transfer Coefficients

NOTE: The calculation shown here are an estimate of the heat transfer coefficients. These have been used in the simulations, however these values do **not** change based on site location nor do have any time dependant behaviour within the simulation. **The values found here are treated as constant for all simulation cases.**

External convective heat transfer coefficient, h_{wind} was calculated using the McAdams formula which relates wind speed to the heat transfer coefficient.

$$h_{wind} = 5.7 + 3.8 * V$$

Where V is the wind speed in m/s.

For example, the average wind speed in New Delhi is 6.7mph (ref fig x) which is roughly 3m/s. Hence,

$$h_{wind,New\ Delhi} = 5.7 + 3.8 * 3 = \mathbf{17.1\ W/m^2K}$$

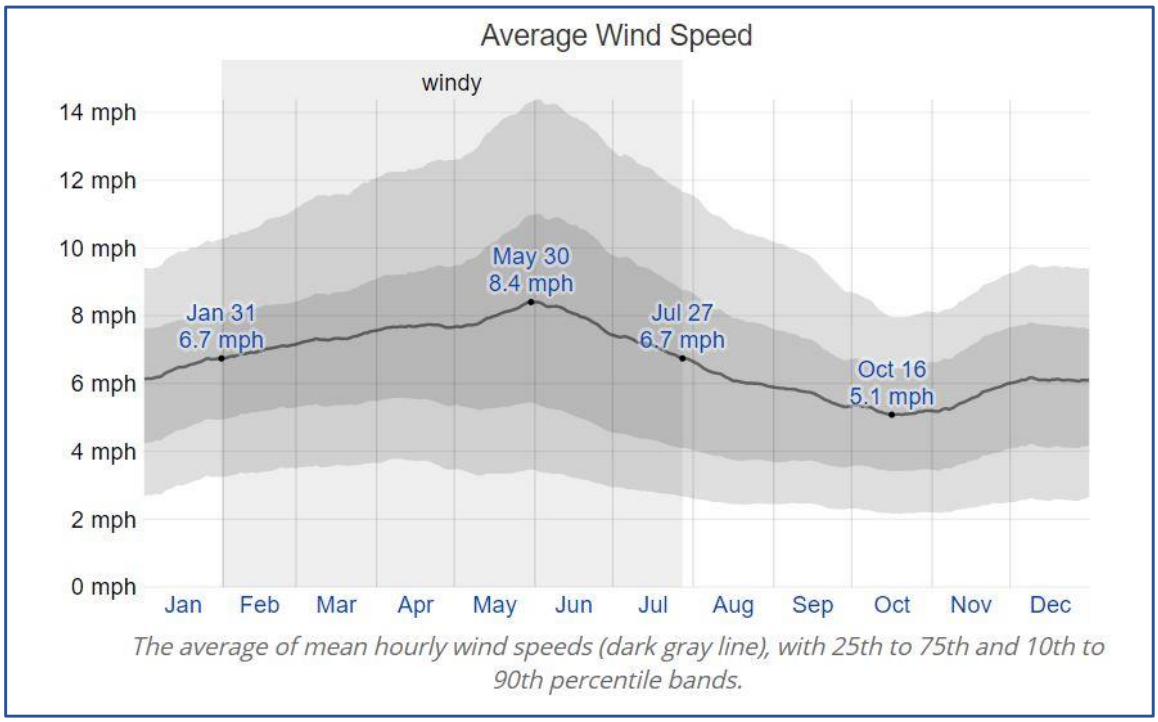

Figure B-1: Hourly Average wind speed in New Delhi
Source: https://weatherspark.com/y/109174/Average-Weather-in-New-Delhi-India-Year-Round

Internal convective heat transfer coefficient, h_{int} was calculated using the procedure outlined in the ASHRAE: Fundamentals Handbook which is empirically based on the Grashof (*Gr*), Prandtl (*Pr*) and Rayleigh (*Ra*) numbers.

$$Gr = \frac{g * \beta * {l_c}^3 * \Delta T}{\nu^2}$$

$$Ra = Gr * Pr$$

Where, g is acceleration due to gravity, ß is the volume expansion coefficient, l_c is the characteristic length, ΔT is the temperature difference and ν is the kinematic viscosity.

Once these empirical numbers are known the Nusselt number (Nu) can be calculated depending on the type of flow, which is characterized based on the value of Ra.

$$Nu = \begin{cases} 0.68 + \dfrac{0.67 * Ra^{1/4}}{[1 + (0.492/Pr)^{9/16}]^{4/9}} & ; for\ 10^{-1} < Ra < 10^{9} \\ \left\{0.825 + \dfrac{0.387 * Ra^{1/6}}{[1 + (0.492/Pr)^{9/16}]^{8/27}}\right\}^2 & ; for\ 10^{9} < Ra < 10^{12} \\ \left\{0.825 + \dfrac{0.387 * Ra^{1/6}}{[1 + (0.437/Pr)^{9/16}]^{8/27}}\right\}^2 & ; for\ 10^{-1} < Ra < 10^{12} \end{cases}$$

Knowing the Nu number, the convective heat transfer coefficient can be calculated as follows

$$h_{conv} = \frac{Nu * k_a}{l_{ch}}$$

Where k_a is the thermal conductivity of the fluid.

For example,

If the height of the room is 3m (l_c) and the temperature difference is 2°C (ΔT) we have,

$$Gr = \frac{9.81 * 0.00343 * 3^3 * 2}{(15.11 * 10^{-6})^2} = 7.96 * 10^9$$

For building applications, the Prandtl no. is usually 0.72. which gives:

$$Ra = 7.95 * 10^9 * 0.72 = 5.72 * 10^9$$

$$\Rightarrow Nu = \left\{0.825 + \frac{0.387 * (5.72 * 10^9)^{1/6}}{[1 + (0.492/0.72)^{9/16}]^{8/27}}\right\}^2 = 211.96$$

$$\Rightarrow h_{conv} = \frac{211.96 * 0.025}{3} = \mathbf{1.77 W/m^2 K}$$

Radiative heat transfer coefficient, α_r has been calculated by the following formula for objects at room temperature (23°C) and emissivities of 0.95.

$$\alpha_r = \sigma * \frac{({T_1}^2 + {T_2}^2) * (T_1 + T_2)}{(1/\varepsilon_1) + (1/\varepsilon_2) - 1}$$

$$\alpha_r = 5.67 * 10^{-8} * \frac{(296^2 + 296^2) * (296 + 296)}{(1/0.95) + (1/0.95) - 1}$$

$$\Rightarrow \alpha_r = \mathbf{5.32 W/m^2 K}$$

Appendix C

Fictitious Cavity Method

Fictitious surfaces (1) and (4) and a fictitious cavity surrounded by surfaces (1) to (4) are defined for convenience. For example, a view factor from (3) to (5), F_{35} is assumed to be F_{31} because long wave radiation between surfaces (3) and (5) occurs through surface (1). (Park, 2003)

From the summation rule, we obtain,

$$F_{11} + F_{12} + F_{13} + F_{14} = 1$$

$$F_{21} + F_{22} + F_{23} + F_{24} = 1$$

$$F_{31} + F_{32} + F_{33} + F_{34} = 1$$

$$F_{41} + +F_{42} + F_{43} + F_{44} = 1$$

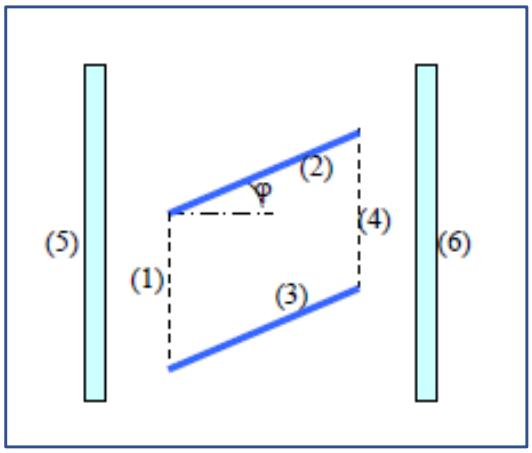

Figure C-1: Surface Notation for Fictitious Cavity Method
SOURCE: Park, 2003

For shape factor of surface (1), it is evident that

$$F_{11} = 0$$

$$F_{12} = 1 - \sin(\frac{90 + \varphi}{2})$$

$$F_{13} = 1 - \sin(\frac{90 - \varphi}{2})$$

$$F_{14} = 1 - F_{12} - F_{13} = \sqrt{2} * \cos\left(\frac{\varphi}{2}\right) - 1$$

Surfaces (2) and (3) and be representative of the venetian blind slats at an angle φ with the horizontal and surfaces (5) and (6) can be representative of the inner and external envelope of the DSF. This implies that the view factor among the glazings and the blind can be written as:

$$F_{glz\ to\ blind} = F_{52} + F_{53} = F_{12} + F_{13}$$

$$F_{glz\ to\ glz} = F_{56} = F_{14}$$

Appendix D

Reduction Factors for Incident Solar Radiation on the Components

Note 1: this section does not account for the reduction due to the shading device, i.e. The shading coefficient. This is explained in chapter 3, section 3.1.2

Note 2: the reduction factor is used to evaluate incident direct/diffuse solar radiation on a component, this should not be confused with the heat gain from solar radiation absorbed by the component.

For the external glazing, i.e. node no. 1:
There is no reduction in the solar loads due to any other layers of the façade, therefore we have,

$$Q_{diff,1} = Q_{diff}$$

$$Q_{dir,1} = Q_{dir}$$

There is no once reflected component nor is there any segmentation based on shading as the entire glazing unit is exposed equally to the solar radiation.

For the shading device, i.e. node no. 3:
There is a reduction on the incident solar radiation as it passes through the external envelope, therefore we have,

$$Q_{diff,3} = Q_{diff} * (\tau_1) = Q_{diff} * RF_{diff,3}$$

$$Q_{dir,3} = Q_{dir} * (\tau_1) = Q_{dir} * RF_{dir,3}$$

$$Q_{re,i} = Q_{dir} * \rho_s * (\tau_1) = Q_{dir} * RF_{dir,3} * \rho_s$$

The effective shading depth "D" for the segmentation along the height of the shading device is the distance between the external glazing and the shading device. Based on this segmentation, a combination of the above components of incident radiation will be applicable.

For the outer surface of the inner envelope, i.e. node no. 5:
There is a reduction on the incident solar radiation as it passes through the external envelope, therefore we have,

$$Q_{diff,5} = Q_{diff} * (\tau_1) = Q_{diff} * RF_{diff,5}$$

$$Q_{dir,5} = Q_{dir} * (\tau_1) = Q_{dir} * RF_{dir,5}$$

$$Q_{re,5} = Q_{dir} * \rho_s * (\tau_1) = Q_{dir} * RF_{dir,5} * \rho_s$$

The effective shading depth "D" for the segmentation along the height of the surface is the distance between the external glazing and the internal envelope. Based on this segmentation, a combination of the above components of incident radiation will be applicable.

For the inner surface of the inner envelope, i.e. node no. 6:
There is a reduction on the incident solar radiation as it passes through the external envelope as well as the external glazing layer in the double-glazed system, therefore we have,

$$Q_{diff,6} = Q_{diff} * (\tau_1 + \tau_5) = Q_{diff} * RF_{diff,6}$$

$$Q_{dir,6} = Q_{dir} * (\tau_1 + \tau_5) = Q_{dir} * RF_{dir,6}$$

$$Q_{re,6} = Q_{dir} * \rho_s * (\tau_1 + \tau_5) = Q_{dir} * RF_{dir,6} * \rho_s$$

The effective shading depth "D" for the segmentation along the height of the surface is the distance between the external glazing and the internal envelope. Based on this segmentation, a combination of the above components of incident radiation will be applicable.

Appendix E

Glazing Properties and Variable Setup

The tables below show all the optical properties and U-values of the different glazing systems employed for the simulations carried forth in this study. These values are derived from the WINDOW 7.7 programme.

In Green: Glazing systems used as inner (4/16/4 argon gas) and external (clear 6mm) in the verification procedure with design builder as well as in the base configuration of the DSF in the behavioural analysis.

In Red: Glazing system used in the single skin façade for comparative assessment of the DSF.

Note: The transmission for all double-glazing systems (trans 1 and trans 2) are derived from the properties of simulating the individual glazing lights as the window 7.7 program provides the overall transmission of the full system in the case of double-glazing and not that of the individual glazing lights. This was done to accommodate the methodology employed for computing solar

Table E-1: Glazing optical properties and U-

Glazing	U-Value	Optical Details	Angle										
			0 °	10 °	20 °	30 °	40 °	50 °	60 °	70 °	80 °	90 °	Diffuse
Tinted DG 4/12.7/3 Argon gas	2.56	ABS 1	0.416	0.418	0.423	0.431	0.441	0.453	0.462	0.456	0.389	0	0.435
		TRANS 1	0.539	0.537	0.532	0.523	0.509	0.486	0.446	0.369	0.214	0	0.463
		ABS 2	0.036	0.037	0.037	0.037	0.037	0.036	0.034	0.029	0.019	0	0.034
		TRANS 2	0.834	0.833	0.821	0.827	0.818	0.797	0.749	0.637	0.389	0	0.753
Reflective DG 13.2/12.7/3 Argon Gas	2.47	ABS 1	0.199	0.201	0.204	0.206	0.205	0.205	0.208	0.206	0.162	0	0.201
		TRANS 1	0.186	0.188	0.185	0.182	0.179	0.173	0.158	0.129	0.078	0	0.163
		ABS 2	0.011	0.011	0.011	0.011	0.012	0.012	0.011	0.01	0.008	0	0.001
		TRANS 2	0.834	0.833	0.821	0.827	0.818	0.797	0.749	0.637	0.389	0	0.753
clear DB 4/16/4 argon gas	2.72	ABS 1	0.054	0.054	0.055	0.057	0.06	0.063	0.068	0.074	0.079	0	0.062
		TRANS 1	0.871	0.871	0.87	0.866	0.858	0.838	0.79	0.675	0.417	0	0.792
		ABS 2	0.043	0.043	0.044	0.045	0.046	0.047	0.047	0.043	0.033	0	0.044
		TRANS 2	0.871	0.871	0.87	0.866	0.858	0.838	0.79	0.675	0.417	0	0.792
clear 4mm	5.88	ABS	0.051	0.051	0.052	0.054	0.056	0.058	0.061	0.063	0.062	0	0.057
		TRANS	0.871	0.871	0.87	0.866	0.858	0.838	0.79	0.675	0.417	0	0.792
High Performance DG 6/12/3 LowE, argon	1.33	ABS 1	0.34	0.343	0.348	0.35	0.348	0.347	0.347	0.336	0.258	0	0.337
		TRANS 1	0.258	0.26	0.256	0.252	0.247	0.239	0.219	0.178	0.107	0	0.225
		ABS 2	0.011	0.011	0.011	0.011	0.011	0.011	0.011	0.01	0.008	0	0.011
		TRANS 2	0.834	0.833	0.821	0.827	0.818	0.797	0.749	0.637	0.389	0	0.753

Table E-1: Glazing optical properties and U-value (Contd.)

Glazing	U-Value	Optical Details	Angle										
			0 °	10 °	20 °	30 °	40 °	50 °	60 °	70 °	80 °	90 °	Diffuse
Clear 6mm	5.82	ABS	0.159	0.16	0.163	0.167	0.173	0.18	0.185	0.186	0.17	0	0.173
		TRANS	0.771	0.77	0.767	0.761	0.75	0.727	0.68	0.575	0.346	0	0.689
Reflective 13.2mm	5.39	ABS	0.193	0.194	0.198	0.199	0.198	0.197	0.198	0.19	0.144	0	0.192
		TRANS	0.186	0.188	0.185	0.182	0.179	0.173	0.158	0.129	0.078	0	0.163
Tinted 5.8mm	5.82	ABS	0.623	0.622	0.627	0.634	0.642	0.647	0.641	0.602	0.471	0	0.681
		TRANS	0.327	0.325	0.32	0.312	0.299	0.282	0.255	0.207	0.117	0	0.271
High Performance DG 10/1/3 LowE, Vacuum	0.59	ABS 1	0.255	0.258	0.262	0.264	0.264	0.264	0.267	0.264	0.208	0.001	0.258
		TRANS 1	0.254	0.255	0.252	0.248	0.244	0.235	0.216	0.176	0.106	0	0.222
		ABS 2	0.007	0.008	0.008	0.008	0.008	0.008	0.008	0.007	0.005	0	0.007
		TRANS 2	0.834	0.833	0.821	0.827	0.818	0.797	0.749	0.637	0.389	0	0.753
LowE DB 9.4/12.7/3 LowE, Argon gas	1.47	ABS 1	0.155	0.157	0.168	0.175	0.179	0.187	0.212	0.246	0.229	0.001	0.191
		TRANS 1	0.638	0.642	0.634	0.624	0.612	0.59	0.542	0.441	0.265	0	0.558
		ABS 2	0.049	0.049	0.05	0.05	0.051	0.052	0.05	0.044	0.032	0	0.048
		TRANS 2	0.834	0.833	0.821	0.827	0.818	0.797	0.749	0.637	0.389	0	0.753
Clear 3mm	5.91	ABS	0.091	0.092	0.094	0.096	0.1	0.104	0.108	0.11	0.105	0	0.101
		TRANS	0.834	0.833	0.831	0.827	0.818	0.797	0.749	0.637	0.389	0	0.753

loads in the MATLAB/Simulink model which is based on the optical properties of individual glazing lights. The absorption (ABS 1 and ABS 2) on the other hand were taken from the double-glazing system as a whole since it more accurately represents the distribution of heat among the two glazing lights.

The visible light transmission of the DSF as a whole was calculated by multiplying the individual transmissions of the inner and external envelope and this was kept as close to that of the single skin used in the performance comparison to equate for day light quality.

Table 2: Visible light transmission of various glazing units

Glazing	Visible Light Transmission
Clear 6mm	0.88
Reflective 13.2mm	0.33
Tinted 5.8mm	0.66
High Performance DG 6/12/3 LowE, argon	0.52
LowE DB 9.4/12.7/3 LowE, Argon gas	0.79
High Performance DG 10/1/3 LowE, Vacuum	0.61
Tinted DG 4/12.7/3 Argon gas	0.72

The following image describes the file setup for the glazing data used in the MATLAB/Simulink model. The program is configured to read the values in the cells of the 2-D array and employ them as needed.

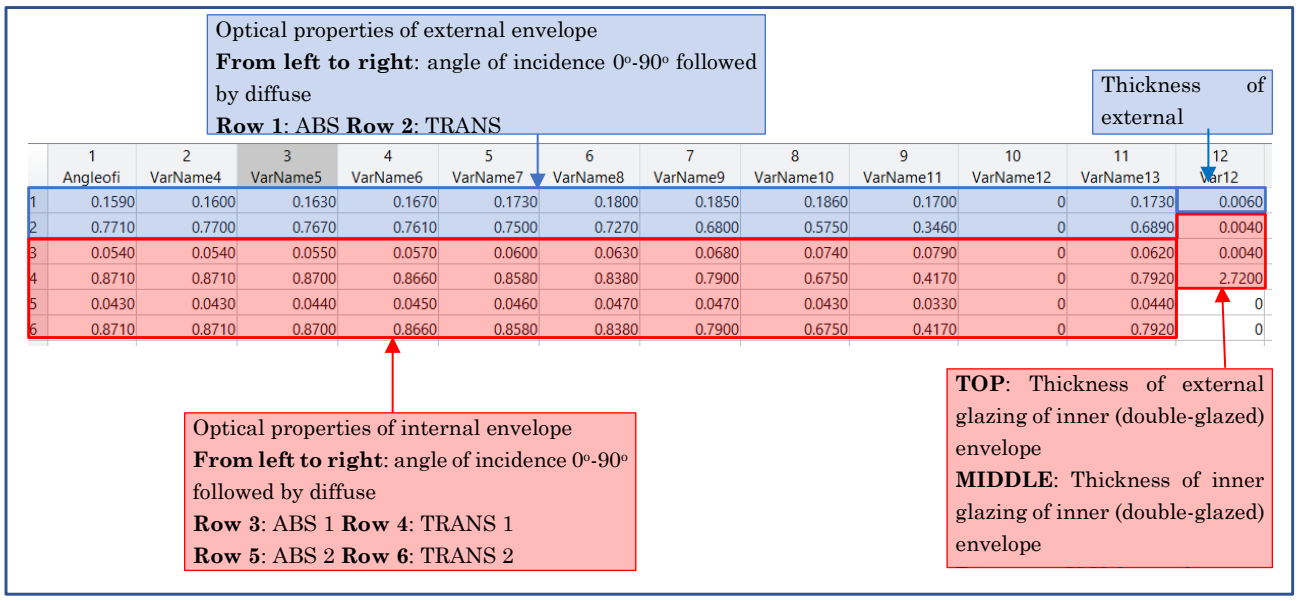

	1 Angleofi	2 VarName4	3 VarName5	4 VarName6	5 VarName7	6 VarName8	7 VarName9	8 VarName10	9 VarName11	10 VarName12	11 VarName13	12 Var12
1	0.1590	0.1600	0.1630	0.1670	0.1730	0.1800	0.1850	0.1860	0.1700	0	0.1730	0.0060
2	0.7710	0.7700	0.7670	0.7610	0.7500	0.7270	0.6800	0.5750	0.3460	0	0.6890	0.0040
3	0.0540	0.0540	0.0550	0.0570	0.0600	0.0630	0.0680	0.0740	0.0790	0	0.0620	0.0040
4	0.8710	0.8710	0.8700	0.8660	0.8580	0.8380	0.7900	0.6750	0.4170	0	0.7920	2.7200
5	0.0430	0.0430	0.0440	0.0450	0.0460	0.0470	0.0470	0.0430	0.0330	0	0.0440	0
6	0.8710	0.8710	0.8700	0.8660	0.8580	0.8380	0.7900	0.6750	0.4170	0	0.7920	0

Figure E-1: The setup of the Matlab table for storing various glazing data. (The table is converted to a 2D array in the initiation function)

Appendix F

Initialization MATLAB code

```
% Version 4: with shading and mech ventilation control,
% internal temp based on adaptive thermal comfort


clear;% clear all data in the workspace
clc; % clear screen
%----------WEATHER DATA INPUT----------------------------------------------

load("te_delhi.mat");       %load temperature data
load("Q_delhi");            %load solar radiation data
load("LW_delhi");           %load LW sky radiation data
Qze=table2array(Q);
orient=     5;              %1-N 2-NE 3-E 4-SE 5-S 6-SW 7-W 8-NW
Q_sol_dir=zeros(8760,2);
Q_sol_diff=zeros(8760,2);
for i=1:8760                %set required dir and diff solar rad matrices
    Q_sol_dir(i,2) = Qze(i,orient+1);
    Q_sol_dir(i,1) = Qze(i,1);
    Q_sol_diff(i,2)= Qze(i,orient+19);
    Q_sol_diff(i,1)= Qze(i,1);
end


tan_theta = zeros (8760,2); %setting tan(theta) for cavity overhang shading
angle_normal2plane = zeros (8760,1);
for i=1:8760

    if Qze(i,19) >=0
        theta = acosd(Qze(i,19));  %theta is angle of incidence, ie measured from normal to
plain
        angle_normal2plane (i) = theta;
        tan_theta(i,2) = tand(90-theta);
    end

    if angle_normal2plane (i) >= 360
        angle_normal2plane (i) = angle_normal2plane (i)-360;
    end

    tan_theta(i,1) = i*3600;

    if tan_theta(i,2) == inf
        tan_theta(i,2) = -1;
    end

end
```

```
%---------LOAD MATERIAL DATA FOR GLAZING OPTICAL PROPERTIES----------------

load("G7.mat");% ADJUST FOR GL DETAILS
T = table2array(mat_data);


%-------THERMAL COMFORT DATA to SET INTERNAL TEMPERATURE------------------

load("int_temp_delhi.mat");
T_i     =zeros(8760,2);
count   =1;
for i=1:8760
    T_i(i,1)    = i*3600;
        if i<31*24
            T_i(i,2)    =int_temp(1,1);
        elseif i>=31*24 && i<(31+28)*24
            T_i(i,2)    =int_temp(2,1);
        elseif i>=(31+28)*24 && i<(31+28+31)*24
            T_i(i,2)    =int_temp(3,1);
        elseif i>=(31+28+31)*24 && i<(31+28+31+30)*24
            T_i(i,2)    =int_temp(4,1);
        elseif i>=(31+28+31+30)*24 && i<(31+28+31+30+31)*24
            T_i(i,2)    =int_temp(5,1);
        elseif i>=(31+28+31+30+31)*24 && i<(31+28+31+30+31+30)*24
            T_i(i,2)    =int_temp(6,1);
        elseif i>=(31+28+31+30+31+30)*24 && i<(31+28+31+30+31+30+31)*24
            T_i(i,2)    =int_temp(7,1);
        elseif i>=(31+28+31+30+31+30+31)*24 && i<(31+28+31+30+31+30+31+31)*24
            T_i(i,2)    =int_temp(8,1);
        elseif i>=(31+28+31+30+31+30+31+31)*24 && i<(31+28+31+30+31+30+31+31+30)*24
            T_i(i,2)    =int_temp(9,1);
        elseif i>=(31+28+31+30+31+30+31+31+30)*24 && i<(31+28+31+30+31+30+31+31+30+31)*24
            T_i(i,2)    =int_temp(10,1);
        elseif i>=(31+28+31+30+31+30+31+31+30+31)*24 &&
i<(31+28+31+30+31+30+31+31+30+31+30)*24
            T_i(i,2)    =int_temp(11,1);
        elseif i>=(31+28+31+30+31+30+31+31+30+31+30)*24 &&
i<=(31+28+31+30+31+30+31+31+30+31+30+31)*24
            T_i(i,2)    =int_temp(12,1);
        end

end







% ------PHYSICAL INPUT -----------------------------------------------------

% constants
rho_air         = 1.2;      % mass density of air (kg/m3)
c_air           = 1000;     % specific heat capacity of air J/kgK

%Facade dimensions
```

```
ht              = 3;  %height (m)
w               = 10;  %width (m)

%Facade material properties

% layer 1: outer single glazing
layer(1).d      = T(1,12);   % thickness (m)
layer(1).rho    = 2530;      % mass density (kg/m3)
layer(1).c      = 840;       % specific heat capacity (J/kgK)
layer(1).la     = 0.971;     % heat conduction coefficient (W/mK)


% layer 2: air cavity between outer envelope and shading device
layer(2).d      = 0.65;      % thickness (m)
layer(2).rho    = rho_air;   % mass density (kg/m3)
layer(2).c      = c_air;     % specific heat capacity (J/kgK)
layer(2).la     = 0.0262;    % heat conduction coefficient (W/mK)

% layer 3: shading device (aluminium)
layer(3).d      = 0.0001;        % thickness (m)
layer(3).rho    = 2700;          % mass density (kg/m3)
layer(3).c      = 900;           % specific heat capacity (J/kgK)
layer(3).la     = 205;           % heat conduction coefficient (W/mK)
l3              = layer(2).d;    % shading depth

% layer 4: air cavity between shading device and inner envelope
layer(4).d      = layer(2).d;    % thickness (m),
layer(4).rho    = rho_air;       % mass density (kg/m3)
layer(4).c      = c_air;         % specific heat capacity (J/kgK)
layer(4).la     = 0.0262;        % heat conduction coefficient (W/mK)

%layer 5: external pane of double glazing, inner envelope
layer(5).d      = T(2,12);       % thickness (m), loaded from glazing data
layer(5).rho    = 2530;          % mass density (kg/m3)
layer(5).c      = 840;           % specific heat capacity (J/kgK)
layer(5).la     = 1;             % heat conduction coefficient (W/mK)
l5 = layer(2).d + layer(4).d ;  % shading depth

% layer 6: internal pane of double glazing, inner envelope
layer(6).d      = T(3,12);       % thickness (m), loaded from glazing data
layer(6).rho    = 2530;          % mass density (kg/m3)
layer(6).c      = 840;           % specific heat capacity (J/kgK)
layer(6).la     = 1;             % heat conduction coefficient (W/mK)
l6 = l5;  %shading depth




% ------SIMULATION INPUT -------------------------------------------------

T_intial        = 22;              % initial temp in all nodes(deg C)
start_time      = 0*86400;         % start simulation (s)
stop_time       = 365*86400;       % stop simulation (s)
```

```
% ------DISCRETISATION INPUT -------------------------------------------

K               = 12;       % number of nodes in vertical direction
Ar              = w*ht/K;   % area per node (m2)
n_fr            = K*6;      % total number of free nodes in facade
n_int           = 6*K+1;    % node no. of internal air
n_ext           = 6*K+2;    % node no. of external air
n_tot           = n_ext;    % total no. of nodes


%------HEAT TRANSFER AND AIR FLOW PARAMETERS------------------------------

a_cvE           = 17.7;                                     % convective coeff external W/m2K
a_cvIC          = 2.2;                                    % convective coeff inside cavity
W/m2K
a_cvSD          = 4;                                        % convective coeff for shading
device W/m2K
a_cvIR          = 1.7;                                      % convective coeff inside room
W/m2K
a_rad           = 5;                                        % radiation coeff W/m2K
%AirCh           = 080.0;                                    % air changes per hour h^-1
%vf_rate         = AirCh*(layer(2).d+layer(4).d)*ht*w/(2*3600);  % volumetric flow rate in
m3/s based on air changes, either side of blinds
vf_rate         = 600/3600;                                 % Possible to fix, m3/s for either
side of the blinds
mf_rate         = vf_rate*rho_air;                          % mass flow rate in kg/m3
r_i             = 1/(a_rad + a_cvIR);                       % tot surf resistance internal
m2K/W
r_e             = 1/(a_cvE + a_rad);                      % tot surf resistance external(W/m2K)
U_glz_actual    = T(4,12);     % U value of double glazing (W/m2K), loaded from glazing data
U_glz           = 1/((1/U_glz_actual)-0.17) ;               % adjusting value to remove
surface resistance(W/m2K)


%-------VIEW FACTORS-------------------------------------------------------
%without blinds:
angle_off       = 0;
F_13            = 2-sind((90+angle_off)/2)-sind((90-angle_off)/2);
F_31            = F_13;
F_15            = sqrt(2)*cosd(angle_off/2)-1;
F_51            = F_15;
F_35            = F_13;
F_53            = F_35;
F_56            = 1;
F_65            = F_56;

%with blinds:
angle_on        = 45;
F_13b           = 2-sind((90+angle_on)/2)-sind((90-angle_on)/2);
F_31b           = F_13b;
F_15b           = sqrt(2)*cosd(angle_on/2)-1;
F_51b           = F_15b;
F_35b           = F_13b;
F_53b           = F_35b;
F_56b           = 1;
```

```
F_65b           = F_56b;


%----------CREATING "S" MATRIX, STIFFNESS MATRIX WITHOUT BLINDS------------

S=zeros(n_fr); %total unknown nodes

for i=1:K   %for external envelope
    S(i,i)      = Ar*((1/r_e) + a_cvIC + a_rad*(F_13+F_15)); %(1,1)
    S(i,i+K)    = -Ar*a_cvIC;                                %(1,2)
    S(i,i+2*K)  = -Ar*a_rad*F_13;                            %(1,3)
    S(i,i+4*K)  = -Ar*a_rad*F_15;                            %(1,5)
end

for i=K+2:2*K   %air cavity between outer envelope and shading device
                  %all nodes except bottom node
    S(i,i)      = Ar*(a_cvIC + a_cvSD)+rho_air*c_air*vf_rate;   %(2,2)
    S(i,i-K)    = -Ar*a_cvIC;                                   %(2,1)
    S(i,i+K)    = -Ar*a_cvSD;                                   %(2,3)
    S(i,i-1)    = -rho_air*c_air*vf_rate;                   %(2(k),2(k-1))
end

for i=2*K+1:3*K       %nodes at blinds
    S(i,i)      = Ar*(2*a_cvSD + a_rad*(F_31+F_35));        %(3,3)
    S(i,i-K)    = -Ar*a_cvSD;                               %(3,2)
    S(i,i-2*K)  = -Ar*a_rad*F_31;                           %(3,1)
    S(i,i+K)    = -Ar*a_cvSD;                               %(3,4)
    S(i,i+2*K)  = -Ar*a_rad*F_35;                           %(3,5)
end

for i=3*K+2:4*K   %air cavity between inner envelope and shading device
                    %all nodes except bottom
    S(i,i)      = Ar*(a_cvIC + a_cvSD)+rho_air*c_air*vf_rate;   %(4,4)
    S(i,i+K)    = -Ar*a_cvIC;                                   %(4,5)
    S(i,i-K)    = -Ar*a_cvSD;                                   %(4,3)
    S(i,i-1)    = -rho_air*c_air*vf_rate;                   %(4(k),4(k-1))
end

for i=4*K+1:5*K     %for external glazing surface of inner envelope
    S(i,i)      = Ar*(a_cvIC + a_rad*(F_51+F_53)+U_glz);    %(5,5)
    S(i,i-K)    = -Ar*a_cvIC;                               %(5,4)
    S(i,i-2*K)  = -Ar*a_rad*F_53;                           %(5,3)
    S(i,i-4*K)  = -Ar*a_rad*F_51;                           %(5,1)
    S(i,i+K)    = -Ar*U_glz;                                %(5,6)
end

for i=5*K+1:6*K     %for internal glzing surface of inner envelope
    S(i,i)      = Ar*((1/r_i) + U_glz);                     %(6,6)
    S(i,i-K)    = -Ar*U_glz;                                %(6,5)
end

 %setting bottom air nodes
 S(K+1,K+1)     = Ar*(a_cvIC + a_cvSD)+rho_air*c_air*vf_rate;   %(2,2)
 S(K+1,1)       = -Ar*a_cvIC;                                   %(2,1)
 S(K+1,2*K+1)   = -Ar*a_cvSD;                                   %(2,3)
```

```
 S(3*K+1,3*K+1) = Ar*(a_cvIC + a_cvSD)+rho_air*c_air*vf_rate;   %(4,4)
 S(3*K+1,4*K+1) = -Ar*a_cvIC;                                   %(4,5)
 S(3*K+1,2*K+1) = -Ar*a_cvSD;                                   %(4,3)



%-------CREATING "S_blind" MATRIX, STIFFNESS MATRIX WITH BLINDS------------

 S_blind        = S;            %initialize to same as "S"
%change view factors:
 for i=1:K   %for external envelope
    S_blind(i,i)      = Ar*((1/r_e) + a_cvIC + a_rad(F_13b+F_15b)); %(1,1)
    S_blind(i,i+2*K)  = -Ar*a_rad*F_13b;                            %(1,3)
    S_blind(i,i+4*K)  = -Ar*a_rad*F_15b;                            %(1,5)
end

for i=2*K+1:3*K       %nodes at blinds
    S_blind(i,i)      = Ar*(2*a_cvSD + a_rad*(F_31b+F_35b));       %(3,3)
    S_blind(i,i-2*K)  = -Ar*a_rad*F_31b;                          %(3,1)
    S_blind(i,i+2*K)  = -Ar*a_rad*F_35b;                          %(3,5)
end

for i=4*K+1:5*K     %for external glazing surface of inner envelope
    S_blind(i,i)      = Ar*(a_cvIC + a_rad(F_51b+F_53b)+U_glz);    %(5,5)
    S_blind(i,i-2*K)  = -Ar*a_rad*F_53b;                          %(5,3)
    S_blind(i,i-4*K)  = -Ar*a_rad*F_51b;                          %(5,1)

end



%-----CREATING "Sb" MATRIX, KNOWN TEMPERATURE COUPLINGS-------------------

Sb=zeros(n_fr,2);
for i=1:K  %for external glazing nodes
           %all constants other than ext temperature
    Sb(i,2)       = -Ar*(1/r_e);
end
for i=5*K+1:6*K  %for internal glazing nodes
                 %all constants other than int temperature
    Sb(i,1)       = -Ar*(1/r_i);
end
%advection, all constants other than ext temperature
Sb(K+1,2)   = -rho_air*c_air*vf_rate;      %bottom node @2 and ext air
Sb(3*K+1,2) = -rho_air*c_air*vf_rate;      %bottom node @4 and ext air
        %in simulink Sb should have T int first, then T ext in input MUX



%-----SETTING PARTIAL STIFFNESS MATRIX FOR ADVECTION ADJUSTMENT-----------
```

```
%by default, ventilation is set at vf_rate, this component when added to the
%stiffness matrix makes the terms of advective component zero by subtraction
%from pre-set stiffness matrix, creating ventilation OFF STATE

T_v_set     = 10;           %temperature set point for ventilation

%for "S" and "S_blind"
S_adjust = zeros(n_fr);
for i=K+2:2*K   %air cavity between outer envelope and shading device
                  %all nodes except bottom node
    S_adjust(i,i)      = rho_air*c_air*vf_rate;             %(2,2)
    S_adjust(i,i-1)    = -rho_air*c_air*vf_rate;            %(2(k),2(k-1))
end
for i=3*K+2:4*K   %air cavity between inner envelope and shading device
                    %all nodes except bottom
    S_adjust(i,i)      = rho_air*c_air*vf_rate;             %(4,4)
    S_adjust(i,i-1)    = -rho_air*c_air*vf_rate;            %(4(k),4(k-1))
end
 S_adjust(K+1,K+1)     = rho_air*c_air*vf_rate;             %(2,2)
 S_adjust(3*K+1,3*K+1)  = rho_air*c_air*vf_rate;            %(4,4)

%for "Sb"
Sb_adjust=zeros(n_fr,2);
Sb_adjust(K+1,2)   = -rho_air*c_air*vf_rate;    %bottom node @2 and ext air
Sb_adjust(3*K+1,2) = -rho_air*c_air*vf_rate;    %bottom node @4 and ext air


%-----------CREATING "M" MATRIX, MASS MATRIX-----------------------------

M=zeros(n_fr);
for i=1:6
    for k=1:K
        n = (i-1)*K+k;
        switch i
            case {1}     %ext glazing
                M(n,n)= layer(1).d*Ar*layer(1).c*layer(1).rho;
            case {2}     %air cav between ext glz and blinds
                M(n,n)= layer(2).d*Ar*layer(2).c*layer(2).rho;
            case {3}     %blinds
                M(n,n)= layer(3).d*Ar*layer(3).c*layer(3).rho;
            case {4}     %air cav between int glz and blinds
                M(n,n)= layer(4).d*Ar*layer(4).c*layer(4).rho;
            case {5}     %outer pane of double glazing
                M(n,n)= layer(5).d*Ar*layer(5).c*layer(5).rho;
            case {6}     %inner pane of double glazing
                M(n,n)= layer(6).d*Ar*layer(6).c*layer(6).rho;
        end
    end
end


%-----CREATING "Q" MATRIX, SOLAR/INTERNAL HEAT LOADS-----------------------
%only area
%dir/diff and abs will be taken in secondary function in simulink
```

```
SC_on   = 0.52;
SC_off  = 0.98;

Q=zeros(n_fr,1); %-----for blinds not active-----------------------------
for i=1:K                           %outer glazing
    Q(i,1)  = Ar;
end
for i=2*K+1:3*K                     %blind
    Q(i,1)  = Ar;
end
for i=4*K+1:5*K                     %outer pane of double glazing
    Q(i,1)  =  Ar*SC_off;
end
for i=5*K+1:6*K                     %inner pane of double glazing
    Q(i,1)  = Ar*SC_off;
end


Q_blind=Q; %-----------for blinds active---------------------------------
%includes area and reduction factor for blind
for i=1:K                               %outer glazing
    Q_blind(i,1)  = Ar;
end
for i=2*K+1:3*K                         %blind
    Q_blind(i,1)  = Ar;
end
for i=4*K+1:5*K                         %outer pane of double glazing
    Q_blind(i,1)  = Ar*SC_on;
end
for i=5*K+1:6*K                         %inner pane of double glazing
    Q_blind(i,1)  = Ar*SC_on;
end
```

Published with MATLAB® R2018b

Appendix G

Simulink Model

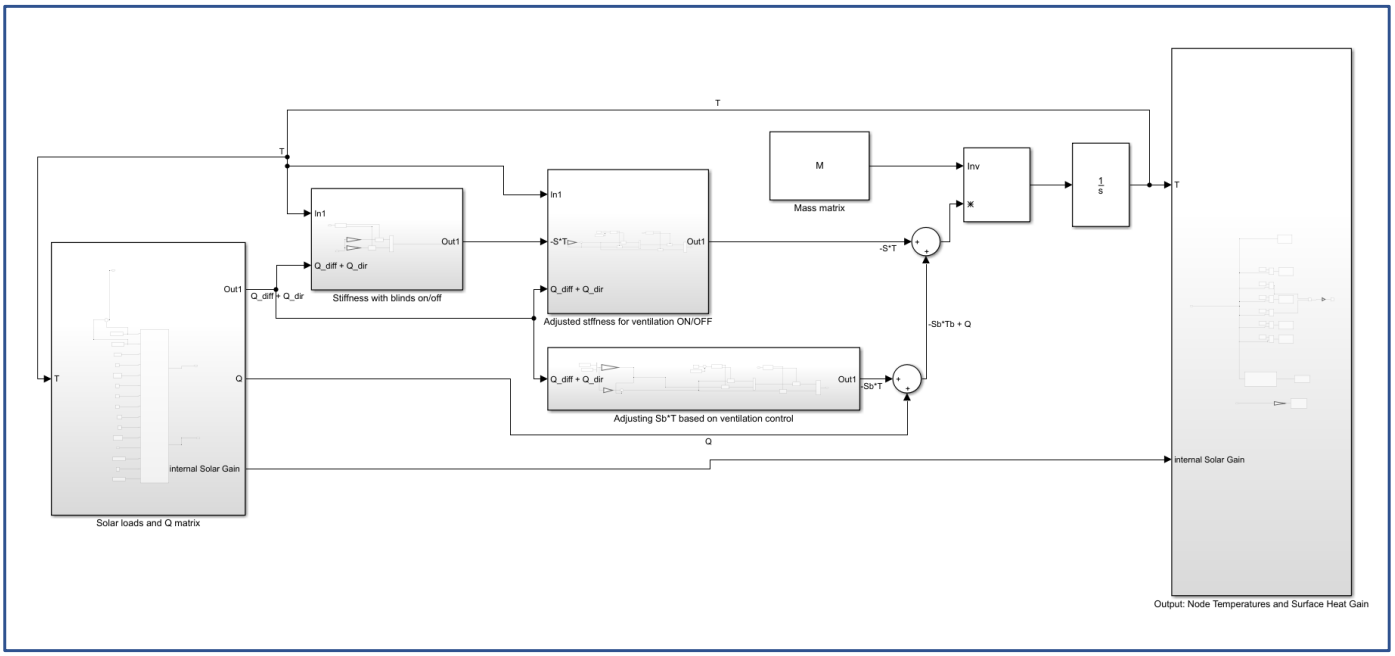

Figure G-1:Full Simulink Model

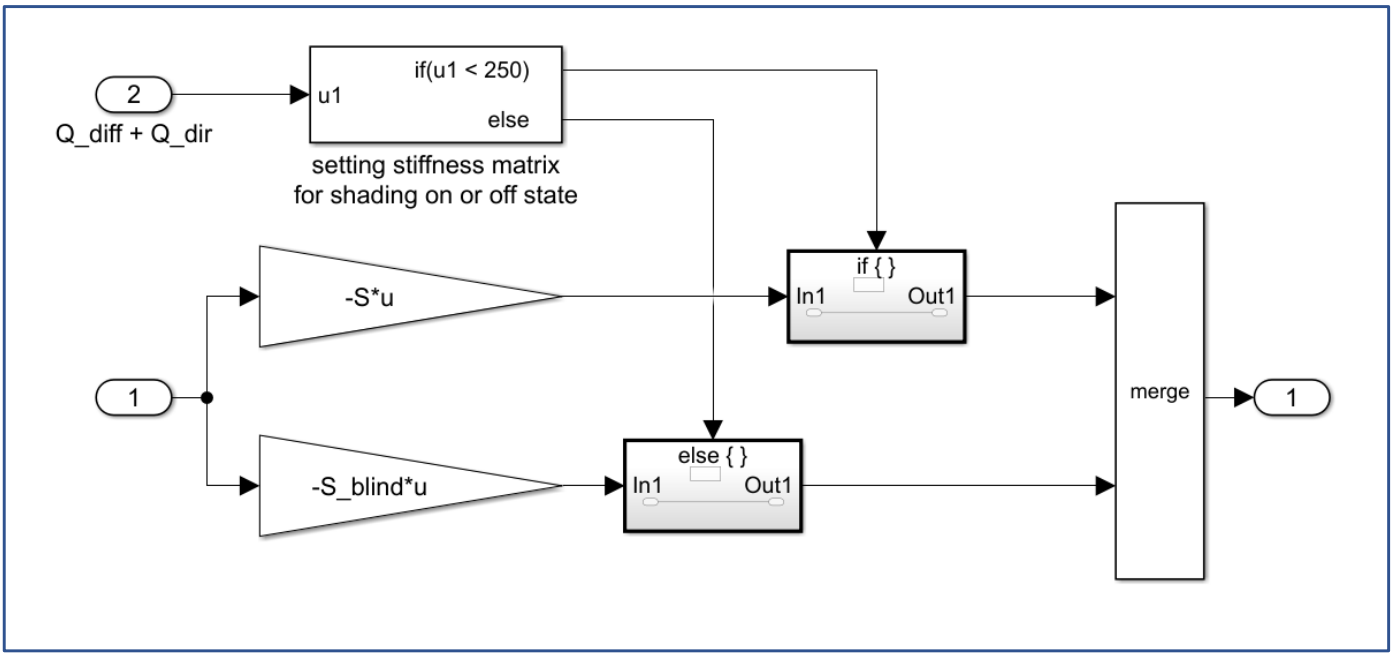

Figure G-2: Simulink Block for selecting stiffness matrix based on blind off or on condition

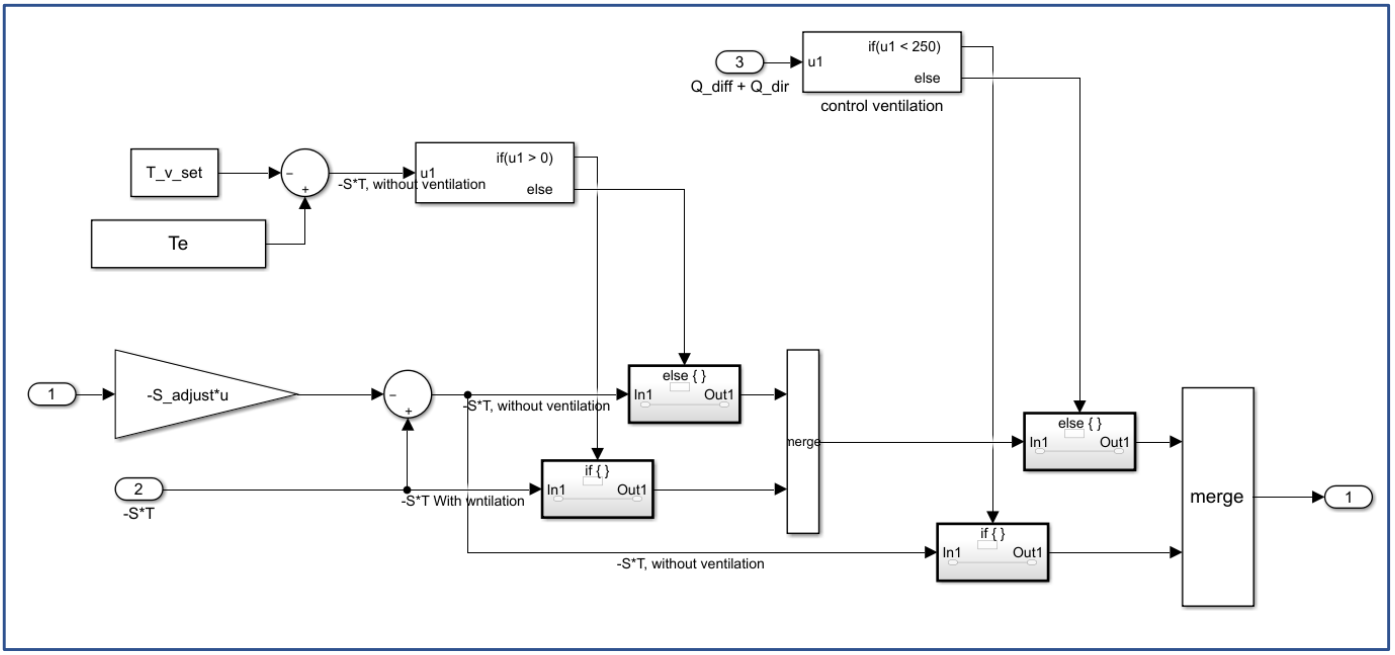

Figure G-3: Simulink Block for adjusting stiffness matrix based on ventilation on or off condition

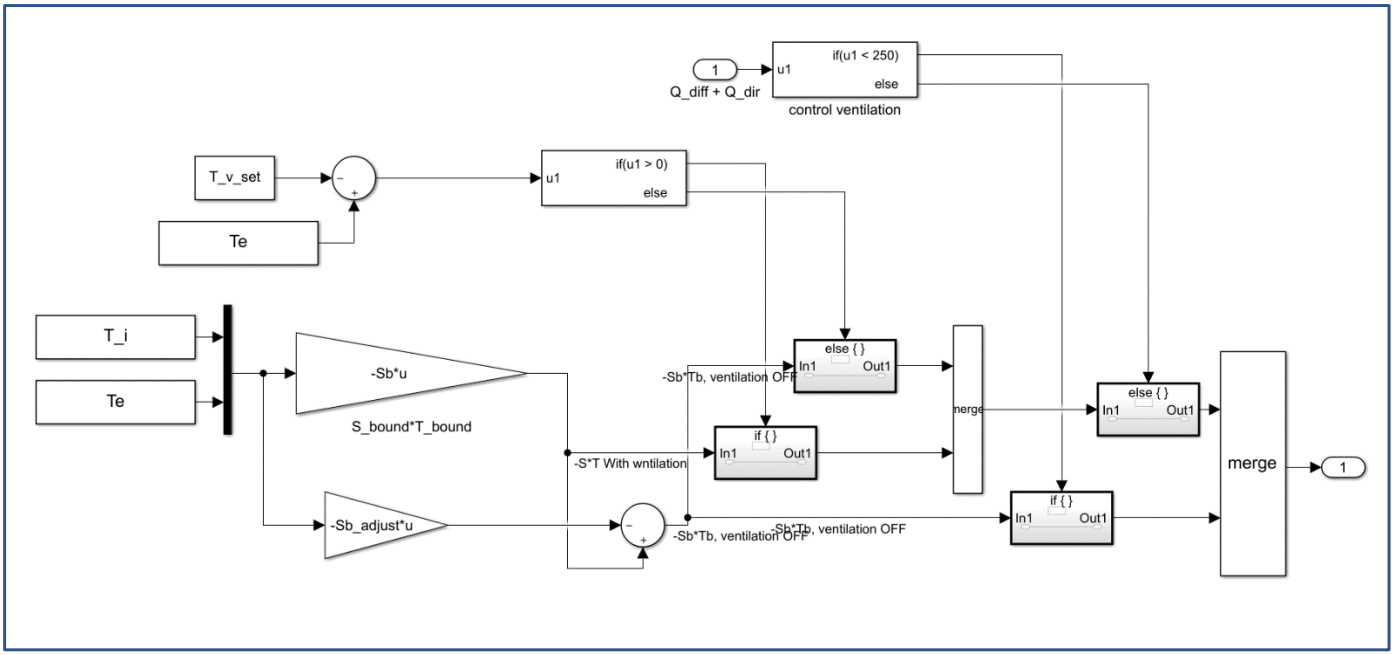

Figure G-4: Simulink Block for adjusting bound node stiffness matrix based on ventilation on or off condition

Matlab function within Simulink “output” block to calculate total surface heat gain or loss to the inside at each time step:

```
function y = fcn(u,K,T_i,Ar,r_i)
sum =0;

for i=5*K+1:6*K         %all nodes on inner-most glazing surface (node case 6)
    del_T   = u(i)-T_i; %temperature difference with air
    sum     = sum + (del_T*Ar*(1/r_i)); %calculating total heat flow through the
facade
end



y = sum;
```

Published with MATLAB® R2018b

Matlab function within Simulink “solar load and Q matrix” block to calculate Q matrix and solar heat gain at each time step:

```
function [Qze,INT_SOL] = solar_load(dir,diff,
tan_theta,Q,Q_blind,l3,l5,l6,K,ht,mat_data,Tg,Ta,Ar,LW)
%inputs fed in from simulink
%function used to set Q matrix based on angle of dir solar radiation and shading
coeff

T = mat_data;               %matrix containing angular dependant optical properties

%---------SETTING CONDITION FOR BLIND ON OR OFF-----------------------------------
if (dir+diff)>= 250
    x = Q_blind;
    a = x;
    abs_blind   = 0.34;     %absorption for blinds on (45deg)
else
    x = Q;
    a = x;
    abs_blind   = 0.001;    %absorption for blinds off (0deg)
end

%---SETTING SHADING LENGTH------------------------------------------------
h3 = l3*tan_theta;
h5 = l5*tan_theta;
h6 = l6*tan_theta;

%----SETTING HT OF ONCE REFLECTED FROM BASE-------------------------------
if l3*tan_theta < ht                        %for blind
    hre3    = l3*tan_theta;
elseif ht <= l3*tan_theta < 2*ht
    hre3    = 2*ht-l3*tan_theta;
else
```

```
    hre3    = 0;
end

if l5*tan_theta < ht                        %for node 5
    hre5    = l5*tan_theta;
elseif ht <= l5*tan_theta < 2*ht
    hre5    = 2*ht-l5*tan_theta;
else
    hre5    = 0;
end

hre6    = hre5;                             %for node 6

%-------SETTING INCIDENT ANGLE FOR INTERPOLATION----------------------------------
if tan_theta == -1
    theta = 90;
else
    theta = atand(tan_theta);
end

%----SELECTING PROPERTIES BASED ON SOLAR ANGLE---------------------------
if tan_theta < 0
    abs_1 = 0;
    abs_5 = 0;
    abs_6 = 0;
    t_1 = 0;
    t_5 = 0;
    t_6 = 0;
else

    y    = theta/10;
    ind1 = floor(y) +1;             %set lower angle index to refer table
    ind2 = ind1 + 1;                %set upper angle index to refer table
    ang1 = (ind1-1)*10;             %lower angle limit
    ang2 = ang1 + 10;               %upper angle limit

    if ind1 == 10
        ind2 = ind1;
        ang2 = ang1;
    end
    %"interpol" function linearly interpolates required values from the table
    %for direct radiation
    abs_1 = intpol(ang1,ang2,T(1,ind1),T(1,ind2),theta);
    abs_5 = intpol(ang1,ang2,T(3,ind1),T(3,ind2),theta);
    abs_6 = intpol(ang1,ang2,T(5,ind1),T(5,ind2),theta);
    t_1 = intpol(ang1,ang2,T(2,ind1),T(2,ind2),theta);
    t_5 = intpol(ang1,ang2,T(4,ind1),T(4,ind2),theta);
    t_6 = intpol(ang1,ang2,T(6,ind1),T(6,ind2),theta);
end

%for diffused radiation
abs_diff_1 = T(1,11);
abs_diff_5 = T(3,11);
abs_diff_6 = T(5,11);
t_diff_1 = T(2,11);
```

```
t_diff_5 = T(4,11);
t_diff_6 = T(6,11);

%reduction factors for incident radiation (for glazings), blind factor (SC)
%is included in initial Q or Q_blind matrix from initialization code
rf_1 = 1;
rf_5 = t_1;
rf_6 = t_1*t_5;
rf_1_diff = 1;
rf_5_diff = t_diff_1;
rf_6_diff = t_diff_1*t_diff_5;

%for blind
%absorption is defined with selection on Q matrix based on blind condition
rf_3        = rf_5;
rf_3_diff   = rf_5_diff;


br          = 0.27;%reflection coeff from base of the


%---SETTING "x" AS Q-------------------------------------------------------

for i=1:K                                   %outer glazing
    x(i,1)  = x(i,1)*(dir*abs_1*rf_1 + diff*abs_diff_1*rf_1_diff);
end

for i=2*K+1:3*K                             %blind
    j=i-2*K;
    if (j*ht/K) < ht-h3 && (j*ht/K) >= hre3
       x(i,1)  = x(i,1)*(dir*rf_3 + diff*rf_3_diff)*abs_blind;
    elseif (j*ht/K) >= ht-h3
       x(i,1)  = x(i,1)*(diff*rf_3_diff)*abs_blind;
    else
        x(i,1)  = x(i,1)*(dir*rf_3*(1+br) + diff*rf_3_diff)*abs_blind;
    end

end

for i=4*K+1:5*K                             %outer pane of double glazing
    j=i-4*K;
    if (j*ht/K) < ht-h5 && (j*ht/K) >= hre5
       x(i,1)  = x(i,1)*(dir*abs_5*rf_5 + diff*abs_diff_5*rf_5_diff);
    elseif (j*ht/K) >= ht-h5
       x(i,1)  = x(i,1)*(diff*abs_diff_5*rf_5_diff);
    else
        x(i,1)  = x(i,1)*(dir*abs_5*rf_5*(br+1) + diff*abs_diff_5*rf_5_diff);
    end
end

for i=5*K+1:6*K                             %inner pane of double glazing
    j=i-5*K;
    if (j*ht/K) < ht-h6 && (j*ht/K) >= hre6
       x(i,1)  = x(i,1)*(dir*abs_6*rf_6 +diff*abs_diff_6*rf_6_diff);
    elseif (j*ht/K) >= ht-h6
```

```
        x(i,1)  = x(i,1)*(diff*abs_diff_6*rf_6_diff);
    else
        x(i,1)  = x(i,1)*(dir*abs_6*rf_6*(br+1) +diff*abs_diff_6*rf_6_diff);
    end
end

%--------------INTERNAL SOLAR GAIN INTO THE ROOM-------------------------
sum = 0;
for i=5*K+1:6*K                             %inner pane of double glazing
    j=i-5*K;
    if (j*ht/K) < ht-h6 && (j*ht/K) >= hre6
       sum  = sum + a(i,1)*(dir*t_6*rf_6 +diff*t_diff_6*rf_6_diff);
    elseif (j*ht/K) >= ht-h6
       sum  = sum + a(i,1)*(diff*t_diff_6*rf_6_diff);
    else
       sum  = sum + a(i,1)*(dir*t_6*rf_6*(br+1) +diff*t_diff_6*rf_6_diff);
    end
end


%--LW SKY RADIATION (not used in simulation due to unexpected behaviour)---
%TaK         = Ta +273.14;       % AIR TEMP convert to K
%TgK         = Tg +273.14;       % GLAZING TEMP convert to K
%sigma       = 5.67*10^-8;       % stefan boltzmann constant
%eps         = 0.95;             % emissivity of glass
%f           = 0.5;              % glazing to sky/ground vf

%for i=1:K
%    x(i,1)  = x(i,1) - eps*Ar*sigma*TgK(i,1)^4;     % subtracting radiative heat
loss from glazing
%    x(i,1)  = x(i,1) + f*eps*Ar*(LW+sigma*TaK^4);   % adding heat gain from sky
and ground, ground temp sam as air
%end


INT_SOL = sum;
Qze = x;
```

Published with MATLAB® R2018b

Appendix H

Graphical Plots for Verification

The graphical plots from the out puts of M/S and DB comparing the temperature distribution (external glazing, cavity air and inner-most glazing) and heat flows (total heat gain, solar heat gain and surface heat gain) are presented. The hourly variation in these quantities is presented for three weeks, 18th to 24th of March, June and December.

The simulation conducted are for the configuration of the DSF as described in Ch4 in New Delhi at North and South orientations (fig D1 to D4). Additional simulations with higher ventilation rates (fig D5 and D6) are presented as well. Lastly the simulation outputs when sky and ground long wave radiation were included in the calculation, for both 100 m^3/hr and 600m^3/hr ventilation rates, are presented (fig D7 to D10).

Note1: Temperature of the cavity air in M/S is calculated as the average temperature of the air nodes either side of the blind, i.e., node number 2 and 4 as depicted in fig 3.1

Note 2: The comparison is presented for the temperatures and heat gain of zone 3 of the DB model (height between 1m and 1.5m of the façade). Similarly, layer 6 of the M/S model was chosen (at K=12). Both were subsequently equated to the full façade area for the total heat flow estimations**.**

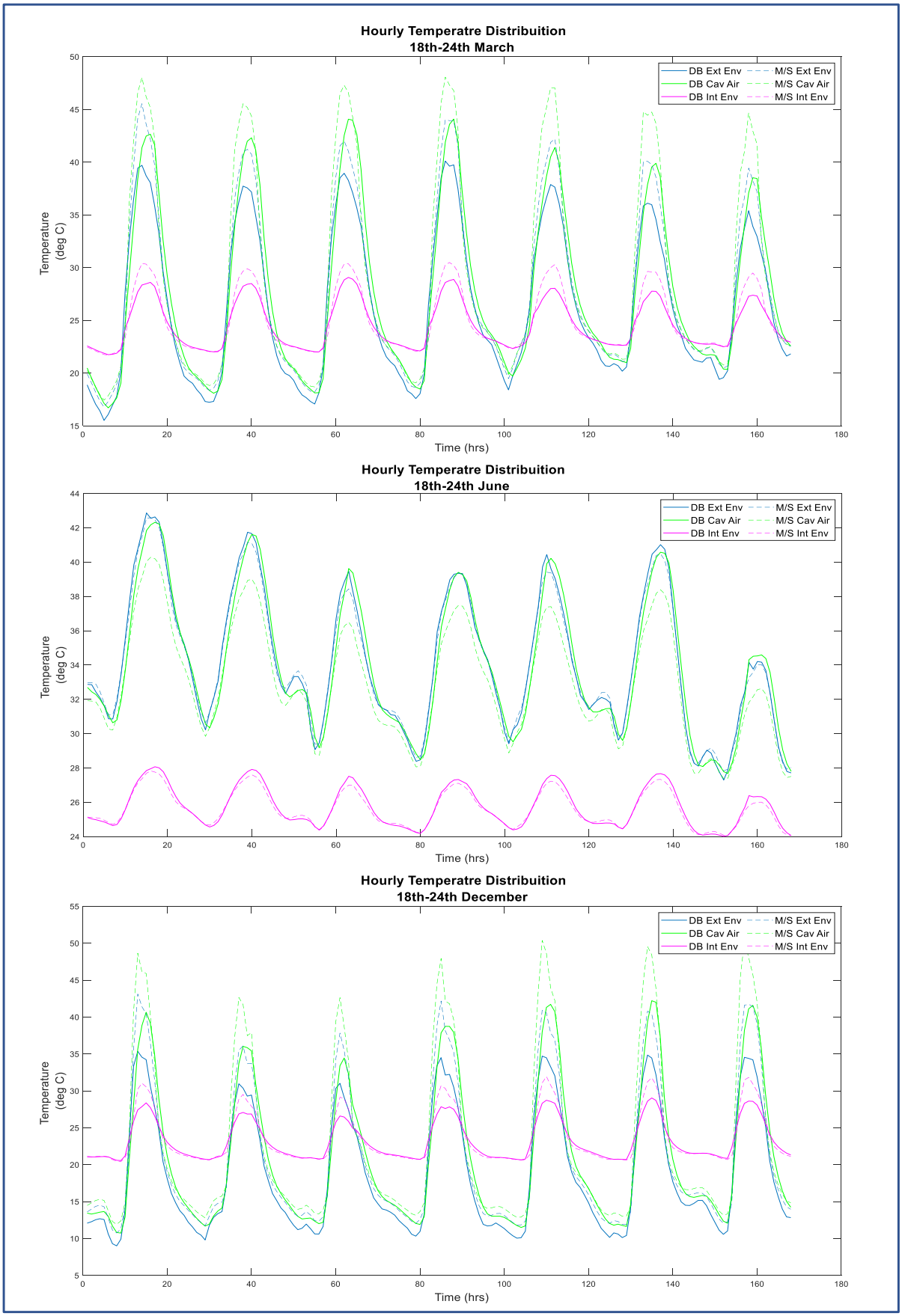

Figure H-1: Temperature Distributions in South Facing DSF at 100m³/hr ventilation rate, neglecting external sky and ground radiation

NOTE: Y-axis not at same scale/origin

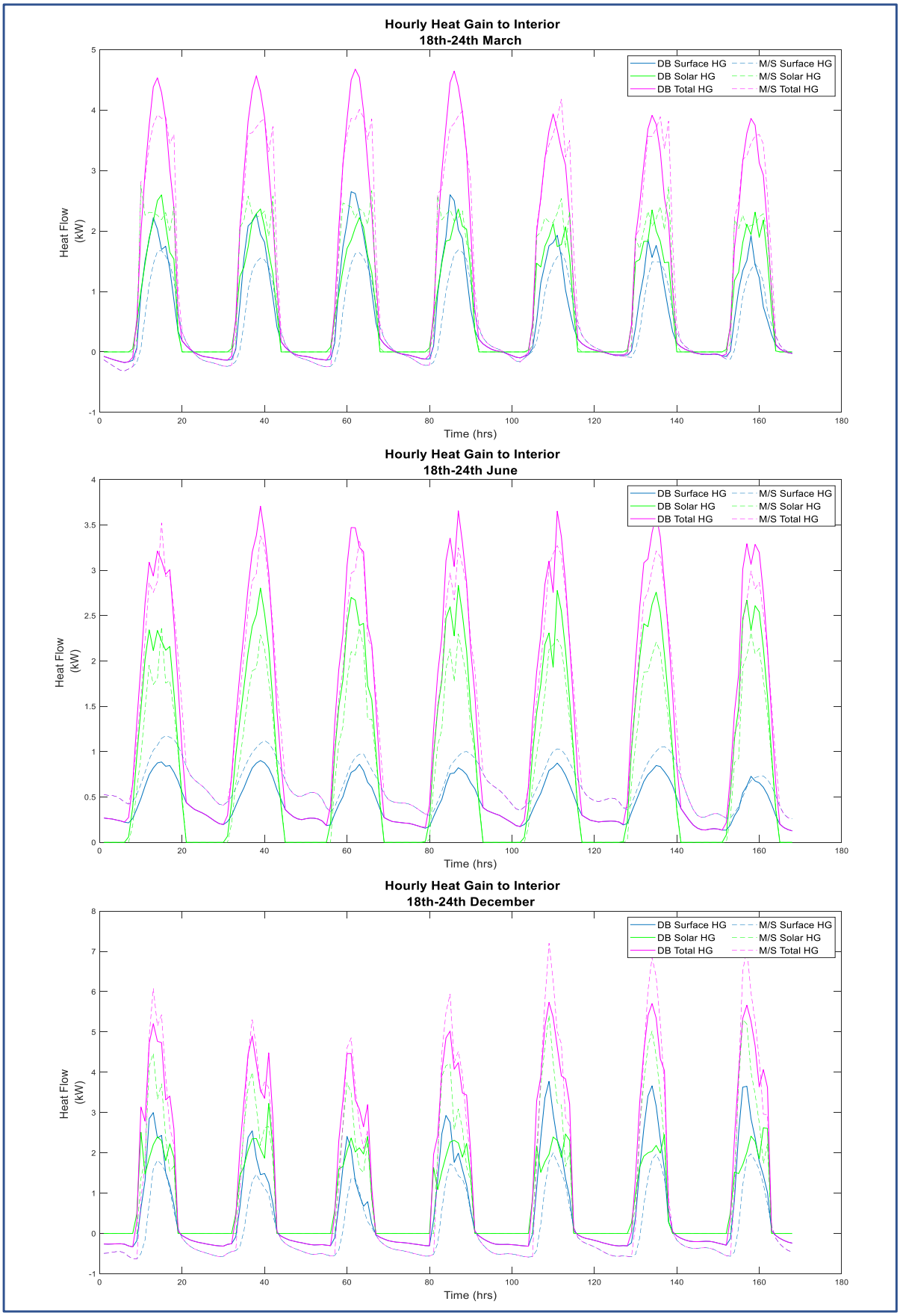

Figure H-2: Heat gain to interior room in South facing DSF at 100m³/hr ventilation rate, neglecting external sky and ground radiation

NOTE: Y-axis not at same scale/origin

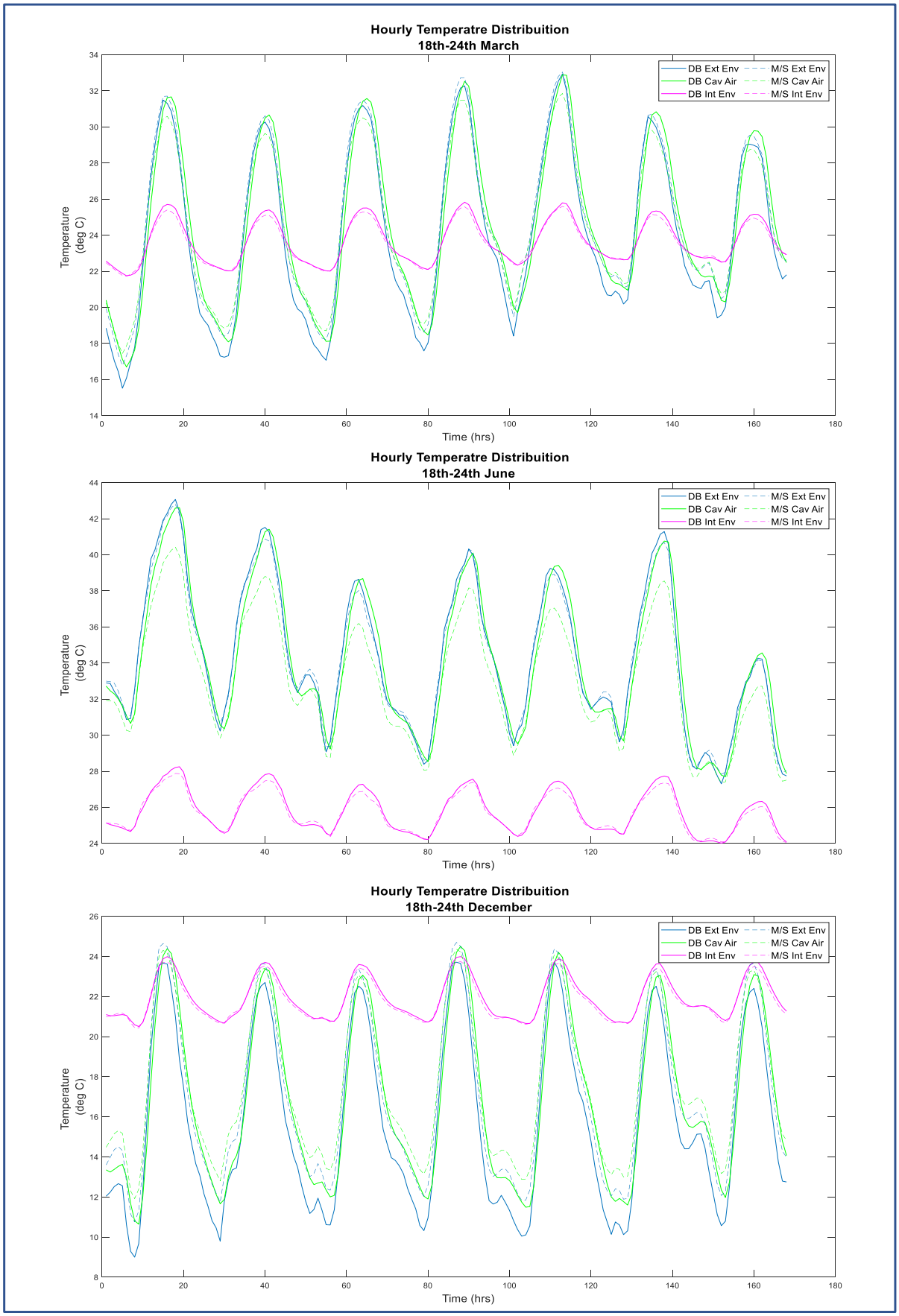

Figure H-3: Temperature distribution in North facing DSF at 100m³/hr ventilation rate, neglecting external sky and ground radiation

NOTE: Y-axis not at same scale/origin

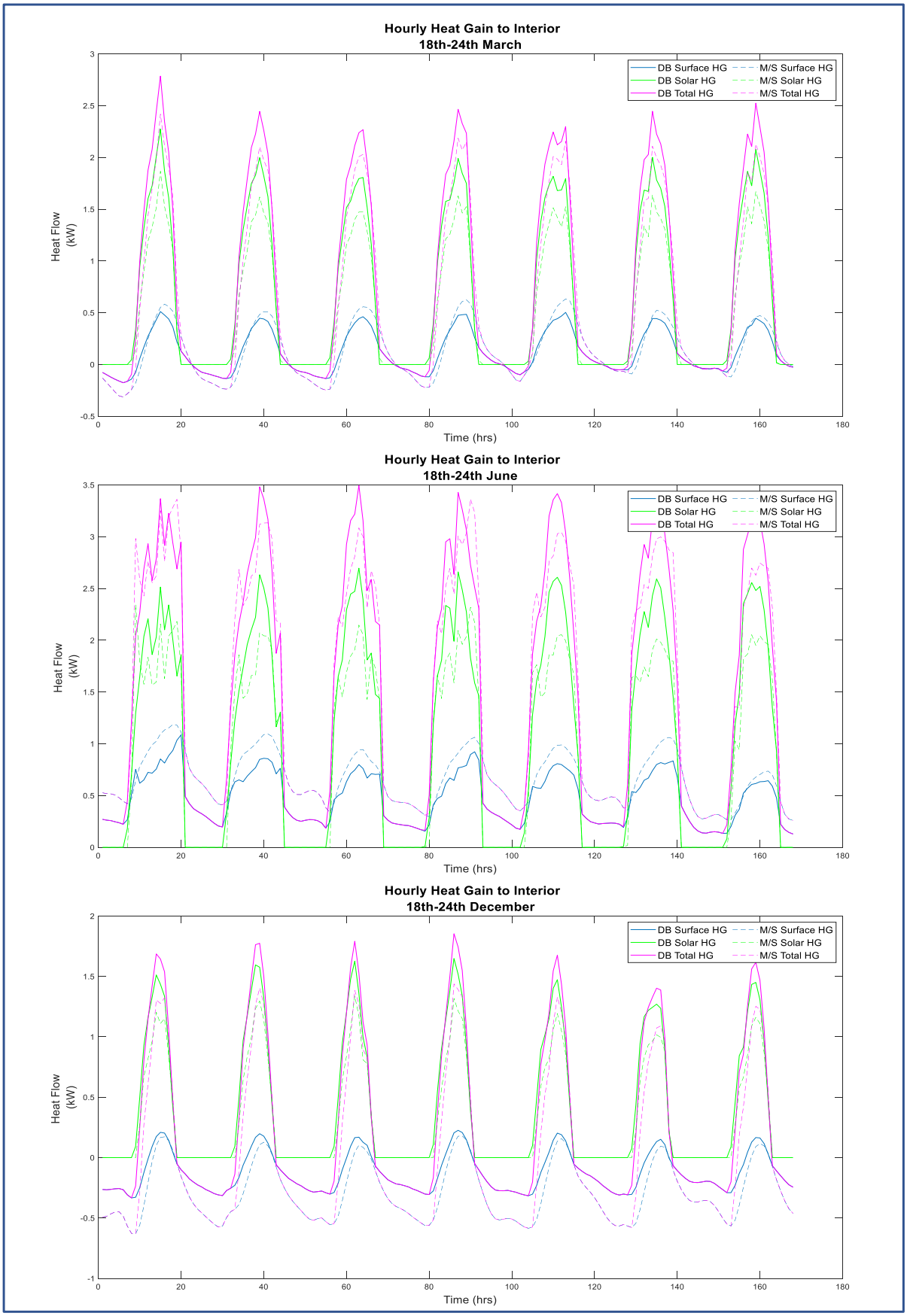

Figure H-4: Heat Gain to the interior room in North facing DSF at 100m³/hr ventilation rate, neglecting external sky and ground radiation

NOTE: Y-axis not at same scale/origin

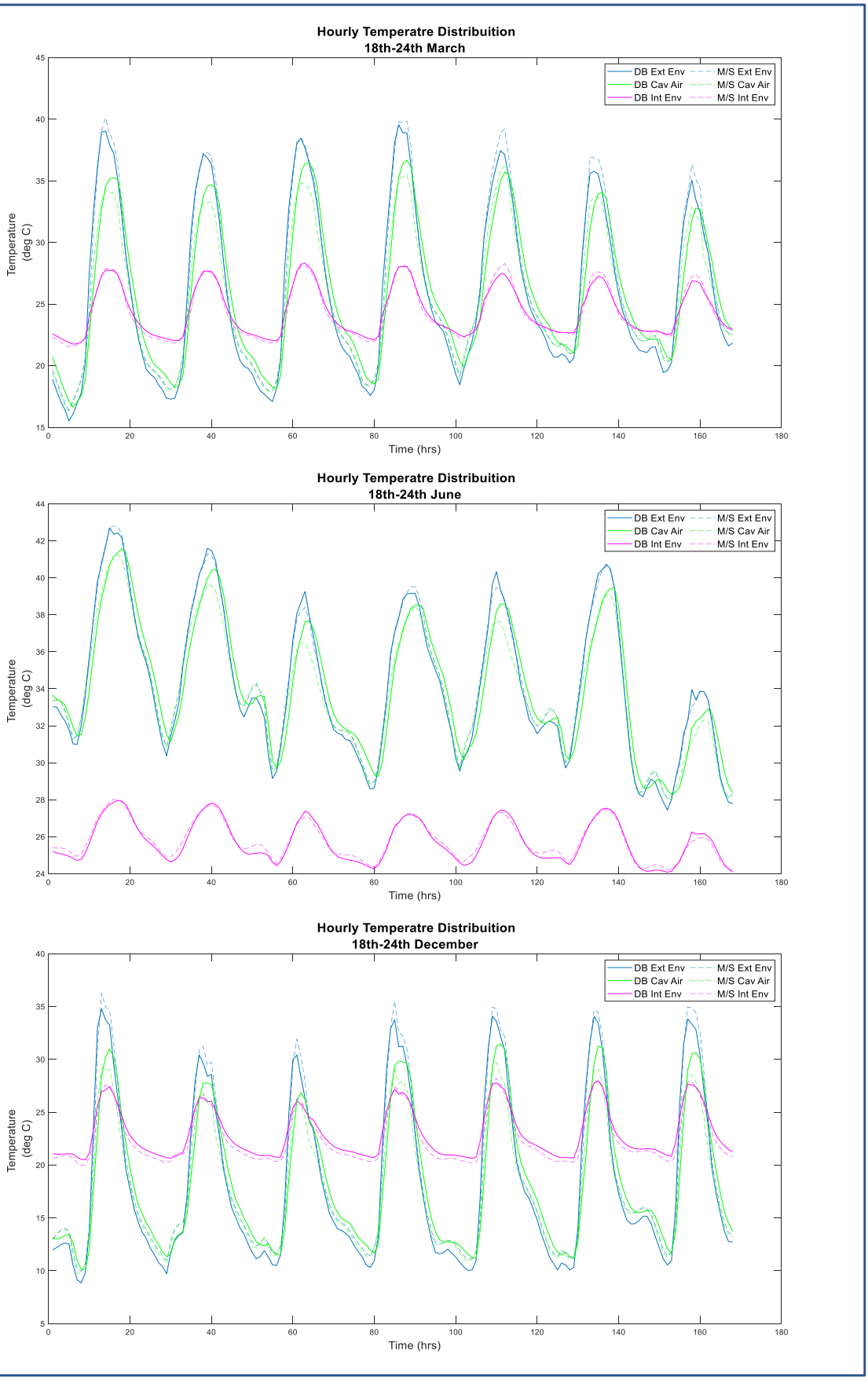

Figure H-5: Temperature Distributions in South Facing DSF at 600m³/hr ventilation rate, neglecting external sky and ground radiation

NOTE: Y-axis not at same scale/origin

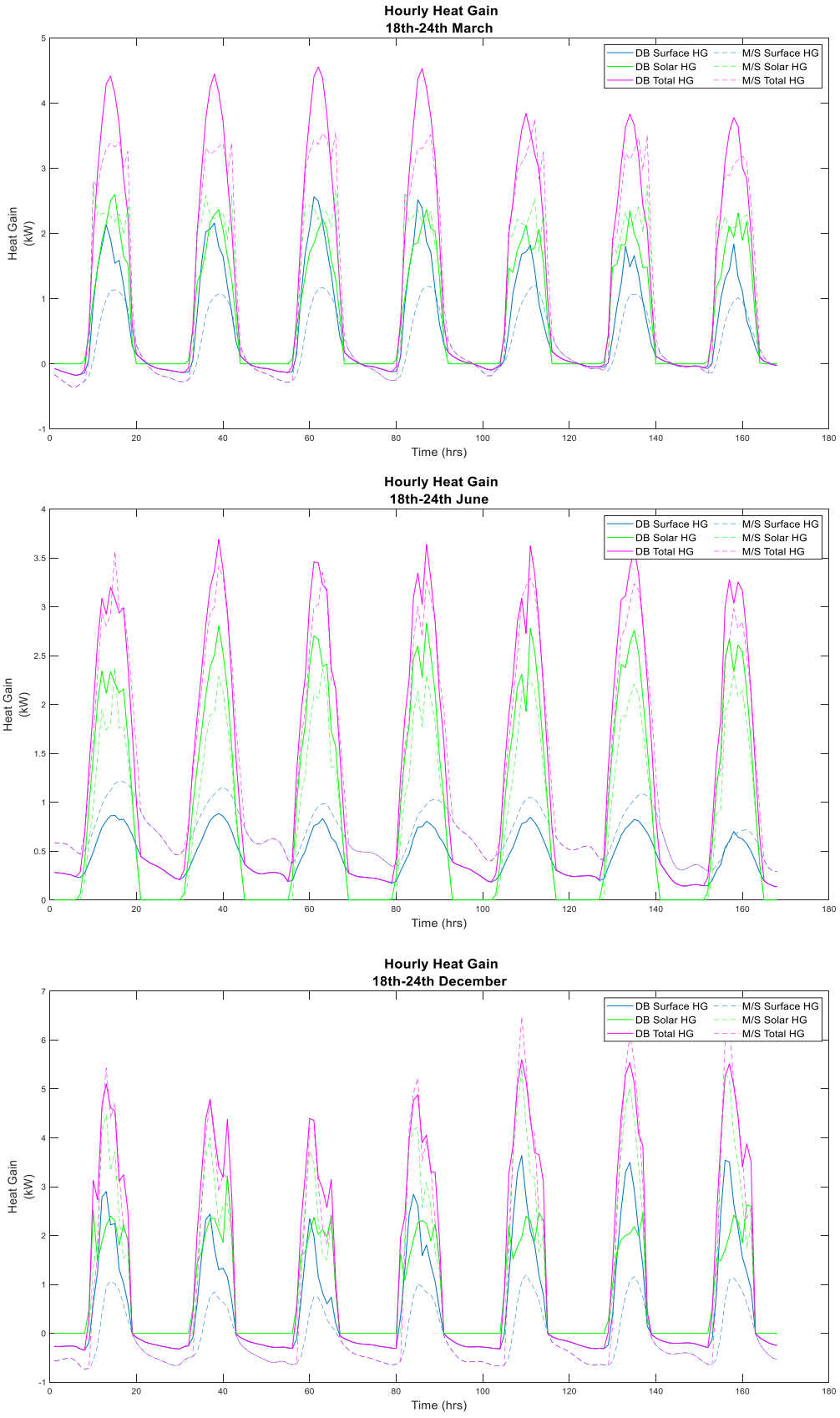

Figure H-6: Heat Gain to the interior room in South Facing DSF at 600m³/hr ventilation rate, neglecting external sky and ground radiation

NOTE: Y-axis not at same scale/origin

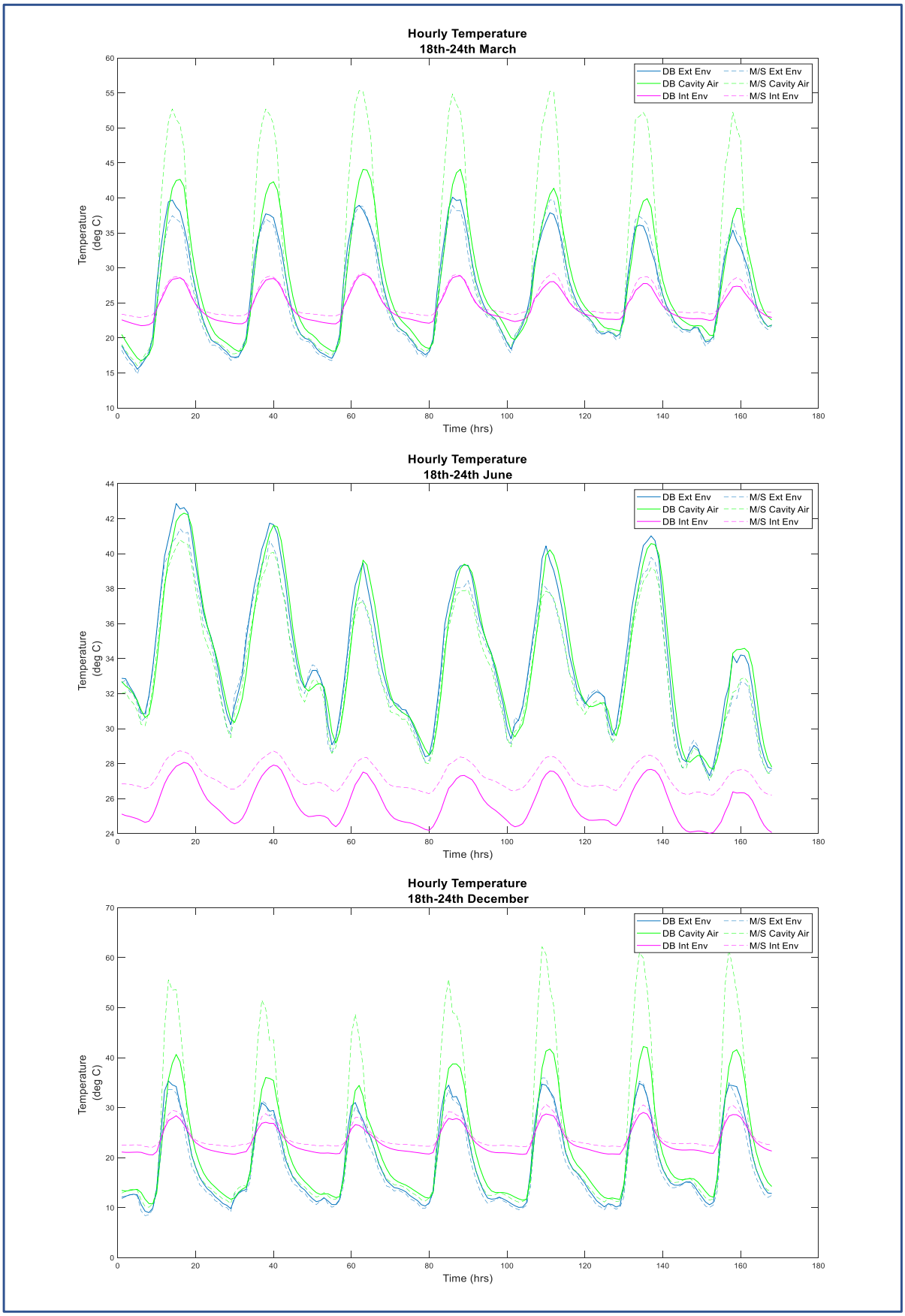

Figure H-7: Temperature Distributions in South Facing DSF at 100m³/hr ventilation rate, with external sky and ground radiation

NOTE: Y-axis not at same scale/origin

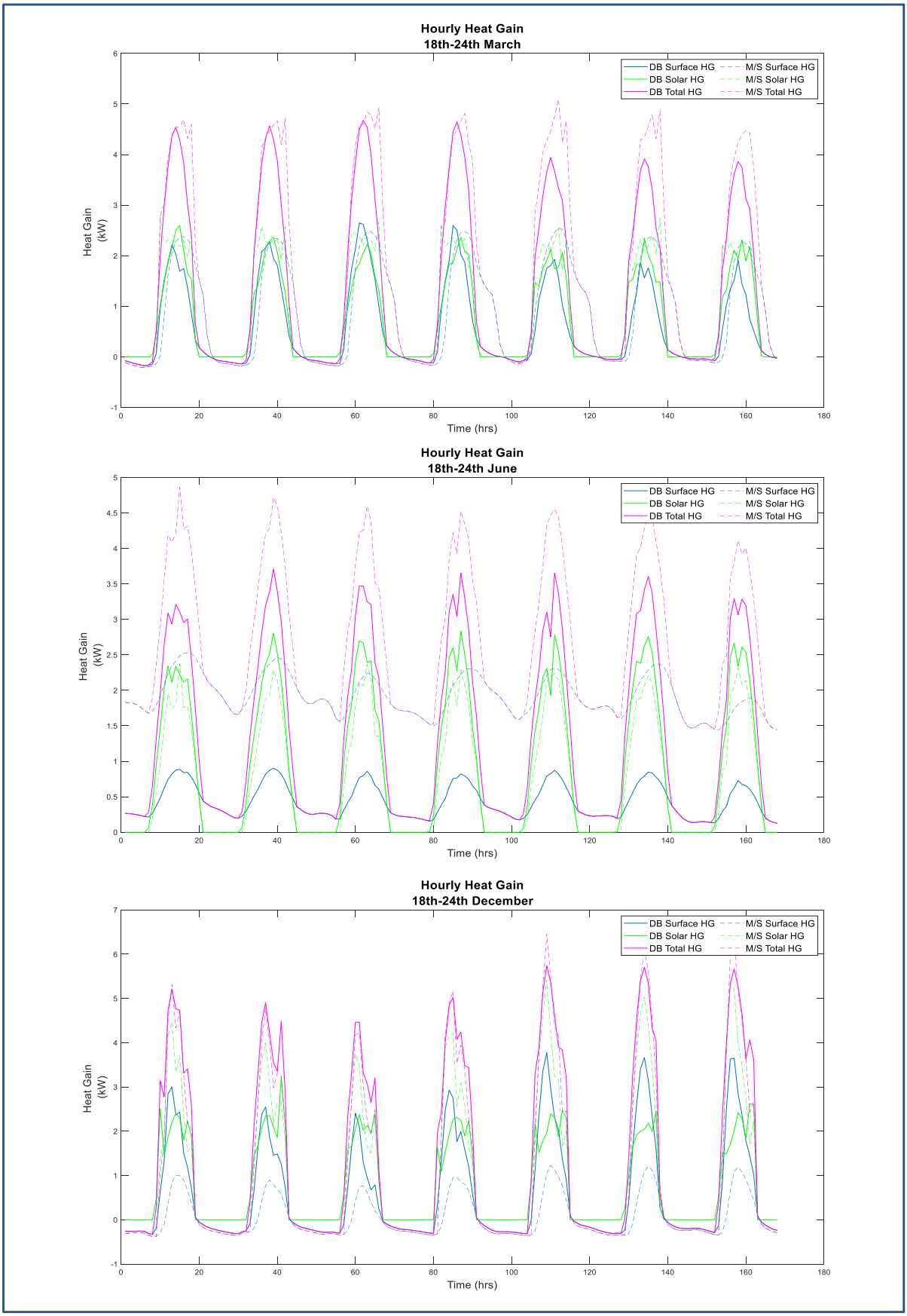

Figure H-8: Heat gain to interior room in South facing DSF at 100m³/hr ventilation rate, with external sky and ground radiation

NOTE: Y-axis not at same scale/origin

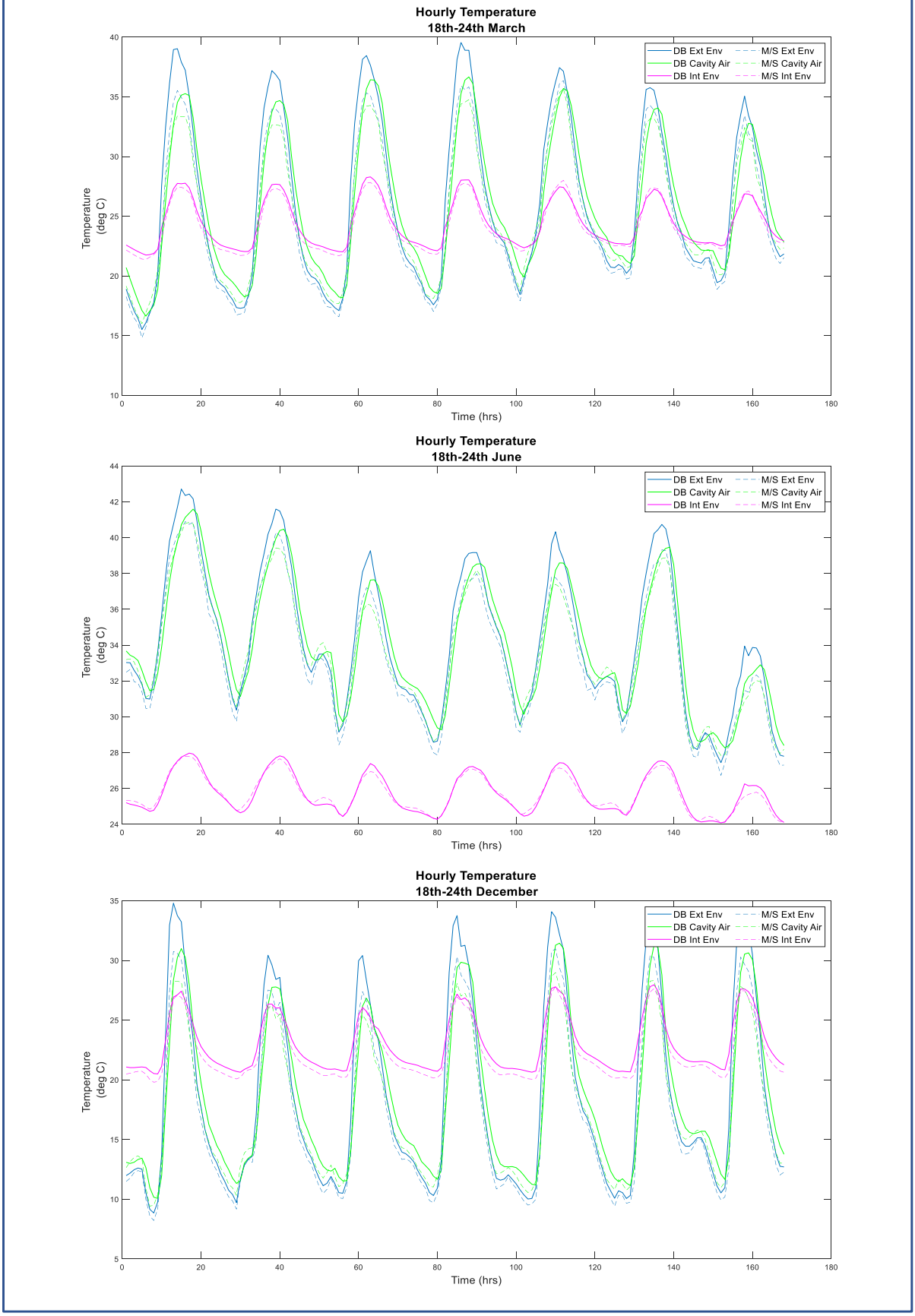

Figure H-9: Temperature Distributions in South Facing DSF at 600m³/hr ventilation rate, with external sky and ground radiation

NOTE: Y-axis not at same scale/origin

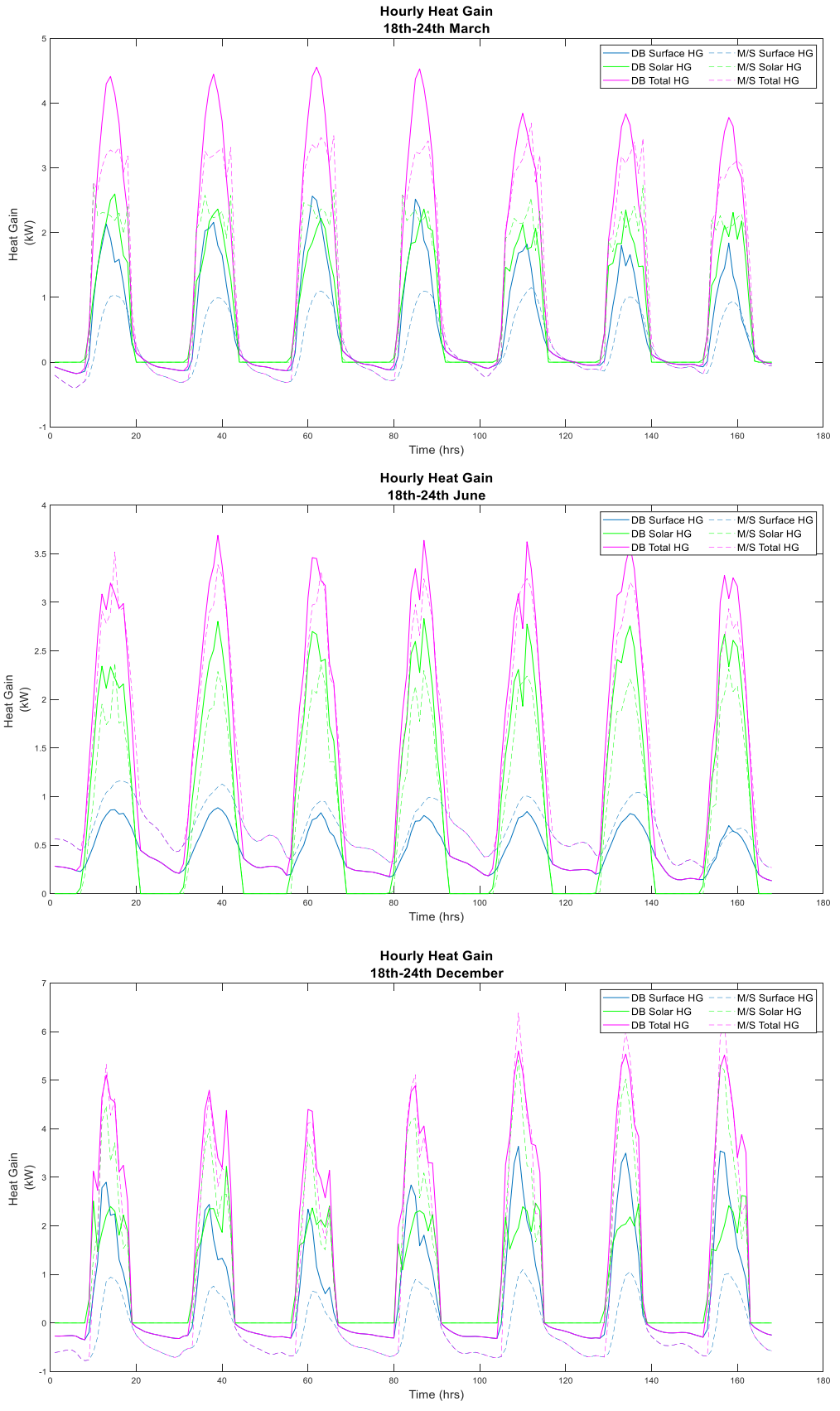

Figure H-10: Heat gain to interior room in South facing DSF at 600m³/hr ventilation rate, with external sky and ground radiation

NOTE: Y-axis not at same scale/origin

Appendix I

Behavioural Analysis Results for the DSF

Note: Data for thermal comfort parameter is not included as the thermal comfort was never compromised in any of the cases, i.e., inner-most glazing temperature never exceeded 45°C (for warm walls) and never went below 16°C (for cool walls)

The details for the different sites and orientation for variations in the base configuration with respect to cavity width, ventilation rate and glazing systems can be found in the tables as mentioned below. The parameters relating to heat transfer are expressed per meter length of façade.

CITY	ORIENTATION	TABLE NO.
New Delhi	South	1-3
	North	4-6
	East	7-9
Chennai	South	10-12
	North	13-15
	East	16-18
Kathmandu	South	19-21
	North	22-24
	East	25-27
Jaisalmer	South	28-30
	North	31-33
	East	34-36
Kolkata	South	37-39
	North	40-42
	East	43-45
Bhopal	South	46-48
	North	49-51
	East	52-54

South Façade in New Delhi

Table I-1: Variation in performance parameters for different ventilation rates in the base model

AC per hour	Vent Rate per m length of facade	Total Heat Gain to Room per m length of facade	Solar Heat Gain to Room per m length of facade	Surface Heat Gain to Room per m length of facade	Total Heat Loss from Room per m length of facade	Hrs with glazing surf above 28°C	Hrs with cavity air above 40°C
/h	m3/hr	kWh	kWh	kWh	kWh	hrs	hrs
0	0	1324.7	943	381.7	99.8	2672	1429
10	15	1292.3	943	349.3	99.9	2608	1141
14	21	1280.7	943	337.7	99.9	2577	874
20	30	1267.2	943	324.2	99.9	2531	542
40	60	1241.9	943	298.9	99.9	2382	127
80	120	1223	943	279.9	100	2253	57
160	240	1211.2	943	268.1	100	2149	34
320	480	1204.6	943	261.5	100	2091	30
400	600	1203.2	943	260.2	100	2076	30

Table I-2: Variation in performance parameters for different cavity widths in the base case, tested for constant air changes and volumetric flow rate

Applied Ventilation	Observed Vent Quantity	Cavity Width	Total Heat Gain to Room per m length of facade	Solar Heat Gain to Room per m length of facade	Surface Heat Gain to Room per m length of facade	Total Heat Loss from Room per m length of facade	Hrs with glazing surf above 28°C	Hrs with cavity air above 40°C
		m	kWh	kWh	kWh	kWh	hrs	hrs
80AC	480 m3/hr	0.2	1288	978.1	309.9	100	2436	208
80AC	1200 m3/hr	0.5	1223	943	279.9	100	2253	57
80AC	1920 m3/hr	0.8	1174.2	907.1	267.2	99.9	2173	35
80AC	2400 m3/hr	1	1144.1	882.6	261.5	99.9	2122	30
80AC	2880 m3/hr	1.2	1114.5	857.7	256.8	99.8	2068	27
80AC	3600 m3/hr	1.5	1070.5	820	250.5	99.7	1987	24
1200m3/hr	200 AC	0.2	1261.3	978.1	283.2	100.1	2253	53
1200m3/hr	80 AC	0.5	1223	943	279.9	100	2253	57
1200m3/hr	50 AC	0.8	1182.9	907.1	275.8	99.9	2251	49
1200m3/hr	40 AC	1	1155.8	882.6	273.2	99.8	2237	44
1200m3/hr	33.34 AC	1.2	1128.2	857.7	270.5	99.8	2215	42
1200m3/hr	23.67 AC	1.5	1086.2	820	266.2	99.7	2176	39

Table I-3: Variation in performance parameters of different glazing systems on the external and internal envelope on the base configuration

Façade Configuration		Total Heat Gain to Room per m length of facade	Solar Heat Gain to Room per m length of facade	Surface Heat Gain to Room per m length of facade	Heat Loss from Room per m length of facade	Hrs with glazing surf above 28°C	Hrs with cavity air above 40°C
External Glazing (single)	**Internal Glazing (double)**	**kWh**	**kWh**	**kWh**	**kWh**	**hrs**	**hrs**
clear 6mm	Clear DG 4/16/4 argon gas	1223	943	279.9	100	2253	57
clear 6mm	LowE DB 9.4/12.7/3 LowE, Argon gas	867.3	635.6	231.7	60.9	1716	211
clear 6mm	Tinted DG 4/12.7/3 Argon gas	976.8	528.3	448.5	95.8	3124	319
clear 6mm	High Performance DG 10/1/3 LowE, Vacuum	359.1	253	106.1	27.6	3	427
Tinted 5.8mm	Clear DG 4/16/4 argon gas	639.6	374	265.6	100.5	2063	150
Reflective 13.2mm	Clear DG 4/16/4 argon gas	399.9	223.9	175.9	101.3	1182	16
Tinted 5.8mm	LowE DB 9.4/12.7/3 LowE, Argon gas	442.9	252.1	190.7	62.1	1077	329
Tinted 5.8mm	High Performance DG 10/1/3 LowE, Vacuum	188.4	100.3	88	28.3	0	491

North Façade in New Delhi

Table I-4: Variation in performance parameters for different ventilation rates in the base model

AC per hour	Vent Rate per m length of facade	Total Heat Gain to Room per m length of facade	Solar Heat Gain to Room per m length of facade	Surface Heat Gain to Room per m length of facade	Total Heat Loss from Room per m length of facade	Hrs with glazing surf above 28°C	Hrs with cavity air above 40°C
/h	m3/hr	kWh	kWh	kWh	kWh	hrs	hrs
0	0	751.4	578.6	172.9	102.4	1327	11
10	15	751.4	578.6	172.9	102.4	1327	11
14	21	751.4	578.6	172.9	102.4	1327	11
20	30	751.4	578.6	172.9	102.4	1327	11
40	60	751.4	578.6	172.8	102.4	1327	10
80	120	751.4	578.6	172.8	102.4	1327	9
160	240	751.4	578.6	172.8	102.4	1327	9
320	480	751.4	578.6	172.8	102.4	1327	9
400	600	751.4	578.6	172.8	102.4	1327	9

Table I-5: Variation in performance parameters for different cavity widths in the base case, tested for constant air changes and volumetric flow rate

Applied Ventilation	Observed Vent Quantity	Cavity Width	Total Heat Gain to Room per m length of facade	Solar Heat Gain to Room per m length of facade	Surface Heat Gain to Room per m length of facade	Total Heat Loss from Room per m length of facade	Hrs with glazing surf above 28°C	Hrs with cavity air above 40°C
		m	kWh	kWh	kWh	kWh	hrs	hrs
80AC	480 m3/hr	0.2	752.5	579.5	173	102.4	1328	11
80AC	1200 m3/hr	0.5	751.4	578.6	172.8	102.4	1327	9
80AC	1920 m3/hr	0.8	749.3	576.7	172.6	102.3	1322	9
80AC	2400 m3/hr	1	748.7	576.2	172.5	102.2	1320	9
80AC	2880 m3/hr	1.2	747.5	575.1	172.4	102.2	1320	9
80AC	3600 m3/hr	1.5	745.8	573.6	172.2	102.1	1320	8
1200m3/hr	200 AC	0.2	752.5	579.5	173	102.4	1328	9
1200m3/hr	80 AC	0.5	751.4	578.6	172.8	102.4	1327	9
1200m3/hr	50 AC	0.8	749.3	576.7	172.6	102.3	1322	9
1200m3/hr	40 AC	1	748.7	576.2	172.5	102.2	1320	9
1200m3/hr	33.34 AC	1.2	747.5	575.1	172.4	102.2	1320	9
1200m3/hr	23.67 AC	1.5	745.8	573.6	172.2	102.1	1320	8

Table I-6: Variation in performance parameters of different glazing systems on the external and internal envelope on the base configuration

Façade Configuration		Total Heat Gain to Room per m length of facade	Solar Heat Gain to Room per m length of facade	Surface Heat Gain to Room per m length of facade	Heat Loss from Room per m length of facade	Hrs with glazing surf above 28°C	Hrs with cavity air above 40°C
External Glazing (single)	**Internal Glazing (double)**	**kWh**	**kWh**	**kWh**	**kWh**	**hrs**	**hrs**
clear 6mm	Clear DG 4/16/4 argon gas	751.4	578.6	172.8	102.4	1327	9
clear 6mm	LowE DB 9.4/12.7/3 LowE, Argon gas	538.3	388.2	150	63.7	968	156
clear 6mm	Tinted DG 4/12.7/3 Argon gas	623.8	322.3	301.5	99.3	2217	288
clear 6mm	High Performance DG 10/1/3 LowE, Vacuum	225.7	154.5	71.3	29.5	17	437
Tinted 5.8mm	Clear DG 4/16/4 argon gas	422	228.2	193.8	105.3	1502	113
Reflective 13.2mm	Clear DG 4/16/4 argon gas	280	137	143	108.6	911	3
Tinted 5.8mm	LowE DB 9.4/12.7/3 LowE, Argon gas	294.2	153.2	141.1	66.6	852	315
Tinted 5.8mm	High Performance DG 10/1/3 LowE, Vacuum	128	60.9	67.1	31.2	1	554

East Façade in New Delhi

Table I-7: Variation in performance parameters for different ventilation rates in the base model

AC per hour	Vent Rate per m length of facade	Total Heat Gain to Room per m length of facade	Solar Heat Gain to Room per m length of facade	Surface Heat Gain to Room per m length of facade	Total Heat Loss from Room per m length of facade	Hrs with glazing surf above 28°C	Hrs with cavity air above 40°C
/h	m3/hr	kWh	kWh	kWh	kWh	hrs	hrs
0	0	1180.4	854.5	325.9	100.5	2228	1004
10	15	1158.2	854.5	303.7	100.5	2164	794
14	21	1150.1	854.5	295.6	100.5	2122	677
20	30	1140.5	854.5	286	100.5	2074	503
40	60	1122.6	854.5	268.1	100.5	1994	241
80	120	1109.1	854.5	254.6	100.5	1938	87
160	240	1100.7	854.5	246.2	100.5	1898	35
320	480	1096	854.5	241.5	100.5	1877	21
400	600	1095	854.5	240.5	100.5	1874	19

Table I-8: Variation in performance parameters for different cavity widths in the base case, tested for constant air changes and volumetric flow rate

Applied Ventilation	Observed Vent Quantity	Cavity Width	Total Heat Gain to Room per m length of facade	Solar Heat Gain to Room per m length of facade	Surface Heat Gain to Room per m length of facade	Total Heat Loss from Room per m length of facade	Hrs with glazing surf above 28°C	Hrs with cavity air above 40°C
		m	kWh	kWh	kWh	kWh	hrs	hrs
80AC	480 m3/hr	0.2	1154.1	878.2	275.9	100.6	2019	312
80AC	1200 m3/hr	0.5	1109.1	854.5	254.6	100.5	1938	87
80AC	1920 m3/hr	0.8	1074.6	828.9	245.6	100.4	1901	50
80AC	2400 m3/hr	1	1054.1	812.6	241.5	100.4	1887	36
80AC	2880 m3/hr	1.2	1031.9	793.8	238.1	100.3	1867	25
80AC	3600 m3/hr	1.5	1001	767.4	233.6	100.2	1837	22
1200m3/hr	200 AC	0.2	1135.1	878.2	256.9	100.6	1938	85
1200m3/hr	80 AC	0.5	1109.1	854.5	254.6	100.5	1938	87
1200m3/hr	50 AC	0.8	1080.7	828.9	251.8	100.4	1938	86
1200m3/hr	40 AC	1	1062.5	812.6	249.9	100.4	1931	85
1200m3/hr	33.34 AC	1.2	1041.7	793.8	247.9	100.3	1925	85
1200m3/hr	23.67 AC	1.5	1012.1	767.4	244.8	100.2	1900	84

Table I-9: Variation in performance parameters of different glazing systems on the external and internal envelope on the base configuration

Façade Configuration		Total Heat Gain to Room per m length of facade	Solar Heat Gain to Room per m length of facade	Surface Heat Gain to Room per m length of facade	Heat Loss from Room per m length of facade	Hrs with glazing surf above 28°C	Hrs with cavity air above 40°C
External Glazing (single)	**Internal Glazing (double)**	**kWh**	**kWh**	**kWh**	**kWh**	**hrs**	**hrs**
clear 6mm	Clear DG 4/16/4 argon gas	1109.1	854.5	254.6	100.5	1938	87
clear 6mm	LowE DB 9.4/12.7/3 LowE, Argon gas	791.1	576.1	215	62.2	1557	287
clear 6mm	Tinted DG 4/12.7/3 Argon gas	894.2	478.9	415.2	96.7	2840	370
clear 6mm	High Performance DG 10/1/3 LowE, Vacuum	329.3	229.2	100.1	28.6	98	579
Tinted 5.8mm	Clear DG 4/16/4 argon gas	588.9	339.4	249.5	101.1	1943	148
Reflective 13.2mm	Clear DG 4/16/4 argon gas	371.6	202.9	168.7	101.6	1184	20
Tinted 5.8mm	LowE DB 9.4/12.7/3 LowE, Argon gas	410.3	228.9	181.4	63.1	1167	363
Tinted 5.8mm	High Performance DG 10/1/3 LowE, Vacuum	175.9	91.1	84.8	29	19	589

South Façade in Chennai

Table I-10: Variation in performance parameters for different ventilation rates in the base model

AC per hour	Vent Rate per m length of facade	Total Heat Gain to Room per m length of facade	Solar Heat Gain to Room per m length of facade	Surface Heat Gain to Room per m length of facade	Total Heat Loss from Room per m length of facade	Hrs with glazing surf above 28°C	Hrs with cavity air above 40°C
/h	m3/hr	kWh	kWh	kWh	kWh	hrs	hrs
0	0	1113.7	753.4	360.4	6.1	1309	800
10	15	1098.9	753.4	345.5	6.1	1242	472
14	21	1093.7	753.4	340.4	6.1	1194	291
20	30	1087.7	753.4	334.4	6.1	1140	103
40	60	1076.5	753.4	323.1	6.1	971	3
80	120	1068	753.4	314.7	6	816	0
160	240	1062.8	753.4	309.4	6	723	0
320	480	1059.8	753.4	306.5	6	668	0
400	600	1059.2	753.4	305.9	6	656	0

Table I-11: Variation in performance parameters for different cavity widths in the base case, tested for constant air changes and volumetric flow rate

Applied Ventilation	Observed Vent Quantity	Cavity Width	Total Heat Gain to Room per m length of facade	Solar Heat Gain to Room per m length of facade	Surface Heat Gain to Room per m length of facade	Total Heat Loss from Room per m length of facade	Hrs with glazing surf above 28°C	Hrs with cavity air above 40°C
		m	kWh	kWh	kWh	kWh	hrs	hrs
80AC	480 m3/hr	0.2	1094.5	766.6	327.9	6.1	1023	14
80AC	1200 m3/hr	0.5	1068	753.4	314.7	6	816	0
80AC	1920 m3/hr	0.8	1049.2	739.9	309.3	6	732	0
80AC	2400 m3/hr	1	1036.9	730	306.9	6	681	0
80AC	2880 m3/hr	1.2	1023.7	718.9	304.8	6	617	0
80AC	3600 m3/hr	1.5	1004.3	702.2	302.2	6	546	0
1200m3/hr	200 AC	0.2	1082.6	766.6	316	6.1	829	0
1200m3/hr	80 AC	0.5	1068	753.4	314.7	6	816	0
1200m3/hr	50 AC	0.8	1053.1	739.9	313.1	6	805	0
1200m3/hr	40 AC	1	1042.1	730	312.1	6	782	0
1200m3/hr	33.34 AC	1.2	1029.9	718.9	311	6	744	0
1200m3/hr	23.67 AC	1.5	1011.3	702.2	309.2	6	695	0

Table I-12: Variation in performance parameters of different glazing systems on the external and internal envelope on the base configuration

Façade Configuration		Total Heat Gain to Room per m length of facade	Solar Heat Gain to Room per m length of facade	Surface Heat Gain to Room per m length of facade	Heat Loss from Room per m length of facade	Hrs with glazing surf above 28°C	Hrs with cavity air above 40°C
External Glazing (single)	Internal Glazing (double)	kWh	kWh	kWh	kWh	hrs	hrs
clear 6mm	Clear DG 4/16/4 argon gas	1068	753.4	314.7	6	816	0
clear 6mm	LowE DB 9.4/12.7/3 LowE, Argon gas	759.8	505.9	253.9	3.5	62	1
clear 6mm	Tinted DG 4/12.7/3 Argon gas	881.1	420	461.1	5.9	2756	34
clear 6mm	High Performance DG 10/1/3 LowE, Vacuum	320.9	201.3	119.6	1.5	0	132
Tinted 5.8mm	Clear DG 4/16/4 argon gas	614.8	297.3	317.4	6.1	815	0
Reflective 13.2mm	Clear DG 4/16/4 argon gas	423.5	178.5	245	6	12	0
Tinted 5.8mm	LowE DB 9.4/12.7/3 LowE, Argon gas	427.1	199.7	227.4	3.6	0	58
Tinted 5.8mm	High Performance DG 10/1/3 LowE, Vacuum	187.1	79.5	107.6	1.6	0	292

North Façade in Chennai

Table I-13: Variation in performance parameters for different ventilation rates in the base model

AC per hour	Vent Rate per m length of facade	Total Heat Gain to Room per m length of facade	Solar Heat Gain to Room per m length of facade	Surface Heat Gain to Room per m length of facade	Total Heat Loss from Room per m length of facade	Hrs with glazing surf above 28°C	Hrs with cavity air above 40°C
/h	m3/hr	kWh	kWh	kWh	kWh	hrs	hrs
0	0	946	658.8	287.2	6.1	601	296
10	15	943.3	658.8	284.5	6.1	597	199
14	21	942.4	658.8	283.6	6.1	595	148
20	30	941.3	658.8	282.4	6.1	589	100
40	60	939.2	658.8	280.4	6.1	565	32
80	120	937.6	658.8	278.8	6.1	546	3
160	240	936.6	658.8	277.8	6.1	527	0
320	480	936.1	658.8	277.3	6.1	516	0
400	600	936	658.8	277.1	6.1	514	0

Table I-11: Variation in performance parameters for different cavity widths in the base case, tested for constant air changes and volumetric flow rate

Applied Ventilation	Observed Vent Quantity	Cavity Width	Total Heat Gain to Room per m length of facade	Solar Heat Gain to Room per m length of facade	Surface Heat Gain to Room per m length of facade	Total Heat Loss from Room per m length of facade	Hrs with glazing surf above 28°C	Hrs with cavity air above 40°C
		m	kWh	kWh	kWh	kWh	hrs	hrs
80AC	480 m3/hr	0.2	944.9	663.3	281.6	6.1	577	45
80AC	1200 m3/hr	0.5	937.6	658.8	278.8	6.1	546	3
80AC	1920 m3/hr	0.8	931.2	653.7	277.4	6	519	1
80AC	2400 m3/hr	1	927.2	650.4	276.8	6	502	0
80AC	2880 m3/hr	1.2	923.5	647.2	276.3	6	496	0
80AC	3600 m3/hr	1.5	917.8	642.3	275.6	6	479	0
1200m3/hr	200 AC	0.2	942.7	663.3	279.4	6.1	548	3
1200m3/hr	80 AC	0.5	937.6	658.8	278.8	6.1	546	3
1200m3/hr	50 AC	0.8	931.9	653.7	278.1	6	533	3
1200m3/hr	40 AC	1	928.1	650.4	277.7	6	527	3
1200m3/hr	33.34 AC	1.2	924.5	647.2	277.3	6	523	1
1200m3/hr	23.67 AC	1.5	919.1	642.3	276.8	6	508	1

Table I-12: Variation in performance parameters of different glazing systems on the external and internal envelope on the base configuration

Façade Configuration		Total Heat Gain to Room per m length of facade	Solar Heat Gain to Room per m length of facade	Surface Heat Gain to Room per m length of facade	Heat Loss from Room per m length of facade	Hrs with glazing surf above 28°C	Hrs with cavity air above 40°C
External Glazing (single)	Internal Glazing (double)	kWh	kWh	kWh	kWh	hrs	hrs
clear 6mm	Clear DG 4/16/4 argon gas	937.6	658.8	278.8	6.1	546	3
clear 6mm	LowE DB 9.4/12.7/3 LowE, Argon gas	670.5	442	228.5	3.5	81	26
clear 6mm	Tinted DG 4/12.7/3 Argon gas	785.5	366.9	418.5	5.9	2178	97
clear 6mm	High Performance DG 10/1/3 LowE, Vacuum	285	175.9	109.1	1.6	0	185
Tinted 5.8mm	Clear DG 4/16/4 argon gas	554.7	259.8	295	6.1	719	8
Reflective 13.2mm	Clear DG 4/16/4 argon gas	388.1	156	232.1	6.1	115	0
Tinted 5.8mm	LowE DB 9.4/12.7/3 LowE, Argon gas	386.9	174.3	212.6	3.6	4	101
Tinted 5.8mm	High Performance DG 10/1/3 LowE, Vacuum	170.9	69.4	101.5	1.6	0	258

East Façade in Chennai

Table I-16: Variation in performance parameters for different ventilation rates in the base model

AC per hour	Vent Rate per m length of facade	Total Heat Gain to Room per m length of facade	Solar Heat Gain to Room per m length of facade	Surface Heat Gain to Room per m length of facade	Total Heat Loss from Room per m length of facade	Hrs with glazing surf above 28°C	Hrs with cavity air above 40°C
/h	m3/hr	kWh	kWh	kWh	kWh	hrs	hrs
0	0	1269.8	865.7	404.1	6	1632	1125
10	15	1249.7	865.7	384	6.1	1567	904
14	21	1242.6	865.7	376.9	6.1	1523	757
20	30	1234.3	865.7	368.6	6.1	1468	518
40	60	1218.8	865.7	353.1	6	1362	149
80	120	1207.2	865.7	341.5	6	1252	22
160	240	1200	865.7	334.3	6	1197	2
320	480	1195.9	865.7	330.2	6	1148	0
400	600	1195.1	865.7	329.4	6	1138	0

Table I-17: Variation in performance parameters for different cavity widths in the base case, tested for constant air changes and volumetric flow rate

Applied Ventilation	Observed Vent Quantity	Cavity Width	Total Heat Gain to Room per m length of facade	Solar Heat Gain to Room per m length of facade	Surface Heat Gain to Room per m length of facade	Total Heat Loss from Room per m length of facade	Hrs with glazing surf above 28°C	Hrs with cavity air above 40°C
		m	kWh	kWh	kWh	kWh	hrs	hrs
80AC	480 m3/hr	0.2	1237.4	878.4	359	6.1	1394	252
80AC	1200 m3/hr	0.5	1207.2	865.7	341.5	6	1252	22
80AC	1920 m3/hr	0.8	1184.9	850.2	334.7	6	1202	5
80AC	2400 m3/hr	1	1173.6	841.7	331.9	6	1176	2
80AC	2880 m3/hr	1.2	1160.2	830.6	329.6	6	1161	2
80AC	3600 m3/hr	1.5	1139.3	812.7	326.6	6	1128	0
1200m3/hr	200 AC	0.2	1221	878.4	342.6	6.1	1256	22
1200m3/hr	80 AC	0.5	1207.2	865.7	341.5	6	1252	22
1200m3/hr	50 AC	0.8	1190.2	850.2	340.1	6	1248	23
1200m3/hr	40 AC	1	1180.8	841.7	339.1	6	1243	23
1200m3/hr	33.34 AC	1.2	1168.7	830.6	338.1	6	1236	24
1200m3/hr	23.67 AC	1.5	1149.1	812.7	336.4	6	1220	25

Table I-18: Variation in performance parameters of different glazing systems on the external and internal envelope on the base configuration

Façade Configuration		Total Heat Gain to Room per m length of facade	Solar Heat Gain to Room per m length of facade	Surface Heat Gain to Room per m length of facade	Heat Loss from Room per m length of facade	Hrs with glazing surf above 28°C	Hrs with cavity air above 40°C
External Glazing (single)	**Internal Glazing (double)**	**kWh**	**kWh**	**kWh**	**kWh**	**hrs**	**hrs**
clear 6mm	Clear DG 4/16/4 argon gas	1207.2	865.7	341.5	6	1252	22
clear 6mm	LowE DB 9.4/12.7/3 LowE, Argon gas	861.7	584.7	277	3.5	579	76
clear 6mm	Tinted DG 4/12.7/3 Argon gas	988.6	486.2	502.3	5.9	2852	127
clear 6mm	High Performance DG 10/1/3 LowE, Vacuum	363.2	232.6	130.6	1.6	0	345
Tinted 5.8mm	Clear DG 4/16/4 argon gas	683.3	344.9	338.3	6.1	1274	13
Reflective 13.2mm	Clear DG 4/16/4 argon gas	463	205.8	257.2	6	206	0
Tinted 5.8mm	LowE DB 9.4/12.7/3 LowE, Argon gas	476.7	233.1	243.7	3.6	113	116
Tinted 5.8mm	High Performance DG 10/1/3 LowE, Vacuum	208.1	92.7	115.4	1.6	0	417

South Façade in Kathmandu

Table I-19: Variation in performance parameters for different ventilation rates in the base model

AC per hour	Vent Rate per m length of facade	Total Heat Gain to Room per m length of facade	Solar Heat Gain to Room per m length of facade	Surface Heat Gain to Room per m length of facade	Total Heat Loss from Room per m length of facade	Hrs with glazing surf above 28°C	Hrs with cavity air above 40°C
/h	m3/hr	kWh	kWh	kWh	kWh	hrs	hrs
0	0	1211.4	996.3	215.1	173.6	1341	812
10	15	1180.9	996.3	184.6	173.7	1155	378
14	21	1170.2	996.3	173.9	173.7	1050	177
20	30	1157.7	996.3	161.4	173.8	895	80
40	60	1134.4	996.3	138.1	173.8	580	73
80	120	1116.8	996.3	120.5	173.9	359	73
160	240	1105.8	996.3	109.5	173.9	271	72
320	480	1099.7	996.3	103.4	173.9	229	72
400	600	1098.4	996.3	102.1	173.9	221	72

Table I-20: Variation in performance parameters for different cavity widths in the base case, tested for constant air changes and volumetric flow rate

Applied Ventilation	Observed Vent Quantity	Cavity Width	Total Heat Gain to Room per m length of facade	Solar Heat Gain to Room per m length of facade	Surface Heat Gain to Room per m length of facade	Total Heat Loss from Room per m length of facade	Hrs with glazing surf above 28°C	Hrs with cavity air above 40°C
		m	kWh	kWh	kWh	kWh	hrs	hrs
80AC	480 m3/hr	0.2	1176.2	1027.8	148.4	174	669	73
80AC	1200 m3/hr	0.5	1116.8	996.3	120.5	173.9	359	73
80AC	1920 m3/hr	0.8	1071.8	963.7	108.1	173.7	284	71
80AC	2400 m3/hr	1	1043.4	941	102.5	173.6	255	69
80AC	2880 m3/hr	1.2	1016.7	918.9	97.7	173.5	212	69
80AC	3600 m3/hr	1.5	974.6	883.3	91.3	173.4	158	69
1200m3/hr	200 AC	0.2	1151.6	1027.8	123.8	174	360	73
1200m3/hr	80 AC	0.5	1116.8	996.3	120.5	173.9	359	73
1200m3/hr	50 AC	0.8	1079.9	963.7	164.1	173.7	350	71
1200m3/hr	40 AC	1	1054.4	941	164.1	173.6	333	70
1200m3/hr	33.34 AC	1.2	1029.5	918.9	164.1	173.5	307	69
1200m3/hr	23.67 AC	1.5	989.3	883.3	164.1	173.3	257	69

Table I-21: Variation in performance parameters of different glazing systems on the external and internal envelope on the base configuration

Façade Configuration		Total Heat Gain to Room per m length of facade	Solar Heat Gain to Room per m length of facade	Surface Heat Gain to Room per m length of facade	Heat Loss from Room per m length of facade	Hrs with glazing surf above 28°C	Hrs with cavity air above 40°C
External Glazing (single)	Internal Glazing (double)	kWh	kWh	kWh	kWh	hrs	hrs
clear 6mm	Clear DG 4/16/4 argon gas	1116.8	996.3	120.5	173.9	359	73
clear 6mm	LowE DB 9.4/12.7/3 LowE, Argon gas	797.8	672.5	125.3	105.4	172	107
clear 6mm	Tinted DG 4/12.7/3 Argon gas	872.1	559.1	313	168.4	1941	185
clear 6mm	High Performance DG 10/1/3 LowE, Vacuum	322.7	267.6	55.1	47.8	0	134
Tinted 5.8mm	Clear DG 4/16/4 argon gas	502.4	396.1	106.3	179	98	32
Reflective 13.2mm	Clear DG 4/16/4 argon gas	242.4	236.8	5.6	185.8	0	0
Tinted 5.8mm	LowE DB 9.4/12.7/3 LowE, Argon gas	350.3	267.5	82.8	110.2	3	45
Tinted 5.8mm	High Performance DG 10/1/3 LowE, Vacuum	142.5	106.5	36.1	50.4	0	56

North Façade in Kathmandu

Table I-22: Variation in performance parameters for different ventilation rates in the base model

AC per hour	Vent Rate per m length of facade	Total Heat Gain to Room per m length of facade	Solar Heat Gain to Room per m length of facade	Surface Heat Gain to Room per m length of facade	Total Heat Loss from Room per m length of facade	Hrs with glazing surf above 28°C	Hrs with cavity air above 40°C
/h	m3/hr	kWh	kWh	kWh	kWh	hrs	hrs
0	0	657.1	639.6	17.5	185.4	92	50
10	15	654.5	639.6	14.9	185.4	82	37
14	21	653.7	639.6	14.1	185.4	74	34
20	30	652.7	639.6	13.1	185.4	67	25
40	60	650.8	639.6	11.2	185.5	58	9
80	120	649.3	639.6	9.8	185.5	44	0
160	240	648.4	639.6	8.8	185.5	34	0
320	480	647.9	639.6	8.3	185.5	32	0
400	600	647.8	639.6	8.2	185.5	32	0

Table I-23: Variation in performance parameters for different cavity widths in the base case, tested for constant air changes and volumetric flow rate

Applied Ventilation	Observed Vent Quantity	Cavity Width	Total Heat Gain to Room per m length of facade	Solar Heat Gain to Room per m length of facade	Surface Heat Gain to Room per m length of facade	Total Heat Loss from Room per m length of facade	Hrs with glazing surf above 28°C	Hrs with cavity air above 40°C
		m	kWh	kWh	kWh	kWh	hrs	hrs
80AC	480 m3/hr	0.2	652.5	640.5	12	185.6	60	13
80AC	1200 m3/hr	0.5	649.3	639.6	9.8	185.5	44	0
80AC	1920 m3/hr	0.8	647.1	638.3	8.8	185.4	36	0
80AC	2400 m3/hr	1	645.8	637.4	8.4	185.3	34	0
80AC	2880 m3/hr	1.2	644.7	636.6	8.1	185.2	33	0
80AC	3600 m3/hr	1.5	642.9	635.3	7.6	185	32	0
1200m3/hr	200 AC	0.2	650.5	640.5	10	185.6	44	0
1200m3/hr	80 AC	0.5	649.3	639.6	9.8	185.5	44	0
1200m3/hr	50 AC	0.8	647.8	638.3	9.5	185.3	44	0
1200m3/hr	40 AC	1	646.7	637.4	9.3	185.2	44	0
1200m3/hr	33.34 AC	1.2	645.8	636.6	9.2	185.1	44	0
1200m3/hr	23.67 AC	1.5	644.2	635.3	8.9	185	44	0

Table I-24: Variation in performance parameters of different glazing systems on the external and internal envelope on the base configuration

Façade Configuration		Total Heat Gain to Room per m length of facade	Solar Heat Gain to Room per m length of facade	Surface Heat Gain to Room per m length of facade	Heat Loss from Room per m length of facade	Hrs with glazing surf above 28°C	Hrs with cavity air above 40°C
External Glazing (single)	Internal Glazing (double)	kWh	kWh	kWh	kWh	hrs	hrs
clear 6mm	Clear DG 4/16/4 argon gas	649.3	639.6	9.8	185.5	44	0
clear 6mm	LowE DB 9.4/12.7/3 LowE, Argon gas	469.7	428.9	40.8	114.9	24	1
clear 6mm	Tinted DG 4/12.7/3 Argon gas	514.9	356	158.8	181.6	614	4
clear 6mm	High Performance DG 10/1/3 LowE, Vacuum	188.6	170.6	17.9	53.6	0	3
Tinted 5.8mm	Clear DG 4/16/4 argon gas	290.8	252	38.8	197.7	28	0
Reflective 13.2mm	Clear DG 4/16/4 argon gas	142.7	151.4	-8.7	210.8	0	0
Tinted 5.8mm	LowE DB 9.4/12.7/3 LowE, Argon gas	204.2	169	35.2	124.3	5	1
Tinted 5.8mm	High Performance DG 10/1/3 LowE, Vacuum	82.9	67.2	15.6	58.6	0	2

East Façade in Kathmandu

Table I-25: Variation in performance parameters for different ventilation rates in the base model

AC per hour	Vent Rate per m length of facade	Total Heat Gain to Room per m length of facade	Solar Heat Gain to Room per m length of facade	Surface Heat Gain to Room per m length of facade	Total Heat Loss from Room per m length of facade	Hrs with glazing surf above 28°C	Hrs with cavity air above 40°C
/h	m3/hr	kWh	kWh	kWh	kWh	hrs	hrs
0	0	973.1	863.8	109.3	170.6	627	289
10	15	958.5	863.8	94.8	170.6	509	74
14	21	953.4	863.8	89.7	170.6	437	26
20	30	947.5	863.8	83.7	170.6	347	8
40	60	936.2	863.8	72.4	170.6	173	8
80	120	927.7	863.8	63.9	170.6	93	8
160	240	922.3	863.8	58.6	170.6	61	8
320	480	919.3	863.8	55.6	170.6	45	8
400	600	918.7	863.8	55	170.6	43	8

Table I-26: Variation in performance parameters for different cavity widths in the base case, tested for constant air changes and volumetric flow rate

Applied Ventilation	Observed Vent Quantity	Cavity Width	Total Heat Gain to Room per m length of facade	Solar Heat Gain to Room per m length of facade	Surface Heat Gain to Room per m length of facade	Total Heat Loss from Room per m length of facade	Hrs with glazing surf above 28°C	Hrs with cavity air above 40°C
		m	kWh	kWh	kWh	kWh	hrs	hrs
80AC	480 m3/hr	0.2	951.8	874.8	77	170.8	219	8
80AC	1200 m3/hr	0.5	927.7	863.8	63.9	170.6	93	8
80AC	1920 m3/hr	0.8	909.3	850.8	58.5	170.4	69	6
80AC	2400 m3/hr	1	897.5	841.7	55.8	170.3	58	6
80AC	2880 m3/hr	1.2	887.1	833.4	53.7	170.2	51	6
80AC	3600 m3/hr	1.5	869.3	818.4	50.9	170.1	43	6
1200m3/hr	200 AC	0.2	939.9	874.8	65.1	170.8	93	8
1200m3/hr	80 AC	0.5	927.7	863.8	63.9	170.6	93	8
1200m3/hr	50 AC	0.8	913.2	850.8	93	170.4	91	6
1200m3/hr	40 AC	1	902.9	841.7	93	170.3	90	6
1200m3/hr	33.34 AC	1.2	893.4	833.4	93	170.2	81	6
1200m3/hr	23.67 AC	1.5	876.6	818.4	93	170.1	75	6

Table I-27: Variation in performance parameters of different glazing systems on the external and internal envelope on the base configuration

Façade Configuration		Total Heat Gain to Room per m length of facade	Solar Heat Gain to Room per m length of facade	Surface Heat Gain to Room per m length of facade	Heat Loss from Room per m length of facade	Hrs with glazing surf above 28°C	Hrs with cavity air above 40°C
External Glazing (single)	**Internal Glazing (double)**	**kWh**	**kWh**	**kWh**	**kWh**	**hrs**	**hrs**
clear 6mm	Clear DG 4/16/4 argon gas	927.7	863.8	63.9	170.6	93	8
clear 6mm	LowE DB 9.4/12.7/3 LowE, Argon gas	671	585	86.1	105.2	9	8
clear 6mm	Tinted DG 4/12.7/3 Argon gas	727.7	487	240.7	165.3	1339	65
clear 6mm	High Performance DG 10/1/3 LowE, Vacuum	271.8	232.7	39	48.4	0	17
Tinted 5.8mm	Clear DG 4/16/4 argon gas	413.5	345.7	67.8	176.1	8	1
Reflective 13.2mm	Clear DG 4/16/4 argon gas	192.1	205.6	-13.5	182.2	0	0
Tinted 5.8mm	LowE DB 9.4/12.7/3 LowE, Argon gas	292	234.3	57.7	109.2	0	2
Tinted 5.8mm	High Performance DG 10/1/3 LowE, Vacuum	118.7	93.2	25.6	50.3	0	3

South Façade in Jaisalmer

Table I-28: Variation in performance parameters for different ventilation rates in the base model

AC per hour	Vent Rate per m length of facade	Total Heat Gain to Room per m length of facade	Solar Heat Gain to Room per m length of facade	Surface Heat Gain to Room per m length of facade	Total Heat Loss from Room per m length of facade	Hrs with glazing surf above 28°C	Hrs with cavity air above 40°C
/h	m3/hr	kWh	kWh	kWh	kWh	hrs	hrs
0	0	1481.6	1019.6	462	84.1	2887	1741
10	15	1445.4	1019.6	425.7	84.2	2835	1484
14	21	1432.3	1019.6	412.6	84.2	2815	1293
20	30	1417	1019.6	397.4	84.2	2779	1018
40	60	1388.5	1019.6	368.9	84.3	2687	522
80	120	1367.2	1019.6	347.5	84.3	2604	278
160	240	1353.9	1019.6	334.3	84.3	2525	146
320	480	1346.5	1019.6	326.9	84.3	2480	116
400	600	1345	1019.6	325.3	84.3	2470	113

Table I-29: Variation in performance parameters for different cavity widths in the base case, tested for constant air changes and volumetric flow rate

Applied Ventilation	Observed Vent Quantity	Cavity Width	Total Heat Gain to Room per m length of facade	Solar Heat Gain to Room per m length of facade	Surface Heat Gain to Room per m length of facade	Total Heat Loss from Room per m length of facade	Hrs with glazing surf above 28°C	Hrs with cavity air above 40°C
		m	kWh	kWh	kWh	kWh	hrs	hrs
80AC	480 m3/hr	0.2	1437.9	1056.8	381.1	84.3	2719	636
80AC	1200 m3/hr	0.5	1367.2	1019.6	347.5	84.3	2604	278
80AC	1920 m3/hr	0.8	1313.9	980.5	333.4	84.2	2548	175
80AC	2400 m3/hr	1	1280.3	953.2	327.1	84.2	2526	144
80AC	2880 m3/hr	1.2	1249.1	927.2	321.9	84.1	2503	132
80AC	3600 m3/hr	1.5	1198.6	883.6	315	84	2454	116
1200m3/hr	200 AC	0.2	1407.9	1056.8	351	84.4	2605	277
1200m3/hr	80 AC	0.5	1367.2	1019.6	347.5	84.3	2604	278
1200m3/hr	50 AC	0.8	1323.6	980.5	343.2	84.2	2603	284
1200m3/hr	40 AC	1	1293.4	953.2	340.3	84.2	2608	286
1200m3/hr	33.34 AC	1.2	1264.5	927.2	337.3	84.1	2603	284
1200m3/hr	23.67 AC	1.5	1216.2	883.6	332.6	84	2587	280

Table I-30: Variation in performance parameters of different glazing systems on the external and internal envelope on the base configuration

Façade Configuration		Total Heat Gain to Room per m length of facade	Solar Heat Gain to Room per m length of facade	Surface Heat Gain to Room per m length of facade	Heat Loss from Room per m length of facade	Hrs with glazing surf above 28°C	Hrs with cavity air above 40°C
External Glazing (single)	Internal Glazing (double)	kWh	kWh	kWh	kWh	hrs	hrs
clear 6mm	Clear DG 4/16/4 argon gas	1367.2	1019.6	347.5	84.3	2604	278
clear 6mm	LowE DB 9.4/12.7/3 LowE, Argon gas	968.2	689	279.2	50.9	2157	579
clear 6mm	Tinted DG 4/12.7/3 Argon gas	1097.2	573.1	524.1	81.1	3454	715
clear 6mm	High Performance DG 10/1/3 LowE, Vacuum	402.6	274.2	128.4	23.1	22	962
Tinted 5.8mm	Clear DG 4/16/4 argon gas	735.4	406.2	329.2	84.9	2502	387
Reflective 13.2mm	Clear DG 4/16/4 argon gas	475.8	242.5	233.4	85.4	1482	85
Tinted 5.8mm	LowE DB 9.4/12.7/3 LowE, Argon gas	508.4	274.6	233.8	52	1422	654
Tinted 5.8mm	High Performance DG 10/1/3 LowE, Vacuum	217.6	109.3	108.4	23.6	0	932

North Façade in Jaisalmer

Table I-31: Variation in performance parameters for different ventilation rates in the base model

AC per hour	Vent Rate per m length of facade	Total Heat Gain to Room per m length of facade	Solar Heat Gain to Room per m length of facade	Surface Heat Gain to Room per m length of facade	Total Heat Loss from Room per m length of facade	Hrs with glazing surf above 28°C	Hrs with cavity air above 40°C
/h	m3/hr	kWh	kWh	kWh	kWh	hrs	hrs
0	0	812.5	589.5	223.1	86.8	1546	37
10	15	812.5	589.5	223.1	86.8	1546	37
14	21	812.5	589.5	223.1	86.8	1546	37
20	30	812.5	589.5	223.1	86.8	1546	37
40	60	812.5	589.5	223.1	86.8	1546	37
80	120	812.5	589.5	223.1	86.8	1546	37
160	240	812.5	589.5	223.1	86.8	1546	37
320	480	812.5	589.5	223.1	86.8	1546	37
400	600	812.5	589.5	223.1	86.8	1546	37

Table I-32: Variation in performance parameters for different cavity widths in the base case, tested for constant air changes and volumetric flow rate

Applied Ventilation	Observed Vent Quantity	Cavity Width	Total Heat Gain to Room per m length of facade	Solar Heat Gain to Room per m length of facade	Surface Heat Gain to Room per m length of facade	Total Heat Loss from Room per m length of facade	Hrs with glazing surf above 28°C	Hrs with cavity air above 40°C
		m	kWh	kWh	kWh	kWh	hrs	hrs
80AC	480 m3/hr	0.2	814.1	590.8	223.3	86.9	1548	37
80AC	1200 m3/hr	0.5	812.5	589.5	223.1	86.8	1546	37
80AC	1920 m3/hr	0.8	810.1	587.3	222.9	86.7	1543	37
80AC	2400 m3/hr	1	808.7	586.1	222.7	86.7	1543	36
80AC	2880 m3/hr	1.2	807.4	584.9	222.5	86.6	1544	36
80AC	3600 m3/hr	1.5	805.2	582.9	222.3	86.6	1541	36
1200m3/hr	200 AC	0.2	814.1	590.8	223.3	86.9	1548	37
1200m3/hr	80 AC	0.5	812.5	589.5	223.1	86.8	1546	37
1200m3/hr	50 AC	0.8	810.1	587.3	222.9	86.7	1543	37
1200m3/hr	40 AC	1	808.7	586.1	222.7	86.7	1543	36
1200m3/hr	33.34 AC	1.2	807.4	584.9	222.5	86.6	1544	36
1200m3/hr	23.67 AC	1.5	805.2	582.9	222.3	86.6	1541	36

Table I-33: Variation in performance parameters of different glazing systems on the external and internal envelope on the base configuration

Façade Configuration		Total Heat Gain to Room per m length of facade	Solar Heat Gain to Room per m length of facade	Surface Heat Gain to Room per m length of facade	Heat Loss from Room per m length of facade	Hrs with glazing surf above 28°C	Hrs with cavity air above 40°C
External Glazing (single)	**Internal Glazing (double)**	**kWh**	**kWh**	**kWh**	**kWh**	**hrs**	**hrs**
clear 6mm	Clear DG 4/16/4 argon gas	812.5	589.5	223.1	86.8	1546	37
clear 6mm	LowE DB 9.4/12.7/3 LowE, Argon gas	580.1	395.6	184.4	53.6	821	295
clear 6mm	Tinted DG 4/12.7/3 Argon gas	680.9	328.5	352.4	84.4	2517	441
clear 6mm	High Performance DG 10/1/3 LowE, Vacuum	245.4	157.4	88	24.8	0	702
Tinted 5.8mm	Clear DG 4/16/4 argon gas	476.7	232.6	244.1	89.5	1791	226
Reflective 13.2mm	Clear DG 4/16/4 argon gas	331.2	139.6	191.5	92	971	21
Tinted 5.8mm	LowE DB 9.4/12.7/3 LowE, Argon gas	331.3	156.1	175.2	56.3	620	511
Tinted 5.8mm	High Performance DG 10/1/3 LowE, Vacuum	145.6	62.1	83.5	26.3	0	865

East Façade in Jaisalmer

Table I-34: Variation in performance parameters for different ventilation rates in the base model

AC per hour	Vent Rate per m length of facade	Total Heat Gain to Room per m length of facade	Solar Heat Gain to Room per m length of facade	Surface Heat Gain to Room per m length of facade	Total Heat Loss from Room per m length of facade	Hrs with glazing surf above 28°C	Hrs with cavity air above 40°C
/h	m3/hr	kWh	kWh	kWh	kWh	hrs	hrs
0	0	1409.1	992.7	416.5	84.6	2690	1272
10	15	1381.1	992.7	388.4	84.6	2646	1085
14	21	1370.9	992.7	378.2	84.7	2605	971
20	30	1359	992.7	366.3	84.7	2567	817
40	60	1336.7	992.7	344.1	84.6	2480	467
80	120	1320	992.7	327.4	84.6	2406	218
160	240	1309.6	992.7	317	84.6	2363	125
320	480	1303.8	992.7	311.2	84.6	2317	86
400	600	1302.6	992.7	310	84.6	2310	83

Table I-35: Variation in performance parameters for different cavity widths in the base case, tested for constant air changes and volumetric flow rate

Applied Ventilation	Observed Vent Quantity	Cavity Width	Total Heat Gain to Room per m length of facade	Solar Heat Gain to Room per m length of facade	Surface Heat Gain to Room per m length of facade	Total Heat Loss from Room per m length of facade	Hrs with glazing surf above 28°C	Hrs with cavity air above 40°C
		m	kWh	kWh	kWh	kWh	hrs	hrs
80AC	480 m3/hr	0.2	1364.7	1012.3	352.4	84.7	2500	571
80AC	1200 m3/hr	0.5	1320	992.7	327.4	84.6	2406	218
80AC	1920 m3/hr	0.8	1287.5	969.9	317.6	84.6	2369	130
80AC	2400 m3/hr	1	1267.5	954.3	313.3	84.5	2361	119
80AC	2880 m3/hr	1.2	1249.7	939.9	309.9	84.4	2348	107
80AC	3600 m3/hr	1.5	1218.7	913.2	305.5	84.4	2326	97
1200m3/hr	200 AC	0.2	1341.3	1012.3	329	84.7	2407	215
1200m3/hr	80 AC	0.5	1320	992.7	327.4	84.6	2406	218
1200m3/hr	50 AC	0.8	1295.1	969.9	325.2	84.6	2404	220
1200m3/hr	40 AC	1	1277.9	954.3	323.6	84.5	2405	223
1200m3/hr	33.34 AC	1.2	1262	939.9	322.1	84.4	2403	221
1200m3/hr	23.67 AC	1.5	1232.8	913.2	319.6	84.4	2398	217

Table I-36: Variation in performance parameters of different glazing systems on the external and internal envelope on the base configuration

Façade Configuration		Total Heat Gain to Room per m length of facade	Solar Heat Gain to Room per m length of facade	Surface Heat Gain to Room per m length of facade	Heat Loss from Room per m length of facade	Hrs with glazing surf above 28°C	Hrs with cavity air above 40°C
External Glazing (single)	**Internal Glazing (double)**	**kWh**	**kWh**	**kWh**	**kWh**	**hrs**	**hrs**
clear 6mm	Clear DG 4/16/4 argon gas	1320	992.7	327.4	84.6	2406	218
clear 6mm	LowE DB 9.4/12.7/3 LowE, Argon gas	941.8	673.8	267.9	51.9	1915	618
clear 6mm	Tinted DG 4/12.7/3 Argon gas	1061.9	561.3	500.6	81.8	3289	733
clear 6mm	High Performance DG 10/1/3 LowE, Vacuum	393.3	268	125.3	23.7	35	1138
Tinted 5.8mm	Clear DG 4/16/4 argon gas	715.3	398.8	316.4	85.4	2377	355
Reflective 13.2mm	Clear DG 4/16/4 argon gas	463.9	236.7	227.3	85.4	1495	59
Tinted 5.8mm	LowE DB 9.4/12.7/3 LowE, Argon gas	498.9	270.9	228	52.8	1372	742
Tinted 5.8mm	High Performance DG 10/1/3 LowE, Vacuum	214.8	107.8	107	24.1	0	1139

South Façade in Bhopal

Table I-37: Variation in performance parameters for different ventilation rates in the base model

AC per hour	Vent Rate per m length of facade	Total Heat Gain to Room per m length of facade	Solar Heat Gain to Room per m length of facade	Surface Heat Gain to Room per m length of facade	Total Heat Loss from Room per m length of facade	Hrs with glazing surf above 28°C	Hrs with cavity air above 40°C
/h	m3/hr	kWh	kWh	kWh	kWh	hrs	hrs
0	0	1313.3	944.7	368.6	76.9	2338	1443
10	15	1280.9	944.7	336.2	77	2297	1167
14	21	1269.3	944.7	324.7	77	2266	949
20	30	1255.8	944.7	311.1	77	2229	599
40	60	1230.5	944.7	285.9	77	2115	121
80	120	1211.6	944.7	266.9	77	1973	62
160	240	1199.8	944.7	255.1	77.1	1890	42
320	480	1193.2	944.7	248.6	77.1	1835	31
400	600	1191.9	944.7	247.2	77.1	1829	29

Table I-38: Variation in performance parameters for different cavity widths in the base case, tested for constant air changes and volumetric flow rate

Applied Ventilation	Observed Vent Quantity	Cavity Width	Total Heat Gain to Room per m length of facade	Solar Heat Gain to Room per m length of facade	Surface Heat Gain to Room per m length of facade	Total Heat Loss from Room per m length of facade	Hrs with glazing surf above 28°C	Hrs with cavity air above 40°C
		m	kWh	kWh	kWh	kWh	hrs	hrs
80AC	480 m3/hr	0.2	1274.5	977.8	296.7	77.1	2159	183
80AC	1200 m3/hr	0.5	1211.6	944.7	266.9	77	1973	62
80AC	1920 m3/hr	0.8	1165.2	910.7	254.5	77	1918	47
80AC	2400 m3/hr	1	1136	887.1	249	76.9	1885	41
80AC	2880 m3/hr	1.2	1107.2	863.1	244.1	76.9	1834	36
80AC	3600 m3/hr	1.5	1064.1	826	238.1	76.8	1775	30
1200m3/hr	200 AC	0.2	1247.9	977.8	270	77.1	1976	60
1200m3/hr	80 AC	0.5	1211.6	944.7	266.9	77	1973	62
1200m3/hr	50 AC	0.8	1173.9	910.7	263.2	77	1968	57
1200m3/hr	40 AC	1	1147.7	887.1	260.6	76.9	1963	57
1200m3/hr	33.34 AC	1.2	1120.9	863.1	257.8	76.9	1956	57
1200m3/hr	23.67 AC	1.5	1079.8	826	253.8	76.8	1935	54

Table I-39: Variation in performance parameters of different glazing systems on the external and internal envelope on the base configuration

Façade Configuration		Total Heat Gain to Room per m length of facade	Solar Heat Gain to Room per m length of facade	Surface Heat Gain to Room per m length of facade	Heat Loss from Room per m length of facade	Hrs with glazing surf above 28°C	Hrs with cavity air above 40°C
External Glazing (single)	**Internal Glazing (double)**	**kWh**	**kWh**	**kWh**	**kWh**	**hrs**	**hrs**
clear 6mm	Clear DG 4/16/4 argon gas	1211.6	944.7	266.9	77	1973	62
clear 6mm	LowE DB 9.4/12.7/3 LowE, Argon gas	861	637.2	223.8	46.3	1526	214
clear 6mm	Tinted DG 4/12.7/3 Argon gas	967	529.6	437.4	74.1	3217	265
clear 6mm	High Performance DG 10/1/3 LowE, Vacuum	356.1	253.6	102.5	20.8	0	387
Tinted 5.8mm	Clear DG 4/16/4 argon gas	628.2	375.1	253.1	77.1	1831	139
Reflective 13.2mm	Clear DG 4/16/4 argon gas	387.4	224.4	163	76.8	662	19
Tinted 5.8mm	LowE DB 9.4/12.7/3 LowE, Argon gas	436	253.1	182.9	46.9	740	285
Tinted 5.8mm	High Performance DG 10/1/3 LowE, Vacuum	185	100.7	84.3	21.1	0	396

North Façade in Bhopal

Table I-40: Variation in performance parameters for different ventilation rates in the base model

AC per hour	Vent Rate per m length of facade	Total Heat Gain to Room per m length of facade	Solar Heat Gain to Room per m length of facade	Surface Heat Gain to Room per m length of facade	Total Heat Loss from Room per m length of facade	Hrs with glazing surf above 28°C	Hrs with cavity air above 40°C
/h	m3/hr	kWh	kWh	kWh	kWh	hrs	hrs
0	0	786.2	619.6	166.6	77.9	789	24
10	15	786.1	619.6	166.5	77.9	789	16
14	21	786	619.6	166.5	77.9	789	10
20	30	786	619.6	166.4	77.9	789	8
40	60	785.9	619.6	166.3	77.9	788	7
80	120	785.8	619.6	166.2	77.9	788	4
160	240	785.7	619.6	166.1	77.9	788	4
320	480	785.7	619.6	166.1	77.9	788	4
400	600	785.7	619.6	166.1	77.9	788	4

Table I-41: Variation in performance parameters for different cavity widths in the base case, tested for constant air changes and volumetric flow rate

Applied Ventilation	Observed Vent Quantity	Cavity Width	Total Heat Gain to Room per m length of facade	Solar Heat Gain to Room per m length of facade	Surface Heat Gain to Room per m length of facade	Total Heat Loss from Room per m length of facade	Hrs with glazing surf above 28°C	Hrs with cavity air above 40°C
		m	kWh	kWh	kWh	kWh	hrs	hrs
80AC	480 m3/hr	0.2	789	622.4	166.6	78	789	8
80AC	1200 m3/hr	0.5	785.8	619.6	166.2	77.9	788	4
80AC	1920 m3/hr	0.8	782.2	616.4	165.8	77.9	786	4
80AC	2400 m3/hr	1	780.2	614.7	165.5	77.8	785	4
80AC	2880 m3/hr	1.2	777.9	612.6	165.3	77.8	782	4
80AC	3600 m3/hr	1.5	773.7	608.8	164.9	77.7	780	4
1200m3/hr	200 AC	0.2	788.9	622.4	166.5	78	789	4
1200m3/hr	80 AC	0.5	785.8	619.6	166.2	77.9	788	4
1200m3/hr	50 AC	0.8	782.2	616.4	165.8	77.9	786	4
1200m3/hr	40 AC	1	780.3	614.7	165.6	77.8	785	4
1200m3/hr	33.34 AC	1.2	777.9	612.6	165.4	77.8	782	4
1200m3/hr	23.67 AC	1.5	773.8	608.8	165	77.7	780	4

Table I-42: Variation in performance parameters of different glazing systems on the external and internal envelope on the base configuration

Façade Configuration		Total Heat Gain to Room per m length of facade	Solar Heat Gain to Room per m length of facade	Surface Heat Gain to Room per m length of facade	Heat Loss from Room per m length of facade	Hrs with glazing surf above 28°C	Hrs with cavity air above 40°C
External Glazing (single)	Internal Glazing (double)	kWh	kWh	kWh	kWh	hrs	hrs
clear 6mm	Clear DG 4/16/4 argon gas	785.8	619.6	166.2	77.9	788	4
clear 6mm	LowE DB 9.4/12.7/3 LowE, Argon gas	564.4	416	148.4	47.6	498	161
clear 6mm	Tinted DG 4/12.7/3 Argon gas	649.4	345.4	304	75.5	2309	260
clear 6mm	High Performance DG 10/1/3 LowE, Vacuum	235.9	165.5	70.4	21.8	0	403
Tinted 5.8mm	Clear DG 4/16/4 argon gas	431.4	244.6	186.8	79.5	978	104
Reflective 13.2mm	Clear DG 4/16/4 argon gas	277	146.8	130.3	80.9	511	2
Tinted 5.8mm	LowE DB 9.4/12.7/3 LowE, Argon gas	301.6	164.3	137.4	49.4	378	302
Tinted 5.8mm	High Performance DG 10/1/3 LowE, Vacuum	130.4	65.4	65.1	22.7	0	479

East Façade in Bhopal

Table I-43: Variation in performance parameters for different ventilation rates in the base model

AC per hour	Vent Rate per m length of facade	Total Heat Gain to Room per m length of facade	Solar Heat Gain to Room per m length of facade	Surface Heat Gain to Room per m length of facade	Total Heat Loss from Room per m length of facade	Hrs with glazing surf above 28°C	Hrs with cavity air above 40°C
/h	m3/hr	kWh	kWh	kWh	kWh	hrs	hrs
0	0	1320.5	968.7	351.8	77.5	2090	1124
10	15	1291.9	968.7	323.2	77.5	2042	857
14	21	1281.6	968.7	312.9	77.5	2006	698
20	30	1269.6	968.7	300.9	77.5	1951	530
40	60	1247.2	968.7	278.5	77.5	1806	275
80	120	1230.3	968.7	261.6	77.5	1659	138
160	240	1219.8	968.7	251.1	77.5	1574	53
320	480	1214	968.7	245.3	77.5	1526	26
400	600	1212.7	968.7	244	77.5	1513	25

Table I-43: Variation in performance parameters for different cavity widths in the base case, tested for constant air changes and volumetric flow rate

Applied Ventilation	Observed Vent Quantity	Cavity Width	Total Heat Gain to Room per m length of facade	Solar Heat Gain to Room per m length of facade	Surface Heat Gain to Room per m length of facade	Total Heat Loss from Room per m length of facade	Hrs with glazing surf above 28°C	Hrs with cavity air above 40°C
		m	kWh	kWh	kWh	kWh	hrs	hrs
80AC	480 m3/hr	0.2	1272.7	986	286.7	77.6	1852	332
80AC	1200 m3/hr	0.5	1230.3	968.7	261.6	77.5	1659	138
80AC	1920 m3/hr	0.8	1201.2	949.2	252	77.4	1598	75
80AC	2400 m3/hr	1	1183.8	935.9	247.8	77.4	1564	53
80AC	2880 m3/hr	1.2	1167.4	922.8	244.5	77.3	1543	43
80AC	3600 m3/hr	1.5	1139.7	899.4	240.4	77.3	1508	39
1200m3/hr	200 AC	0.2	1249.1	986	263.1	77.6	1659	138
1200m3/hr	80 AC	0.5	1230.3	968.7	261.6	77.5	1659	138
1200m3/hr	50 AC	0.8	1208.9	949.2	259.7	77.4	1660	139
1200m3/hr	40 AC	1	1194.2	935.9	258.3	77.4	1652	144
1200m3/hr	33.34 AC	1.2	1179.8	922.8	256.9	77.3	1644	146
1200m3/hr	23.67 AC	1.5	1154	899.4	254.6	77.3	1636	145

Table I-44: Variation in performance parameters of different glazing systems on the external and internal envelope on the base configuration

Façade Configuration		Total Heat Gain to Room per m length of facade	Solar Heat Gain to Room per m length of facade	Surface Heat Gain to Room per m length of facade	Heat Loss from Room per m length of facade	Hrs with glazing surf above 28°C	Hrs with cavity air above 40°C
External Glazing (single)	Internal Glazing (double)	kWh	kWh	kWh	kWh	hrs	hrs
clear 6mm	Clear DG 4/16/4 argon gas	1230.3	968.7	261.6	77.5	1659	138
clear 6mm	LowE DB 9.4/12.7/3 LowE, Argon gas	881.6	657.7	223.9	47.3	1226	369
clear 6mm	Tinted DG 4/12.7/3 Argon gas	984.2	547.8	436.4	74.7	3097	406
clear 6mm	High Performance DG 10/1/3 LowE, Vacuum	365.9	261.6	104.2	21.5	68	572
Tinted 5.8mm	Clear DG 4/16/4 argon gas	640.7	389.3	251.4	77.7	1559	189
Reflective 13.2mm	Clear DG 4/16/4 argon gas	393.4	231	162.5	77.1	726	20
Tinted 5.8mm	LowE DB 9.4/12.7/3 LowE, Argon gas	449	264.4	184.6	47.8	750	408
Tinted 5.8mm	High Performance DG 10/1/3 LowE, Vacuum	191.4	105.2	86.2	21.6	0	536

South Façade in Kolkata

Table I-46: Variation in performance parameters for different ventilation rates in the base model

AC per hour	Vent Rate per m length of facade	Total Heat Gain to Room per m length of facade	Solar Heat Gain to Room per m length of facade	Surface Heat Gain to Room per m length of facade	Total Heat Loss from Room per m length of facade	Hrs with glazing surf above 28°C	Hrs with cavity air above 40°C
/h	m3/hr	kWh	kWh	kWh	kWh	hrs	hrs
0	0	1123.1	815.7	307.4	49.6	2060	1041
10	15	1100.9	815.7	285.2	49.6	2026	759
14	21	1093.2	815.7	277.5	49.6	2001	544
20	30	1084.2	815.7	268.5	49.6	1970	283
40	60	1067.4	815.7	251.6	49.6	1892	31
80	120	1054.7	815.7	239	49.6	1802	6
160	240	1046.9	815.7	231.2	49.6	1727	3
320	480	1042.5	815.7	226.8	49.6	1689	2
400	600	1041.6	815.7	225.9	49.6	1682	1

Table I-47: Variation in performance parameters for different cavity widths in the base case, tested for constant air changes and volumetric flow rate

Applied Ventilation	Observed Vent Quantity	Cavity Width	Total Heat Gain to Room per m length of facade	Solar Heat Gain to Room per m length of facade	Surface Heat Gain to Room per m length of facade	Total Heat Loss from Room per m length of facade	Hrs with glazing surf above 28°C	Hrs with cavity air above 40°C
		m	kWh	kWh	kWh	kWh	hrs	hrs
80AC	480 m3/hr	0.2	1092.9	834.5	258.4	49.7	1921	64
80AC	1200 m3/hr	0.5	1054.7	815.7	239	49.6	1802	6
80AC	1920 m3/hr	0.8	1027.1	796	231.1	49.6	1743	3
80AC	2400 m3/hr	1	1010.8	783	227.8	49.6	1719	3
80AC	2880 m3/hr	1.2	993.3	768.5	224.9	49.5	1698	3
80AC	3600 m3/hr	1.5	968.5	747.2	221.3	49.5	1643	2
1200m3/hr	200 AC	0.2	1075.2	834.5	240.7	49.7	1804	6
1200m3/hr	80 AC	0.5	1054.7	815.7	239	49.6	1802	6
1200m3/hr	50 AC	0.8	1032.9	796	236.9	49.6	1801	6
1200m3/hr	40 AC	1	1018.7	783	235.6	49.5	1798	6
1200m3/hr	33.34 AC	1.2	1002.5	768.5	234.1	49.5	1795	6
1200m3/hr	23.67 AC	1.5	979.1	747.2	231.9	49.5	1768	6

Table I-48: Variation in performance parameters of different glazing systems on the external and internal envelope on the base configuration

Façade Configuration		Total Heat Gain to Room per m length of facade	Solar Heat Gain to Room per m length of facade	Surface Heat Gain to Room per m length of facade	Heat Loss from Room per m length of facade	Hrs with glazing surf above 28°C	Hrs with cavity air above 40°C
External Glazing (single)	Internal Glazing (double)	kWh	kWh	kWh	kWh	hrs	hrs
clear 6mm	Clear DG 4/16/4 argon gas	1054.7	815.7	239	49.6	1802	6
clear 6mm	LowE DB 9.4/12.7/3 LowE, Argon gas	751.9	549.1	202.8	30	1357	28
clear 6mm	Tinted DG 4/12.7/3 Argon gas	849.2	456.2	393	47.7	3057	50
clear 6mm	High Performance DG 10/1/3 LowE, Vacuum	312.5	218.5	94	13.5	0	102
Tinted 5.8mm	Clear DG 4/16/4 argon gas	557.6	323	234.6	49.7	1803	15
Reflective 13.2mm	Clear DG 4/16/4 argon gas	350.9	193.6	157.3	49.7	563	1
Tinted 5.8mm	LowE DB 9.4/12.7/3 LowE, Argon gas	388.4	217.5	170.9	30.4	611	49
Tinted 5.8mm	High Performance DG 10/1/3 LowE, Vacuum	166.3	86.5	79.7	13.7	0	183

North Façade in Kolkata

Table I-49: Variation in performance parameters for different ventilation rates in the base model

AC per hour	Vent Rate per m length of facade	Total Heat Gain to Room per m length of facade	Solar Heat Gain to Room per m length of facade	Surface Heat Gain to Room per m length of facade	Total Heat Loss from Room per m length of facade	Hrs with glazing surf above 28°C	Hrs with cavity air above 40°C
/h	m3/hr	kWh	kWh	kWh	kWh	hrs	hrs
0	0	762.3	593.7	168.6	50.1	910	2
10	15	762.3	593.7	168.6	50.1	910	2
14	21	762.3	593.7	168.6	50.1	910	1
20	30	762.3	593.7	168.6	50.1	910	1
40	60	762.3	593.7	168.6	50.1	910	0
80	120	762.3	593.7	168.6	50.1	910	0
160	240	762.3	593.7	168.5	50.1	910	0
320	480	762.3	593.7	168.5	50.1	910	0
400	600	762.3	593.7	168.5	50.1	910	0

Table I-50: Variation in performance parameters for different cavity widths in the base case, tested for constant air changes and volumetric flow rate

Applied Ventilation	Observed Vent Quantity	Cavity Width	Total Heat Gain to Room per m length of facade	Solar Heat Gain to Room per m length of facade	Surface Heat Gain to Room per m length of facade	Total Heat Loss from Room per m length of facade	Hrs with glazing surf above 28°C	Hrs with cavity air above 40°C
		m	kWh	kWh	kWh	kWh	hrs	hrs
80AC	480 m3/hr	0.2	763.3	594.6	168.7	50.2	909	0
80AC	1200 m3/hr	0.5	762.3	593.7	168.6	50.1	910	0
80AC	1920 m3/hr	0.8	760.9	592.5	168.4	50.1	910	0
80AC	2400 m3/hr	1	760.4	592.1	168.3	50	909	0
80AC	2880 m3/hr	1.2	759.6	591.4	168.2	50	908	0
80AC	3600 m3/hr	1.5	758.3	590.2	168.1	50	905	0
1200m3/hr	200 AC	0.2	763.3	594.6	168.7	50.2	909	0
1200m3/hr	80 AC	0.5	762.3	593.7	168.6	50.1	910	0
1200m3/hr	50 AC	0.8	760.9	592.5	168.4	50.1	910	0
1200m3/hr	40 AC	1	760.4	592.1	168.3	50	909	0
1200m3/hr	33.34 AC	1.2	759.6	591.4	168.2	50	908	0
1200m3/hr	23.67 AC	1.5	758.3	590.2	168.1	50	905	0

Table I-51: Variation in performance parameters of different glazing systems on the external and internal envelope on the base configuration

Façade Configuration		Total Heat Gain to Room per m length of facade	Solar Heat Gain to Room per m length of facade	Surface Heat Gain to Room per m length of facade	Heat Loss from Room per m length of facade	Hrs with glazing surf above 28°C	Hrs with cavity air above 40°C
External Glazing (single)	Internal Glazing (double)	kWh	kWh	kWh	kWh	hrs	hrs
clear 6mm	Clear DG 4/16/4 argon gas	762.3	593.7	168.6	50.1	910	0
clear 6mm	LowE DB 9.4/12.7/3 LowE, Argon gas	548.4	398	150.4	30.8	627	15
clear 6mm	Tinted DG 4/12.7/3 Argon gas	631.6	330.4	301.2	48.5	2404	51
clear 6mm	High Performance DG 10/1/3 LowE, Vacuum	230.2	158.4	71.8	14.1	0	110
Tinted 5.8mm	Clear DG 4/16/4 argon gas	421.9	233.9	188	50.9	1177	10
Reflective 13.2mm	Clear DG 4/16/4 argon gas	273.3	140.5	132.7	51.6	328	0
Tinted 5.8mm	LowE DB 9.4/12.7/3 LowE, Argon gas	295.9	156.8	139.1	31.7	421	57
Tinted 5.8mm	High Performance DG 10/1/3 LowE, Vacuum	128.7	62.4	66.3	14.6	0	201

East Façade in Kolkata

Table I-52: Variation in performance parameters for different ventilation rates in the base model

AC per hour	Vent Rate per m length of facade	Total Heat Gain to Room per m length of facade	Solar Heat Gain to Room per m length of facade	Surface Heat Gain to Room per m length of facade	Total Heat Loss from Room per m length of facade	Hrs with glazing surf above 28°C	Hrs with cavity air above 40°C
/h	m3/hr	kWh	kWh	kWh	kWh	hrs	hrs
0	0	1068.2	789.9	278.3	49.8	1858	775
10	15	1051.6	789.9	261.7	49.8	1804	547
14	21	1045.8	789.9	255.9	49.8	1784	397
20	30	1039	789.9	249.1	49.8	1753	239
40	60	1026.3	789.9	236.4	49.8	1641	41
80	120	1016.8	789.9	226.8	49.8	1563	3
160	240	1010.8	789.9	220.9	49.8	1512	0
320	480	1007.5	789.9	217.5	49.8	1488	0
400	600	1006.8	789.9	216.8	49.8	1484	0

Table I-53: Variation in performance parameters for different cavity widths in the base case, tested for constant air changes and volumetric flow rate

Applied Ventilation	Observed Vent Quantity	Cavity Width	Total Heat Gain to Room per m length of facade	Solar Heat Gain to Room per m length of facade	Surface Heat Gain to Room per m length of facade	Total Heat Loss from Room per m length of facade	Hrs with glazing surf above 28°C	Hrs with cavity air above 40°C
		m	kWh	kWh	kWh	kWh	hrs	hrs
80AC	480 m3/hr	0.2	1039.9	799	240.9	49.8	1680	72
80AC	1200 m3/hr	0.5	1016.8	789.9	226.8	49.8	1563	3
80AC	1920 m3/hr	0.8	1001.2	779.7	221.5	49.7	1527	0
80AC	2400 m3/hr	1	991.5	772.3	219.2	49.7	1508	0
80AC	2880 m3/hr	1.2	982.4	765	217.4	49.7	1497	0
80AC	3600 m3/hr	1.5	969.1	753.9	215.2	49.6	1479	0
1200m3/hr	200 AC	0.2	1026.5	799	227.5	49.8	1561	3
1200m3/hr	80 AC	0.5	1016.8	789.9	226.8	49.8	1563	3
1200m3/hr	50 AC	0.8	1005.6	779.7	225.9	49.7	1559	3
1200m3/hr	40 AC	1	997.5	772.3	225.2	49.7	1556	3
1200m3/hr	33.34 AC	1.2	989.4	765	224.5	49.7	1555	3
1200m3/hr	23.67 AC	1.5	977.2	753.9	223.4	49.6	1544	3

Table I-54: Variation in performance parameters of different glazing systems on the external and internal envelope on the base configuration

Façade Configuration		Total Heat Gain to Room per m length of facade	Solar Heat Gain to Room per m length of facade	Surface Heat Gain to Room per m length of facade	Heat Loss from Room per m length of facade	Hrs with glazing surf above 28°C	Hrs with cavity air above 40°C
External Glazing (single)	Internal Glazing (double)	kWh	kWh	kWh	kWh	hrs	hrs
clear 6mm	Clear DG 4/16/4 argon gas	1016.8	789.9	226.8	49.8	1563	3
clear 6mm	LowE DB 9.4/12.7/3 LowE, Argon gas	729.4	533.4	196	30.5	1217	37
clear 6mm	Tinted DG 4/12.7/3 Argon gas	823.3	443.6	379.7	48	3004	63
clear 6mm	High Performance DG 10/1/3 LowE, Vacuum	304.3	212.2	92.1	13.9	0	188
Tinted 5.8mm	Clear DG 4/16/4 argon gas	542.4	314.7	227.6	49.9	1627	15
Reflective 13.2mm	Clear DG 4/16/4 argon gas	341.8	187.8	154	49.7	645	0
Tinted 5.8mm	LowE DB 9.4/12.7/3 LowE, Argon gas	380.4	212.6	167.8	30.8	774	78
Tinted 5.8mm	High Performance DG 10/1/3 LowE, Vacuum	163.6	84.6	79.1	14	0	251

Appendix J

Sensitivity Analysis for Heat Transfer Coefficients

NOTE: This analysis was carried on the base configuration of the DSF for New Delhi site in South orientation.

Table J-1: Percentage change of various measurement parameters for changes in heat transfer coefficients. Change factor indicates the factor by which the original value in the methodology is/are multiplied by, unless otherwise mentioned. If *(NA)* is present for a value, it implies an unrealistic situation owing to the boundary conditions or control schemes. Thus, these values may be discarded.

Heat transfer coefficient	**Change factor**	**Total Heat Gain to Room per m length of facade**	**Surface Heat Gain to Room per m length of facade**	**Total Heat Loss from Room per m length of facade**	**Hrs with glazing surf above 28°C**	**Hrs with cavity air above 40°C**
		%	%	%	%	%
Ext Convection	0.5	-1.2	-5.2	5.5	-3.9	-15.8
	2	1	4.2	-4	4.3	29.8
All Convection coeffs. within cavity	2	0.9	4	-6.1 *(**NA**, cavity ventilation is off)*	5.7	-8.8
	4	-0.5	-2.1	-27.2 *(**NA**, cavity ventilation is off)*	17.5	-26.3
	6	0.7	3	-22.4 *(**NA**, cavity ventilation is off)*	4.3	-56.1
Radiation coeff.	Set as per objects at 40°C	-1.6	-7	-13.5	13.1	17.5

Appendix K

Carbon Footprint Estimation

For the purpose of assessing the carbon footprint of the electricity used to compensate for heat gain through the respective DSF and single skin the following factors and assumptions are made:

Table K-1: Various assumed quantities for estimating carbon footprint

Coefficient of performance (COP) of air conditioning unit	3
Working hours for the AC unit (based on working schedule in offices)	08:00 to 18:00
Number of working days per week	5
Transmission loss in electricity grid (L_{trans})	10%
Efficiency of coal burning power plant (η_{PL})	40%
Thermal energy content of coal (TEC_{coal})	6150 kWh/ton
CO_2 produced by combustion of 1 ton of coal (M_{co2})	2860 kg

The calculation is made for an office building with 10 floors (F), 3m height (H) each and a façade length (L) of 50m. The site selected is New Delhi and it is assumed that the façade is South facing. Based on the MATLAB/Simulink model, the annual heat gain for working hours per meter width (HG_m) of the optimized DSF configuration is 353.4kW/m while that of the single skin is 711.6kW/m. This results in the following:

Table K-2: Calculation details for carbon footprint estimation

Quantity	Magnitude		Remarks
	DSF	**Single Skin**	
Annual heat gain to be compensated (HG_a)	126234.7 kWh	254134.6 kWh	$HG_a = HG_m * L * F$
Electricity needed (E)	42078.2 kWh	84711.6 kWh	$E = HG_a / COP$
Electricity to be produced at power plant (E_{PP})	46753.6 kWh	94123.9 kWh	$E_{PP} = E / (1-L_{trans}/100)$
Electricity produced from combustion 1 ton of coal (E_{coal})	3690 kWh		$E_{coal} = TEC_{coal} *(\eta_{PL}/100)$
Amount of coal burnt (M)	12.7 ton	25.5 ton	$M = E_{PP} / E_{coal}$
Amount of CO_2 produced, i.e. **Carbon footprint** (CFP)	**36.2 ton**	**72.9 ton**	$CFP = M * M_{co2}$

Hence, by employing a DSF instead of the fully glazed single skin a **reduction of 36.7 ton (0.07 ton per meter length)** in the carbon footprint is achieved.

Note: Energy used for mechanical ventilation in the DSF is neglected in this calculation since it accounts for less than 1% of overall energy needed